Stereo–Chemical Control of Organic Reactions in the Interlamellar Region of Cation–Exchanged Clay Minerals

By

Vinod Vishwapathi

A thesis submitted in partial fulfilment for the requirements for the degree of Doctor of Philosophy at the University of Central Lancashire

March 2015

STUDENT DECLARATION FORM

Concurrent registration for two or more academic awards

Either *I declare that while registered as a candidate for the research degree, I have not been a registered candidate or enrolled student for another award of the University or other academic or professional institution

_____

Material submitted for another award

Either *****I declare that no material contained in the thesis has been used in any other submission for an academic award and is solely my own work

_____

(state award and awarding body and list the material below):

* *delete as appropriate*

Collaboration

Where a candidate's research programme is part of a collaborative project, the thesis must indicate in addition clearly the candidate's individual contribution and the extent of the collaboration. Please state below:

Signature of Candidate _____

Type of Award _____PhD (Doctor of Philosophy)_____

School School of Forensics and Investigative Sciences_____

Abstract

Carbene intermediates can be generated by thermal, photochemical and transition metal catalysed processes from diazoalkanes.[1] The carbene intermediates are very reactive and can add across double bonds to give 3–membered rings (cyclopropanes),[2] insert into –OH bonds to give esters[3] or ethers[4] and insert into neighbouring –C–H bonds to give 4 or 5–membered rings, such as *β*– and γ–lactams[5,6] or γ–lactones.[7] Copper salts and complexes were amongst the first catalysts to be used for carbene generation from diazoalkanes.[8] However, current tendencies are to use very expensive, especially, platinum group salts and complexes to generate the carbene intermediates, as yields and specificity tend to be higher.[2,9] We have found that Cu^{2+}–exchanged clay minerals (e.g. Wyoming bentonite) and zeolites (zeolite A), have proven to be very competitive in yield with such transition metal catalysts and they have the added advantage that the restricted reaction space within the zeolite pore or clay interlayer favours the more planar/less bulky product. With the clay minerals, when the layer spacing is kept low by judicious choice of mineral or solvent, the selectivity is improved.

Herein we report a wide range of carbene addition (cyclopropane formation) and –C–H insertion reactions (*β*–lactam, *γ*–lactam and *β*–lactone formation) catalysed by the Cu^{2+}–exchanged clay minerals and the stereo–chemical consequences of carrying out the reactions within the clay interlayer. Preliminary studies on the successful formation of aziridines from azides via nitrene intermediates with Cu^{2+}–exchanged clay minerals are also reported.

For my

Loving Mom and Dad

Acknowledgments

First and foremost I would like to thank my director of studies Dr Richard W McCabe for his constant support, and his continuous guidance and encouragement throughout my research work.

I would also like to thank Prof Gary Bond for giving me funding for research and also valuable time to spend with him throughout the research and for giving me opportunity to present my work in various conferences.

I am also very thankful to member of my supervisory team Dr Rob Smith for his guidance, valuable support and encouragement. I also thank to Dr Jennifer Elizabeth Readman for her guidance in XRD and XRF and Dr Stephen Johns for his support and guidance in the lab.

I would like to thank the members of the technical department; Tamar Garcia, Sal Tracey, Jim Donnelly, Patrick Cookson, Steven Kirby and staff in the Forensic chemistry department for always being so helpful and friendly. I also thank to my lab mates Dr Adeyi Okoh, Hajira Faki, Dr Samridhi lal, Sandeep Kadam for making my time enjoyable and sharing knowledge in chemistry all the time. I would like to express my thanks to my friend Dr Vishnu Vardhan Reddy, Alessandro Sinopoli for providing modelling data, and house mates for constant encouragement.

Finally, my appreciation goes to my family members: mother, dad, brother Vinay kumar, sister Sujatha, brother-in-law Kasoju Govardhan and my sweet sons-in-law Sumanth, Akhil and my loving wife Saritha and sweet son.

Table of figures

List of Abbreviations

Å	Angstrom
ACN	Acetonitrile
BTC	Benzene-1,3,5-tricarboxylate
^{13}C-NMR	Carbon Nuclear Magnetic Resonance
$CHCl_3$	Chloroform
$CDCl_3$	Chloroform deuterated
COSY	Correlation spectroscopy
$Cu(acac)_2$	Copper(II) acetylacetonate
CF_3SO_3H	Trifluoromethanesulfonic acid
DIOX	1,4–dioxane
DCC	*N,N'*-Dicyclohexylcarbodiimide
DEPT	Distortionless Enhancement by Polarisation Transfer
D_2O	Deuterium oxide
DMSO	Dimethyl sulfoxide
DMF	Dimethylformamide
Δd	Interlayer distance
ee	Enantiomeric excess
Er	Enantiomer ratio
EDG	Electron-donating group
EWG	Electron-withdrawing group
E^+	Electrophile
Et	Ethyl
EtOAc	Ethyl acetate
EDA	Ethyl diazoacetate
ESIMS	Electron Spray Ionisation Mass Spectrometry
^{1}H–NMR	Proton Nuclear Magnetic Resonance
HCl	Hydrochloric acid
HSQC	Heteronuclear Single Quantum Correlation
HOMO	Highest occupied molecular orbital
IRMOF	Isoreticular Metal Organic Framework
LUMO	Lowest unoccupied molecular orbital

MeOH	Methanol
MOF	Metal-Organic Framework
MO	Molecular Orbital
NOESY	Nuclear Overhauser effect spectroscopy
p–TSAz	*p*-Toluenesulfonyl azide
PhCN	Benzonitrile
PhEDA	Ethyl 2-phenyldiazoacetate
PCB	*p*-Carboxybenzenesulfonazide
$PhCH_3$	Toluene
PMP	*p*-methoxyphenyl
TsCl	*p*-Toluenesulfonyl chloride
THF	Tetrahydrofuran
THP	Tetrahydropyran
TON	Turn Over Number
VIs	Vertically Integrated Sectors
ZSM-5	Zeolite Socony Mobil #5

1 Chapter: General Introduction

1.1 Background

Clays and modified clay minerals are layered materials and zeolites are cage structures with molecular sized pores. These minerals are used widely as catalysts for numerous synthetic organic reactions[10] such as diazotisation reactions,[6] formation of ethers, esters, lactones and cyclic anhydrides, synthesis of heterocyclic compounds and for several named reactions, e.g. aldol condensation, Michael addition, Diels-Alder reaction and Friedel-Crafts alkylation and acylation.[11] Most of these catalytic reactions are carried out either in the interlamellar region of the clay minerals[12] or within the pores of the zeolite and, due to steric constraints, they often prefer to proceed via less bulky intermediates to produce stereo- and regio-specific products.[13,14]

1.2 Aims of the research

By exchanging the usual sodium or calcium ions present in between the aluminosilicate layers of clay minerals or within the pores of zeolites, for low valent transition metals, such as Cu^{2+} or Rh^{2+}, a catalytic site highly restricted in size and shape can be produced. This leads to the possibility that, due to steric constraints, the less bulky isomer should be formed in these molecular dimension regions. Thus, chemical reactions carried out in these restricted environments would prefer to proceed via less bulky intermediates or transition states.[12,15]

Thus, the main aims of this project were:

i. To catalyse novel organic synthesis by generating reactive intermediates, such as carbenes (formed from diazoalkanes) or nitrenes (formed from azides), within the interlamellar region of a cation–exchanged clay mineral or zeolite pore.
ii. To utilise the ability to modify the interlamellar distance of clay minerals to help control the regio- and stereo-chemical outcome of reactions carried out within the clay layers compared to free solution, i.e. reactions via less bulky intermediates should be more favoured within the restricted interlamellar region of the clay.

iii. To create a chiral environment within the clay interlamellar region to improve the enantioselectivity of asymmetric synthetic chemical reactions.

The project was begun by generating carbene intermediates, catalytically, within the interlayer region or pore region of a cation exchanged clay mineral or zeolite. Since these aluminosilicate catalysts can have shape and size selectivity,[12] they can be used to control the stereochemical outcome of organic reactions. This follows on from previous work in the group on clay mineral catalysed Diels-Alder reactions where a larger proportion of the less bulky, but less kinetically favoured *exo*-isomer can be produced within the clay catalyst.[12] We are interested in using these carbene intermediates in the syntheses of molecules related to *β*-lactam antibiotics and pyrethrin pesticides; syntheses that proceed mainly through carbene generation in the interlayer or pore region, followed by cyclisation reactions, to produce regio–isomers of potentially biologically active chiral compounds.

β-Lactams have been generated by intramolecular carbene insertion reactions by the action of transition metal catalysts (e.g. Cu^{2+}) on diazoalkanes.[1] Similarly, these reactive intermediates can also be trapped by alkenes to give cyclopropanes and this has been used to produce chrysanthemic acid derivatives that are precursors of pyrethrin pesticides.[2] This cyclopropanation reaction is one of the most important transformations in organic synthesis, because of its versatile applications in natural product synthesis.[2]

1.3 Clay minerals as catalysts

Clay minerals are useful for laboratory and industrial catalysts with excellent product, regio- and stereo-selectivity[10,15] and as heterogeneous catalysts they have distinct advantages over homogeneous catalysts because of easy workup of the reaction mixture, i.e. the clay mineral catalyst can be removed easily. Clay minerals are layered silicates, which were found to be crystalline by X–ray diffraction studies.[16,17] Clays and clay–supported chiral metal complexes have been used in asymmetric synthesis as they can absorb one enantiomer from a racemate differentially or absorb enantiomers equally from a non–racemic mixture; of which bentonite (montmorillonite) is found to be the best example.[18] Initially, research on catalysis with clay minerals concentrated on either cation exchange of the clay to increase Brønsted or Lewis

acidity, or activation of the clay by treatment with strong acid,[10,15] but more recent publications[19] show the use of clay catalysts in redox processes, generation of reactive intermediates such as carbenes,[20] carbocations, carbanions and also as supports for metal salts and complexes.[21]

1.3.1 Structures of clay minerals

Clay is a term used in mineralogy to describe inorganic materials in the soil that have a particle size of less than 2μm.[22] They are also classed as layered silicates or phyllosilicates.[16] Clay minerals are mainly made–up of two distinct building blocks (Figure 1): tetrahedral (mainly SiO_2) and octahedral (mainly Al_2O_3, but possibly MgO). The tetrahedra usually have silicon in the centre surrounded on four corners by oxygen atoms, whilst the octahedra usually have six oxygen atoms or hydroxyl groups surrounding an aluminium or magnesium ion at the centre.

Silica tetrahedra

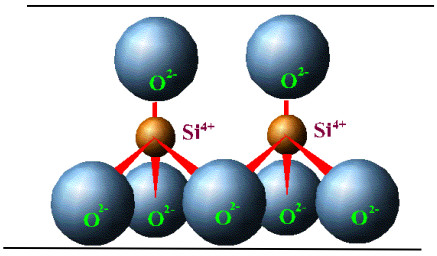

(Tetrahedral sheets)

Alumina octahedra

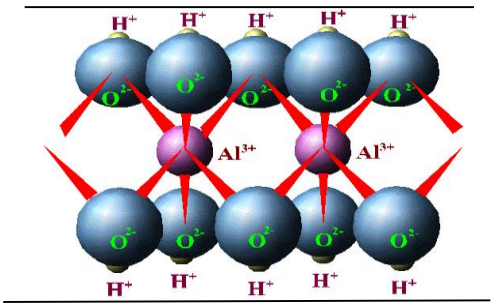

(Octahedral sheets)

Figure 1 The tetrahedral silica sheet and octahedral alumina sheets of clay minerals.

In the clay minerals the tetrahedral sheet is comprised mainly of silica tetrahedra, while the octahedral sheets consist of aluminium, magnesium or iron oxides/hydroxides. The basic lamellar structure of clay minerals is obtained through combination of the tetrahedral and octahedral sheets by sharing oxygens between the sheets. Different clay minerals are formed by having different combinations of these two units (e.g. $1_T : 1_O$ or $2_T : 1_O$) and by

substituting one cation for another. The interlamellar region is usually hydrated. Some typical compositions of the most common minerals are:

1. Illite $[K_{1.6}Si_{6.4}Al_{5.6}O_{20}(OH)_4] + (H_2O)_x$
2. Vermiculite $[Mg_{6.6}Si_{6.8}Al_{1.2}O_{20}(OH)_4] + (H_2O)_x$
3. Montmorillonite $[Na_{0.6}Al_{3.4}Mg_{0.6}Si_8O_{20}(OH)_4] + (H_2O)_x$
4. Hectorite $[Li_{1.0}Mg_{5.5}Si_8O_{20}(OH)_4] + (H_2O)_x$

Most naturally occurring clay minerals have layer charges due to isomorphous substitution,[23] which is the "substitution of one atom by another of similar size in the crystal lattice without changing the crystal structure of the mineral".[23] Isomorphous substitution of Al^{3+} for Si^{4+} in the tetrahedral layer or of Mg^{2+} for Al^{3+} in the octahedral layer results in a net negative charge on the clay sheet.[23,24] This negative charge is neutralised by cations (e.g. Na^+, K^+, Ca^{2+} or Mg^{2+}) in the interlamellar region that separates adjacent layers of platelets. This structure (Figure 2) makes montmorillonite chemically stable.

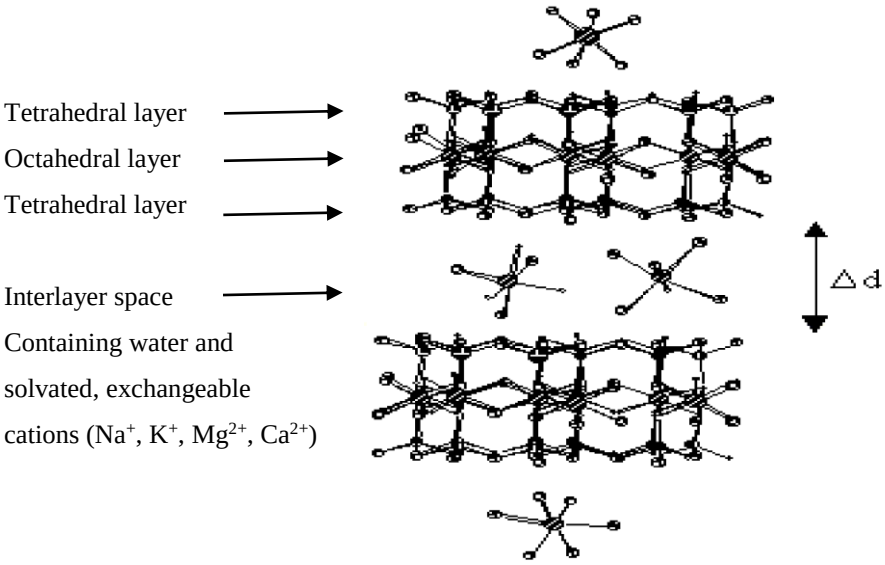

Figure 2 The basic structure of montmorillonite,[17,25] a T: O: T dioctahedral arrangement with water and aquated cations in the interlayer space. Where Δd is the interlayer space.

The specific characteristics of a montmorillonite vary due to: the size of the surface negative charge; where the charge resides (i.e. mainly on the tetrahedral or octahedral layer) and what interlayer cations are present. The natural cations can be exchanged for more useful cations

that can increase the catalytic activity of the mineral. Where Δd is the distance between the two layers of the clay mineral.

1.3.2 Acid activation of clay minerals

Smectite (swelling) clays are often treated with a strong mineral acid (acid activated)[22] to give materials of high surface area (increasing from *ca.* 60 $m^{-2}g^{-1}$ to *ca.* 300 $m^{-2}g^{-1}$), which have excellent activity as adsorbents[26] and catalysts.[27] The process of acid activation is quite severe (> 5 mol dm^{-3} hot mineral acid for several hours) and destroys the bentonite layer structure as it removes iron, aluminium and magnesium from the octahedral layer. Most of the edges of the bentonite clay particles become very disordered by the replacement of exchangeable cations Al^{3+} and H^{+}–cations, which was shown by Scanning Electron Microscopy (SEM).[28,29] The characteristic surface properties of clays have long been used in bleaching and other adsorptive processes. For such purposes, individual clays possess widely differing properties.[30] Acid–treated bentonites were once important catalysts in catalytic cracking,[31] but they have now been superseded by zeolites. Another application of acid–activated clays is as a developer for carbonless copying paper,[28] which requires a high brightness of the material. Acid activation improves the brightness mainly by removal of structural Fe^{3+}-cations, which usually cause the clay to be a grey or yellow colour.

Bentonite and Sepiolite types of clays have been studied intensively since they have catalytic and adsorptive properties. Some of the adsorptive properties of bentonite include the removal of a number of chemical species: e.g. amines (e.g. desorption of cyclohexylamine and pyridine from an acid-treated Wyoming bentonite),[32] organic pigments (e.g. adsorption of *β*-carotenes form acetone solution on modified bentonite),[33] cations (Ni, Zn), phenols and ketones[34] and pesticides.[35] Sepiolite, a Mg silicate, because of its strong adsorbing power, has been used as a deodorant[36] and to adsorb methylene blue,[37] ammonium cations and ammonia,[38] tetrahydropyran, tetrahydrofuran and 1,4-dioxane.[39] The desorption of tetrahydropyran, tetrahydrofuran and 1,4-dioxane from Na^{+}, Ca^{2+}, Al^{3+} and Cr^{3+}-exchanged montmorillonite has been studied using variable temperature infrared spectroscopy and thermogravimetric analysis.[39]

1.3.3 Structures of zeolites

Zeolites are framework aluminosilicates with accessible molecular size pores. Generally, Si^{4+} ions in the framework are replaced by Al^{3+} cations, which cause the framework to have a negative charge that is neutralised by exchangeable cations such as Na^{+}, K^{+} or Ca^{2+} in normal usage.[40] We were interested in two types of zeolites, 4A molecular sieves and ZSM-5, for this project.

Type A molecular sieves have the cage structure shown in Figure 3[41] and 4A molecular sieves have the approximate elemental composition: Si Al Na O_4,[42] as *ca*. half of the Si^{4+} cations in the framework have been replaced by Al^{3+}-cations giving a negative charge that is neutralised by Na^{+}. Typically, 4 Na^{+} cations reside in the opening of the 7.4 Å pores reducing the accessible pore diameter to *ca.* 4 Å (Figure 3).[41]

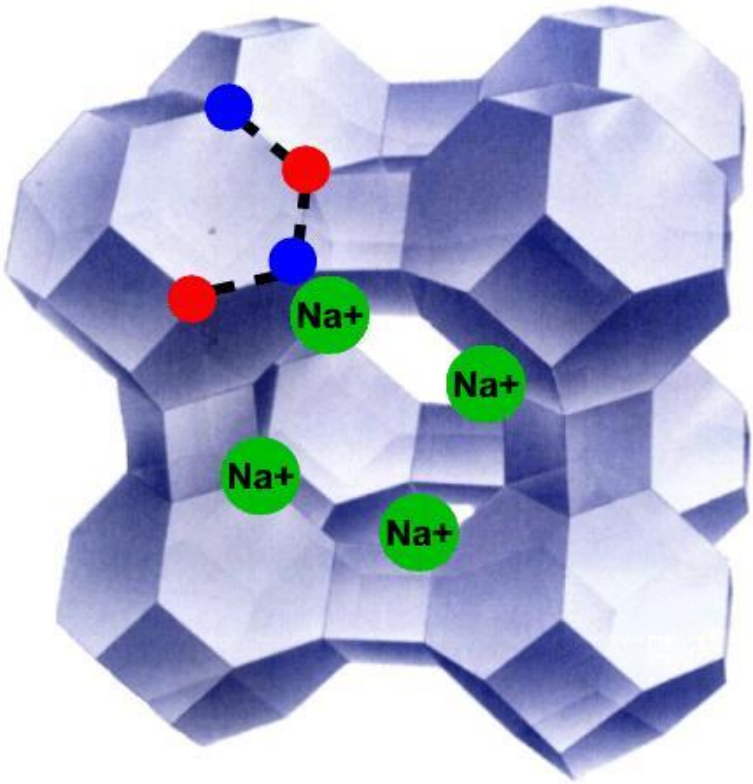

Figure 3 Structure of zeolite A showing positioning of Na^{+} cations in 4A molecular sieves.[41] (red, Si and blue, Al)

The ionic radius of 6-coordinate Na^+ is 1.02 Å,[43,44] giving a diameter of 2.04 Å plus the co-ordinated waters, which reduces the accessible pore diameter to about 4 Å. However, only two Cu^{2+} cations will be required in the pore entrance, due to the 2+ charge, and the diameter of 6 co-ordinate Cu^{2+} is 1.46 Å plus co-ordinated waters.[43] Thus, assuming that the Cu^{2+} cations will be as far apart as possible, the pore "entrance" should become a slot with maximum width 7.4 Å, but reduced to about 5 Å in "height", thus giving a size restriction of about 5 Å for the smallest dimension of an isomer that might migrate out of the Cu^{2+}-exchanged A zeolite.

ZSM-5 zeolite has the structure shown in Figure 4 with pore diameters of 5.4 Å,[45] but as the Si/Al ratio is generally kept to 50-200, the effects of different cations on pore diameters should be minimal.

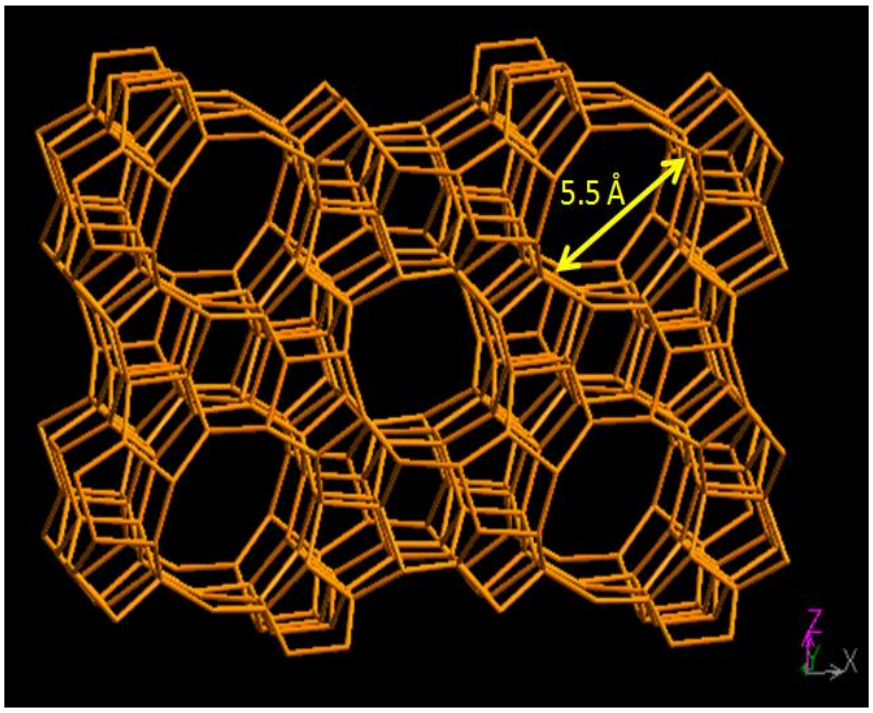

*IZA-SC: http://iza-online.org

Figure 4 Pore structure of ZSM-5.[45,46]

1.4 Clay minerals as catalysts in synthetic organic reactions

1.4.1 Ether formation

Primary alcohols **2** react with terminal alkenes **1** (e.g. 1-hexene) slowly at 150°C to form 2-alkyl **3** and 3–alkyl ethers **4** in the presence of M^{3+}- or M^{2+}-exchanged montmorillonites (e.g. aluminium cation-exchanged montmorillonite) via rearrangement of the secondary carbocation intermediate (Scheme 1).[47] These reactions are not truly catalytic as the interlayer water cannot be replenished effectively without reducing the acidity of the clay too far.

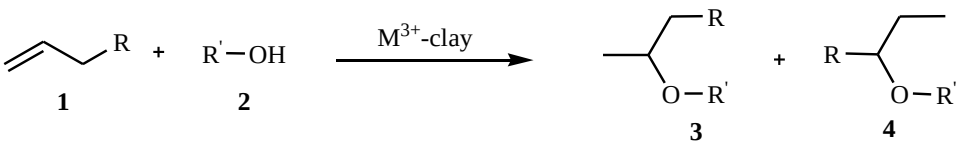

Scheme 1 Formation of ethers in the presence of Al^{3+}-cation-exchanged montmorillonite.

M^{2+}-exchanged clay minerals show some catalytic activity for this reaction, whilst M^{+}-exchanged clays are essentially unreactive, thus confirming that the Brønsted acidity of the clay minerals is mainly due to dissociation of water molecules in the hydration sphere of exchangeable interlayer cations (Scheme 2).[15]

$$[M(OH_2)_n]^{m+} \rightleftharpoons [M(OH_2)_{n-1}OH]^{(m-1)+} + H^+$$

Scheme 2 Dissociation of water molecules in the hydration sphere of the interlayer exchangeable cations.

When isobutene **5** is reacted with methanol in the presence of clay minerals exchanged with different interlamellar cations, methyl tertiary-butyl ether (MTBE) **6** is produced in > 50% yields with trivalent (e.g. Fe^{3+}, Cr^{3+} or Al^{3+}) exchanged cations (Scheme 3). With acid-activated clay catalysts (e.g. K-10, KSF and K306 from Süd Chemie) > 50% yield was obtained with K-10, KSF clays and low yields were obtained with K306 with monovalent or divalent interlamellar cations. Because of the greater polarising power of trivalent cations the interdependence of the acidity of the interlayer water[48] and the Al^{3+}-interlamellar cations gave high yields in K-10 or KSF, but low yields in K306, possibly due to the presence of 85% silica in this highly acid activated material.

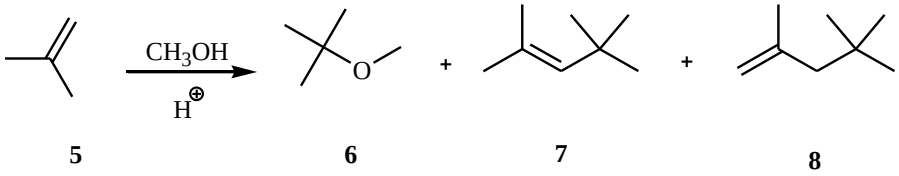

Scheme 3 Formation of methyl tertiary-butyl ether 6 from isobutene 5 and methanol in the presence of acid catalysts.

When the same reaction was performed with different solvents such as tetrahydrofuran, 1,4-dioxane, *n*-pentane, diethylene glycol, diethyl ether, *N*-methylmorpholine and 1,2-dimethoxyethane; different yields were obtained. This illustrates the important role of the solvent in determining the distribution of reactants and products that can be formed either in the interlamellar region, if it is accessible, or outside the clay if not. *n*-Pentane gives low yields as the interlayer regions become inaccessible as the interlayer distance becomes very small and reactions occur predominantly on the outer surface. In contrast, it was found that solvents that caused higher interlayer spacing, as determined from X-ray diffraction data, also gave low yields. This is a result of a balance of two effects: (i) more coordinating solvents tend to push the layers apart, thus making the interlayer cations more accessible; however, (ii) these more coordinating solvents reduce the acidity of the protons present in the interlayer resulting in slower reactions.

Equimolar amounts of glycerol **9** with benzyl alcohol **10** were reacted in the presence of different ZSM-5 type catalysts (Table 1), to give mixtures of monobenzyl glyceryl ethers **11** and **12**, dibenzyl glyceryl ethers **13** and **14** and dibenzyl ether **15** (Scheme 4). The yields of monobenzyl glyceryl ether, dibenzyl glyceryl ether and dibenzyl ether vary with a series of ZSM-5 type catalysts having different pore sizes and SiO_2 to Al_2O_3 ratios (Table 1).[49]

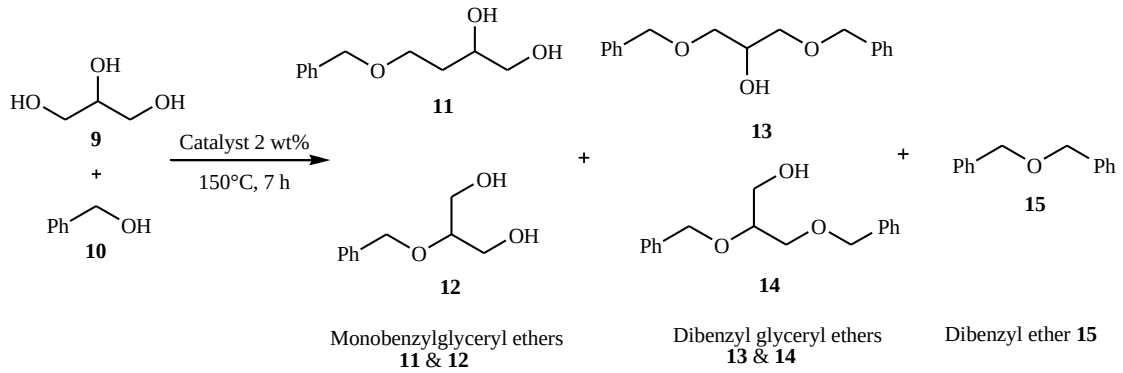

Scheme 4 Catalysed reaction of glycerol 9 with benzyl alcohol 10.[49]

Table 1: Zeolite catalysed etherficaton of glycerol with benzyl alcohol

Type of catalyst	Pore size (Å)	SiO_2/Al_2O_3	Yield % of **11** & **12**	Yield % of **13** & **14**	Yield % of **15**
Beta type	7	75	24	5	3
ZSM-5 type	5	80	57	1	2
ZSM-5 type	5	30	80	<1	<1
ZSM-5 type	5	50	86	<1	<1

The results from the Table 1 showed zeolite catalysts were effective for the synthesis of monobenzyl glyceryl ethers, formed more than 95% selectivity, especially using ZSM-5 type with (SiO_2/Al_2O_3 = 30 and 50, respectively) target compounds **11** and **12** were obtained in > 80% yields; when compared to ZSM-5 (SiO_2/Al_2O_3 = 80) which gave only 57% of the target compounds **11** and **12**. With the increase in ratio of SiO_2 to Al_2O_3 the hydrophilicity of the surface of ZSM-5 also increases. The results from Table 1 shows that both the pore size and hydrophilic-lipophilic surface of zeolites will govern the selectivities and yields of reaction products.

1.4.2 Synthesis of heterocyclic compounds

Dihydrothiazines such as **18**, synthesised from thioamide **16** and *α,β*–unsaturated ketone **17** in the presence of acid catalysts,[50] are important in the synthesis of cephalosporin antibiotics. Similar types of reactions in toluene with Al^{3+}–, Cr^{3+}– or Fe^{3+}–exchanged montmorillonites as a catalyst, also gives dihydrothiazines (Scheme 5).[50]

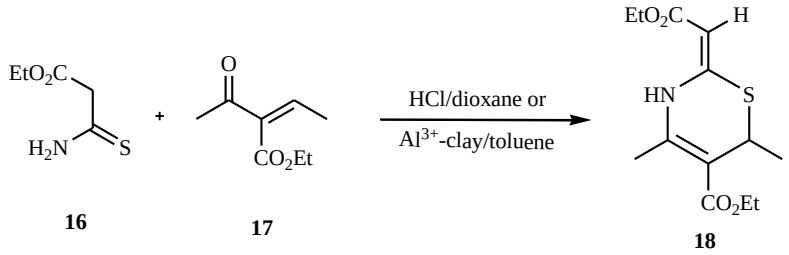

Scheme 5 Synthesis of dihydrothiazines from thioamides and *α,β*-unsaturated ketones.

From the literature,[51] formation of 3-substitiuted isoquinolines **19** was catalysed by clay mineral supported transition metal catalysts (Ag^{I}–K10 clay)[51] at 100°C in DMF for 6 h (Scheme 6).[52] Control experiments showed that no desired product was obtained in the absence of clay catalyst at room temperature, or even at 100°C. Reactions were carried out at different temperatures (50, 75 and 100°C), with the optimum yield at 100°C. The use of K10 clay had several advantages, like ease of handling, non-corrosiveness and low cost.

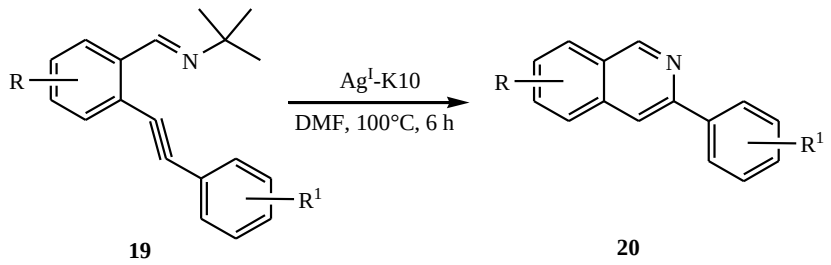

Scheme 6 Synthesis of 3-substitiuted isoquinolines in the presence of Ag^{I}–K10 clay catalyst.

A further example, employing microwave irradiation of a mixture of *α*–tosyloxyketones **21** and thioamides **22** in the presence of montmorillonite K-10 clay gave bridgehead thiazoles **23** (3–aryl–5,6–dihydroimidazo[2,1–*b*][1,3]thiazoles) (Scheme 7);[53] a method that is easy and quick, when compared to conventional methods of synthesis, which are normally difficult, require a longer heating time and employ highly active *α*–haloketones[54] or *α*-tosyloxyketones[55] under strongly acidic conditions. The reactions of tosyloxyketones with ethylenethioureas remain incomplete on heating in an oil bath (conventional method); whereas, in a microwave–accelerated method using montmorillonite K-10 clay as adsorbent and catalyst, the reaction completed within a very short time scale (~3 min) with excellent yields.[53]

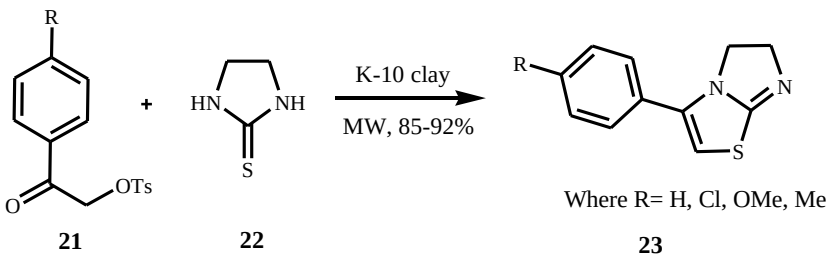

Scheme 7 Preparation of bridgehead thiazoles using montmorillonite K-10 clay.

Various proportions (0.25, 0.50 and 0.75 x CEC) of organic amines adsorbed on Al-PILC catalysts[56] have been used to catalyse the reaction of aromatic aldehydes **25** with *ortho*-phenylenediamine or *ortho*-aminothiophenol **24**[57] to form benzimidazole **26** and benzothiazole derivatives **27** (Scheme 8). In the synthesis of benzimidazole and benzothiazole derivatives there is an influence of number and size of the pillars in the interlayer region, which influenced the cation exchange capacity (CEC) of the clay mineral.

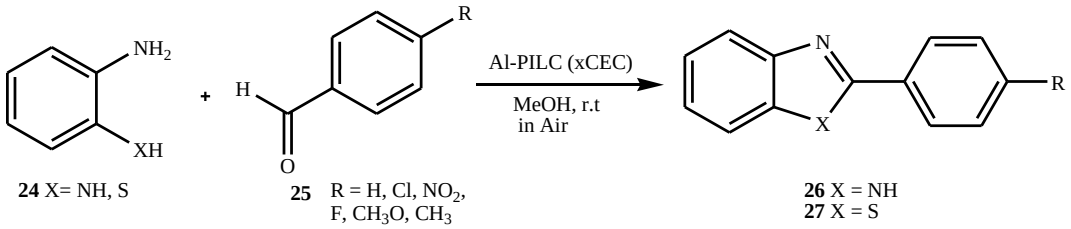

Al-PILC (xCEC) - Aluminum Oxide-Pillared clay with preadsorption of diethylamine

where x is the ratio ($^1/_4$, $^1/_2$ or $^3/_4$) *vs*. CEC of the PILC, of the diethylamine used.

Scheme 8 Synthesis of 2-arylbenzimidazoles and benzothiazoles catalysed by diethylamine supported on Al-pillared clay.[56]

1.4.3 Formation of aziridine derivatives

Dibromo compounds **28** react with primary aliphatic amines **29** in the presence of bentonite clay catalyst as a solid support under solvent–free conditions to give functionalised aziridine derivatives[58] **30** and **31** (Scheme 9).[59] Microwave irradiation or classical heating methods both accelerated the aziridine formation.[58,60]

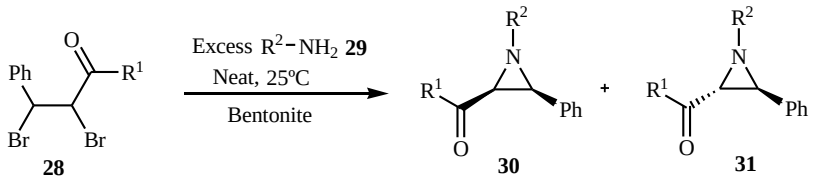

(a) R^1 : Ph	R^2 : $-(C_2H_5)_5$	48%	25%
(b) R^1 : Ph	R^2 : -Bn	80%	0%

Scheme 9 Synthesis of aziridines using bentonite.

From the literature,[61] when ethyl diazoacetate **33** with Schiff bases **32** reacted in the presence of montmorillonite K-10 as catalyst at room temperature for 2 h formed *cis*-aziridines[62] **34** in high diastereoselectivity (>99%) and excellent yields (82–91%) (Scheme 10). It has showed

that K-10 was the best catalyst among the several other acid catalysts, such as $H_4W_{12}SiO_{40}$, Nafion-H, Amberlist-15, and Nafion-H on silicon, in achieving the highest diastereoselectivity.

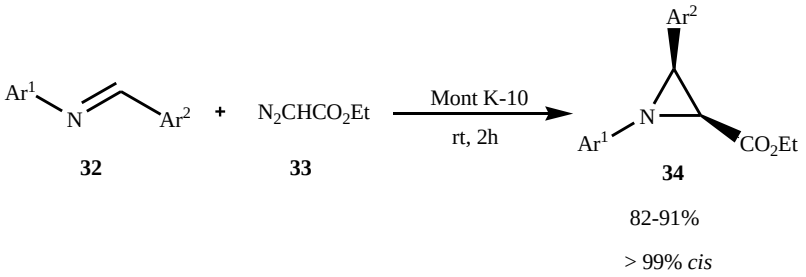

Scheme 10 ***cis*-Aziridine formation from imine 32 and ethyl diazoacetate 33 using montmorillonite K-10 as catalyst.**

1.4.4 Acid catalysed Pinacol-rearrangements

On heating, tertiary 1,2–glycols **35** (e.g. 2,3–diphenylbutan–2,3–diol) undergo acid catalysed Pinacol–rearrangement to give two ketones[63] **37** and **38** in preference to simple dehydration **36**. The Brønsted acidity of montmorillonite clays is suitable for catalysing this rearrangement and excellent results were achieved.[64]

The selectivity of reaction of 2,3–diphenylbutan–2,3–diol **35** adsorbed in the interlayer space of layer silicates (homoionic montmorillonites) has been reported and also by thermal treatment,[65] pinacol rearranges quantitatively to pinacolone in the intracrystalline environment of these solids, the reaction being clearly preferred to the intramolecular dehydration. In the same way, 2,3–diphenyl–2,3–butanediol gives two ketones, the reaction being also different from that taking place in homogeneous conditions. The extent and the selectivity of both reactions have been correlated with the acidity of the interlayer cations (Scheme 11).

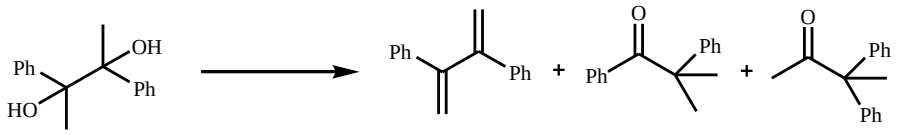

35		36	37	38
	1. Ca^{2+}-montmorillonite in solid, 160ºC, 15 h	28%	9%	60%
	2. DMSO, 190ºC, 14 h	17%	11%	89%

Scheme 11 Pinacol rearrangement of 1,2–diols in the presence of Ca^{2+}-montmorillonite and in homogeneous conditions (DMSO).[65]

Various catalysts such as acidic zeolites, heteropoly acids, metal oxides and cation exchanged clays are the most well-known heterogeneous catalysts for the direct acylation. In organic synthesis out of various solid acid catalysts employed in organic synthesis, acidic clays are the most efficient because of their abundant availability and easy modification.[66]

1.4.5 Aldol reactions

Condensation reaction of glycol aldehydes to monosaccharaides (mainly hexoses) in the presence of Na^{+} montmorillonite as catalyst occurs by an aldol process.[67,68] Similarly, Al^{3+}-exchanged montmorillonites catalyse the cross–aldol addition of silylenol ethers **40** to aldehydes **39**, ketones or acetals,[69] for example, silyl ketene acetals and carbonyls give 3-silyl-ether esters **41** (Scheme 12).[70]

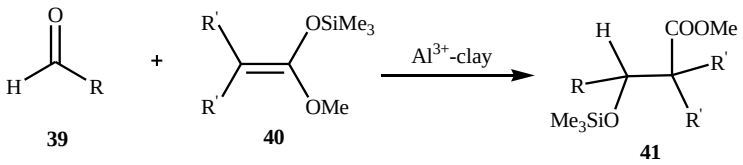

Scheme 12 Cross-aldol reaction of silylenol ethers with ketones in the presence of Al^{3+}-clay.

1.4.6 Cycloaddition reactions (Diels-Alder reaction)

Diels-Alder reactions, such as cyclodimerisation of oleic acid with acid-activated clays, is an industrially important reaction.[71] Another example of a Diels-Alder reaction catalysed by a clay mineral,[72] is the dimerisation of 1,3-butadiene s-*cis* **42** and s-*trans* **42** and in the presence of Cu^+-montmorillonite at 100ºC to form vinyl cyclohexene **43** (Scheme 13).

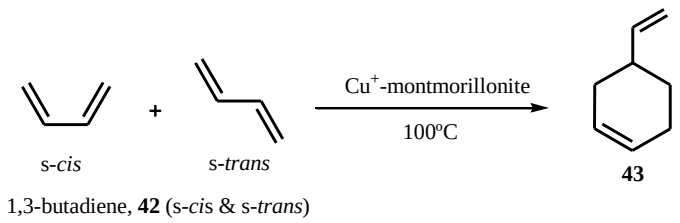

Scheme 13 Cyclodimerisation of 1,3-butadiene with Cu^+-acid–activated clay.

1.4.7 Stereochemistry of Diels-Alder reaction, formation of *endo*-46 and *exo*-47 products

A modest degree of selectivity for the less bulky isomer has been observed in Diels-Alder reactions catalysed by transition metal cation-exchanged clay minerals at ambient temperature in a variety of solvents.[73,74] In the Diels-Alder reaction, *α,β*–unsaturated carbonyl compounds, such as methyl vinyl ketone, methyl acrylate and methyl methacrylate were used as the dienophile and cyclopentadiene, furan, pyrrole or cyclohexa–1,3–diene were employed as the diene.

For example, when cyclopentadiene **44** reacts with methyl vinyl ketone **45** catalysed by various clay minerals (e.g. Cr^{3+}-Tonsil 13, montmorillonite), a mixture of *endo*-**46** and *exo*-**47** isomers was obtained (Scheme 14) that differed from that in free solution. e.g. 9 : 1 With Cr^{3+}-Tonsil 13 clay compared to 19 : 1 in free solution.[12]

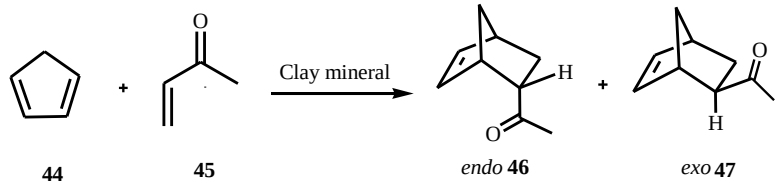

Scheme 14 Diels-Alder reaction of methyl vinyl ketone 45 with 1,3-cyclopentadiene 44 in the presence of cation exchanged clay mineral.

The preferred formation of the *endo*-isomer **46** in uncatalysed reactions at room temperature is explained by the more favourable secondary orbital overlap interactions that occur in the transition state (Figure 5) during formation of the *endo*-isomer **46** when compared to the *exo*-isomer **47**.

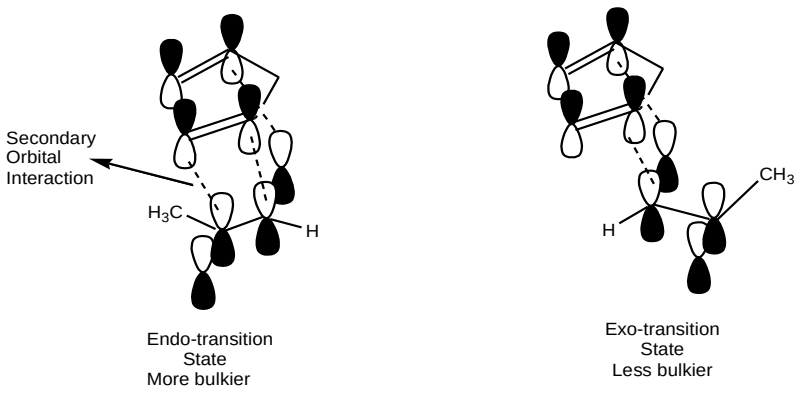

Figure 5 The transition states for the formation of *endo*- 46 and *exo*-isomers 47 in a Diels-Alder reaction.[12]

The ratios of the *endo*- **46** to *exo*- **47** isomers could be changed by manipulation of the inter-layer reaction space of the clay catalyst. Lowering the basal spacing, Δd, gave increased selection for the kinetically less favoured, but less bulky, *exo*-isomer **47**. A small increase in

exo-isomer selectivity was observed with solvents that reduced the interlayer spacing, e.g. see Table 2.

Table 2 Effects of various solvents on the Cr^{3+}-exchanged clay catalysed Diels-Alder reaction of 1,3-cyclopentadiene with methyl vinyl ketone.[12]

Solvents	% Yield in 20 min	*endo*– : *exo*– isomer ratio	Δd/Å
Dichloromethane	92	8.5 : 1	6.8
Chloroform	58	7.0 : 1	7.5
Benzene	87	9.0 : 1	8.7
Chlorobenzene	92	9.1 : 1	7.7
Tetrachloromethane	90	9.2 : 1	7.5

Increasing the layer charge[72] of the Cr^{3+}-exchanged mineral decreased the *endo : exo* ratio, for example: Tonsil-13 montmorillonite (layer charge 0.37) gave an *endo : exo* ratio of 9 : 1, Brett's Fullers earth (layer charge 0.60) gave 6 : 1 and the most spectacular result was obtained with a synthetic expanding vermiculite (layer charge 0.65), which gave 2.5 : 1.

1.4.8 Stereo–control of Diels-Alder reactions in clay minerals

Diels-Alder reactions[75] between various dienes and dienophiles have been catalysed by a montmorillonite supported chiral amine catalyst, (5*S*)-2,2,3-trimethyl-5-phenylethyl-4-imidazolinone hydrochloride with good yields and high enantiomeric excess (*ee*) values compared to the reaction carried out with the non-supported organo-catalyst. The cations present in between the interlayer space of a Na^{+}-montmorillonite **48** were replaced with the chiral amine **49**,[75] thus forming an effective cationic chiral organo catalyst **50** (Figure 6) for carrying out asymmetric Diels-Alder reactions.

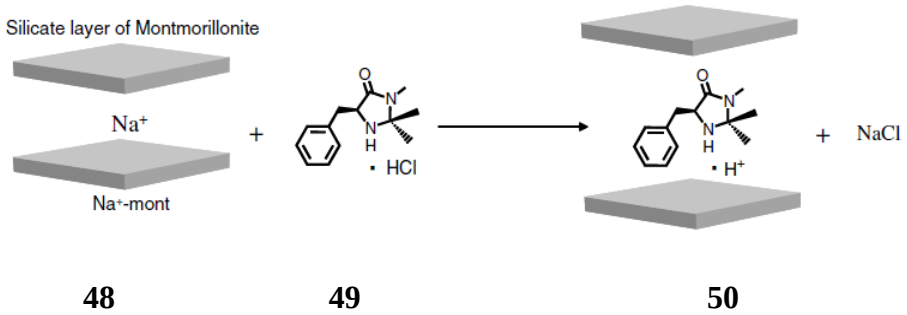

Figure 6 Ion exchange of chiral amine catalyst[75] with Na^+-montmorillonite.

The reaction of cyclohexa-1,3-diene **51** with acrolein **52** in the presence of the chiral amine-montmorillonite in acetonitrile at room temperature with stirring for 48 h afforded a yield of 82% and a high enantioselectivity (*endo* = 92% *ee*, 96 : 4 *endo*-/*exo*- isomers) of the enantio-enriched cycloaddition products *endo*- **53** and *exo*- **54** (Scheme 15). This result was slightly lower than that obtained when employing the homogeneous organocatalyst (82% yield, *endo* = 94% *ee*, 93 : 7 *endo*-/*exo*- isomers).[76]

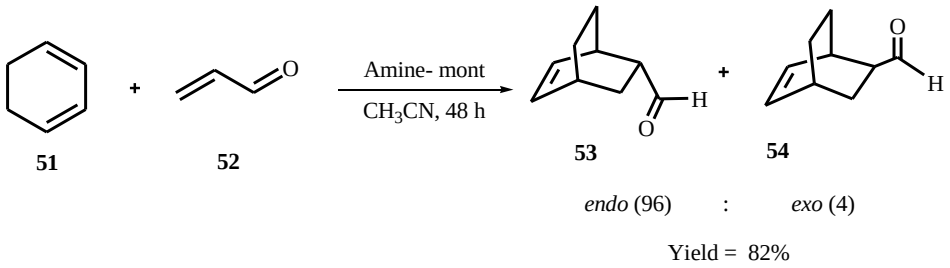

Scheme 15 Asymmetric Diels-Alder reaction catalysed by a chiral organoclay.

The chiral amine-montmorillonite appears to expand the interlayer space[75] of the montmorillonite by acting as a macro counter anion with low nucleophilicity which entraps the organic molecules while maintaining its natural catalytic activity. The chiral catalyst was readily reusable without any decrease in activity or enantioselectivity.

1.5 Carbenes

Carbenes are uncharged, divalent and highly electron deficient species since the carbene carbon has only 6 electrons in the valence shell, making the carbenes highly electrophilic species. Carbenes can be divided into two classes based on the electronic spins, the first one is a singlet state and the second one is a triplet state.

Singlet carbene:

In singlet carbenes[77,78] the two non-bonded valence electrons on the electron-deficient carbon are in the same orbital and they are spin antiparallel giving rise to a diamagnetic, trigonal planar, sp^2 hybridised intermediate with, bond angles of 103º (Figure 7).

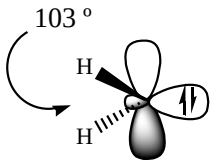

Singlet carbene

Figure 7 sp^2-hybrid structure of singlet state.

Triplet carbene:

In triplet carbenes[78] the two non-bonded valence electrons on the electron deficient carbon are in different orbitals, they have either bent or linear structures with sp^2 or sp hybridised carbons. Most of the carbenes have a non-linear triplet ground state; however, those with heteroatoms such as oxygen, nitrogen, sulfur or halides directly bonded to the divalent carbon are linear. Triplet carbenes are paramagnetic diradicals, whose spin can be observed by electron spin resonance spectroscopy.[79] In the triplet methylene, for example, the bond angle is 125-140º (Figure 8).[80]

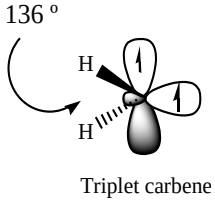

Figure 8 *sp*–hybrid structure of singlet state.

1.5.1 Generation and reactions of carbenes from diazoalkanes

Carbenes can be generated by various methods based on elimination or fragmentation reactions. They mainly involve the breaking of rather weak bonds and the formation of a small thermodynamically stable by-product, such as dinitrogen, from diazo compounds such as ethyl diazoacetate **33** (EDA). Diazo compounds were first prepared by Theodor Curtius[81] in 1883 and they have become widely used precursors in synthetic chemistry. Diazo compounds are unstable and sensitive to light and heat and because of their toxic and explosive nature they should be handled with care. They possess an essentially 1,3–dipolar structure (Scheme 16) and are easy to prepare using the diazo transfer reactions from arenesulfonyl azides.[82]

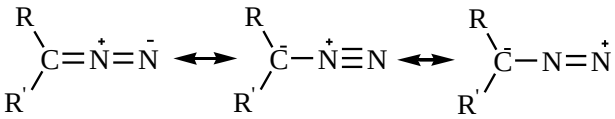

Scheme 16 1,3–Dipolar nature of the diazo group indicating the possibility of resonance stabilisation.

Both thermal and photochemical generation of carbenes produce high energy intermediates, leading to unselective reactions.[83] The stability of various diazo compounds depends on the substituents present. Resonance stabilisation of the carbene by electron withdrawing groups

such as esters can give a more stable intermediate leading to a modest degree of selectivity in reactions.[84]

Under the influence of transition metal catalysts, diazo compounds generate carbene intermediates easily, eliminating dinitrogen as a by-product. Initially, copper powder or copper salts were used for such purposes,[85,86] but more recently there has been greater usage of the highly expensive platinum, rhodium or ruthenium complexes for generating the carbene intermediate.[87] For example, the use of dirhodium(II) tetraacetate, catalysed carbene C-H insertion reactions at room temperature, or slightly above, by Demonceau et al.,[88,89] was a proven breakthrough for selectivity, for example the reaction of ethyl diazoacetate **33** with alkanes **55**, **59** and **64** (Scheme 17).

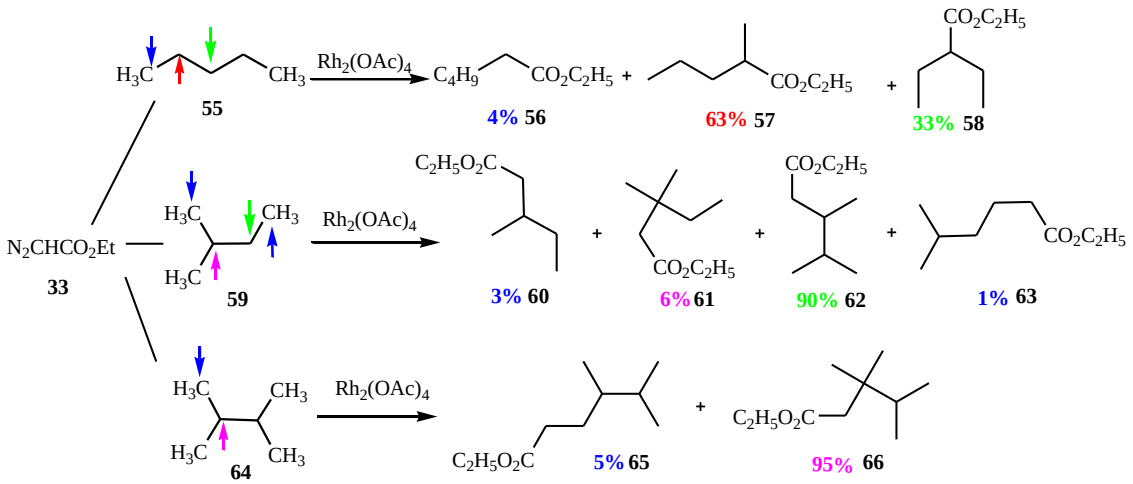

Scheme 17 The reaction of ethyl diazoacetate 33 with alkanes 55, 59 and 64 in the presence of dirhodium(II) tetraacetate.

The carbene intermediates generated from these transition metals are not in the free carbene state, but the carbenes are coordinated to the transition metal and are often referred to as metallocarbenes or carbenoids, which are usually represented by a ligand, L, containing a formal metal–carbon double bond. Transition metal carbenes possess the same electron deficient nature as free carbenes and can undergo the same types of chemical reactions, but in a more selective manner.

1.5.2 The Bamford–Stevens reaction

Diazo compounds which are unstable and low molecular weight are often better used as precursors for carbene generation.[90] For example, the simplest way of preparing diazo precursors is from hydrazines[90] (formed from ketones) in the presence of oxidants such as mercury(II) oxide (HgO),[90] or lead(IV) acetate ($Pb(C_2H_3O_2)_4$).[90,91]

The most widely used carbene precursors are tosylhydrazones which can be prepared readily from aldehydes or ketones by reaction with 4-toluenesulfonyl hydrazide.[92] The tosylhydrazone, **67**, on removal of the acidic –NH proton with a base such as sodium methoxide or sodium hydride, gives the tosyl hydrazine sodium salt **68**, which can be isolated.[93] The tosyl hydrazine sodium salt, under photochemical or thermal conditions, generates the carbene intermediate, **69** as shown below (Scheme 18).[94]

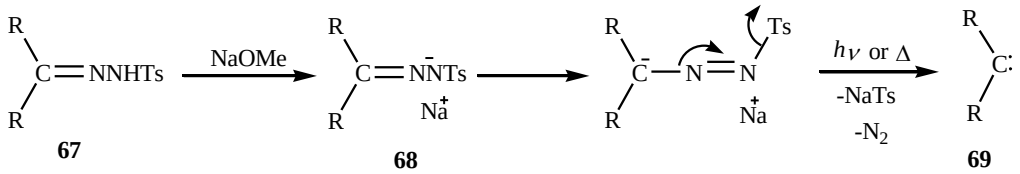

Scheme 18 Bamford–Stevens reaction: formation of carbenes 69 from tosylhydrazones 67.

1.5.3 Carbene generation via Ketenes

Diphenylketene **70** was the first ketene prepared[95] and characterised by Hermann Staudinger in 1905.[95] The preparation involved the reaction of 2–chlorodiphenylacetyl chloride **71** with zinc (Scheme 19).

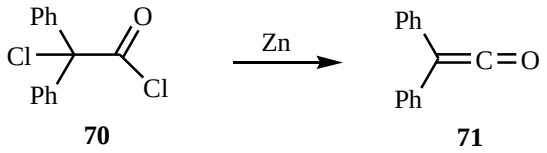

Scheme 19 Diphenylketene 71 formation from 2–chlorodiphenylacetyl chloride 70 in the presence of zinc.

Diphenylketene **71** undergoes thermolysis with loss of –CO to form diphenyl carbene **72**, which then cyclises forming fluorene **73** (Scheme 20).[95]

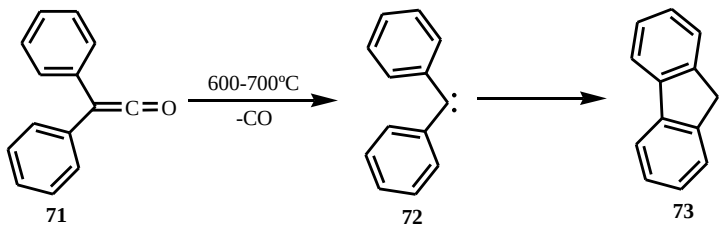

Scheme 20 Diphenylketene cyclisation to form fluorene.

Ketenes, however, are not readily available precursors and they can easily polymerise under the reaction conditions, so are not common precursors for carbenes.

1.5.4 Generation of carbenes from ylides

Ylides[96] are species that consist mainly of a positively charged heteroatom (e.g. X^+ = N, P, S or SO) linked to a carbon atom possessing unpaired electrons.

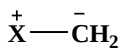

Phosphonium, sulfonium and sulfoxonium ylides
e.g. X = Ph_3P, Me_2S and Me_2SO respectively

Ylides can undergo useful synthetic transformations[97] where they can react in a similar manner to diazo compounds.

Phosphorus and sulfur ylides are well-known reagents in synthetic chemistry and they can react with carbonyl compounds to form alkenes (the Wittig reaction) and epoxides, respectively; while, reaction of the carbene with a second mole of ylide will produce dibenzoylethylene **76**, which can subsequently combine with either **74** or **75** to produce cyclopropane **77**.[96]

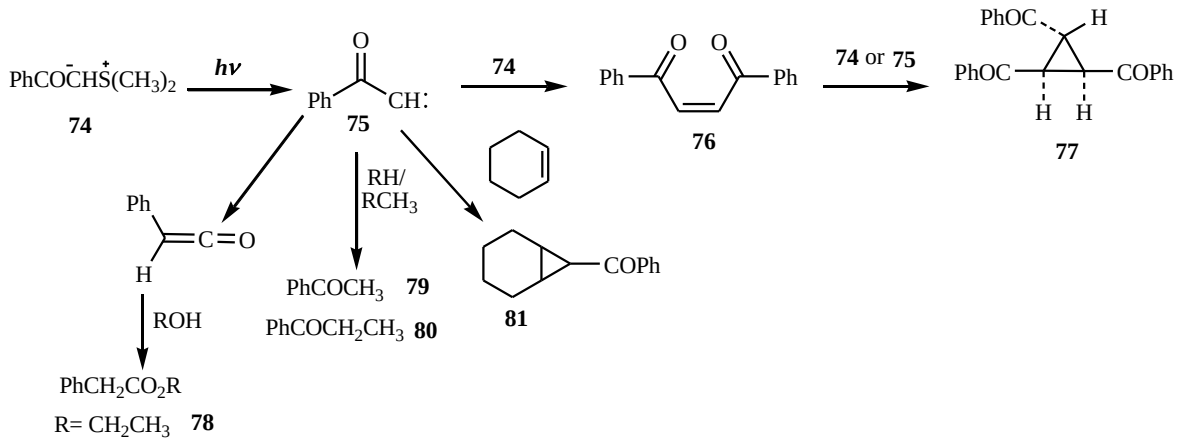

Scheme 21 Photolysis of a sulfur ylide forming cyclopropanes through a carbene intermediate 75.

Photolysis of ylide **74** in the presence of an alcohol and cyclohexene produced the bicyclic cyclopropane **81**, confirming that the reaction was proceeding via carbene intermediate **75**. Irradiation in ethanol gave an approximately 48% yields of three volatile products and 40-45% yield of **78**. The volatile materials were recognised as ethyl phenylacetate **78**, acetophenone **79** and propiophenone **80** (Scheme 21).[96]

1.5.5 Generation of carbenes from epoxides and cyclopropanes

The three membered rings of epoxides and cyclopropanes have steric strain and a high ground state energy, e.g. epoxide **82** can decompose to give carbene intermediate **83** simply on photolysis or heating with formation of the thermodynamically stable fragment, benzaldehyde **84** (Scheme 22).[98]

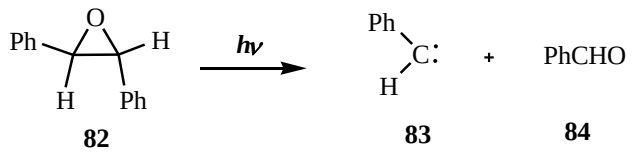

Scheme 22 Carbene generation from an epoxide 82.

Synthesis of an arylcarbene from an epoxide is rarely used.[99] Similarly, the products **86** and **87** formed from cyclopropane **85** decomposition are the reverse of the formation of cyclopropane from carbene and alkene (Scheme 23).[96]

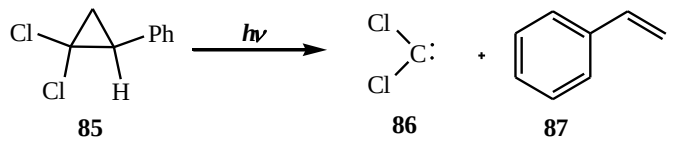

Scheme 23 Carbene generation from cyclopropane 85.

1.5.6 Generation of carbenes from heterocyclic compounds

On irradiation or heating, five membered heterocyclic compounds,[100] decompose to carbenes,[101] e.g. carbene **89**, can be formed by extrusion of thermodynamically stable fragments like ester **90**. For example 1,5-dihydro-1,3,4-oxadiazoles **88** decompose at about

80ºC with loss of dinitrogen followed by the carbonyl fragment to give carbenes **89** (Scheme 24).

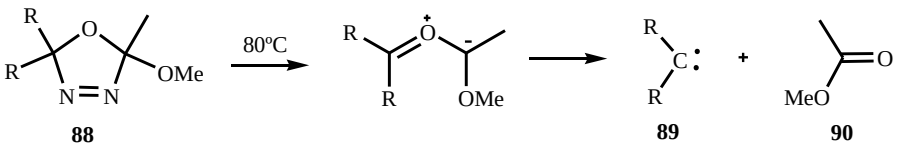

Scheme 24 Decomposition of five–membered heterocyclic compounds 88 to carbenes 89.

1.5.7 Generation of carbenes by α-elimination

α-Elimination is one of the most important routes for generating carbenes. In the early 1950s, Hine and co-workers[102] investigated the mechanism of the hydrolysis of chloroform **91** under basic conditions, with the formation of carbon monoxide **95** and formate **96** as side products. Kinetic studies showed the mechanism for carbene formation involves the rapid formation of the stabilised dichloromethyl anion **93**, then the rate determining loss of chloride by *α*-elimination (Scheme 25), followed by trapping of the carbene by the aqueous solvent to give the hydroxy carbene **94**, which eliminates to **95** and **96**.

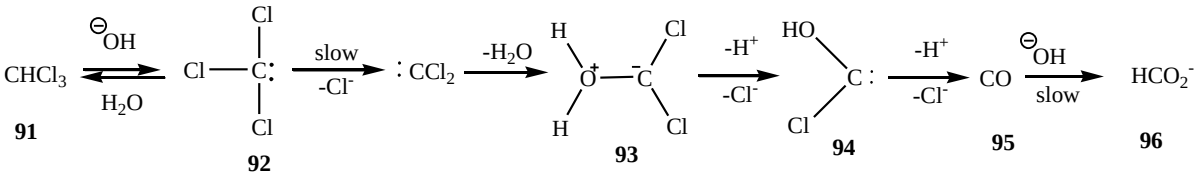

Scheme 25 Generation of carbenes by an *α*-elimination reaction.

1.5.8 Stereochemistry of catalytic carbene insertion reactions and examples

In synthetic chemistry, a general method for making carbocycles and heterocycles is by metal-catalysed decomposition of α–diazocarbonyl compounds[103] forming a new carbon-carbon bond which relates directly to the level of site-(regio) selectivity in the carbon-hydrogen insertion reactions.[104]

For example, the diazo ketone **97**, catalysed by dirhodium(II) tetraacetate, undergoes efficient cyclisation since the methylene C-H and carbenoid centre were in close proximity, so producing cyclopentanone **98** (Scheme 26).[104]

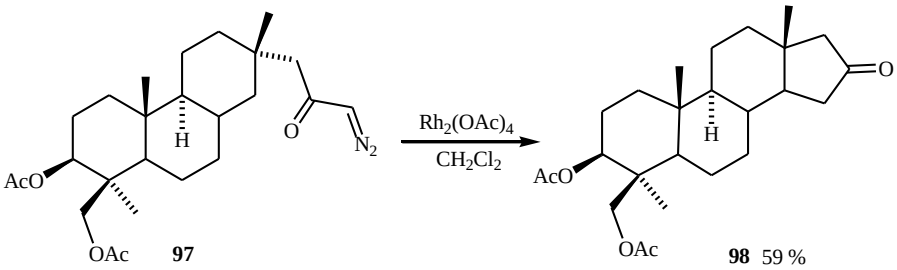

Scheme 26 Dirhodium(II) tetraacetate catalysed C-H insertion in steroid synthesis.[104]

Taber,[105] has shown the high yield formation of cyclopentanes from long chain diazo ketones catalysed by dirhodium(II) tetraacetate and this author also described the reactivity order of insertions to be: 3° C -H > 2° C-H > 1° C-H (Scheme 27).

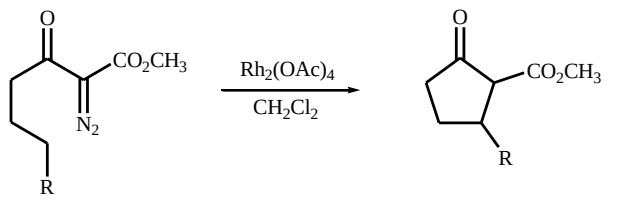

99 R= n-C_8H_{17}
101 R= $CH(CH_3)_2$
103 R= CH_2CH_3

100 R= n-C_8H_{17}, 68 %
102 R= $CH(CH_3)_2$, 55 %
104 R= CH_2CH_3 , 48 %

Scheme 27 Dirhodium(II) tetraacetate catalysed synthesis of cyclopentanes.

In a similar way, Stork showed that the regioselectivity of cyclopentane formation can be modified by the electronic effects of both electron withdrawing (EWG) and electron donating (EDG) groups in a molecule (Scheme 28).[83,106]

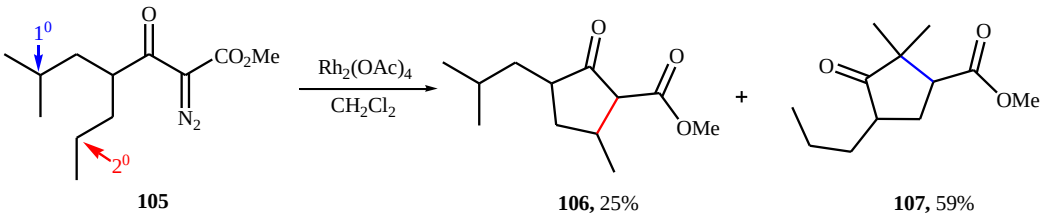

Scheme 28 Conversion of *α*-diazocarbonyl ester 105 to cyclopentanone 107.

In 1982, Doyle,[107] explained that the reactivity of chemically inequivalent C-H bonds equidistant from the diazo group (from which a carbene is generated) of *α*-diazoesters will produce different isomeric ratios with the stereoselectivity depending on steric, conformational and electronic factors in the molecule (Figure 9).

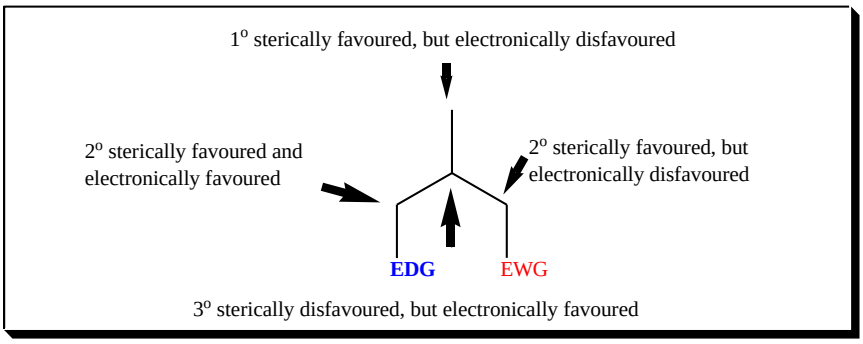

Figure 9 Steric and electronic effects with electron withdrawing and electron donating groups present on the molecule.[107]

In the chemo- and regio-selectivity of the insertion reactions the metal-carbene electrophilicity is one of the most important features. Apart from the catalyst, substituent

change on the carbene carbon is an alternative way of altering the electronic character of the intermediate. For example, the less electron withdrawing groups tend to make diazo compounds more unreactive to metal-carbene formation, even though once formed the intermediate exhibits an increased stability and selectivity (Figure 10)[105,106]

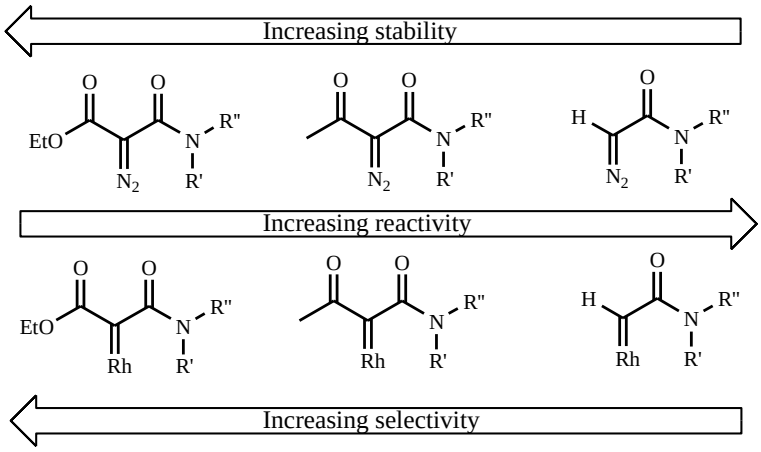

Figure 10 Stability and selectivity in the presence of electron withdrawing groups.[105,108]

In a similar manner, intramolecular bond formation in α-diazoacetamides has also shown various electronic and conformational effects (Scheme 29).

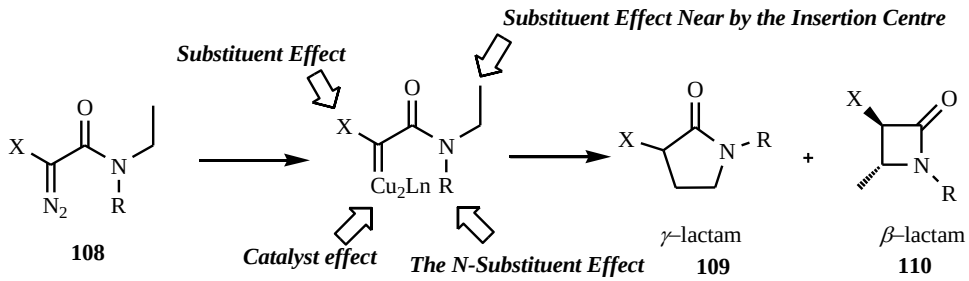

Scheme 29 General scheme for β-lactam 110 and γ-lactam 109 formation from α-diazoacetamides 108.

One of the most important factors in determining the chemo- and regio-selectivity in the intramolecular insertion reactions of α-diazoacetamide is the α-substituent,[109] which controls the electrophilicity of the metal carbene intermediate. Thus, a weaker electron withdrawing

group adjacent to the diazo group makes the molecule less reactive towards metal-carbene formation.[110] For example, when dirhodium(II) tetraacetate is used as catalyst with *N*-benzyl-*N*-*tert*-butyldiazoacetoacetamide **111** (R=CH_3CO), which has a (more stable) *α*-substituent, it afforded the *trans*-*β*-lactam **112** exclusively,[108] whereas carbene addition to the aromatic ring **113** was the only product observed when the deacylated substrate **111** (R=H) (less stable) was treated with $Rh_2(OAc)_4$ (Scheme 30).

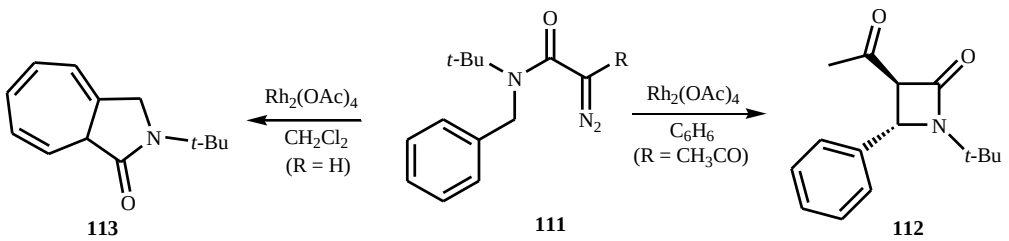

Scheme 30 Effect of the *α*-substituent on product selectivity in the presence of a dirhodium tetraacetate.

Studies reported in the literature[109] on a sequence of diazoacetamides with different substituents on the carbene carbon atom emphasise the *α*-substituent influence on the regioselectivity.[109] Higher selectivity towards *γ*-lactam **119** formation was obtained when less electron-withdrawing substituents were attached to the carbene carbon atom **117** (Scheme 31).

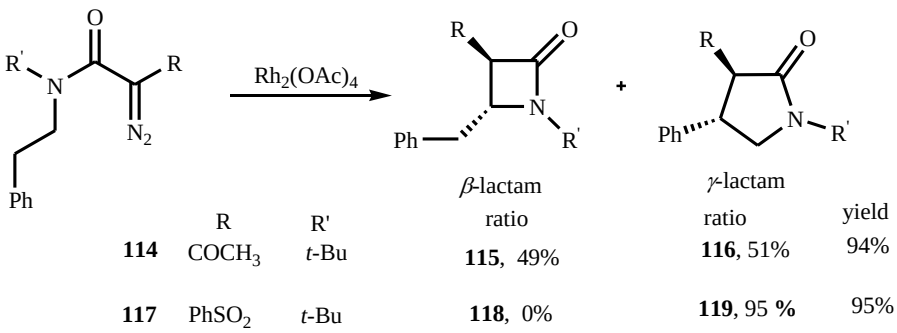

Scheme 31 *α*-Diazoacetamides forming *β*-lactam and a *γ*-lactam in the presence of dirhodium tetraacetate.[108]

Since the benzene sulfonyl group is less electron-withdrawing than its carbonyl counterpart, which stabilises the electrophilic carbenoid carbon, thereby causing the insertion reaction to proceed through a relatively late transition state with the $PhSO_2$ substituent **117**, thus forming the *γ*-lactam ring **119** exclusively.

Nonetheless, as Jung et al.,[111] and Afonso et al.,[112] have rationalised on the basis of the existing literature,[104] the enhanced regioselectivity observed for both *α*-diazoacetamides (R = $COCH_3$, R' = *t*-Bu and R = CO_2CH_3, R' = PMP (*p*-methoxyphenyl)) result from a combination of conformational and stereoelectronic effects (Scheme 32). The carbene electrophilicity appears to be of pivotal importance; presumably because the –C-H insertion proceeds via a later transition state due to the extra stabilisation added by the phenylsulfonyl and phosphoryl moieties, which are not as electron-withdrawing as their carbonyl counterpart in *α*-diazoacetamide.

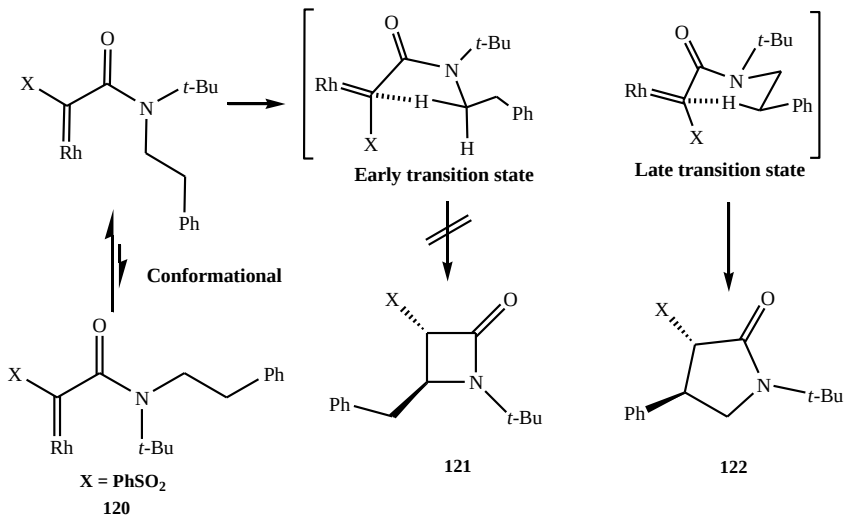

Scheme 32 Favoured transition state forming *γ*-lactam 122.

Scheme 33 shows the *N*-substituent effect, which has a greater influence on the chemo-, regio- and stereo-selectivity[111] of the -C-H insertion processes than electronic factors,[104] for example cyclisation of *α*-diazoacetamide **123** gives a 81 : 19 mixture of *γ*- and *β*-lactams **124**,

125, despite the fact that the *β*-lactam results from the insertion into a more activated C-H bond.

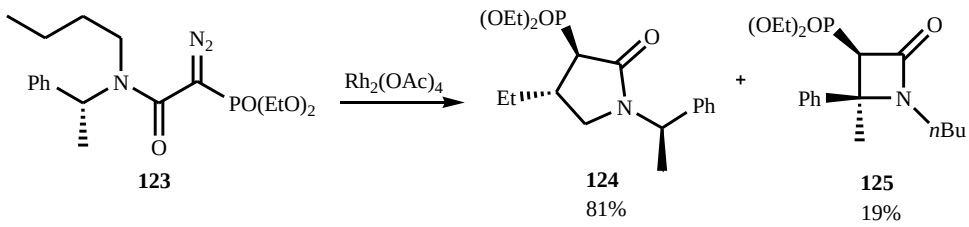

Scheme 33 The effect of the *N*-substituent on the insertion reaction in the presence of dirhodium tetraacetate.

1.5.9 Stereochemistry of catalytic carbene addition reactions

In carbene addition reactions, the stereochemistry depends mainly on whether the addition to alkenes occurs via singlet or triplet spin state carbenes. The orbitals involved in the cyclisation are shown in Figure 11.

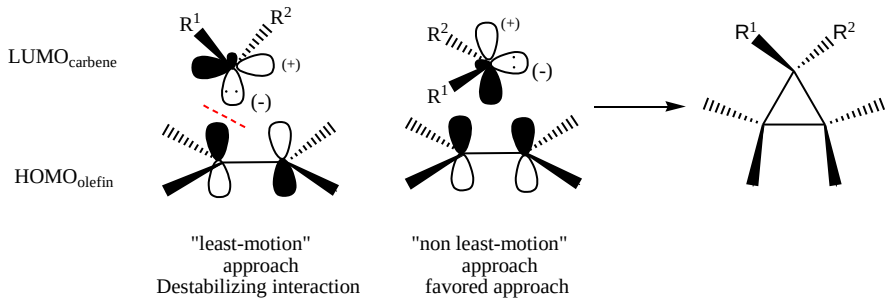

Figure 11 Proposed intermediates of $HOMO_{olefin}$ and $LUMO_{carbene}$ molecular orbitals involved in the determination of the stereochemistry of addition of triplet carbenes to alkenes.

Alkenes react with singlet carbenes in a concerted fashion with retention of the alkene stereochemistry in the cyclopropane products.[113,114] Singlet carbenes react with olefins

through a concerted transition state involving the empty carbene *p*-orbital with the filled π-orbital of the double bond. The "non least motion" approach leads to a favourable molecular orbital interaction between $LUMO_{carbene}$ and $HOMO_{olefin}$ (The "least motion" approach leads to destabilising MO interaction).

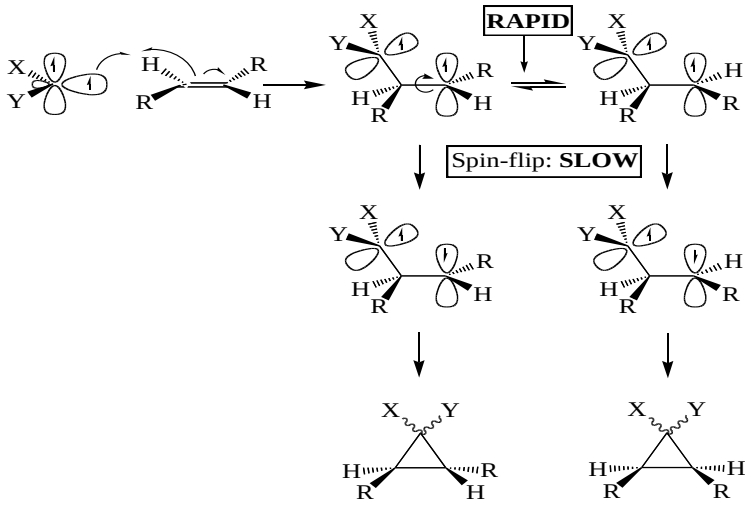

Figure 12 Proposed diradical intermediates involved in the determination of the stereochemistry of addition of triplet carbenes to alkenes.

In contrast, alkenes react with triplet (i.e. diradical) carbenes in a stepwise fashion resulting in the loss of alkene stereochemistry in the cyclopropane product (Figure 12).[115] In 1966 Nozaki and co-workers[116] described the asymmetric catalytic[93] decomposition of ethyl diazoacetate in alkenes as solvent/reactant using a soluble chiral copper(II) complex **126** to give optically active cyclopropanes **127** and **128** with small enantiomeric excesses (Scheme 34); the intermediate being a chiral carbene-copper complex.[117]

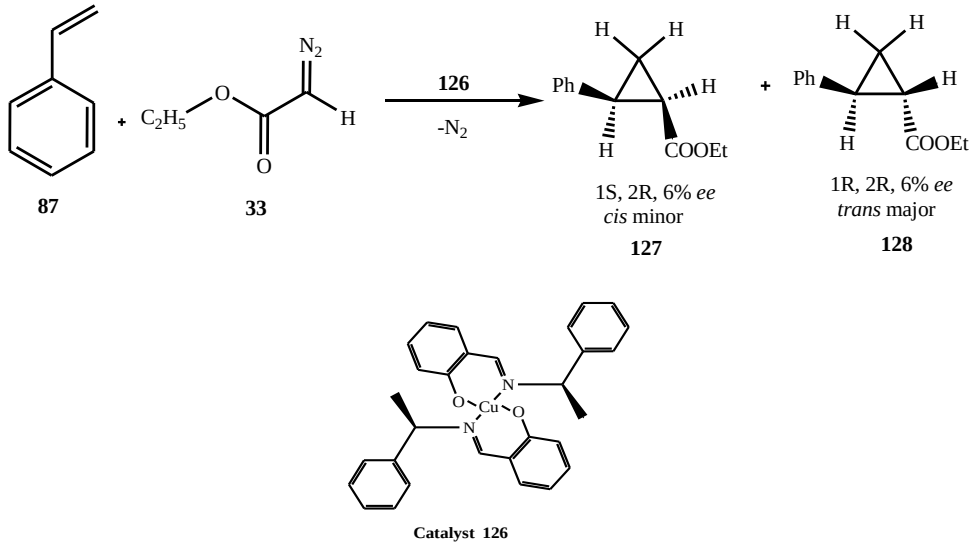

Scheme 34 Asymmetric catalytic decomposition of ethyl diazoacetate 33 with styrene 87 in the presence of chiral copper(II) complex.

This showed the possibility that both yield and selectivity can be improved by using suitable ligands, an excess of styrene to diazoacetate and by slow addition of the diazoacetate. Using lower concentrations of alkenes or a faster addition rate of the diazoacetate leads to increased formation of carbene dimers (diethyl fumarate and diethyl maleate).

The other example for cyclopropane formation is by reacting alkenes with diazoacetate **33** by using metal organic framework (MOF)[117] materials that contain either copper [$Cu_3(BTC)_2$] or gold IRMOF-3-Si-Au centres with diazoacetate (IRMOF: Isoreticular Metal Organic Framework). This is the first example using MOF materials to induce a carbene transfer reaction from a diazo compound (Scheme 35).

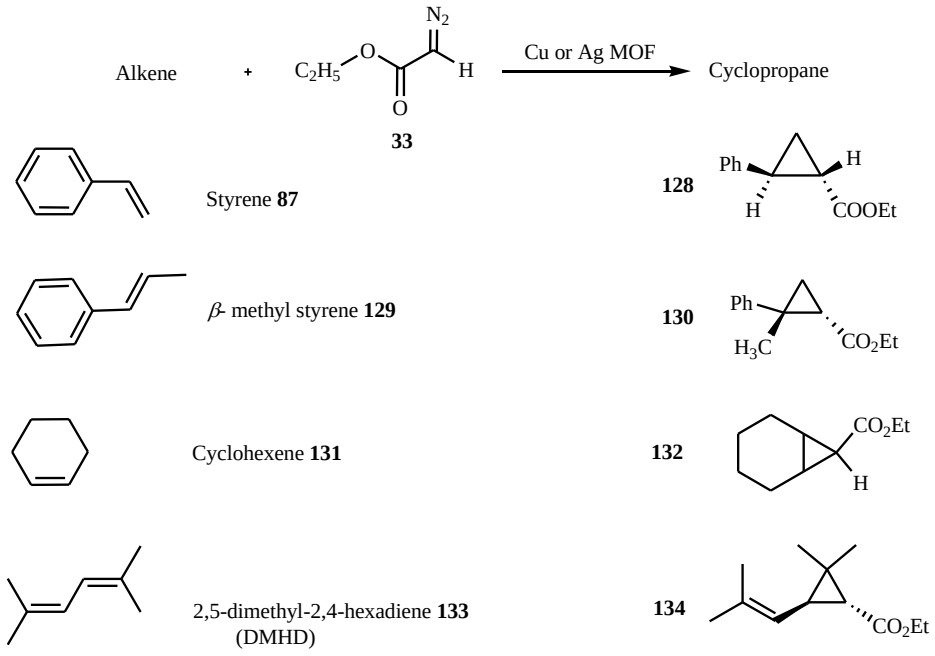

Scheme 35 MOF materials containing either Cu or Au centers used as catalysts for the cyclopropanation of alkenes with ethyl diazoacetate.

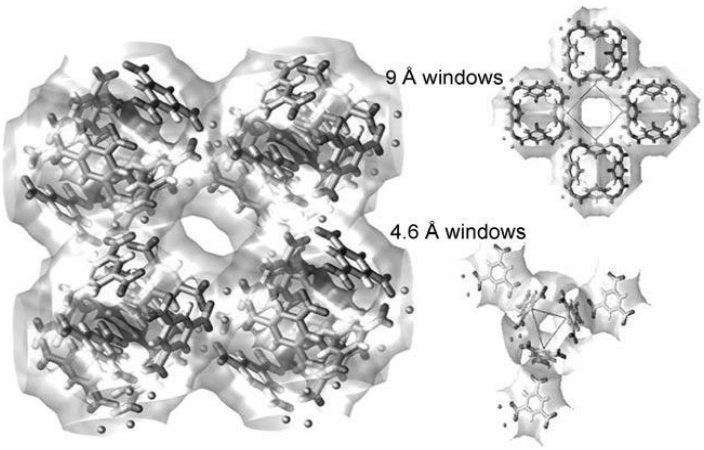

Figure 13 Crystal structure of the [$Cu_3(BTC)_2$] MOF.[117]

Figure 13 shows the typical structure of a MOF material; the (BTC = benzene-1,3,5-tricarboxylate) structure comprises two types of "cage" and two types of "window" that separate these cages. 9 Å windows with a square cross-section interconnect the large cages

and these cages are also connected to tetrahedral-shaped pockets of approximately 6 Å through triangular-shaped windows of approximately 4.6 Å.

By using $Cu_3(BTC)_2$ as catalyst, styrene **87** was converted almost completely into cyclopropanecarboxylate with high yield (98%) and *ca.* 70% *trans*-selectivity. The selectivities for a cyclic olefin (cyclohexene **131**) and a terminal alkene (DMHD **133**) were found to be very high (*ca*. 100%), but with low yield (60%) compared to styrene for the DMHD. However, when using IRMOF-3-Si-Au solid catalyst at room temperature, conversions of up to 42% were obtained for the cyclopropanation of styrene with EDA; this MOF was also an active catalyst for the cyclopropanation of a variety of alkenes with EDA (Table 3). It appears that gold-containing MOFs can also be an interesting solid catalyst for cyclopropanation reactions, although the activity is lower than for the copper containing MOF. Thus activity of the catalyst appears to be due to mainly:

1. The availability of significant numbers of accessible sites due to the open MOF crystal structure (Figure 13).
2. The reversible coordination of organic linkers with the metal atom and
3. The influence of the electrostatic field in the cavity by the partially charged framework.

Table 3 Cyclopropanation of alkenes with a [$Cu_3(BTC)_2$] and IRMOF-3-Si-Au based catalysts with EDA.

	[$Cu_3(BTC)_2$]		IRMOF-3-Si-Au	
Alkenes	Yield [%][a]	d.r [%][b]	Yield	d.r [%][b]
Styrene **87**	98	71	42	54
β-methyl styrene **129**	50	67	40	59
Cyclohexene **131**	99	98	50	100
DMHD **133**	60	100	25	100

[a] Yield of cyclopropane; the remaining diazo compound was converted into coupling products.

[b] Diastereomeric ratio: *trans*/*cis*.

These materials have been shown to be good heterogeneous catalysts with good yields and very high chemo- and diastereo-selectivities (Table 3) which is due to the high surface area inside their pores and their tunable structures (Scheme 35).

1.6 Nitrenes

Nitrenes are six electron, neutral, monovalent, highly reactive nitrogen intermediates and were first suggested by Tiemann in 1891[118] as intermediates in the Lossen rearrangement[119,120] and subsequently adopted by Curtius to explain various reactions of azides.[120] The chemistry of nitrenes closely parallel that of the carbenes in virtually all respects. Like carbenes, nitrenes can also have two spin states depending on whether the two non-bonding electrons have their spins paired (singlet) or parallel (triplet) (Figure 14).

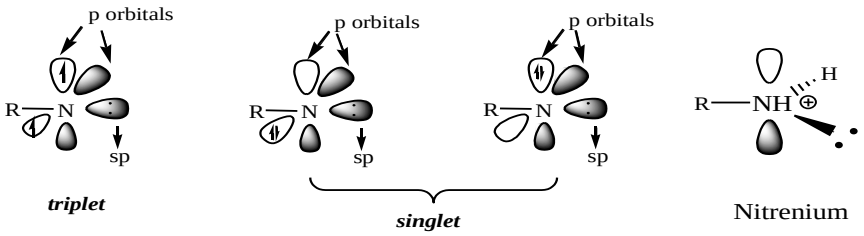

Figure 14 Hybrid structures of nitrene molecule.

1.6.1 Generation of nitrenes

Nitrenes can be generated by methods that parallel those used for carbene generation, for example, from: azides (c.f. diazoalkanes), isocyanates (c.f. ketenes), ylides and by α-elimination from certain heterocycles.[121,122]

1.6.1.1 From azides

The most widely used precursors for nitrene generation are azides. They are similar to diazo compounds as they have a linear 1,3–dipolar structure (Scheme 36)[122] and can be prepared readily by introduction of the N_3^- ion from inorganic salts such as sodium azide.[121]

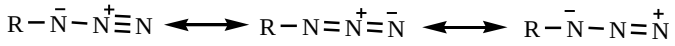

137

Scheme 36 1,3–Dipolar nature of azides.

The thermal stability of the azides depends upon the substituent on the nitrogen. The loss of nitrogen in azide reactions is rate determining being largely interdependent of the nature of the solvent and the concentration of any other compounds present.[123] Whereas most azides decompose thermally in the 100-200ºC range, some are much less stable, particularly those in which the loss of nitrogen can be assisted in some way (Scheme 37).[123]

In some reactions, nitrenes are not involved in product formation, for example in the facile formation of anthranils **139** from *ortho*–azido aromatic ketones **138**,[124] the reaction proceeds by an electrocyclisation followed by loss of nitrogen.[125,126]

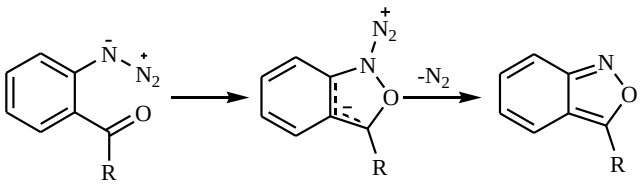

138 **139**

Scheme 37 Decomposition of an *ortho*–substituted aromatic azide 138.

1.6.1.2 Via isocyanate-type molecules

The formation of nitrenes by elimination of –CO to form aryl isocyanates on heating would be analogous to the high temperature formation of carbenes from ketenes and once again an unfeasible synthetic method since the process is energetically unfavourable.[127] The related N-thionylaniline **141** (Ar–N=S=O), which can be prepared readily from anilines **140** and

thionyl chloride, decompose much more readily to nitrenes **142** thermally with extrusion of (-SO) (Scheme 38).[127]

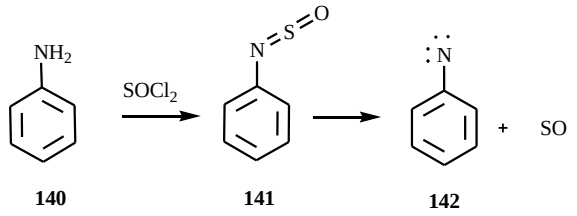

Scheme 38 Formation of an aryl nitrene from a N-thionylaniline.

1.6.1.3 From ylides

The phosphorus and sulfur ylides of nitrogen are known as iminophosphoranes and iminosulfuranes (sulfimides) respectively.[128] Nitrenes can be generated from both of these ylides by irradiation. For example, photolysis of the *S*,*S*–dimethyl sulfimide derived from *N*–phenylbenzamidine **143** (X = SMe_2) gives a high yield of 2–phenylbenzimidazole **148** which proceeds through cyclisation of an intermediate imidoylnitrene **147**, forming an aromatic ring.[129] Thermolysis of the corresponding nitrogen–nitrogen ylide **144** (X = NMe_3), (an aminimide) gives the same product (Scheme 39), as does photolysis of 1,5–diphenyltetrazole **145** and 3,4–diphenyl–1,2,4–oxadiazol–5–one **146**,[130] strongly suggestive of a common nitrene intermediate **147**.

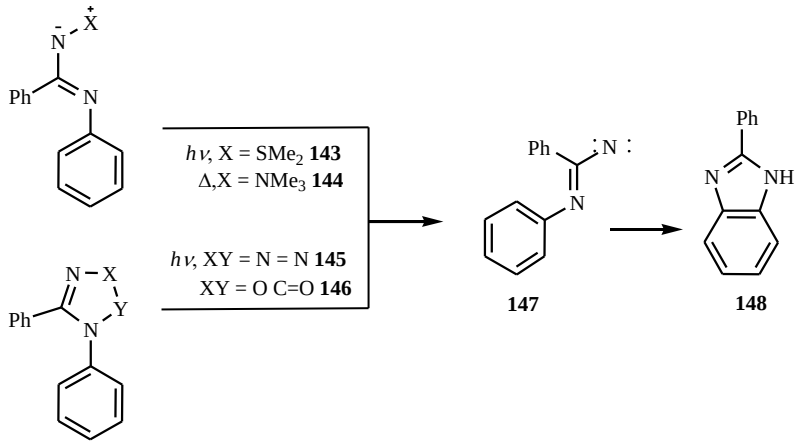

Scheme 39 Cyclisation of imidoylnitrene generated from different precursors.

1.6.2 Nitrene formation from various heterocycles

Five–membered heterocyclic rings, including those with aromatic stabilisation, which are able to undergo fragmentation with extrusion of carbon dioxide (–CO_2) or nitrogen (–N_2) from the five-membered heterocyclic rings, can decompose readily to give nitrenes on irradiation or vapour phase thermolysis, e.g. 1,4,2–dioxazol–5–ones **149** (Scheme 40) lose carbon dioxide on heating or irradiation to form acylnitrenes **150**. Other examples involving tetrazoles[131] or an oxadiazolone[120] are also known.

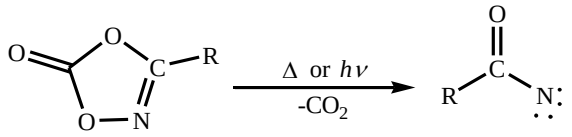

149 **150**

Scheme 40 Nitrene formation via decomposition of 1,4,2–dioxazol–5–ones.

Dibenzothiophene *N*-substituted sulfilimines **151** have the ability to act as photochemical nitrene sources in the presence of several trapping reagents, such as sulfides, olefins, or phosphorus compounds.[132] In these reactions, the corresponding imino–transfer compounds, namely sulfilimines **153**, aziridines **154** and iminophosphoranes **155**, were formed in good yields, indicating that dibenzothiophene *N*-tosyl and *N*-acyl sulfilimines can be good nitrene sources (Scheme 41).[132]

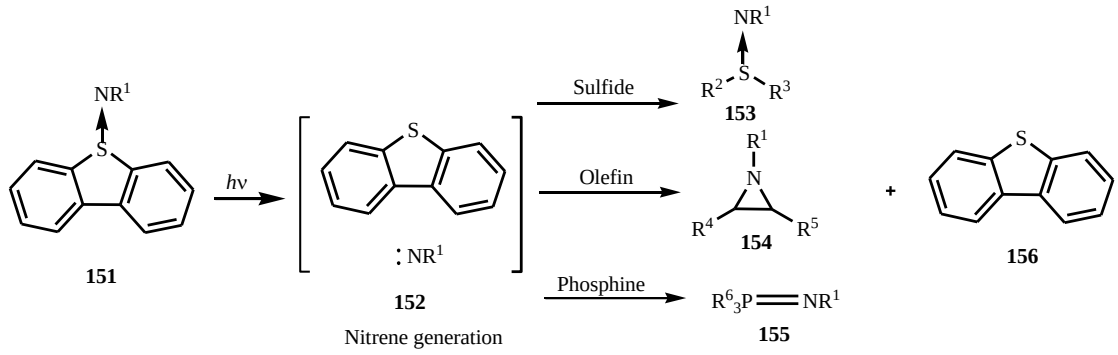

Scheme 41 Generation of nitrenes by the photolysis of *N*-substituted iminodibenzothiophene.

1.6.3 Nitrene formation by α-elimination

As in carbene chemistry, elimination reactions in nitrene chemistry are less significant in their synthetic usefulness. A few substrates, such as *N*,*O*–bis(trimethylsilyl)hydroxylamines **157** (Figure 15),[133] can undergo thermal *α*-elimination.

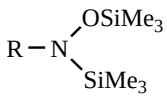

157

Figure 15 *N*,*O*-bis(trimethylsilyl)hydroxylamine.

More often than not, the reactions are base mediated and require a good leaving group on the nitrogen. Since *N*–halo compounds are often unstable and are prone to radical and ionic reactions, the most useful nitrene precursors of this type are *O*-arenesulfonylhydroxylamines ($RNHOSO_2Ar$); this type of reaction is best known for (ethoxycarbonyl)nitrene. By using an organic base such as triethylamine or under phase transfer conditions, *α*-elimination from $EtO_2CNHOSO_2Ar$ **158** appears to give a genuine nitrene intermediate **160**, as a similar

product distribution is obtained as with thermolysis or photolysis of $C_2H_5CO_2N_3$ **159** (Scheme 42).[134,135]

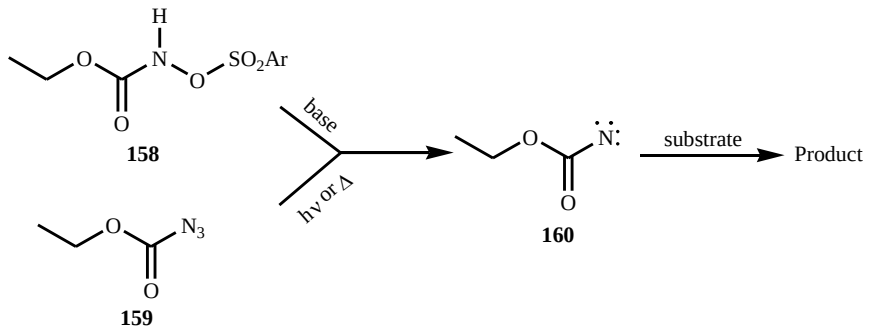

Scheme 42 Generation of (ethoxycarbonyl)nitrene 160 by *α*-elimination.

1.6.4 Stereochemistry of nitrene addition reactions

The chemistry of nitrenes closely parallels that of carbenes in virtually all aspects. Like carbenes, nitrenes may also consist of two spin states depending on whether the two non-bonding electrons have their spins paired or parallel.[136] The energy difference between the singlet and triplet states is usually much larger for nitrenes than for carbenes, being estimated at 145 kJ mol^{-1} for nitrene (–NH) itself compared with 32–42 kJ mol^{-1} for methylene ($-CH_2$).[137] In the most simple linear imidogen nitrene (:N-H), out of six available electrons two form a covalent bond with hydrogen, two of them form a free electron pair and the remaining two electrons occupy degenerate *p* orbitals. The low energy form of the imidogen, which is consistent with Hund's rule, is a triplet with one electron in each of the *p* orbitals and the high energy form is the singlet state with an electron pair filling one *p* orbital and the other one vacant. The main factor is that the nitrogen is more electronegative than carbon and therefore holds its electrons closer to the nucleus, which favours the singlet state. The nature of the substituents on the nitrogen will affect both the multiplicity and the normal electrophilic reactivity of nitrenes, thus strong π–donor substituents like amino groups stabilise the singlet state significantly causing the nitrene to exhibit nucleophilic character.[138] The stereochemistry of addition of nitrenes to alkenes to form aziridines

depends very strongly on whether the singlet or triplet states are involved (Figure 16). Singlet states tend to favour *cis*-addition, while triplet states require spin inversion to occur and this delay allows rotation giving both *cis*- and *trans*-addition.

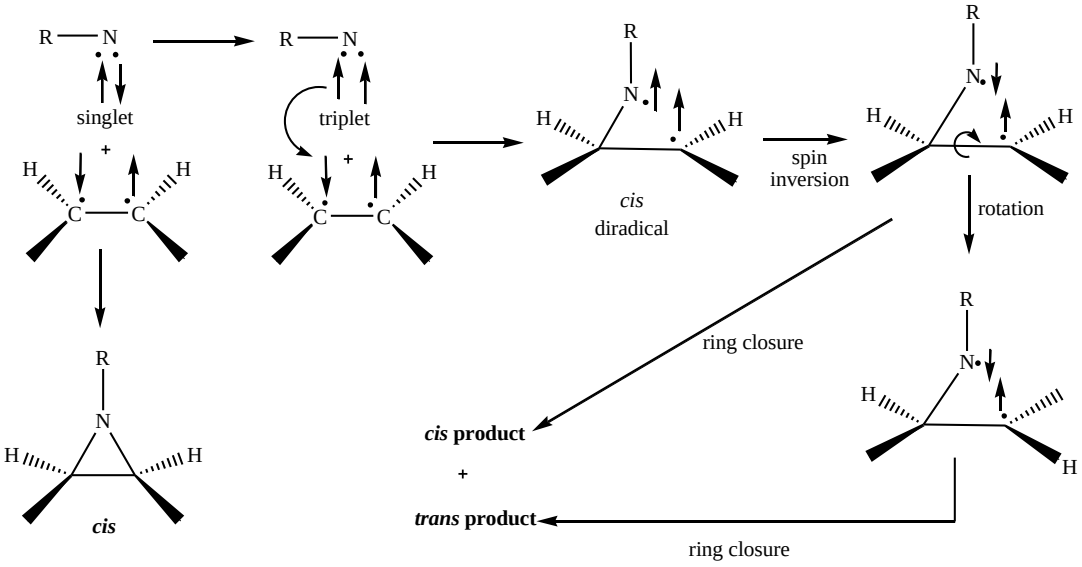

Figure 16 Stereochemistry of nitrene cycloaddition reactions.

Catalytic nitrene formation is useful in aziridine synthesis (Scheme 43). Aziridine **162** can be formed from phenylsulfonyl azide **161** and styrene **87** in the presence of the copper catalysts, copper(II) chloride or $Cu(acac)_2$, with 4A molecular sieves as a co-catalyst which also helps in the removal of water molecules to maintain dry reaction conditions.[139]

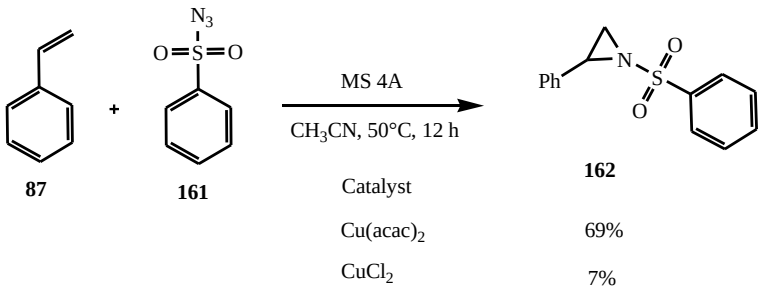

Scheme 43 Formation of aziridine by utilising copper catalysts $Cu(acac)_2$ and $CuCl_2$.

Aziridine **162** can be formed in the presence of the copper catalysts: copper chloride and $Cu(acac)_2$, using 4A molecular sieves as a co-catalyst for reacting phenylsulfonyl azide **161** with styrene **87**. Benzaldehyde was observed as a by-product in these aziridination reactions. Residual water in the reaction mixtures, added with the solvent could hydrolyse the nitrene donor to iodosylbenzene and this is most likely to provide the pathway for the benzaldehyde by-product formation. 4A Molecular sieves as a co-catalyst will help in reducing the formation of by-product by absorption of water molecules.

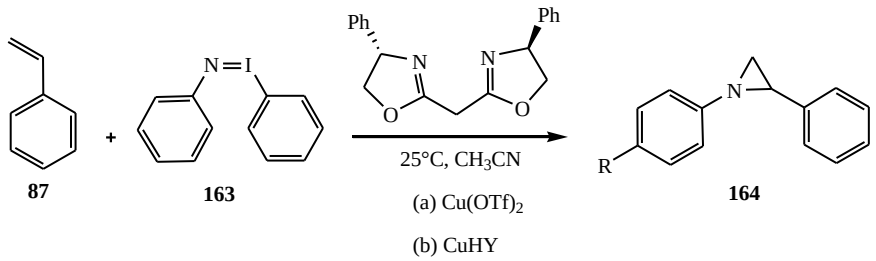

Scheme 44 Formation of aziridine by utilising copper catalyst ($Cu(OTf)_2$) and chiral ligand.

Similarly, formation of aziridine **164** in the presence of copper catalysts from styrene **87** with copper-exchanged zeolite Y (CuHY) or copper(II) triflate (trifluoromethanesulfonate) ($Cu(OTf)_2$ can be carried out using PhI=NTs **163** as nitrene donor (Scheme 44).[140]

The heterogeneous catalyst, CuHY, is found to give enhanced enantioselection for a range of bis(oxazolines) when compared to the homogeneous catalyst; the effect is considered to be due to the confinement of the catalyst within the micropores of the zeolite. With CuHY as heterogeneous catalyst high *ees* were obtained in acetonitrile solvent.

1.7 Project aims

We aim to control the regio- and stereo-control of products based on size selectivity when compared to free solution reactions by carrying them out in the restricted environments within clay minerals and zeolites.

Initially, we will examine the stereochemical consequences of carrying out the synthesis of:

i. *β*-lactam rings in compounds similar to penicillin antibiotics by intramolecular carbene insertion into C-H bonds.
ii. then cyclopropane rings for chrysanthemic acid related pesticides by carbene addition to alkenes.
iii. and finally aziridines via nitrene addition to alkenes.

In the literature[141,142] there are many examples of preparation of carbenes and nitrenes by photochemical, thermal and catalytic (using transition metal catalysts) methods. We will compare the stereochemical outcome of thermal, photochemical and catalytic reactions in free solution with catalysed (Cu^{2+}) reactions within the restricted environment of a clay mineral interlayer or a zeolite pore.

2 Chapter: Carbene Insertion Reactions

2.1 Introduction to carbene and carbene catalysed reactions

Carbenes are highly electron deficient since the carbene carbon has only 6 electrons in the valence shell, making the carbenes highly electrophilic species that can react with many σ– and π–bonds. Carbenes can be generated from diazoalkanes by thermal, photochemical and catalytic means.[143] Catalytic carbene formation processes are usually carried out with transition metal cations, e.g. Cu^{2+}, Rh^{2+} or Pd^{2+} and they tend to give enhanced selectivity and the opportunity for the thermodynamically more favoured product to predominate. It is our intention to generate the carbene intermediate within the restricted environment of either the interlamellar region of a clay mineral or the pore of a zeolite. The clay mineral or zeolite would first be exchanged with Cu^{2+} cations to provide the catalytic site and the carbene could then react to give a product that could be size selected.

Figure 17 illustrates the generation of carbene intermediates within the restricted environment of a clay interlayer or a zeolite pore. The reactive carbene could then react either intramolecularly or with another reactant present within the mineral or zeolite pore.

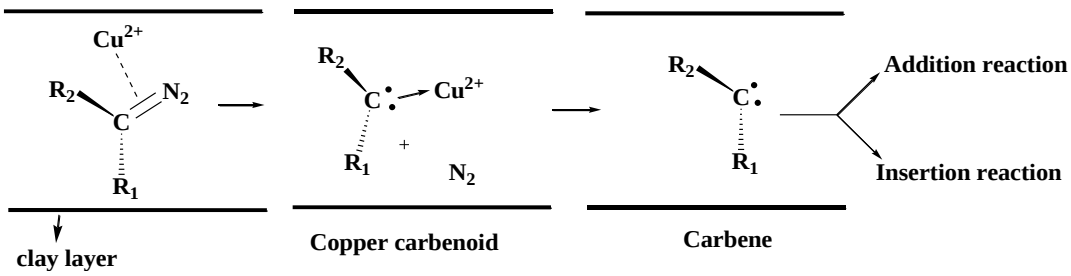

Figure 17 Possible mechanism for copper(II) catalysed carbene generation in clay minerals or zeolites.

There are two major classes of carbene reactions that were of immediate interest as they could provide size selection of isomers while producing compounds with potential bioactivity:

1. Intramolecular carbene insertion into C–H bonds – e.g. in the formation of ring systems such as *β*-lactams which are potential antibiotics (this Chapter).

2. Carbene addition across double bonds (–C = C–) to form cyclopropanes – e.g. synthesis of chrysanthemic acid derivatives which are potential insecticides (Chapter 3).

2.2 Synthesis of diazo ester amides

The methylene group of malonyl compounds can be converted readily to a diazo group by reaction with an azide and a base. Malonic acid half ester[144] derivatives are important intermediates for the synthesis of pharmaceuticals and natural products[145,146] and they can be converted to amides and then ultimately to β-lactams via the malonyl carbene derivative.

Methyl half ester **167** was synthesised from methyl malonate **165** by reacting with potassium hydroxide in methanol to give the half ester salt **166** (Scheme 45), which crystallised out. The salt **166** was converted to the half-ester **167** by reaction with 1M hydrochloric acid.[145] The benzyl half ester **169** was synthesised from malonic acid **168** and benzyl bromide, triethylamine as a base in acetonitrile under reflux (Scheme 45).[147]

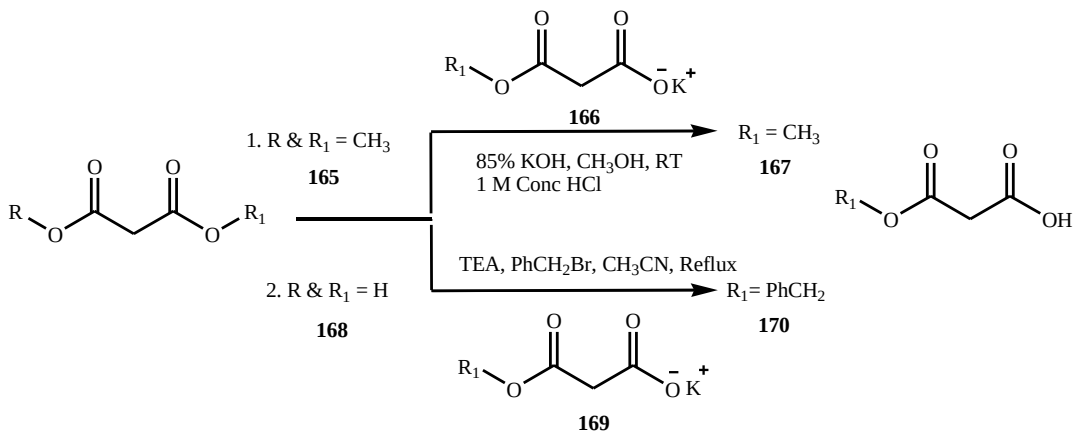

Scheme 45 General method for the preparation of half esters 167 and 170 from methyl malonate and malonic acid.

Then half esters **167**, **170** were converted to amides (Scheme 46) and then to diazo compounds, which were finally converted to *β*-lactams by carbene insertion reactions (Scheme 47).

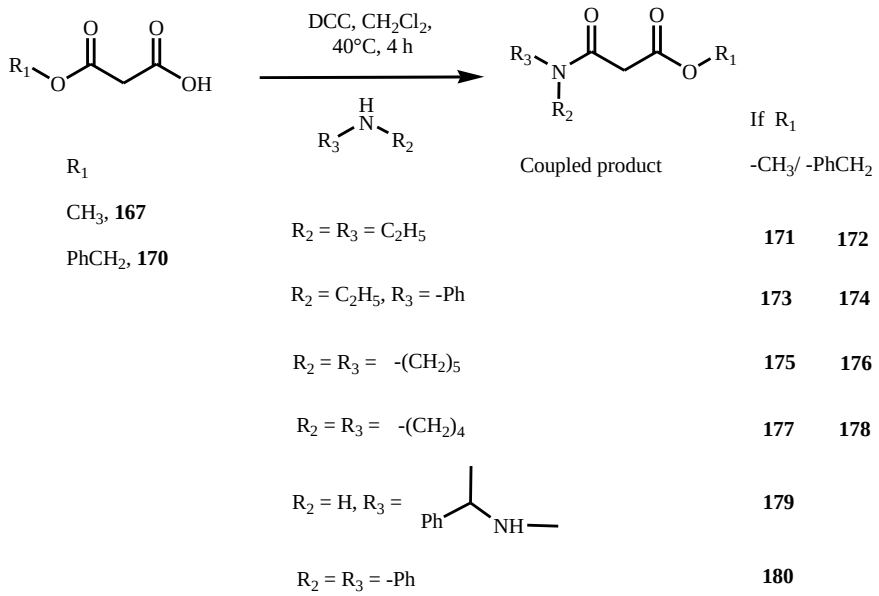

Scheme 46 Proposed synthetic route to coupled products

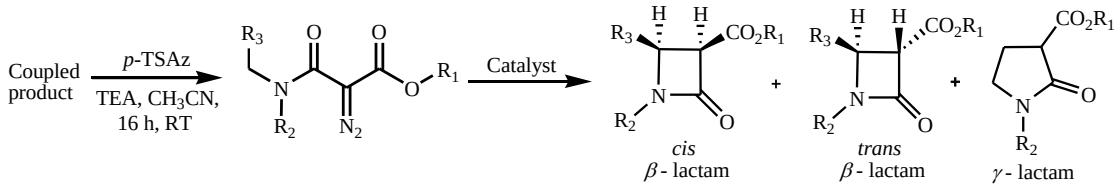

Scheme 47 Proposed synthetic route to *β*-lactams.

The monomethyl malonic acid **167** and monobenzyl malonic acid **170** were then coupled, using *N,N'*-dicyclohexylcarbodiimide (DCC), with a series of acylic (e.g. diethylamine or ethylphenylamine)[7,148] and cyclic aliphatic amines[149,150] (e.g. piperidine or pyrrolidine)[151] to form amides (e.g. See Scheme 46).[152,153] These amides were then reacted with diazo transfer reagent, initially 4-carboxybenzenesulfonyl azide, but subsequently, *p*-toluenesulfonyl azide (*p*-TSAz) **182** to form the dicarbonyl diazo intermediates needed for carbene formation (See Table 4).[7,151]

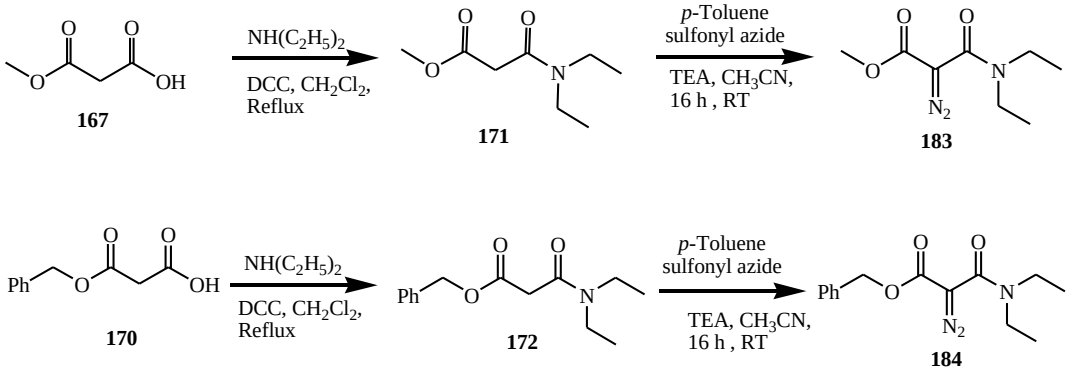

Scheme 48 Example synthesis of an *α*-diazocarbonyl compound.

Insertion of the diazo function at the methylene group flanked by the two carbonyls in the remaining malonyl amides was done in preference with *p*-toluenesulfonyl azide (Scheme 48), as initial reactions done with the more stable *p*-carboxybenzenesulfonyl azide as a diazo transfer reagent, gave separation problems and lower yields of < 50%, with the remaining material left as unreacted starting material and decomposition products. Furthermore, increasing the equivalents of base and heating for longer hours did not improve the yields. Reaction progress was monitored initially by TLC, then by loss of the azide peak at 2200 cm^{-1} in the IR spectrum and by the disappearance of the singlet peak at δ 3.34 in the ^{1}H-NMR spectrum, which corresponds to the methylene ($-CH_2$) flanked between the two carbonyl groups.

Even though, *p*-toluenesulfonyl azide is the more hazardous, with a higher impact sensitivity, lower decomposition initiation temperature and a larger heat of decomposition, it was chosen as the preferred diazo transfer reagent in later reactions as *p*-carboxybenzenesulfonyl azide is a much more expensive reagent that requires 2 moles of base per mole of substrate, which is not ideal for base sensitive substrates. The *p*-TSAz, was prepared in the laboratory by the literature method.[7] Use of *p*-TSAz in the reaction improved the yield to > 50% and also led to fewer separation problems compared to *p*-carboxybenzenesulfonyl azide.

Table 4 Malonyl amides and diazocarbonyl compounds synthesised.

Malonyl amides	Yield %	diazocarbonyl compounds	Yield %
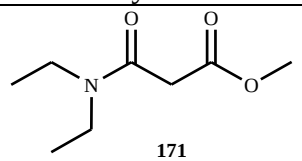 **171**	63	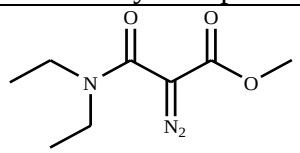 **183**	70
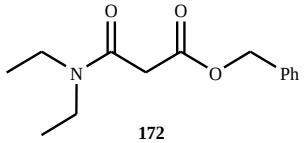 **172**	62	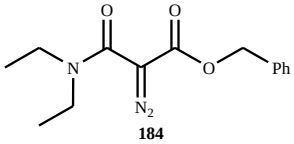 **184**	72
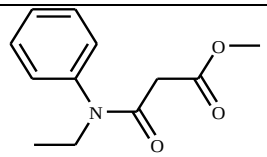 **173**	43	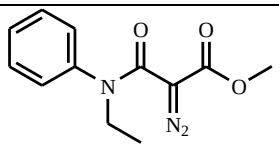 **185**	54
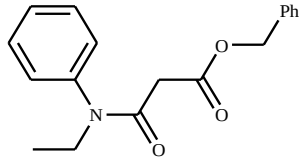 **174**	48	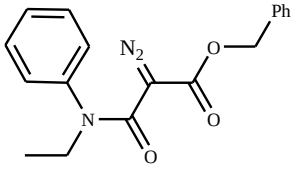 **186**	54
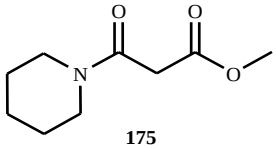 **175**	63	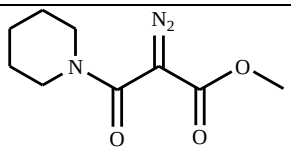 **187**	62
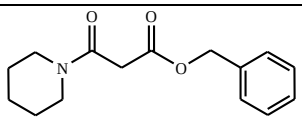 **176**	66	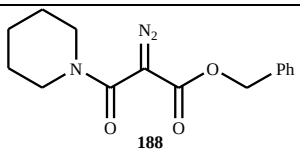 **188**	71
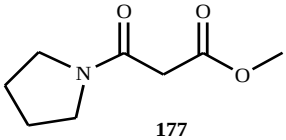 **177**	68	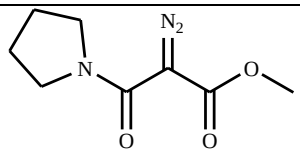 **189**	60
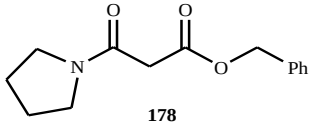 **178**	64	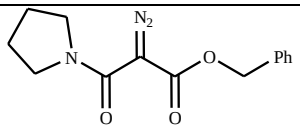 **190**	64
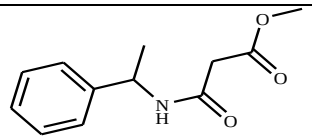 **179**	43	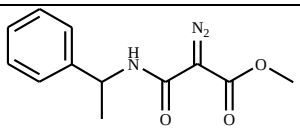 **191**	54
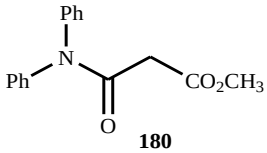 **180**	50	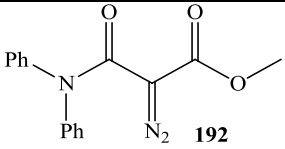 **192**	48

2.3 Catalysed carbene reactions of diazo ester amides

Our main aim was to catalyse novel organic syntheses by generating reactive carbene intermediates from diazoalkanes on Cu(II) cation exchanged within either the interlamellar region of a clay mineral or the pores of a zeolite catalyst. While a zeolite will present a fixed reaction space that can help control the regio- and stereo-chemical outcome of the ring closure reactions; the interlamellar distance of clay minerals can be manipulated, so helping to control a wider range of reactions compared to free solution, i.e. reactions via less bulky intermediates should be more favoured within these restricted regions within the clay minerals.

2.3.1 Reactions of methyl *N,N*-diethylamidodiazomalonate (methyl 2-diazo-2-(diethylcarbamoyl)acetate) 183

Carbene intermediates, formed from methyl *N,N*-diethylamidodiazomalonate **183** by thermal reaction and copper(II) sulfate, Cu(II) clay mineral or Cu(II) zeolite catalysed reactions, yielded a mixture of the *β*-lactam diastereomers **193** and **194** with small amounts of the *γ*-lactam **195** (Scheme 49).

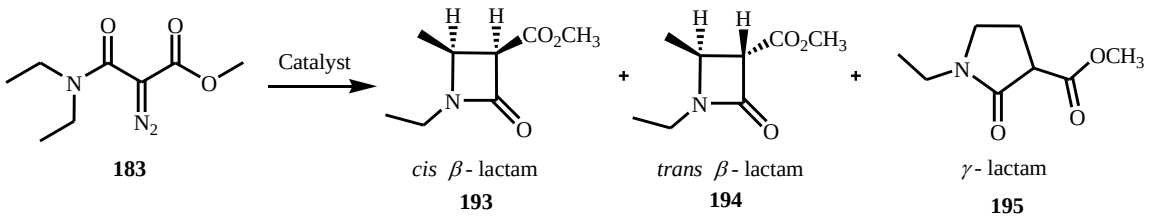

Scheme 49 Synthetic route to *β*-lactams 193 and 194 (39 : 61 ratio) and *γ*-lactam 195.

Intramolecular carbene insertion into an ethyl methylene C–H bond forms a new carbon–carbon (C–C) bond giving a *β*-lactam ring (Scheme 50):

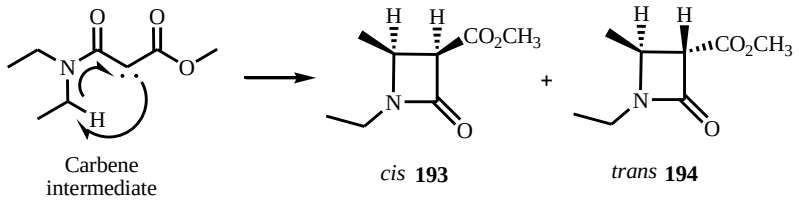

Scheme 50 Mechanism for the formation of *β*-lactam rings 193 and 194.

Another possibility is the intramolecular carbene insertion into the methyl C–H bond to form a new C–C bond giving a *γ*-lactam ring **195** (Scheme 51). This is obviously a less favoured route as only *ca*. 8% yield of this product was produced compared to *ca*. 70% of the *β*-lactams.[104]

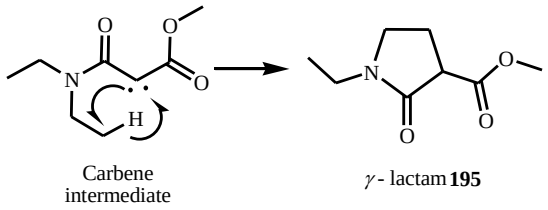

Scheme 51 Mechanism for the formation of the *γ*-lactam ring 195.

2.3.1.1 Assignment of the structures of the *β*-lactam isomers from methyl *N,N*-diethylamidodiazomalonate 183.

A sample containing a mixture of *cis*- and *trans*-diastereomers **193** and **194** and *γ*-lactam **195** was obtained by a reaction of the diazo ester **183** with Cu(II) cation exchanged Wyoming bentonite in benzonitrile or acetonitrile as solvents. These reaction conditions gave good yields of products, typically *ca*. 70% for these reactions and other diazo ester reactions and so were used generally for the product isomer identifications.

The *cis*- and *trans*-diastereomers **193** and **194** (39 : 61 ratio) were identified based on assignment of the ^{1}H-NMR (Figures 22 and 19), ^{13}C-NMR, ^{1}H-^{1}H 2D COSY and ^{1}H-^{1}H 2D NOESY (Figures 23 and 20) spectra of the partially purified *cis*- and *trans*-diastereomers **193** and **194**.

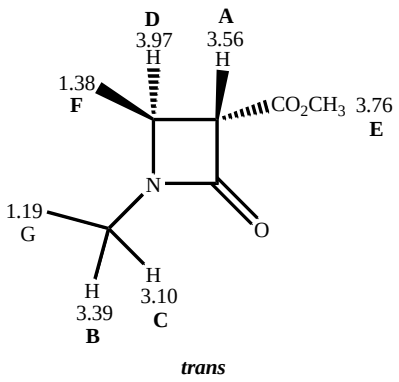

Figure 18 ^{1}H NMR assignments for the *trans*-*β*-lactam isomer 194.

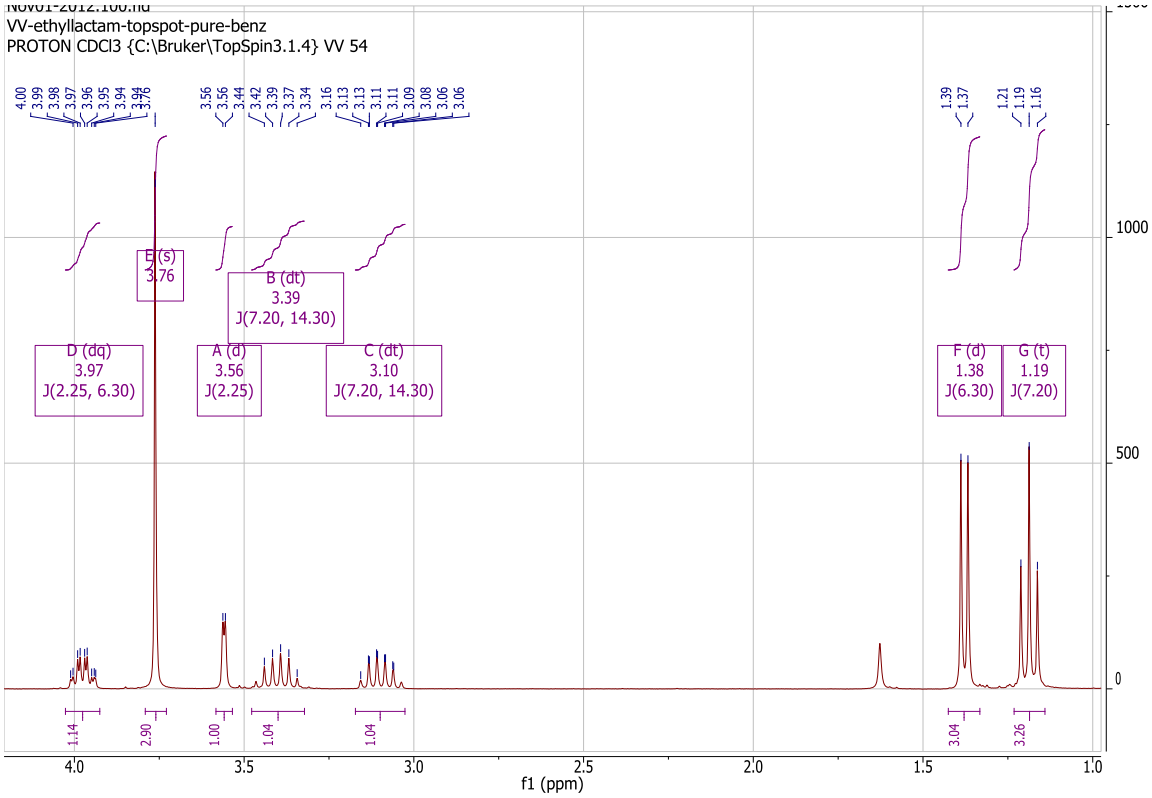

Figure 19 ^{1}H NMR spectrum of *trans*-*β*-lactam diastereomer 194.

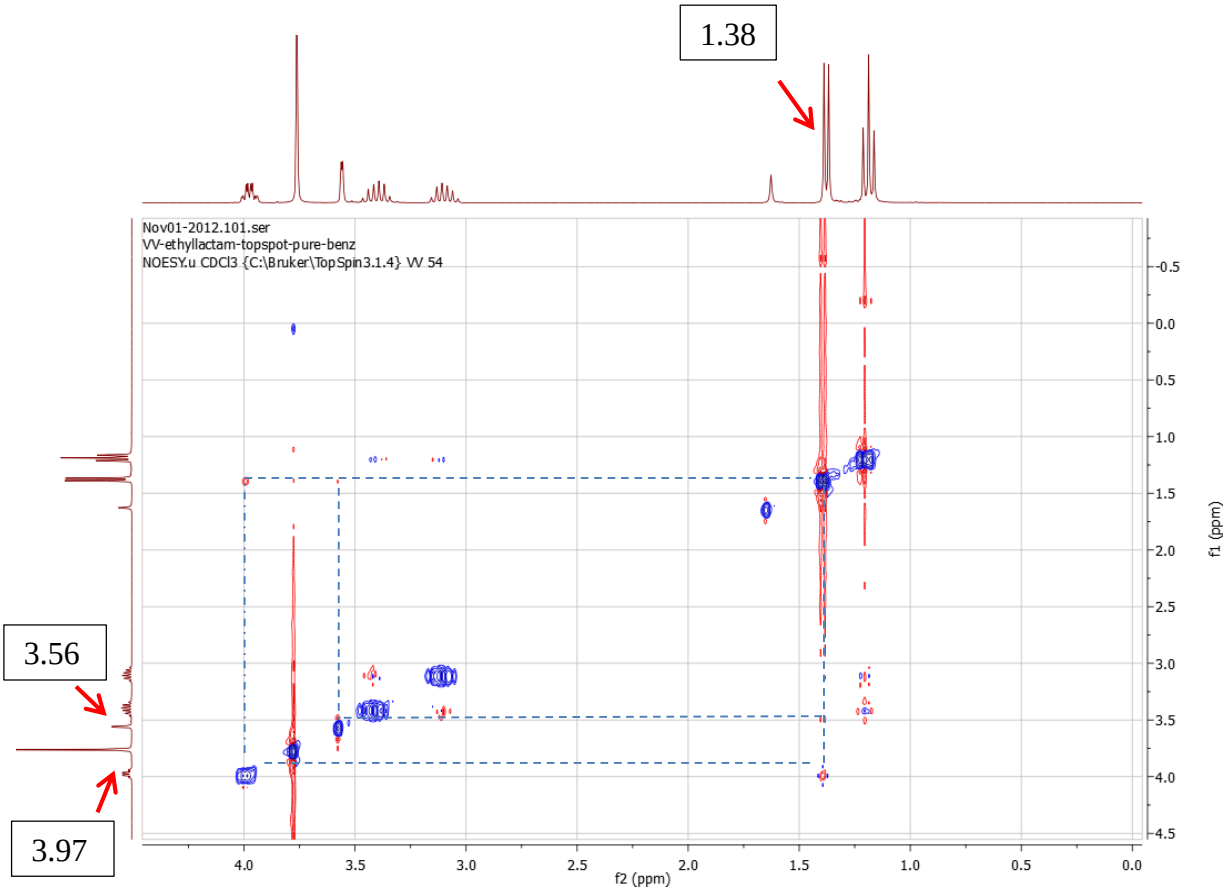

Figure 20 NOESY spectrum of *trans*-*β*-lactam 194.

From the ^{1}H-NMR spectra (Figures 22 and 19), the doublet peaks at δ 4.05 (J = 5.67 Hz) and δ 3.56 (J = 2.25 Hz) were identified as the *cis*- and *trans*-protons in the *β*-lactam ring.

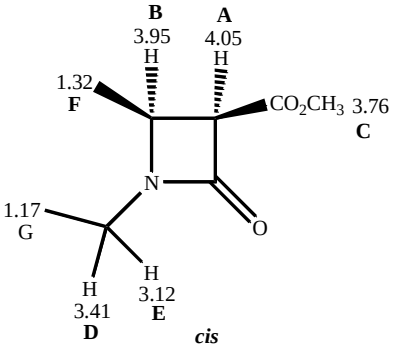

Figure 21 **^{1}H NMR assignments of the *cis*-isomer of *β*-lactam 193.**

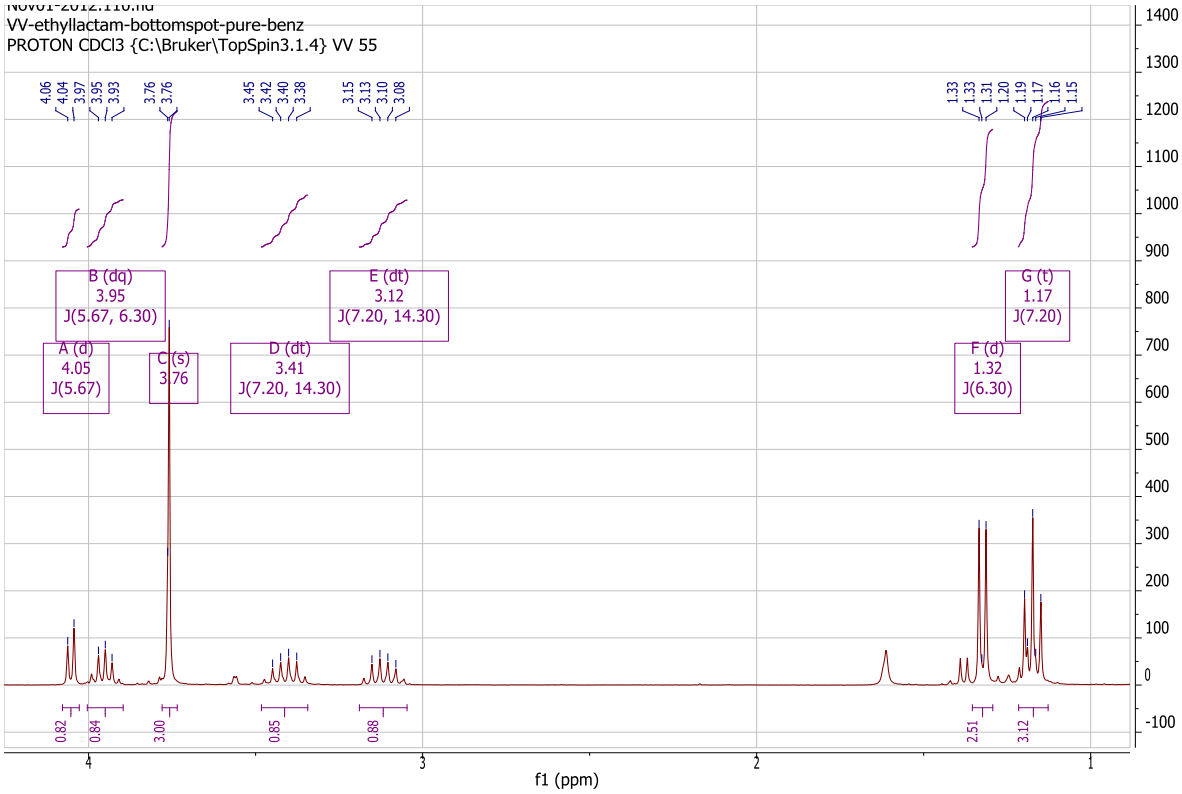

Figure 22 **^{1}H-NMR spectrum of *cis*-isomer of *β*-lactam diastereomer 193.**

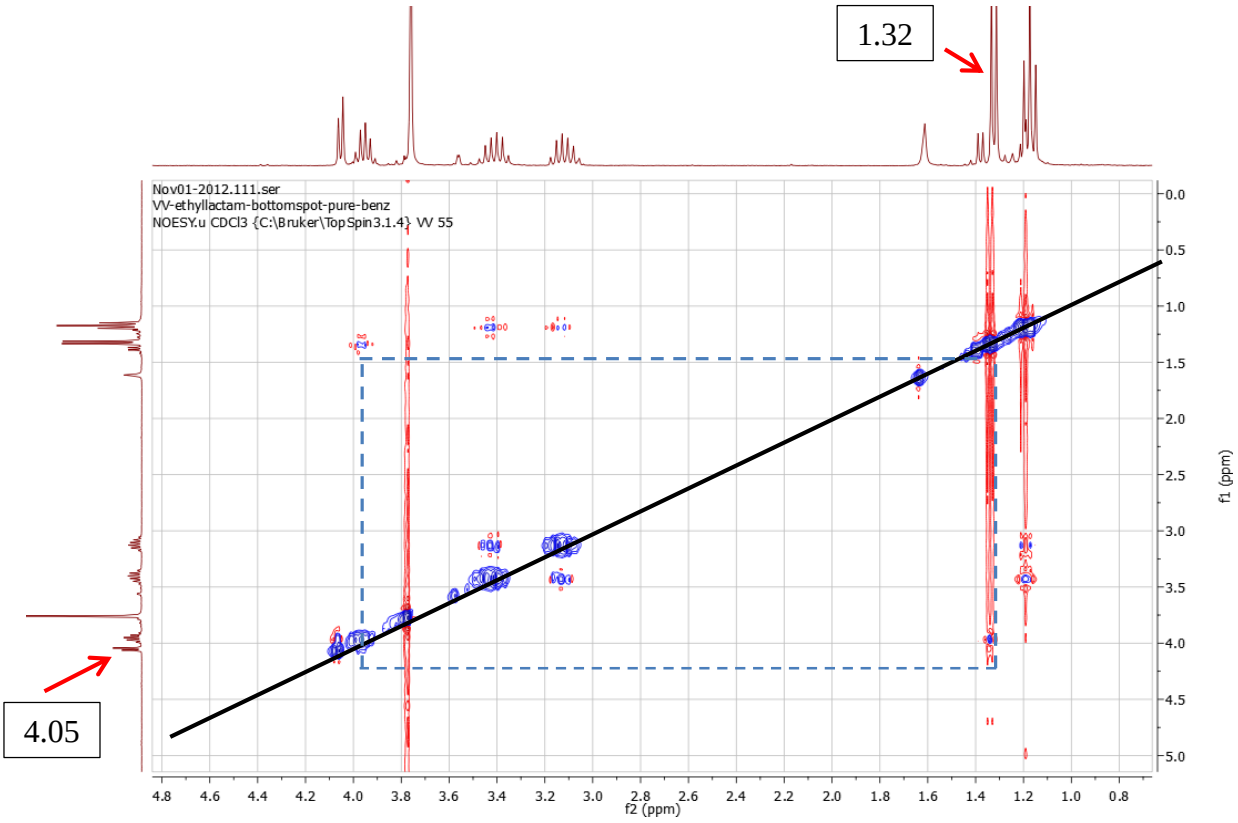

Figure 23 NOESY spectrum of partially purified *cis*-isomer 193.

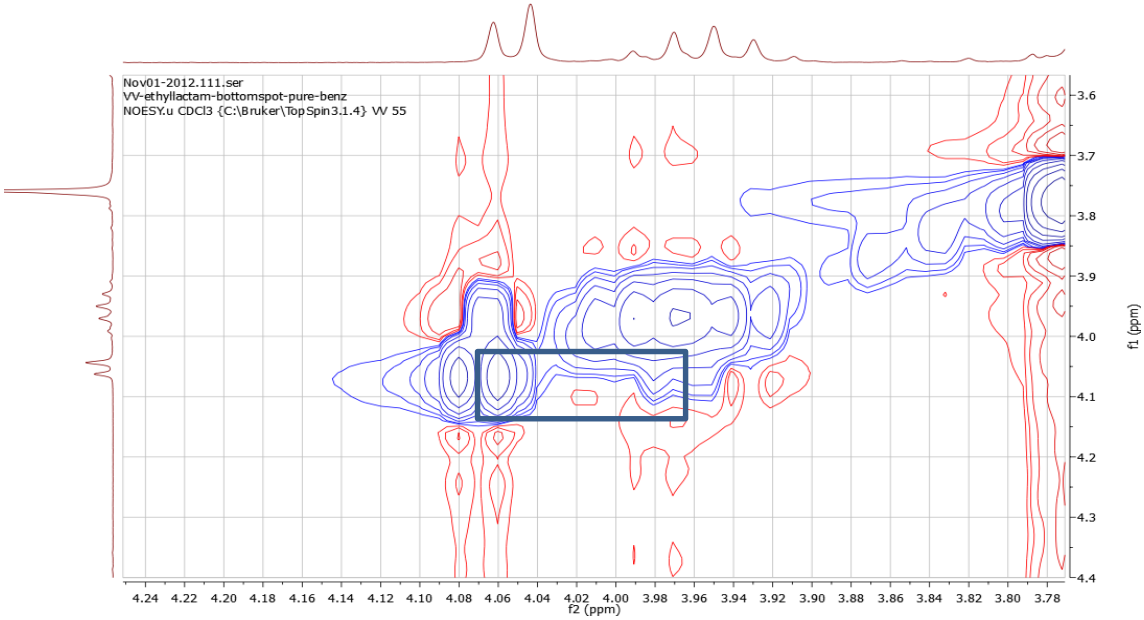

Figure 24 Expansion of *β*-lactam CH region

From the ^{1}H-NMR spectra (Figures 19 and 22), the doublet peaks at δ 3.56 and δ 4.05 were assigned to the *trans*- and *cis*-isomers respectively and thus in benzonitrile as solvent the *trans*-isomer was identified as the major isomer.

The literature values found for the *trans*-*β*-lactam **194** were: ^{1}H-NMR (200 MHz, $CDCl_3$, ppm) δ 3.94 (dq, *J* = 2.25 and 6.17 Hz, 1H), 3.34 (s, 3H), 3.52 (d, *J* = 2.25 Hz, 1H), 3.37 (dt, *J* = 21.54 and 7.26 Hz, 1H), 3.08 (dt, *J* = 21.17 and 6.92 Hz, 1H), 1.36 (d, *J* = 6.17 Hz, 3H), 1.18 (t, *J* = 7.32 Hz, 3H).[7] As can be seen, the quoted *J* values were not matching in the literature,[7] which may be due to print errors or the authors mis-quoting the coupling constant (*J*) values for the *trans*-isomer **194**. However, their values are close enough to help confirm our assignment.

The peak at δ 3.56 (d, *J* = 2.25 Hz, 1H) Figure 19 which corresponds to a –C–H on the *β*-lactam ring, matches well with the literature values 3.52 (d, *J* = 2.25 Hz, 1H), whereas in Figure 22 there is no doublet peak in the δ 3.52 region, as there would be for the *cis*-isomer. The peak at 3.98 (dq, *J* = 2.25 and 6.20 Hz, 1H) matches with the literature value 3.94 (dq, *J* = 2.25 and 6.17 Hz, 1H) and similarly the two pentets of the CH_2 at 3.40 (*J* = 7.26 Hz, 1H) and 3.10 (*J* = 7.22 Hz, 1H).

From Figures 20 and 23, we concluded that there is an NOE effect between resonances δ 1.38 and δ 3.56 in the NOESY spectrum of the *trans*-isomer **194** (Figure 20) and another NOE effect between δ 1.32 and 4.05 in the NOESY spectrum of the *cis*-isomer **193** (Figure 23); suggesting that in both cases these proton pairs are *cis*- to one another.

A small proportion (< 10%) of the *γ*-lactam isomer **195** was also found in the crude ^{1}H NMR spectrum.

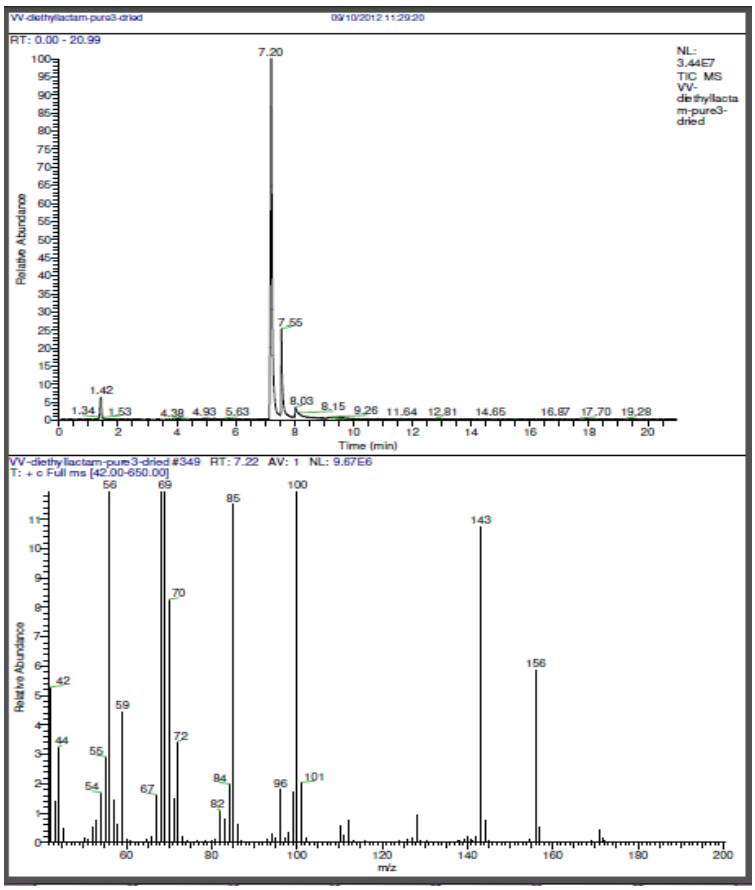

Figure 25 GC-Ms showing the ratio of *cis*- and *trans*-isomers at RT 7.56 and 7.20 min respectively.

From Figure 25 the peaks at RT 7.56 and 7.20 with *m/z* 171, 156, 143, 100. The intense peak at 7.20 corresponds to the *trans*-isomer, which was also confirmed by ^{1}H-NMR spectroscopy (Figures 19 and 22).

2.3.1.2 Computational details for diastereomers

Quantum mechanics calculations were performed to determine accurate energy differences between the diastereomers **193** and **194**. The diastereomer energies were optimised using density functional theory (DFT). For this purpose, the B3LYP function with the 6-31+(d) basis set (B3LYP/6-31+(d)) was employed for all the elements. Minimum energy geometries

were confirmed via vibrational frequency calculations. The Gaussian03 program was used for the calculations.[154]

2.3.1.3 Relative stabilities and bulkiness of the *β*-lactam diastereomers 193 and 194

Using VIs computer modelling, the energy differences of the *cis*- and *trans*-*β*-lactam diastereomers **193** and **194** were calculated:

$E_{cis\text{-isomer}}$ - $E_{trans\text{-isomer}}$ = -592.9164121 – (-592.9169626) Hartree = 0.0005505*627.509391 kcal/mol = 0.3454 kcal/mol.

Thus, the lower energy *trans*-diastereomer **194** would be expected to be the favoured isomer at equilibrium in free solution. However, this is not always the case as formation of a more stable intermediate can lead to a minor product, while a less stable intermediate can lead to a major product. This can be explained by the Curtin-Hammett principle,[155] case–II, the Curtin-Hammett principle in chemical kinetics was proposed by David Yarrow Curtin and Louis Plack Hammett[156] and it mainly states that, for a reaction that has a pair of reactive intermediates or reactants that interconvert rapidly (as is usually the case for conformational isomers), with each going irreversibly to a different product, the product ratio will depend both on the difference in energy between the conformers and the free energy of the transition state going to each product. An example is found in the alkylation of tropanes **196** (Scheme 52).[157,158]

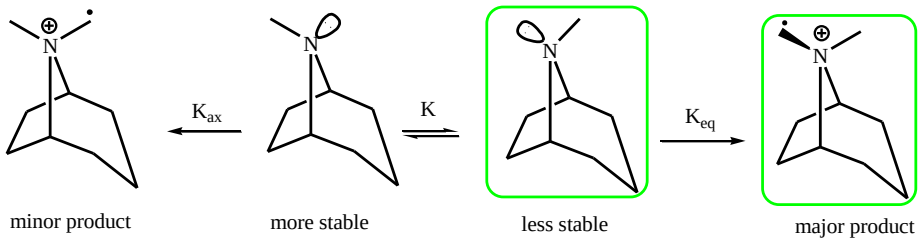

196

Scheme 52 Alkyaltion of tropanes with iodomethane to form the less stable intermediate[155] leading to the major product[158] following the Curtin-Hammett principle.

As a result, the product distribution will not necessarily reflect the equilibrium distribution of the two intermediates. The Curtin-Hammett principle has been invoked to explain selectivity in a variety of stereo- and regio-selective reactions. This is an example of a Curtin-Hammett scenario in which the less-stable intermediate is significantly more reactive than the more stable intermediate that predominates in solution.[158] Because substrate isomerisation is fast, during the course of reaction excess substrate of the more stable form can be converted into the less stable form, which then undergoes rapid and irreversible C–C (carbon–carbon) bond formation to produce the desired product. Thus, many essentially irreversible reactions, give the kinetic product rather than the more stable thermodynamic product, which for most of our *β*-lactams will be the *trans*-diastereomer (Schemes 53 and 54).

Thermodynamically:

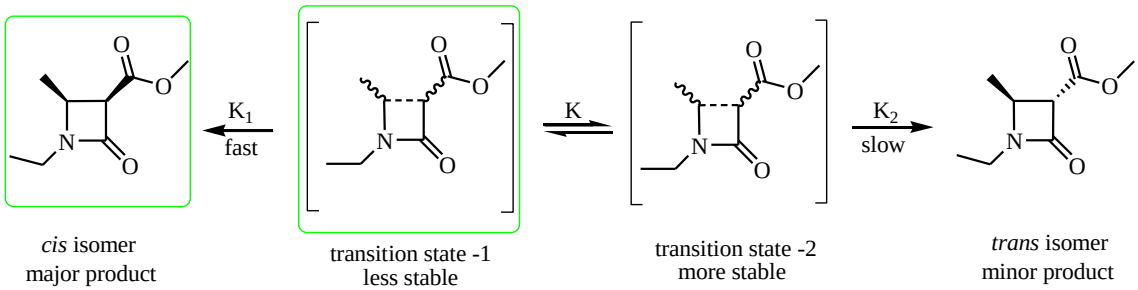

Scheme 53 Formation of more stable *trans*-*β*-lactam 194 under thermodynamic conditions.

Kinetically:

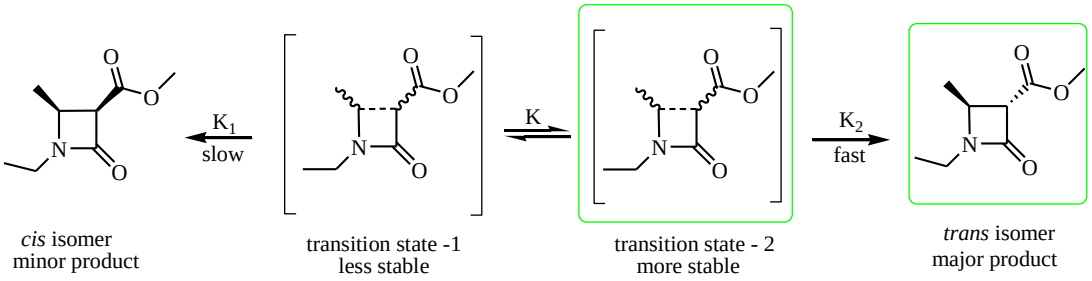

Scheme 54 Formation of less stable *cis*-*β*-lactam 193 under kinetic control conditions.

2.3.1.4 Chem 3D modelling

The structures of the *cis*- and *trans*-diastereomers **193** and **194**, were drawn in ChemDraw then copied to Chem 3D (Ultra, version 9), where the energies of the structures were minimised using the MM2 procedure and the molecules were rotated in 3 dimensions to display their more planar aspects. The models were copied to Microsoft Word, arranged so that they had the same atom and bond sizes and their smallest dimensions compared.[159] Comparison of these energy minimised Chem 3D structures gives a reasonable estimate of the relative sizes of the diastereomers **193** and **194** (Figure 26).

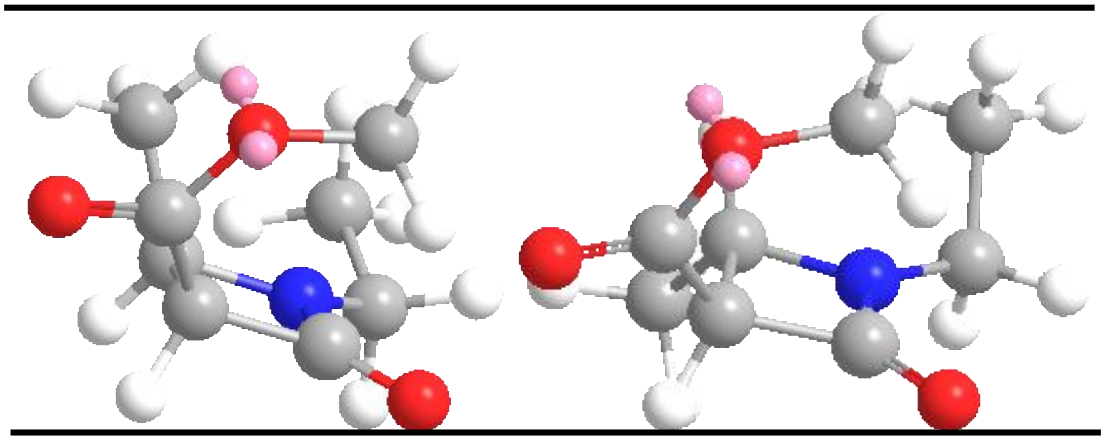

cis **193**, slightly less bulky *trans* **194**, slightly bulky

Figure 26 Chem 3D models of the structures of diastereomers 193 and 194, arranged to show the smallest dimension of the molecules.

The *trans*-diastereomer **194** is more stable and would be expected to predominate slightly in free solution at high temperatures and to become more predominant in low energy catalysed processes. However, the relative "heights" of the *cis*- and *trans*-diastereomers shows that the *cis*-diastereomer **193** should be slightly less bulky and should be formed more readily if the environment is more restricted. In addition it is noticeable that the lower energy *trans*-isomer is less sterically constrained as the molecule is wider and also "longer" (not shown). Size selectivity due to the dimensions of these molecules will be looked for in the catalysed reactions, especially in the restricted environments of the zeolites.

2.3.1.5 Comparison of the carbene insertion reactions of methyl *N,N*-diethylamido-diazomalonate 183

In the literature,[160] photolysis of the related diazo compound *N,N*-diethyldiazoacetamide **197** in 1,4-dioxane as solvent gave 57% of *β*-lactam **198** insertions at the two active –C-H positions of the -NC**H**$_2$ and 43% of *γ*-lactam **199** at the three less active -NCH$_2$C**H**$_3$ positions (Scheme 55).[84,160] Thus we would expect that a mixture of the *β*-lactam and *γ*-lactam should also be formed by methyl *N,N*-diethylamidodiazomalonate **183** under high energy photolytic conditions.

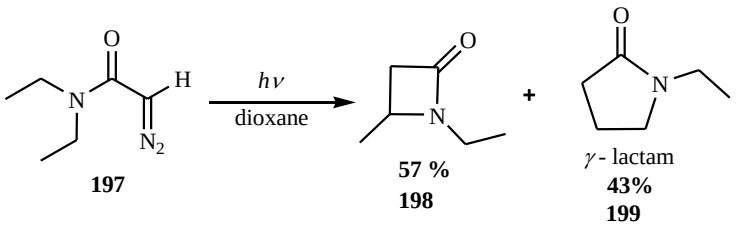

Scheme 55 Photolytic reaction of *N,N*-diethyldiazoacetamide forming *β*-lactam 198 and of *γ*-lactam 199.

Heating methyl *N,N*-diethylamidodiazomalonate **183** under reflux in acetonitrile (*ca*. 80°C) overnight gave *ca*. 60% combined isolated yield of products with *cis/trans* ratio 65 : 35, but there were carbene dimers and unreacted starting material left after >16 hours. A *bis*-acetylacetonatocopper(II) catalysed –C-H insertion reaction, of methyl *N,N*-diethylamidodiazomalonate **183** at 75°C in acetonitrile as solvent, gave a mixture of *β*-lactam diastereomers **193** and **194** with *cis-/trans*-isomer ratio 36 : 64, but with only 40% yield, due to extensive carbene dimer by-product formation along with the *γ*-lactam **195**. These results are similar to those above, for the photolysis of the diazoacetamide **197** (Scheme 55) and are in contrast to a dirhodium tetraacetate catalysed reaction in dichloromethane, which has been reported in the literature to give the *trans*-diastereomer **194** (Scheme 56) exclusively, in 40% yield (the remainder being unreacted starting material),[7] thus showing that a lower energy catalysed reaction can favour the slightly lower energy *trans*-isomer.

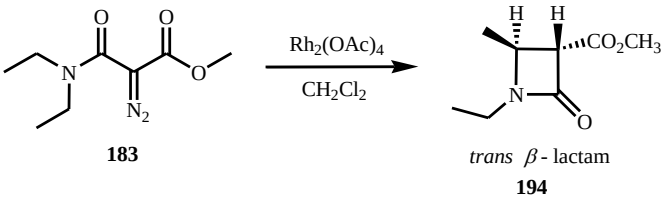

Scheme 56 Catalysed reaction of methyl *N,N*-diethylamidodiazomalonate 183 in the presence of dirhodium tetraacetate, forming the *trans*-*β*-lactam 194 exclusively.

In order to determine whether there was any size selectivity apparent for catalytic reaction of the methyl ester **183** within a clay mineral interlayer, Cu(II)-exchanged Wyoming bentonite was heated with the methyl *N,N*-diethylamidodiazomalonate **183** at 75°C in acetonitrile to give mainly *cis*- and *trans*-*β*-lactams **193** and **194** (*ca*. 70% combined isolated yield) in the ratio 39 : 61 with *ca*. 8% of the *γ*-lactam **195** (Scheme 49). These catalysed reactions were essentially complete in about 1-2 hours, but reflux was continued overnight to ensure complete conversion of diazoalkanes. Other catalysts such as Cu(II)-exchanged zeolites 4A and ZSM-5 were also utilised to find out whether there was selectivity of *cis*- over *trans*-isomer based on their pore sizes.

Both Cu(II) cation exchanged zeolites, should have an accessible pore size of about 5.5 Å (see Section 1.3.3) and reactions in acetonitrile solvent with Cu(II)-exchanged 4A zeolite, gave *ca*. 59% combined isolated yield with a *cis*-/*trans*-isomer ratio of 60 : 40, while ZSM-5 gave *ca*. 60% combined isolated yield with *cis*-/*trans*-isomer ratio of 46 : 54. These results are summarised in Table 5.

Table 5 Summary of isolated yields and isomer ratios for the formation of *β*-lactams 193 and 194 in acetonitrile.

Catalyst	%Yield of *β*-lactams **193** & **194**	*cis-/trans*-diastereomer ratio
No catalyst	60	65 : 35
Cu(II)acac$_2$ catalyst	40	36 : 64
$Rh_2(OAc)_4$ (in CH_2Cl_2)[7]	40 (60% unreacted)	00 : 100 (reported)
Cu(II) Wyoming bentonite	70	39 : 61
Cu(II) 4A zeolite (ca. 5.5 Å).[161] See Section 1.3.3	60	60 : 40
Cu(II) ZSM-5 zeolite (5.4 - 5.6 Å)[162] (Si : Al = (90 : 1)	60	46 : 54

The uncatalysed reaction gives the *cis*-isomer in nearly two-fold excess, suggesting that the reaction is under kinetic control. However, when a good, low energy pathway catalyst such as dirhodium tetraacetate is used the more thermodynamically stable *trans*-isomer is produced almost exclusively. When the less active catalyst Cu(II)acac$_2$ is used the isomer ratio begins to favour the more stable *trans*-isomer as does the reaction catalysed by Cu(II)-Wyoming bentonite, suggesting that there is little size selectivity in the bentonite interlayer in this case. However, the zeolite catalysts with their fixed reaction spaces do begin to show size selectivity with their pore access of ca. 5.5 Å.

Organic solvents can have a profound effect upon the interlayer distance in clay minerals,[84,163] so we were able to manipulate the interlayer distance by changing the reaction solvent for the Cu(II)-Wyoming bentonite catalysed reaction. The interlayer separation of the mineral with various solvents was determined using powder X-ray diffraction of the clay mineral wetted with the solvent. Evaporation of the solvent was minimised at the typical ambient temperature in the XRD instrument of around 35-40°C, by enclosing the sample with Mylar (X-ray film, TF-125). It was assumed, with a fair degree of assurance, that in the reactions carried out, the differences in interlayer separation of each clay mineral would follow a similar trend to those determined for the dried Cu(II)-clay minerals as there were too many solvent/clay mineral combinations to measure during the instrument time available. The yields and isomer ratios obtained with Cu(II)-exchanged Wyoming bentonite in different solvents, that produced differing layer spacings, are compared in Table 6.

Table 6 Yields, isomer ratios and measured (XRD) Δd values for Cu(II)-exchanged Wyoming bentonite in various solvents.

Solvent	%Yield of *β*-lactams **193** & **194**	*cis-/trans*-diastereomer ratio	Interlayer distance of Cu^{2+}-Wyoming bentonite, Δd (Å), assuming the clay layers ≈ 9.6 Å[164]
Acetonitrile	70	39 : 61	3.52
Benzonitrile	67	45 : 55	5.90
Toluene	20	53 : 47	3.36
Acetone	40	36 : 64	3.40
Tetrahydrofuran	38	47 : 53	3.80
Chloroform	50	34 : 66	3.56
Ethylbenzene	*	*	5.02
Dichloromethane	45	30 : 70	3.52
1,4-Dioxane	*	*	5.02

* Less than 10% product formed in ethylbenzene and 1,4-dioxane solvents.

The results from Table 6 show that there are modest solvent effects on selectivity, yield and isomer ratio of diastereomers, but that under the conditions of the experiment (all compared at 80°C or at the reflux temperature of lower boiling solvents), there does not appear to be a simple correlation of measured interlayer distance with preferred formation of the slightly less bulky *cis*-*β*-lactam-isomer, **194**. Benzonitrile and acetonitrile were found to be the best solvents in terms of yields and *cis* : *trans* ratios. Both solvents gave *ca*. 70% combined isolated yield and acetonitrile gave a *cis*-/*trans*-isomer ratio 39 : 61, while benzonitrile gave the *cis*-/*trans*-isomer ratio 45 : 55, however, we had expected the lower Δd with acetonitrile to give more of the less bulky *cis*-isomer. As this is not the case, the solvent packing in the interlayer region must also be affecting the available reaction space. In addition, solvent molecules often stack within clay interlayers (see Figure 27) and this stacking can increase with temperature, thus as the XRD measurements were made at about 35-40°C at the ambient temperature of the diffractometer, whilst the reactions were carried out at 80°C, making the value of the interlayer separation during reaction uncertain.

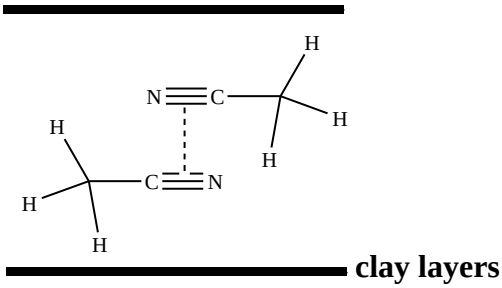

Figure 27 Expansion of interlayer space by the stacking of acetonitrile which may push the layers further apart during heating from 3.52 Å to > 3.52 Å.

With some of the solvents, i.e. 1,4-dioxane, tetrahydrofuran and ethylbenzene the reactions did not proceeded smoothly and many of them formed complex mixtures along with low product formation. The reasons may be due to the carbene intermediate forming carbene dimers or inserting into solvent -C–H bonds such as that shown for tetrahydrofuran in Figure 28.[165,166] Similar solvent insertion reactions could occur with 1,4-dioxane and with the activated $–CH_2$ of ethylbenzene.

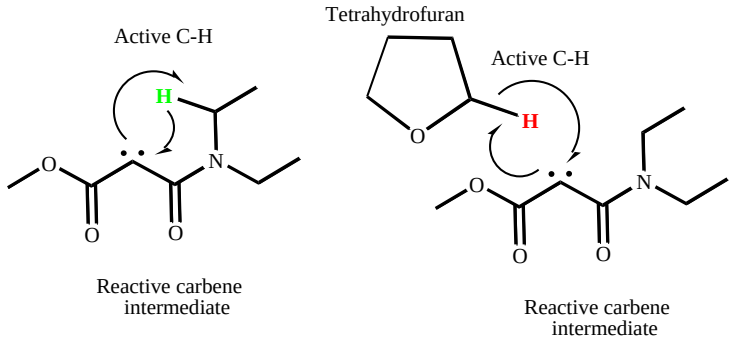

Figure 28 Possible active C–H positions on tetrahydrofuran solvent and reactant in carbene insertion reactions.

2.3.1.6 Effect of varying the layer charge of a clay mineral on the ratio of diastereomers 193 and 194

In order to control the size of the reaction space further, a series of Cu^{2+}-clay mineral catalysts with a variety of layer charges, which should provide increasingly restrictive interlayer reaction spaces as the layer charge increases, were examined. These included (Wyoming bentonite, Brett's Fullers earth, Los Trancos, Fulacolor (acid activated Los Trancos) and a carbene modified Cu(II)-Wyoming bentonite) as described in Section 2.3.1.7 (Scheme 57), each of which has a different interlayer spacing (Δd ranging from 5.92 - 2.52 Å). With the zeolites, there should be little advantage from the pore height with diazoester **183**, but there may be a selection effect due to the greater width of the *trans*-*β*-lactam; these results are collected in Table 7.

These results show that the clay catalysts give lower selectivity for –CH insertion reactions within the interlayer, whereas the zeolites, with their more fixed reaction spaces showed more effective results in terms of selectivity and yields. The reason may be due to the fact that the size of the less bulky *cis*-isomer is ≈ 5.20 Å from the Chem 3D model structures and the interlayer spacing of the clay minerals used can be roughly of the same size as this from XRD measurements after wetting with solvent, while in ZSM-5 zeolite the normal pore size (5.4 Å) was very similar to the width of the less bulky, more planar isomer.

The solvents, acetonitrile and benzonitrile have proven to be the best solvents for *β*-lactam ring formation and exclusion of the *γ*-lactam. This is probably due to the co-ordination of acetonitrile within the interlayer space of the clay minerals, which can push the layers even further apart on heating, which would disfavour the formation of the less bulky/more planar isomer.

The yields for Brett's Fullers earth were lower than for the other minerals, suggesting that the higher layer charge may be restricting access to the Cu(II)-cations in the interlayer. The Los Trancos and Fulacolor gave similar yields to those of Wyoming bentonite. The *cis*-/*trans*-isomer ratios Brett's Fuller earth were 37 : 63 in acetonitrile (56% yield) and 56 : 44 in acetone (30%). Thus suggesting that access to the interlayer is more difficult in acetone, but a more restricted reaction space favours the less bulky *cis*-isomer.

Table 7 Measured yield, isomer ratios and Δd values for clay minerals in various solvents

Cu(II)-exchanged mineral	Solvents	%Yield of *β*-lactams **193** & **194**	*cis-/trans*-diastereomer ratio	Interlayer distance of Cu(II)-clay mineral, Δd (Å), assuming the clay layers ≈ 9.6 Å[164]
Wyoming bentonite	No solvent			2.52
	Acetonitrile	70	39 : 61	3.52
	Benzonitrile	67	45 : 55	5.92
	THF	40	39 : 61	3.8
	Acetone	20	29 : 81	3.4
Modified clay Al-O-EA (see next Section)	No solvent			3.09
	Acetonitrile	66	46 : 54	
	Benzonitrile	65	57 : 43	
	Acetone	39	43 : 57	
	THF	40	39 : 61	
	Toluene		60 : 40	
Brett's Fullers Earth	No solvent			2.52
	Acetonitrile	56	37 : 63	-
	Acetone	30	56 : 44	-
Los Trancos	No solvent			2.64
	Acetonitrile	48	32 : 68	-
	Benzonitrile	55	34 : 66	-
	Toluene	50	45 : 55	-
	THF	53	47 : 53	-
Fulacolor	No solvent			2.74
	Acetonitrile	40	32 : 68	-
	Benzonitrile	48	33 : 77	-
	Toluene	50	46 : 54	-
	Acetone	46	56 : 44	
ZSM-5				Pore size 5.4 - 5.6 Å
	Acetonitrile	60	46 : 54	
	Benzonitrile	62	50 : 50	
	Toluene	70	58 : 42	
4A molecular sieves				The pore size is ca. 5.5 by 7.4 Å, see Chapter 1.3.3.
	Acetonitrile	59	60 : 40	
	Benzonitrile	65	50 : 50	
	Toluene	63	37 : 63	

Acetone and toluene tended to give higher proportions of the *cis*-isomer in most cases, suggesting that their relative bulkiness is further restricting the reaction environment. The

Cu^{2+}-exchanged 4A zeolite catalyst showed decreasing *cis*-isomer selectivity on going from acetonitrile, to benzonitrile to toluene, whereas ZSM-5 showed the opposite effect. This may be due to the larger solvent molecule providing a more restricted reaction environment in the 5.5 Å channels of ZSM-5, whilst the 4A zeolite has a much larger cage to carry out its reactions in (> 11 Å) and is not so dependent on solvent constraints.

2.3.1.7 Modification of the interlayer region of a clay mineral

The hydrogen atoms of the bridging –OH groups of the octahedral layer of a T:O:T clay mineral sits in the central space of the hexasiloxy rings of the tetrahedral layer (Figure 2 in Chapter 1). As diazoalkanes can be used to form carbenes in Cu(II) exchanged clay mineral interlayers, it was hoped that simply reacting a diazo ester, such as ethyl diazoacetate **33**, within an interlayer would insert the carbene into the H-O bond, binding the organic moiety within the clay interlayer region (Scheme 57). This should further restrict the interlayer region and perhaps give higher size selectivity.

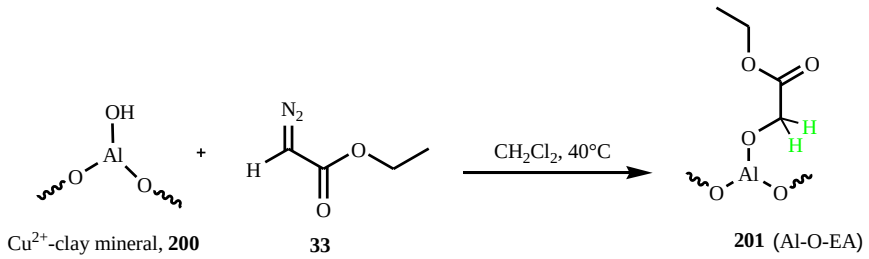

Scheme 57 Carbene insertion onto the Al-OH bond to form more stereo restricted environment.

Ethyl diazoacetate solution in dichloromethane was heated at 40°C with stirring for 18 h with Wyoming bentonite **200** and then washed with dichloromethane to remove excess ethyl diazoacetate and any carbene dimers (dimethyl fumarate and dimethyl maleate) from the interlayer (Scheme 57). FT-IR spectroscopy showed the presence of carbonyl groups in the modified clay mineral **201**; 1731 cm^{-1} for the stretching frequency of the ester –C=O

functional group, confirming binding of the carbene to the clay mineral. The interlayer spacing, Δd, was shown to be 3.09 Å, confirming that the interlayer spacing had increased from the 2.74 Å in the Cu^{2+}-clay.

Some interesting results observed by utilising modified clay mineral **201** were, for example the ratio of *cis-/trans*-isomer ratio 45 : 55 with Cu^{2+}-exchanged Wyoming bentonite in benzonitrile solvent was increased to 57 : 43 with the modified clay mineral **201** (ca. ≈ 70% yield), which has Δd 5.92 Å. By reacting methyl *N,N*-diethylamidodiazomalonate **183** with modified clay **201** in acetonitrile or benzonitrile as solvent, the *cis-/trans*-isomer ratios of 46 : 54 and 57 : 43, respectively, had increased compared to the Cu^{2+}-Wyoming bentonite of 39 : 61 and 45 : 55 in the same solvents. The proportion of the less bulky product was increased in both the solvents, which shows that the modification of the clay mineral (Al-O-EA) had influenced the regioselectivity of the C-H insertion reaction for *β*-lactam formation, but with a consequent increase in the *γ*-CH insertion reaction to form the *γ*-lactam product.

The better competition between the *cis*- and *trans*-isomers **193** and **194** in the modified catalyst **200**, may be due to the more restricted catalytic environment within the clay due to the carbene insertion into the Al-OH bond, slowing down the reaction slightly and allowing the proportion of the kinetic *cis*-product to increase.

In the presence of the modified clay catalyst in toluene solvent the proportion of the *cis*-isomer **193** (60 : 40 with very low yields) had increased nearly to the ratio of the non-catalysed reaction (ca. 60% 65 : 35), once again with increased formation of *γ*-lactam **195** (Figure 29).

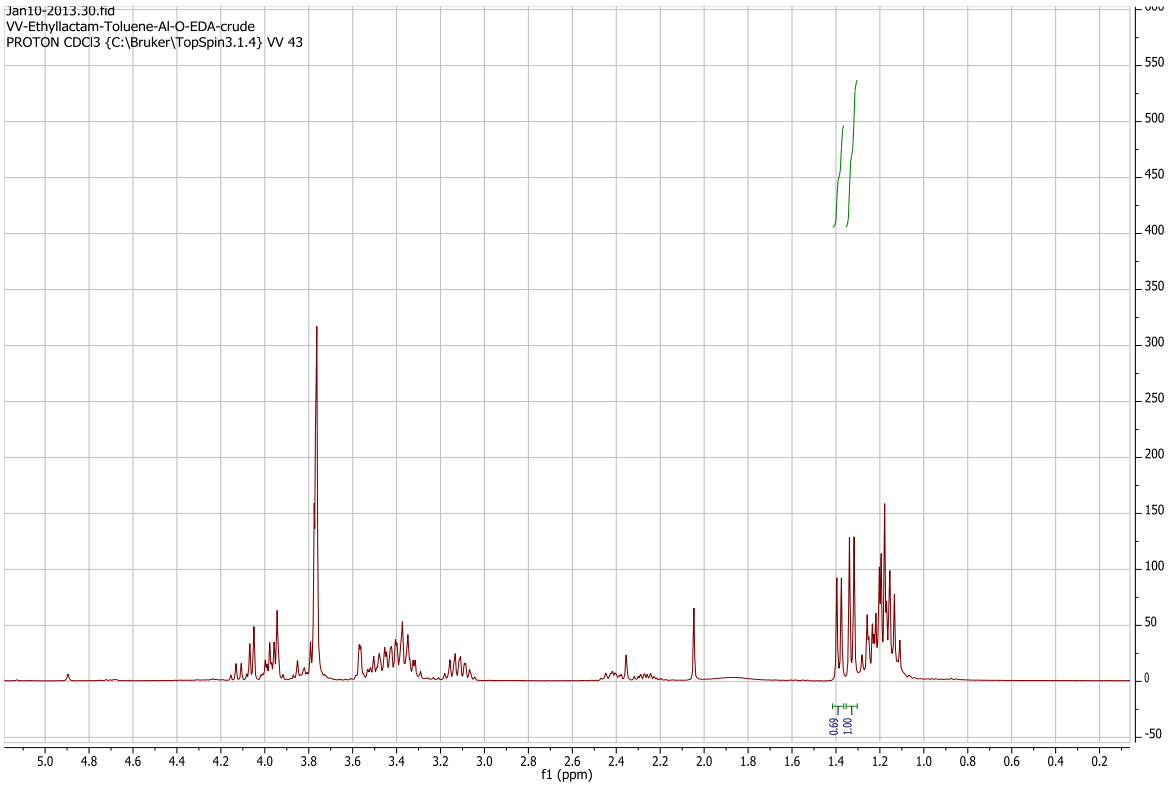

Figure 29 ^{1}H-NMR spectrum of product from the Al-O-EA (modified clay mineral) catalysis of ring closure of methyl *N,N*-diethylamidodiazomalonate in toluene.

2.3.1.8 Conclusions for reactions of methyl *N,N*-diethylamidodiazomalonate 183

Reaction in the interlamellar region of Cu^{2+}-exchanged clay mineral should favour the more planar/less bulky isomer. However we found some interesting results: in most cases when using Cu(II)-exchanged clay mineral and zeolite catalysts in the carbene insertion reaction of **183**, the reactions were much faster than the uncatalysed reactions in all solvents and tended to give higher yields of the *β*-lactam products **193** and **194**, with low proportions of *γ*-lactam **195**. When compared to the dirhodium tetraacetate catalysed reaction from the literature,[7] which appeared to have formed the more thermodynamically stable *trans*-isomer **194**, exclusively, the mineral catalysed processes gave a mixture of *cis-/trans*-isomers with good yields. The proportion of the less bulky *cis*-isomer could be improved by judicious choice of solvent, clay mineral layer charge or zeolite type, but even with the best of these the

proportion of the slightly less bulky *cis*-isomer could not be improved over the catalyst free reaction. This suggests that the catalysed reaction, which usually favours the thermodynamic *trans*-product **194**, can be overcome to a small degree during the reaction of diazo compound **183** in the restricted inner regions of the mineral catalysts, but that the size difference of the *β*-lactam diastereomers **193** and **194** is not great enough to allow great size selection.

The obvious course of action would be to increase the size of the diazoalkane reactant molecule to try and induce size selectivity, thus we next examined benzyl *N,N*-diethylamidodiazomalonate **184**. Originally, we expected the larger size of the benzyl ester group to confer greater steric constraints and improve the selectivity for the less bulky *cis*-isomer **193** or **202**, however, as will be shown in the following sections, this proved to be erroneous due to the planarity of the benzyl group.

2.4 Carbene reactions of benzyl *N,N*-diethylamidodiazomalonate (benzyl 2-diazo-2-(diethylcarbamoyl)acetate) 184

Carbene intermediates were formed from benzyl *N,N*-diethylamidodiazomalonate **184** by photolysis, thermolysis and catalysis with copper(II) sulfate, Cu(II) clay minerals or Cu(II) zeolites to yield a mixture of the *β*-lactam diastereomers **202** and **203** with small amounts of the *γ*-lactam **204** (Scheme 58) by carbene insertion into the nearby C-H bonds.

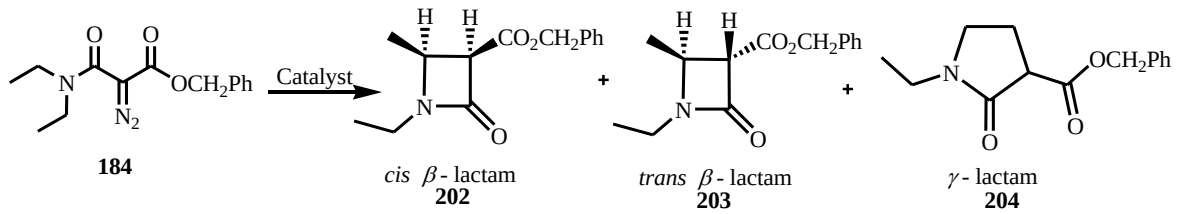

Scheme 58 Synthetic route to *β*-lactams 202 and 203 (35 : 65) and *γ*-lactam 204.

Another possibility is the intramolecular carbene insertion into the terminal CH_3 of the *N*-ethyl group (-NCH_2**CH_3**) in **184** to form a new (carbon–carbon) C–C bond and giving a *γ*-lactam ring **204** (Scheme 59).

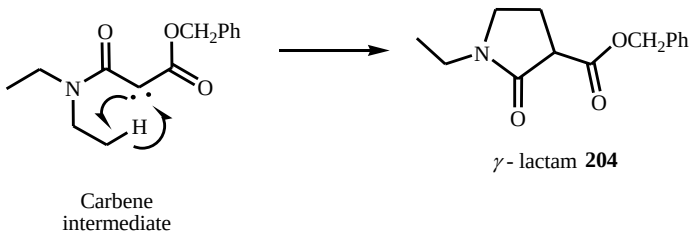

Scheme 59 Mechanism for the formation of the *γ*-lactam ring.

2.4.1.1 Assignment of the structures of the benzyloxy *β*-lactam isomers 202 and 203

The *cis*- and *trans*-diastereomers **202** and **203** (Figure 33 & 31) were identified in a similar manner to the methyl ester isomers **193** and **194**, based on assignment of the ^{1}H NMR (Figures 19 and 22), ^{13}C NMR, ^{1}H-^{1}H 2D COSY and ^{1}H-^{1}H 2D NOESY (Figures 20 and 23) spectra of partially purified *cis*- and *trans*-diastereomers **193** and **194**.

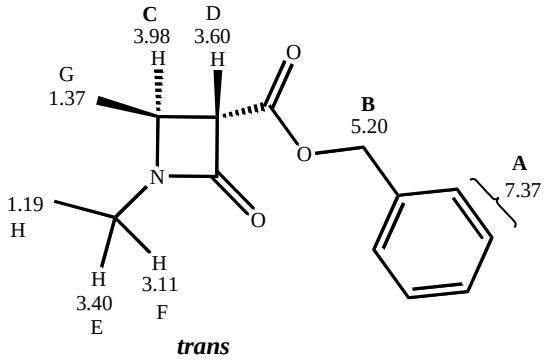

Figure 30 ***trans*-isomer of *β*-lactam 203.**

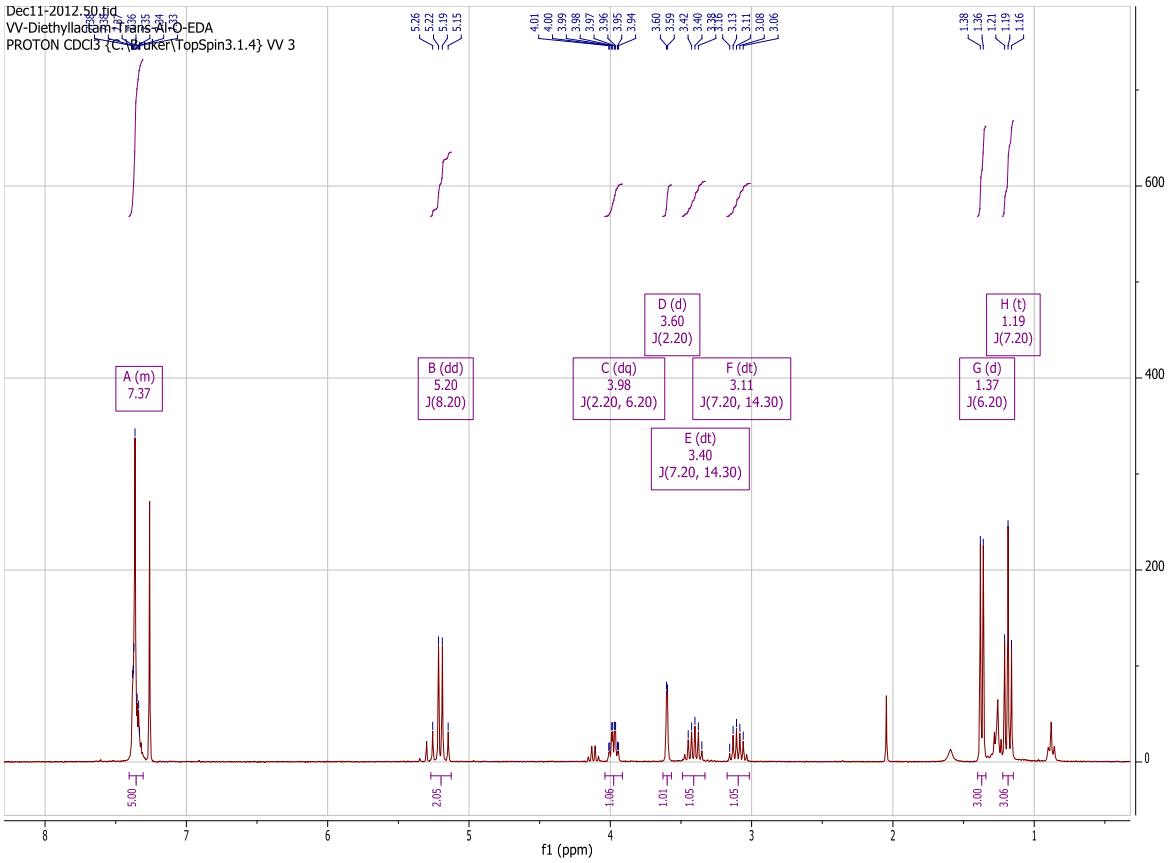

Figure 31 **^{1}H-NMR spectrum of *trans* *β*–lactam diastereomers in the mixture 202 and 203.**

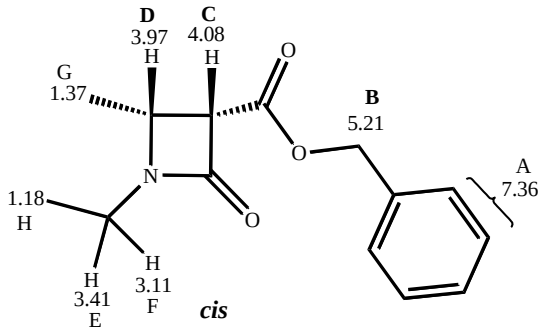

Figure 32 ***cis*-isomer of *β*-lactam 202.**

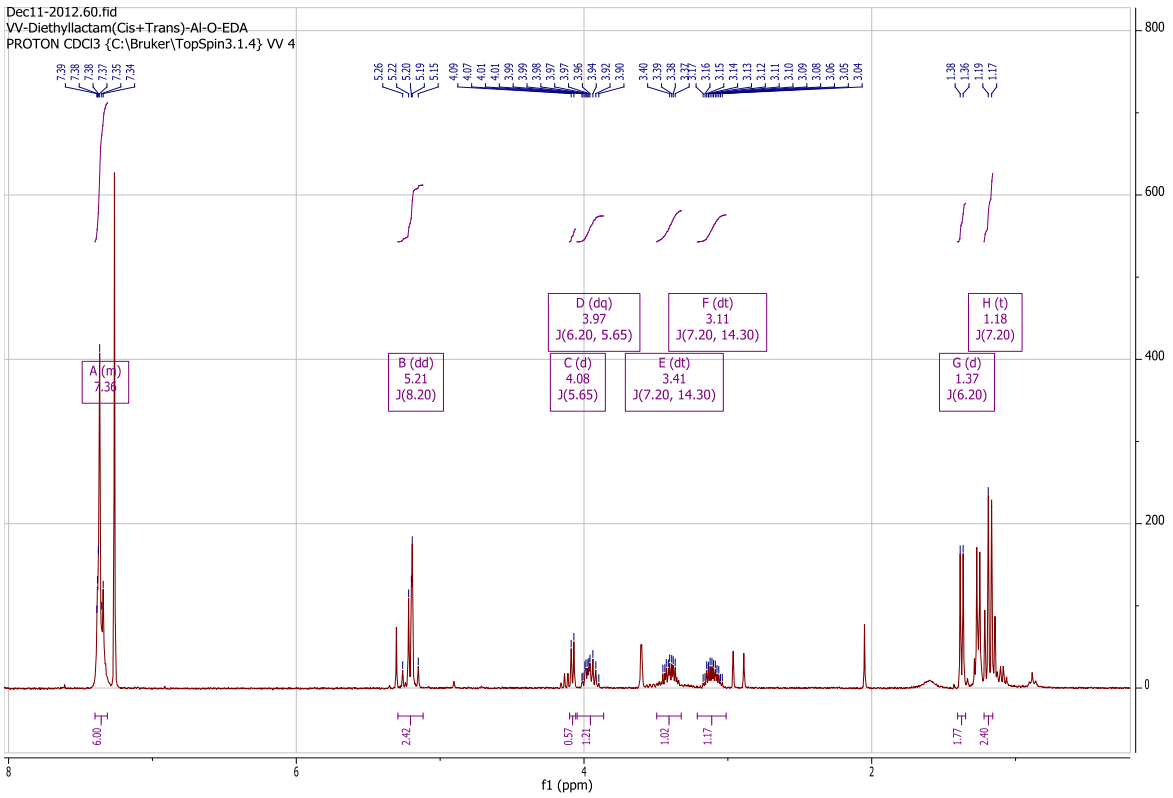

Figure 33 **^{1}H NMR spectrum of *cis* *β*-lactam diastereomer in the mixture 202 and 203.**

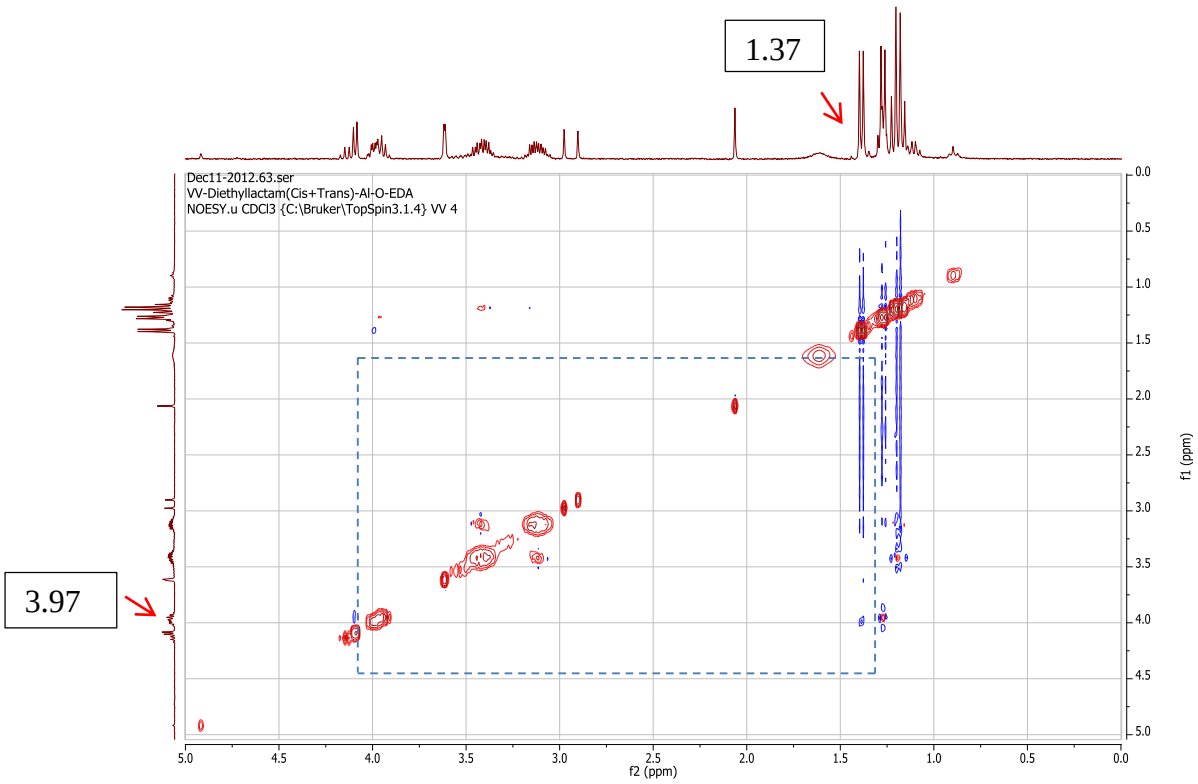

Figure 34 NOESY spectrum of *cis*-*β*-lactam diastereomer in the mixture 202 and 203.

From the ^{1}H-NMR spectra of the benzyl esters **202** and **203** (Figures 33 and 31), the doublet peaks at δ 4.08 (J = 5.65 Hz) and δ 3.60 (J = 2.20 Hz) were identified as the *cis*- and *trans*-protons respectively in the *β*-lactam rings. This is in agreement with the ^{1}H-NMR spectra of the methyl esters (Figures 19 and 22), where the doublet peaks at δ 3.56 (J = 2.25 Hz) and δ 4.05 (J = 5.67 Hz) were attributed to the *cis*- and *trans*-protons respectively in the *β*-lactam rings.

2.4.1.2 Relative stabilities and bulkiness of the *β*-lactam diastereomers 202 and 203

Using VIs computer modelling, the energy differences between of the *cis*- and *trans*-*β*-lactam diastereomers **202** and **203** were calculated:

$E_{cis\text{-isomer}} - E_{trans\text{-isomer}}$ = –823.9178268–(–823.9188763) Hartree = 0.0010495*627.509391 kcal/mol = 0.6585 = kcal/mol.

Thus, the lower energy *trans*-diastereomer **203** would be expected to be the favoured isomer at equilibrium in free solution. In a similar manner as with the methyl esters **193** and **194** (see Section 2.3.1), application of the Curtin-Hammett principle, case 1,[167] once again leads us to expect that a more stable intermediate will lead to the formation of the *trans*-isomer **203** as the major product under thermal conditions (Scheme 60).

However, under kinetic control the intramolecular carbene insertion reaction will undergo carbon–carbon bond formation at a rate dependent on the energy of the transition state. The major isomer (*cis*-) will be formed via the lower energy transition state 1, while the minor isomer (*trans*-) will be formed from the higher energy transition state 2. Thus, according to the Curtin-Hammett principle, case 2,[157] the *cis*-isomer should be the major-isomer under kinetic conditions (Scheme 61).

Thus, we would expect the more stable *trans*-isomer to form as the major product under thermal conditions without catalyst, while with catalysts, under kinetic control, we would expect the less stable isomer to form as the major product. Thus, according to the Curtin-Hammett principle, case 2, the *trans*-isomer should be the major-isomer under thermodynamic conditions (Scheme 61). This would favour our intention to increase the proportion of the less bulky isomer forming within the clay mineral interlamellar region or zeolite pores.

Thermodynamically:

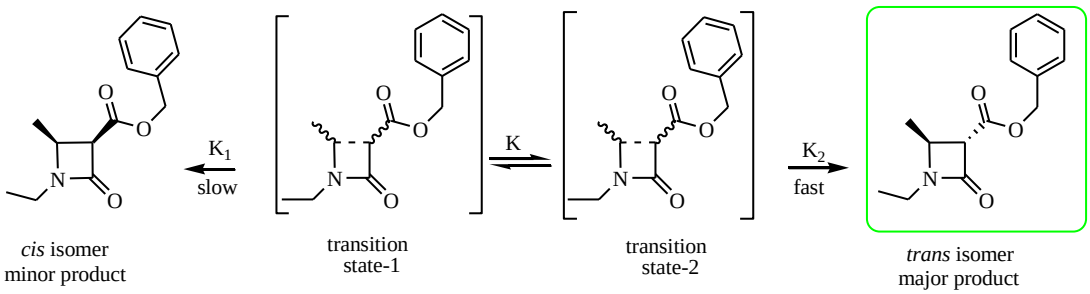

Scheme 60 Expected formation of the more stable *trans*-*β*-lactam 203 under thermodynamic conditions.

Kinetically:

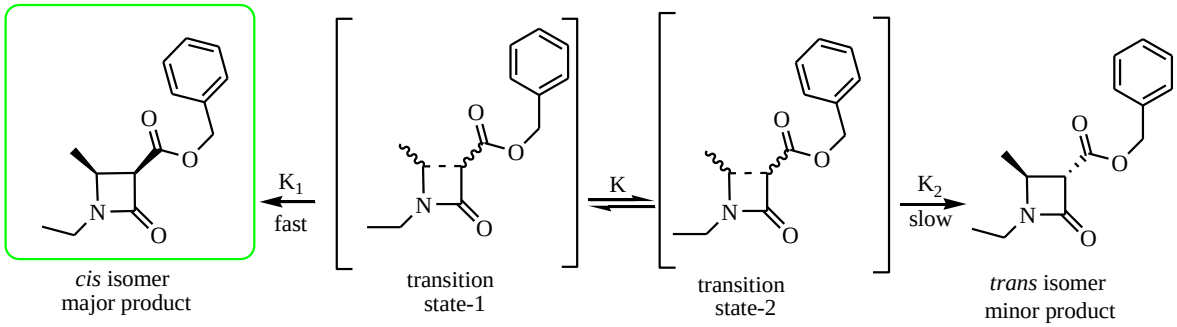

Scheme 61 Formation of less stable *cis*-*β*-lactam 202 under kinetic control conditions.

We had hoped that the greater steric demands of the benzyl group over the methyl group used previously should enhance the selectivity for the less bulky isomer. Once again, changing the solvent, which can be responsible for expanding the interlayer distance, should also have a significant effect on the selectivity over free solution reactions.

Energy minimised Chem 3D structures give an estimate of the relative sizes of the diastereomers (Figure 35).

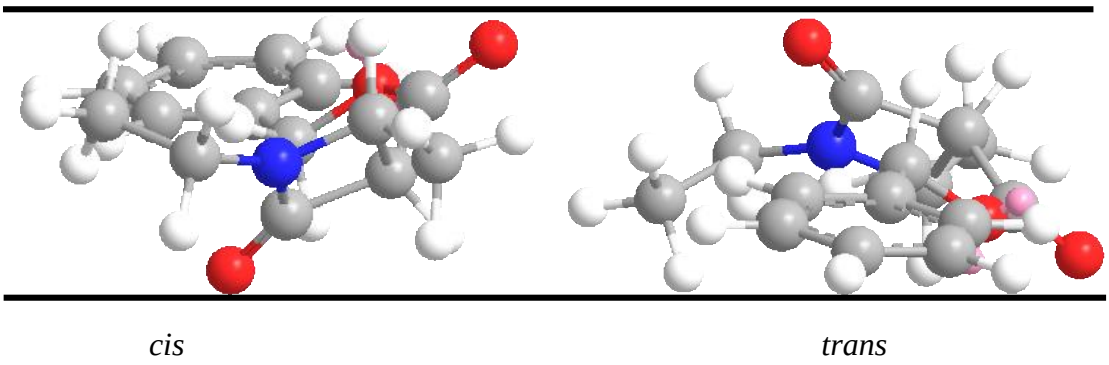

Figure 35 Chem 3D models of the structures of diastereomers 202 and 203.

Unfortunately, due to the planarity of the benzene ring these Chem 3D models (Figure 35) showed that the *cis*- and *trans*-isomers **202** and **203** had very little difference in height, however, the *cis*-isomer is narrower than the *trans*- and this may allow size selectivity.

This leads us to expect that neither the *cis*- nor the *trans*-diastereomer should predominate in free solution with the possibility of the *trans*-isomer becoming more predominant in low energy catalysed processes, whereas, the *cis*-diastereomer **202** is narrower and should be formed more readily in a narrow, restricted environment such as a zeolite pore, but not necessarily in a clay mineral interlayer.

2.4.1.3 Results of carbene reactions of benzyl *N,N*-diethylamidodiazomalonate 184

Similar to methyl *N,N*-diethylamidodiazomalonate **183**, benzyl *N,N*-diethylamidodiazomalonate **184** reacted without catalyst at 75°C in acetonitrile solvent to give a mixture of *β*-lactam diastereomers **202** and **203** with *cis-/trans*-isomer ratio 29 : 71.

Benzyl *N,N*-diethylamidodiazomalonate **184** was heated under reflux with ($Cu(acac)_2$) as catalyst at 75°C in acetonitrile solvent overnight, resulting in a complex mixture containing several by-products, but the *β*-lactam isomers were formed in less than 5% yield.

In order to determine whether there was any change in selectivity on replacing the methyl ester by the more bulky benzyl ester, catalytic reaction of benzyl *N,N*-diethylamidodiazomalonate **184** at 75°C within the clay mineral interlayer of Cu(II)-exchanged Wyoming bentonite in acetonitrile solvent gave a good yield of *cis*- and *trans-β*-lactams **202** and **203** (*ca.* 70% combined isolated yield) in the ratio 35 : 65 with *ca.* 5% of the *γ*-lactam **204** (Scheme 58). Thus, using the clay catalyst increased the proportion of what had been assumed to be the less bulky *cis*-isomer slightly compared to the uncatalysed reaction. Cu(II)-exchanged zeolite catalysts in acetonitrile solvent gave *ca*. 68% combined isolated yield with 4A zeolite with a *cis*-/*trans*-ratio of 71 : 29 and with ZSM-5 *ca*. 66% combined isolated yield with a *cis*-/*trans*-ratio of 62 : 38.

The ratio of *cis*- to *trans*-isomers (71 : 29) almost inverted compared to the uncatalysed reaction and when compared to the ratio obtained for the methyl ester under similar reaction conditions. Thus the benzyl ester **184** does give the less bulky isomer as a major product within the pores of the zeolites, but not within the interlayer space of the clay mineral with both acetonitrile and benzonitrile as solvent.

2.4.1.4 Effects of varying the solvent on the interlayer spacing of clay minerals

As discussed in Section 2.3.1.5 for the methyl ester **183** the solvent can have a profound effect within the clay minerals on the coordination of the carbene intermediate and on the release of the final product from the interlayer space of clay minerals. The effect of solvent on the interlayer space and reaction is shown in Table 8.

Table 8 Yields, isomer ratios and measured (XRD) Δd values for Cu(II)-Wyoming bentonite in various solvents.

Solvent	%Yield of *β*-lactams **202** & **203**	*cis-/trans-* diastereomer ratio	Interlayer distance of Wyoming bentonite, Δd (Å), assuming the clay layers ≈ 9.6 Å[164]
Acetonitrile	59	35 : 65	3.52
Benzonitrile	66	47 : 53	5.90
Toluene	60	55 : 45	3.36
Acetone	28	44 : 56	3.40
Tetrahydrofuran	20	69 : 31	3.80
*Chloroform	-	-	3.56
*Ethylbenzene	-	-	5.02
*Dichloromethane	-	-	3.52
*1,4-Dioxane	-	-	5.02

* Poor yields of product were obtained in the solvents chloroform, ethylbenzene, dichloromethane and 1,4-dioxane.

Interestingly, the proportion of the *cis*-*β*-lactam isomer **202** increased in most other solvents and almost reached 70 : 30 in THF, but unfortunately the yield was low in this case probably due to carbene insertion into solvent C-H bonds. This effect may be due to the increasing bulkiness of the solvent further constraining the reaction space in the mineral interlayer.

2.4.1.5 Effect of varying the layer charge of a clay mineral on the diastereomers 202 and 203

As discussed in Section 2.3.1.5 the effect of increasing the clay mineral layer charge can create a more restricted environment. The effects of changing solvents for the benzyl ester **184** are shown in Table 9.

Table 9 Measured yield, isomer ratios and Δd values for clay minerals in various solvents.

Clay Mineral	Solvents	%Yield of *β*-lactams **202** & **203**	*cis-/trans-* diastereomer ratio	Interlayer distance of Cu(II)-clay mineral, Δd (Å), assuming the clay layers ≈ 9.6 Å[164]
Wyoming bentonite	Acetonitrile	59	33 : 61	3.52
	Benzonitrile	66	47 : 53	5.90
	THF	20	69 : 31	3.80
	Acetone	38	44 : 56	3.40
	Toluene	60	55 : 45	3.36
Modified clay Al-O-EA	No solvent			3.09
	Acetonitrile	48	36 : 64	
	Benzonitrile	78	49 : 51	
Brett's Fullers earth	No solvent			2.52
	Acetonitrile	50	43 : 57	-
ZSM-5				Pore size 5.4 - 5.6 Å
	Acetonitrile	66	62 : 38	
	Benzonitrile	70	54 : 46	
	Acetone	26	33 : 67	
	Toluene	70	62 : 38	
	1,4-dioxane	-	-	
	THF	-	-	
4A molecular sieves				Pore size 5.5 - 7.4 Å
	Acetonitrile	68	71 : 29	
	Benzonitrile	71	75 : 25	
	Acetone	24	76 : 24	
	1,4-dioxane	-	-	
	THF	-	-	

Once again, the lower layer spacing for Brett's Fullers earth enabled more of the less bulky *cis*-isomer to form. Acetone, tetrahydrofuran and 1,4-dioxane were poor solvents in all cases. For the zeolite catalysts, except for acetone, changing the solvent had little effect on the reaction yields or isomer preference. The best yield of *β*-lactams was found with Al-O-EA modified Cu(II)-Wyoming bentonite with benzonitrile solvent, but the isomer ratio was almost 50 : 50.

2.4.1.6 Conclusions for reactions of benzyl *N*,*N*-diethylamidodiazomalonate 184

Due to the ester methyl group in *cis*- and *trans*-*β*-lactam isomers **193** and **194** there is a noticeable difference in the smallest molecular dimension; however, the greater planarity of the benzyl group in the *cis*- and *trans*-*β*-lactam isomers **202** and **203** results in a negligible difference in the smallest dimension of the molecules. There is a reasonable difference in the width of the two isomers, however, (the *cis*-isomer **202** being narrower) and this may lead to size selectivity. Thus we found that size selectivity in Cu(II)-exchanged clay minerals, where there is only one dimension of constraint, was minimal unless sterically demanding solvent or Al-O-EA modifications were present. In contrast, when Cu(II)-exchanged zeolite catalysts, which have two dimensions of constraint within their pores, were used, the narrower *cis*-isomer **202** became highly favoured, the greatest difference being seen for acetonitrile where *ca*. 35% *cis*-isomer **202** was formed in Wyoming bentonite, *ca*. 43% in Brett's Fullers earth and *ca*. 71% in zeolite A.

2.5 Carbene reactions of methyl *N*-ethyl-*N*-phenylamidodiazomalonate (methyl 2-diazo-2-[ethyl(phenyl)carbamoyl]acetate) 185

Similar to diazo compounds **183** and **184**, carbene intermediates were formed from methyl *N*-ethyl-*N*-phenylamidodiazomalonate **185** by thermolysis, while catalysis with Cu(II) clay minerals or Cu(II) zeolites gave a mixture of *β*-lactam diastereomers **205** and **206** as minor products with carbene insertion onto the *ortho*–CH of aromatic ring to form the indolidine **207** as a major product (Scheme 62).

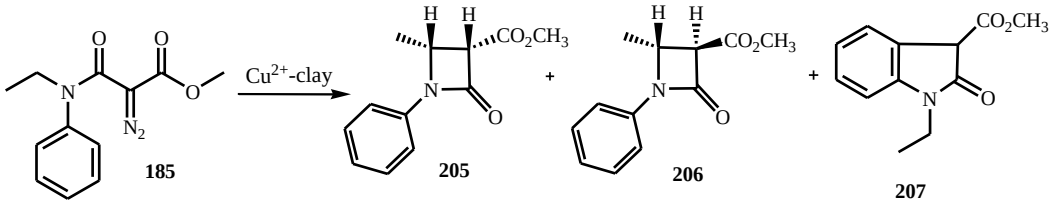

Scheme 62 Methyl *N*–ethyl-*N*-phenylamidodiazomalonate 185 insertion reactions forming *cis*- 205 and *trans*- 206 *β*-lactams (37 : 63) and aromatic C-H insertion reaction product 207.

Intramolecular carbene insertion into an ethyl methylene C–H bond forms a new carbon–carbon (C–C) bond giving a *β*-lactam rings **205** and **206** (Scheme 63).

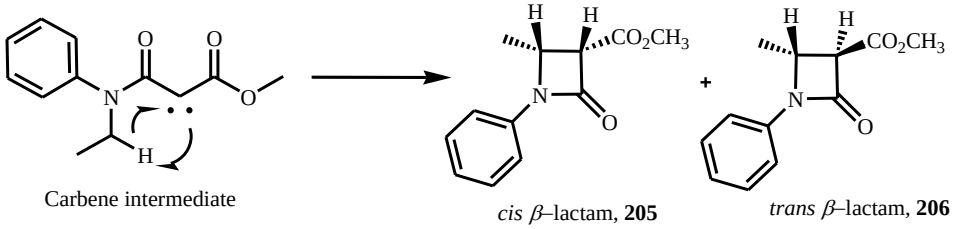

Scheme 63 Mechanism for the formation of *β*-lactam ring.

Another possibility is the intramolecular carbene insertion onto the *ortho* -C-H of the aromatic ring forming indolidine product **207** (Scheme 64).

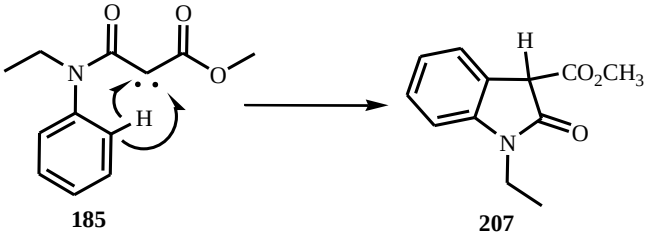

Scheme 64 Carbene insertion into the *ortho*-CH of the aromatic ring to form an indolidine product

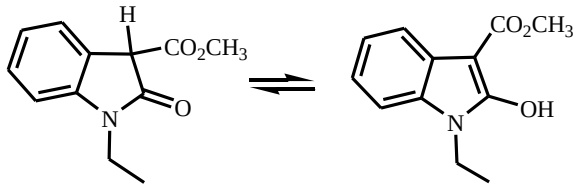

207

Scheme 65 Keto-enol isomerism of indolidine product 207.

2.5.1.1 Structure assignment of the *β*-lactams 205, 206 and indolidine product 207

The *cis*- and *trans*-diastereomers **205** and **206** were identified in a similar manner to the products obtained from methyl ester **183** and benzyl ester **184**, based on the assignment of their ^{1}H NMR spectra of the crude of *cis*- and *trans*-diastereomers **205** and **206**.

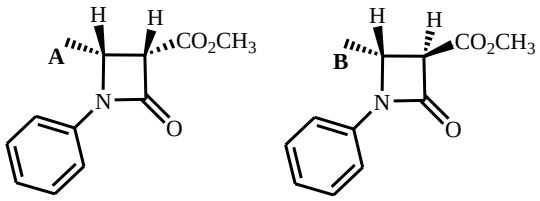

cis β–lactam, **205** *trans β*–lactam, **206**

Figure 36 Crude mixture showing *cis*- and *trans*-diastereomers 205 and 206.

From the crude ^{1}H-NMR spectra of the *β*-lactams **205** and **206** the doublet peaks at δ 1.53 (3H, J = 6.39 Hz) were assigned to the *cis*–isomer and 1.59 (3H, J = 6.11 Hz) to the *trans*-diastereomer. The yields of these products was very low (<10 mg) so further

characterisation was not carried out. The products were more clearly defined in the benzyl ester molecule **186** discussed in Section 2.6.1.1.

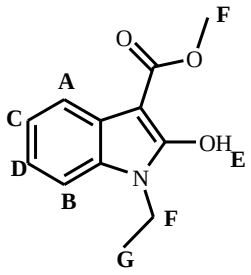

207

Figure 37 Indolidine product 207 resulting from carbene insertion into the *ortho*-aromatic –CH position.

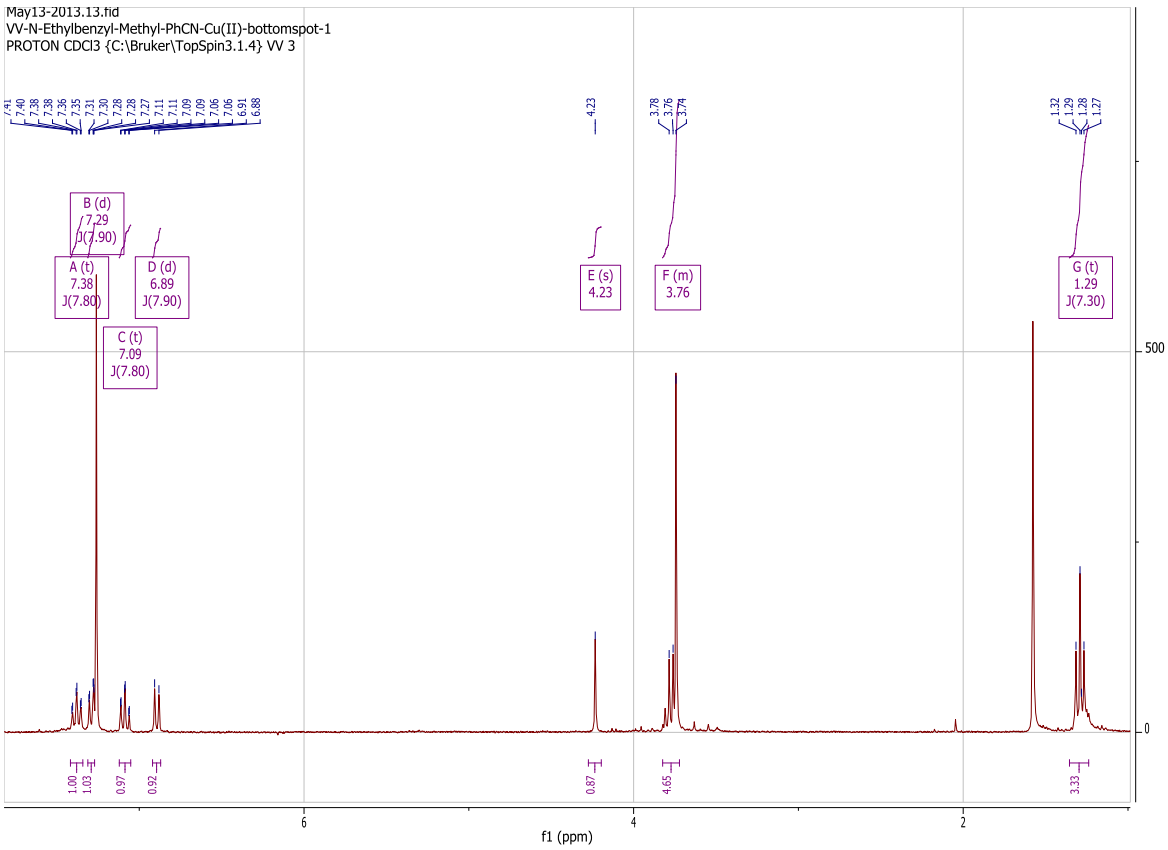

Figure 38 ^{1}H-NMR spectrum of carbene insertion product, forming indolidine 207.

The ^{1}H-NMR spectrum (Figure 38) showing aromatic protons with doublets at δ 6.89 and 7.29 and two triplets at δ 7.09 and 7.38 confirms compound **207** as a disubstituted aromatic

product and a broad (1H) singlet peak at δ 4.23 peak corresponds to –OH which may be due to phenolic compound **207** (Scheme 65) rearrangement of proton at E (Figure 37). The low δ value for the phenolic peak at 4.23 is probably due to the electron rich pyrrole ring lowering the chemical shift of the OH attached and also by H-bonding to the ester C=O.

2.5.1.2 Relative stabilities and bulkiness of the *β*-lactam diastereomers 205 and 206

Using VIs computer modelling, the energy difference of the *cis*- and *trans*-*β*-lactam diastereomers **205** and **206** were calculated:

$E_{cis\text{-isomer}} - E_{trans\text{-isomer}}$ = –745.311475–(–745.312885) Hartree = 0.0014108*627.509391 kcal/mol = 0.8852 kcal/mol. Thus, the lower energy *trans*-diastereomer would be expected to be the favoured isomer at equilibrium in free solution.

Thus the lower energy *trans* diastereomer **206** would be expected to be the favoured isomer in free solution in the similar manner to the methyl and benzyl ester *β*-lactams **193**, **194** and **202**, **203**. However, under kinetic control the carbene insertion reaction should undergo C-C bond formation at a rate dependent on the energy of the transition state. As discussed in section 2.4.1.2 the major (*cis*) isomer **202** will be formed via the lower energy transition state, while the minor (*trans*) isomer **203** will be formed from the higher energy transition state.

In the similar way to **183** and **184**, we expect that under thermal conditions without catalyst the more stable *trans*-isomer **206** should be formed as the major product. While with catalysts, under kinetic control, we would expect the less stable *trans*-isomer **206** to form as the minor isomer and the *cis*-isomer **205** as major product. Catalysed reactions within the interlayer space of clay minerals or the fixed pores of zeolites should increase the proportion of the more planar/less bulky *cis*-isomer. The sterically demanding *N*-phenyl group should enhance the selectivity of the less bulky isomer and it would be expected that changing the solvent within the clay minerals to affect the interlayer distance, should also have significant effect on the selectivity when compared to free solution reactions. Figure 39 shows energy minimised Chem 3D models of the *cis*- **205** and *trans*-*β*-lactam **206** isomers arranged to show

their smallest dimension. The *trans*-isomer **206** can be seen to be the more bulky isomer in this case, by some margin.

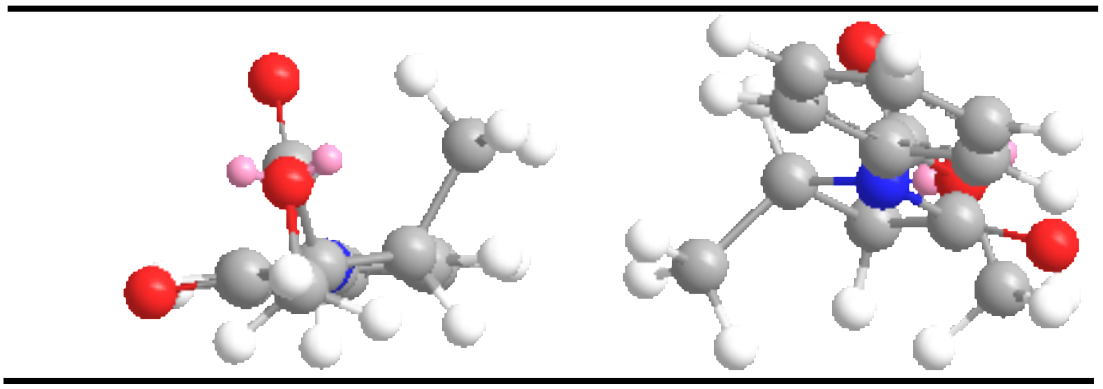

cis-isomer, less bulky *trans*-isomer, bulky

Figure 39 Chem 3D models of the structures of diastereomers 205 and 206.

Based on the Chem 3D structures (Figure 39) and VIs modelling, the *trans*-isomer **206** was found to be the more bulky and the thermodynamically favoured isomer and so should predominate in free solution, but there is the possibility of the less bulky *cis*-isomer becoming more predominant in lower energy catalysed processes. Under the restricted environment of the clay minerals, the *cis*-isomer, which is less bulky/more planar, should be more favoured.

2.5.1.3 Results of carbene reactions of methyl *N*-ethyl-*N*-phenylamidodiazomalonate 185

Similar to the reactions with methyl *N*,*N*-diethylamidodiazomalonate **183** and benzyl *N*,*N*-diethylamidodiazomalonate **184**, *N*-ethyl-*N*-phenylamidodiazomalonate **185** reacted with Cu^{2+}-Wyoming bentonite catalyst at 75°C in acetonitrile solvent to give a less than 10% yield (from crude) of a mixture of *β*-lactam diastereomers *cis*-isomer **205** and *trans*-isomer **206** in the ratio 37 : 63 (minor product) with carbene insertion at the *ortho* C-H of the aromatic ring producing the major indolidine product **207** (Figure 38) in ca. 38% isolated yield, whereas the uncatalysed reaction proceeded mainly through carbene insertion at the *ortho*-CH position of the aromatic ring with no *β*-lactam ring formation. Similarly, in benzonitrile without catalyst the reaction gave mixture of *β*-lactam diastereomers **205** and **206** with *cis*-/*trans*- isomer ratio of 24 : 76 (less than 10% yield from crude) and again the major cyclised products formed and

with Cu^{2+}-Wyoming bentonite, reaction proceeded to form indolidine **207**. When the same reaction was performed without catalyst in $CDCl_3$ solvent, monitoring every hour by ^{1}H-NMR spectroscopy and TLC showed there was little progress of the reaction even after 16 h at 75ºC, with only minor product formation, whereas in the Cu^{2+}-clay mineral, ^{1}H–NMR spectroscopy of the crude mixture showed progress in the reaction leading to carbene insertion into the *ortho* –CH position of the aromatic ring to give the indolidine product **207**.

For the formation of the minor *β*-lactam ring products, *cis*-isomer **205** and *trans*-isomer **206**, there was a strong solvent effect on the regioselectivity, however, the competitive *ortho*–aromatic CH insertion reaction was favoured in all cases.

There are literature examples of carbene insertion reactions into the *ortho* –CH of the aromatic ring to form indolidine products, for example see Scheme 66.[104]

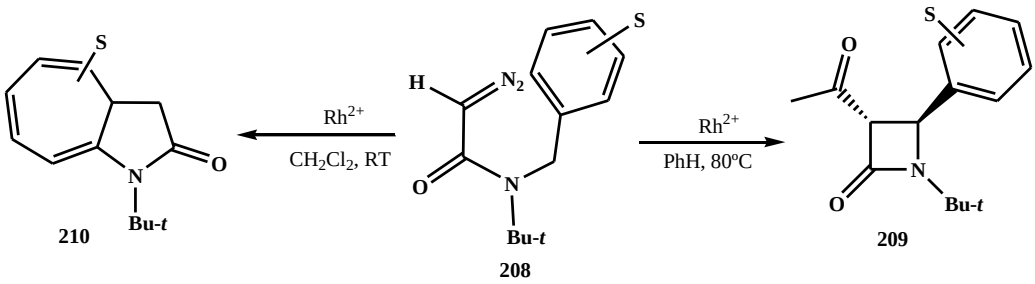

Scheme 66 Carbene insertion reactions forming the *β*-lactam 209 and indolidine 210 products.[104]

Scheme 67 shows the effects of *α*-substituents such as –H **212** and –$COCH_3$ **213**, on the C-H insertion into aromatic rings in the presence of dirhodium tetraacetate catalyst; showing that the *α*-substituent on the carbenoid carbon can have an effect on the chemoselectivity of the rhodium carbenoid.

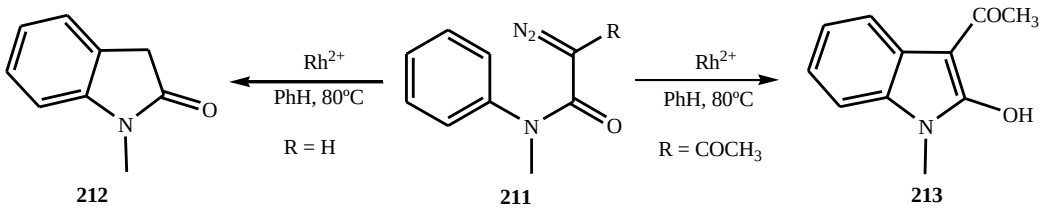

Scheme 67 Efficient carbene –C–H insertion into the aromatic ring with dirhodium tetraacetate.

The above example shows the effect of *N*-substituent and *α*-substituent of the diazo carbonyl compound favouring the carbene insertion at the *ortho*–CH position of the aromatic ring in the presence of a rhodium catalyst. Similarly, the carbene generated from methyl *N*-ethyl-*N*-phenylamidodiazomalonate **185** in the presence of Cu^{2+}-Wyoming bentonite catalyst favoured the insertion into the *ortho*-CH of the aromatic ring to give **207** and less towards the *β*-lactam ring formation *cis*-isomer **205** and *trans*-isomer **206**.

2.5.1.4 Conclusions for reactions of methyl *N*-ethyl-*N*-phenylamidodiazomalonate 185

The Chem 3D models of *cis*- and *trans*-*β*-lactam isomers **205** and **206** (Figure 38), showed that the size difference is mainly due to the bulky phenyl group giving a large "height" difference between the more bulky *trans*-isomer and less bulky *cis*-isomer. We found some quite obvious parallel results on comparison with diazoesters **183** and **184**. By using Cu(II)-exchanged Wyoming bentonite in the carbene insertion reaction of **185**, the reactions were much faster than the uncatalysed reactions in benzonitrile and acetonitrile solvents and gave indolidine **207** as the major product and with much lower yields of the *β*-lactam products **205** and **206**. The results obtained with insertion reactions of **185** are quite similar to literature reports[168] where the reaction favoured the formation of indolidine product **207** (Scheme 62). This shows that the *N*-phenyl substituent in **185** leads to insertion into the *ortho*–CH of the aromatic ring to form the indolidine product rather than the possibility of the less bulky *cis*-isomer **205**. Thus, in this case the Cu^{2+}-exchanged clay minerals can also help in formation of aromatic ring indolidine products.

2.6 Carbene reactions of benzyl *N*–ethylphenylamidodiazomalonate (benzyl 2-diazo-2-[ethyl(phenyl)carbamoyl]acetate) 186

Similar to methyl ester **183**, benzyl *N*–ethyl-*N*-phenylamidodiazomalonate **186** undergoes intramolecular carbene insertion reactions in the presence of Cu^{2+}-Wyoming bentonite catalyst to give a mixture of *β*-lactam ring compounds **214** and **215** as minor products, with carbene insertion into the *ortho*–CH of the aromatic ring to form the indolidine **216** as major product (Scheme 68).

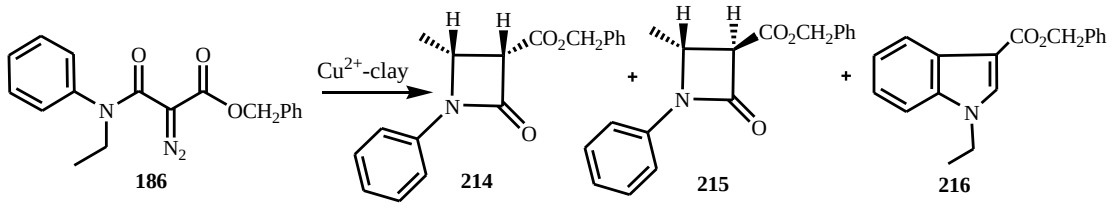

Scheme 68 Benzyl *N*–ethyl-*N*-phenylamidodiazomalonate 186 insertion reactions to form *β*-lactams 214 and 215 (13 : 87) and aromatic -C-H insertion product 216.

The possible carbene insertion reactions with benzyl *N*–ethyl-*N*-phenylamidodiazomalonate **186** are discussed below (Scheme 69).

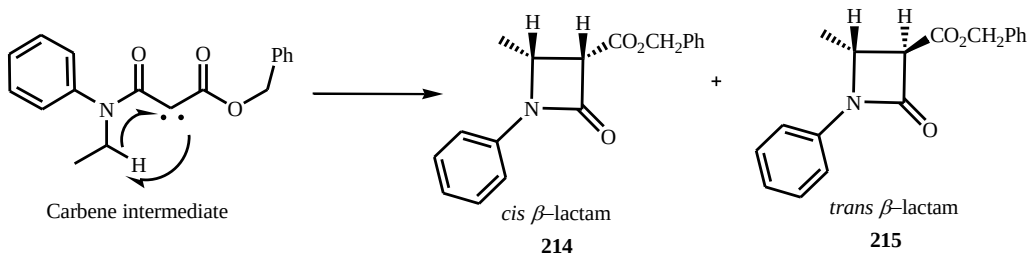

Scheme 69 Formation of *β*-lactam ring compounds 214 and 215.

Another possibility is the intramolecular carbene insertion onto the *ortho* -C-H of the aromatic ring forming indolidine product **216** (Scheme 70).

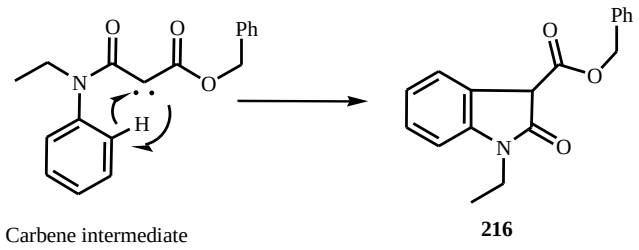

Scheme 70 Carbene insertion into the *ortho*-CH position of the aromatic ring forming indolidine 216.

2.6.1.1 Structure assignment of the *β*-lactam isomers 214, 215 and indolidine 216

The *cis*- and *trans*-diastereomers **214** and **215** were identified in a similar manner to the products obtained from methyl esters **183**, **185** and benzyl ester **184**, based on the assignment of the ^{1}H NMR spectra (Figure 41) of the *cis*- and *trans*-diastereomers **214** and **215**.

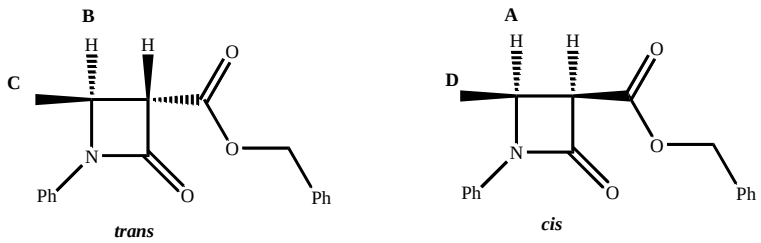

Figure 40 *cis*/*trans β*-lactam diastereomers 214 and 215.

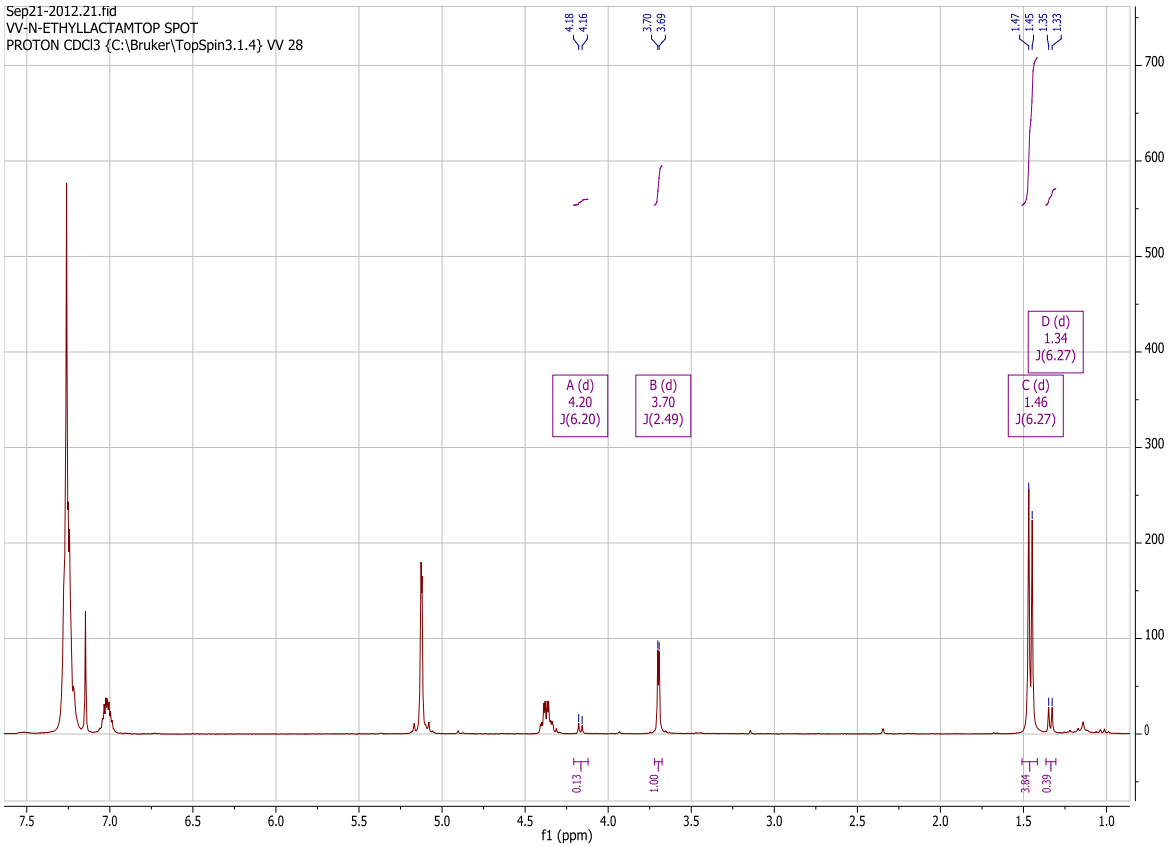

Figure 41 ^{1}H-NMR showing mixture of *cis-/trans-* diastereomers 214 and 215.

From the ^{1}H-NMR spectrum (Figure 41), the coupling constant values at δ 4.20 (d, J = 6.20 Hz, 1H, *N*-CH) were assigned to the *cis*-isomer and δ 3.70 (d, J = 2.49 Hz, 1H, *N*-CH) the *trans*-isomer respectively.

Carbene insertion into the aromatic ring should give the expected indolidine product **216** (Figure 41), but there was also competition with carbene insertion into the active CH of the acetonitrile to form **216a** which was evident from spectral data (Figure 43).

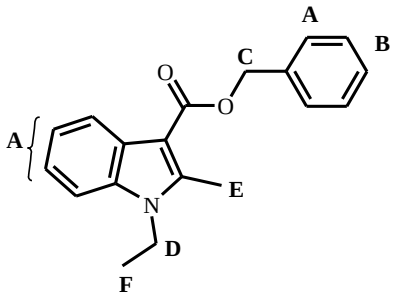

216a

Figure 42 Carbene insertion at aromatic -C-H forming indolidine product 216a.

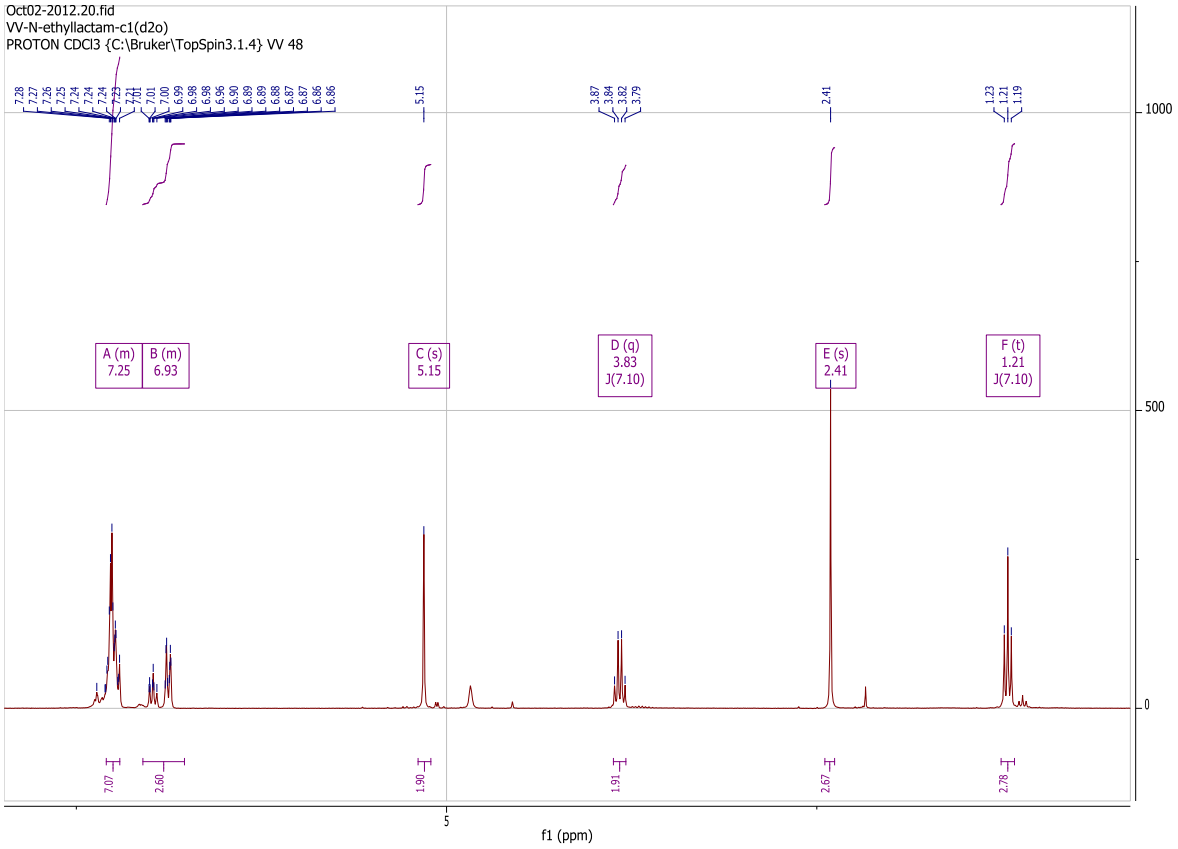

Figure 43 Carbene insertion into the *ortho*–CH of the aromatic ring to form an indolidine product 216a.

The ^{1}H-NMR spectrum (Figure 43) shows a three protons non-coupling methyl singlet, δ 2.43, that is similar to the methyl substituted product found during reaction of diazo

compound **183** in acetonitrile, which may be due to interaction of the solvent, acetonitrile, with the left over active -CH after the predominant insertion of the carbene intermediate into the -CH of the aromatic ring.

2.6.1.2 Relative stabilities and bulkiness of the *β*-lactam diastereomers 214 and 215.

Using VIs computer modelling, the energy differences of the *cis*- and *trans*-*β*-lactam diastereomers **214** and **215** were calculated.

$E_{cis\text{-isomer}}$ - $E_{trans\text{-isomer}}$ = –976.3130908–(–976.3145004) Hartree = 0.0014096*627.509391 kcal/mol = 0.8845 kcal/mol. Thus, the lower energy *trans*-diastereomer would be expected to be the favoured isomer at equilibrium in free solution.

Thus the lower energy *trans* diastereomer **215** would be expected to be the favoured isomer in free solution in a similar manner to **183**, **184** and **185** reactions. As discussed in sections 2.4.1.2 and 2.5.1.2 the major *cis*-isomer **214** will be formed via the lower energy transition state, while the minor *trans*-isomer will be formed from the higher energy transition state.

In a similar way to **183**, **184** and **185**, we would expect that the more stable *trans*-isomer **215** should be formed as the major product, under thermal conditions without catalyst and the *cis*-isomer **214** should be formed as minor product. While with catalysts, under kinetic control, we would expect the less stable *cis*-isomer **214** to form as the major isomer. As expected reaction within the interlayer space of clay minerals or fixed pores of zeolites should increase the proportion of the more planar/less bulky *trans*-isomer **215**. Due to the steric demands of the phenyl group and also on changing solvents within the clay minerals it should be possible to enhance the selectivity for the less bulky isomer when compared to free solution reactions.

Figure 43 shows energy minimised Chem 3D models of the *cis*- **214** and *trans*- **215** isomers arranged to show their smallest dimension. The *cis*-isomer **214** can be seen to be the more bulky isomer in this case, by a small margin.

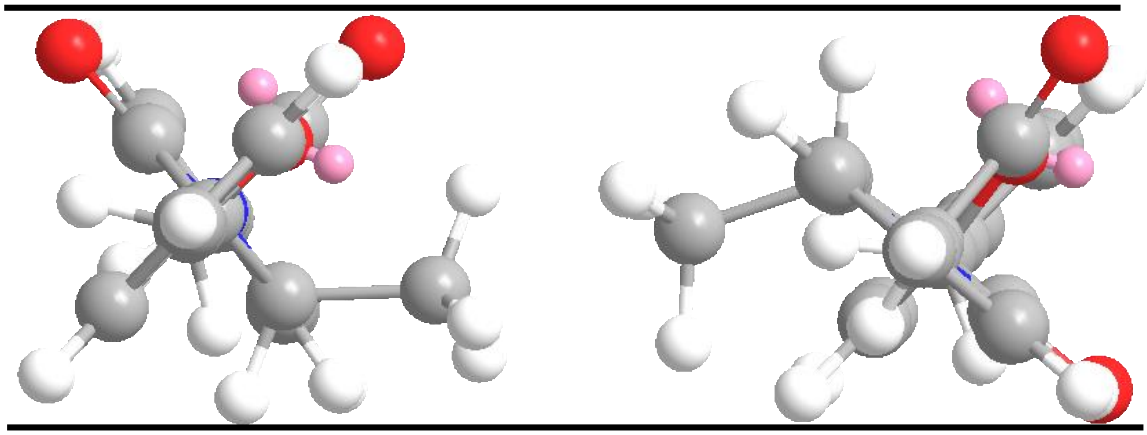

cis- bulky *trans*- less bulky

Figure 44 Chem 3D models of the structures of diastereomers 214 and 215.

Thus, from the Chem 3D model structures (Figure 44) and VIs calculated stabilisation energy values showed that the *trans* isomer is less bulky and lower in energy (-976.3145004) compared to the *cis*-isomer which gives information that the less bulky *trans*-isomer is expected to be the favoured isomer at equilibrium in free solution.

2.6.1.3 Results of carbene reactions of benzyl *N*–ethyl-*N*-phenyldiazomalonate 186.

Similar to diazo compounds **183**, **184** and **185**, compound **186** reacted with Cu^{2+}-Wyoming bentonite at 75°C in acetonitrile solvent to give a mixture of *β*-lactam diastereomers **214** and **215** with *cis*-/*trans*-isomer ratio 13 : 87 (isolated yield *ca*. 10%) (minor product) and also carbene insertion at the *ortho* position of the aromatic ring in ca. 36% isolated yield, whereas the uncatalysed reaction proceeded mainly through carbene insertion at the *ortho*-CH position of the aromatic ring with no *β*-lactam ring formation.

2.6.1.4 Effect of the substituent on the *α*-diazo carbonyl compounds *N*-benzyl-*N*-*tert*-butyl-2-diazoacetamide 206 and methyl 2-diazo-3-(methyl(phenyl)amino)-3-oxopropanoate 209.

From the literature,[169] due to the steric hindrance of the bulky benzyl group, formation of a *β*-lactam ring is more favoured, but when the same reactions were performed without catalyst there was minor product formation and the reaction did not go to completion at 75ºC. Examples of possible carbene insertion reactions dependent upon *N*-substituent were similar to those shown in Scheme 67.

2.6.1.5 Conclusions for reactions of benzyl *N*-ethyl-*N*-phenylamidodiazomalonate 186.

Due to the benzyl ester group in **214** and **215** there is a noticeable difference in the smallest molecular dimension. However, due to the planarity of the *N*-phenyl groups, the *cis*- and *trans*-*β*-lactam isomers **214** and **215** are both narrow so there is little "height" difference, but by comparing the width of the *cis*- and *trans*-*β*-lactam isomers **214** and **215** there is a noticeable difference in size showing the *cis*-isomer is more bulky compared to the *trans*-isomer. This leads us to expect that under free solution reaction conditions the low energy *trans*-isomer should be more favoured. Under catalytic and in free solution reaction conditions, because of a low energy transition state the less bulky *trans*-isomer should be favoured as the major isomer and the more bulky *cis*-isomer as the minor product. Similar to the reaction of methyl *N*-ethyl-*N*-phenylamidodiazomalonate **185**, the benzyl *N*-ethyl—*N*-phenylamidodiazomalonate **186**, would be expected to form the more planar/less bulky isomer within the interlamellar region of Cu^{2+}-exchanged clay minerals. Reactions with the Cu(II)-exchanged Wyoming bentonite were much faster than for the uncatalysed reaction and gave the indolidine product **216a** as the major product and much lower yields of the *β*-lactam products **214** and **215**. The results obtained with insertion reactions of **186** are quite similar to literature reports and the reaction is favoured towards the formation of indolidine product **213**, Scheme 67. This shows that the *N*-phenyl substituent in both **185** and **186** leads to insertion into the *ortho*–CH of the aromatic ring to form indolidine products **207** and **216a**. Thus both examples, **185** and **186**, prove that using Cu^{2+}-exchanged clay mineral catalysts can also help in the formation of indolidine type rings.

Thus we were interested in finding out the stereoselectivity effects within the restricted interlayer space of the clay mineral and fixed pores of zeolites with molecules that have cyclic amines (piperidine and pyrrolidine) attached to the diazo carbonyl group and also the effects of both the methoxy and benzyloxy substituted compounds, due to their differences in molecular sizes.

2.7 Carbene reactions of methyl *N*-piperidinodiazomalonate (methyl 2-diazo-3-oxo-3-(piperidin-1-yl)propanoate) 187.

Carbene intermediates were formed from methyl *N*-piperidinodiazomalonate **187** by photolysis, thermolysis and catalysis with copper(II) sulfate, Cu(II) clay minerals or Cu(II) zeolites to yield a mixture of the *β*-lactam diastereomers **217** and **218** (Scheme 71), together with small amounts of dimers **219** and **220** (Scheme 72) and a small amount of amino acid formed due to *β*-lactam ring cleavage.

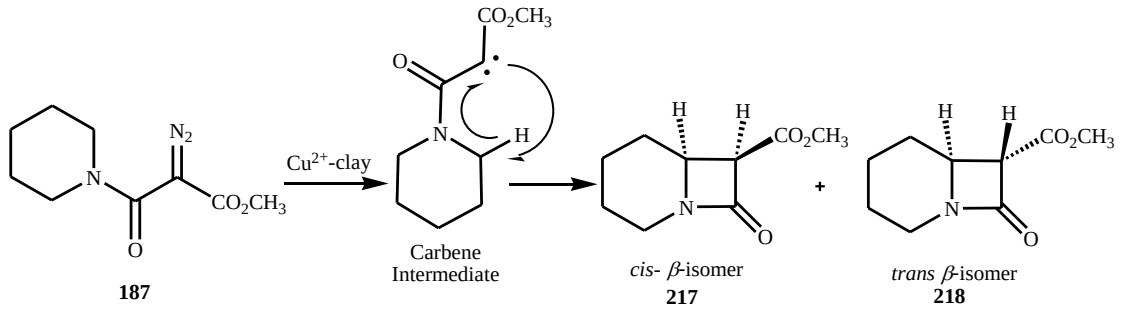

Scheme 71 Methyl *N*-piperidinodiazomalonate 187 insertion reaction forming *β*-lactam ring.

There is also a possibility of dimer formation with carbene addition reactions.

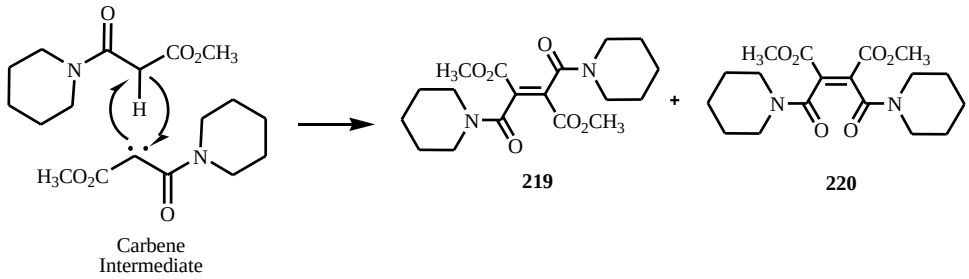

Scheme 72 Methyl *N*-piperidinodiazomalonate 187 insertion reaction forming *trans*-219 and *cis*-220 dimers.

2.7.1.1 Assignment of the structure of the bicyclic *β*-lactam isomer 218

The literature[170] ^{1}H–NMR spectra for the *β*-lactam isomers **217** and **218** were obtained on Varian T60 and A60A spectrometers and are reported in parts per million δ downfield of internal TMS. These ^{1}H-NMR do not provide sufficient information for differentiating between the two isomers **217** and **218**. We attempted to analyse the compounds based on assignment of their ^{1}H-NMR, ^{13}C-NMR, ^{1}H-^{1}H 2D COSY and ^{1}H-^{1}H 2D NOESY spectra. In the literature,[171,172] we found two bicyclic molecules **218a** and **218b** (Figure 45) which were nearly identical to **218** except for having different functional groups at position R (Figure 44). The literature data for **218a** and **218b** were quite useful for predicting the coupling constant (*J*) values and for identifying the δ values and splitting patterns of the piperidine ring hydrogens of **218** (Figure 46). Comparison with the literature values for acid molecule **218a** showed that the δ value at 3.75 (d, *J* = 1.80 Hz, 1H) with a 1.80 Hz coupling constant can be used to establish that the C-6 and C-7 protons are for the *trans β*-lactam.[172]

The ^{1}H NMR spectrum of the partially purified *trans β*-lactam isomer **218** (Figure 46) has a resonance δ 3.69 (d, *J* = 1.90 Hz, 1H), which is consistent with the literature values for analogue **218a**.[172] In a similar manner, the literature values of 7-bromo-1-azabicyclo[4.2.0]octan-8-one **218b** were useful for resolving the splitting pattern of the piperidine ring hydrogens which were close to the values for the *trans β*-lactam **218**, as discussed in Table 10.

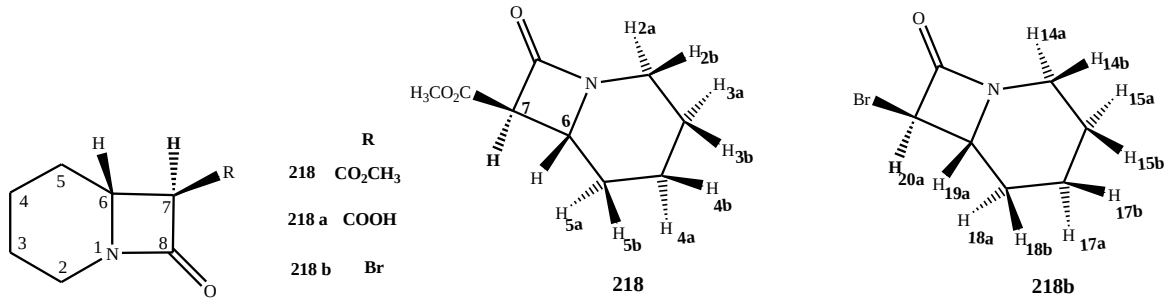

Figure 45 Structures of the substituted bicyclic *β*-lactam isomers

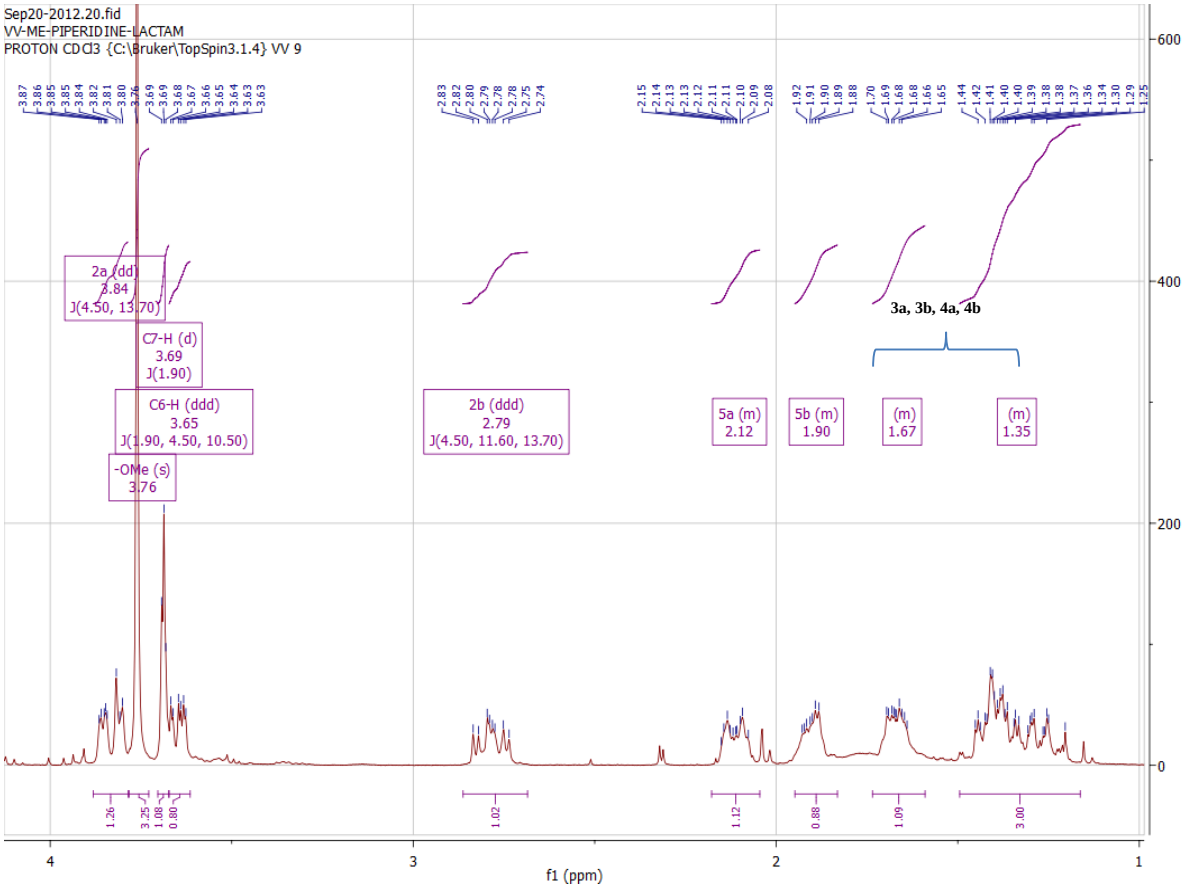

Figure 46 ^{1}H NMR spectrum of partially purified *trans β*-lactam isomer 218

Table 10 Assignments of ^{1}H NMR of bicyclic systems 218 and 218b

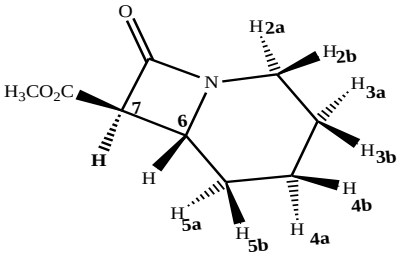 **218**		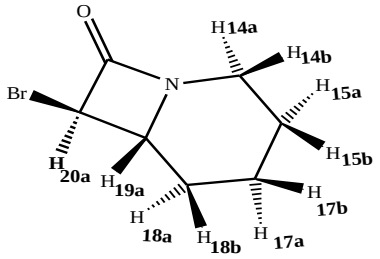 **218b**	
	δ values and (*J*) coupling Constants of **218**		δ values and (*J*) coupling Constants of **218b**
3a, 3b, 4a, 4b	1.16 – 1.73 (m, 4H)	15a, 15b, 16a, 16b	1.18 – 1.70 (m, 4H)
5b	1.83 - 1.95 (m, 1H)	18b	1.85 (m, 1H)
5a	2.05 – 2.18 (m, 1H)	18a	2.12 (m, 1H)
2b	2.79 (ddd, *J* = 4.50, 11.60, 13.70 Hz, 1H)	14b	2.74 (ddd, *J* = 4.33, 11.77, 13.47 Hz, 1H)
C6-H	3.65 (ddd, *J* = 1.90, 4.50, 10.50 Hz, 1H)	19a	3.51 (ddd, *J* = 1.04, 4.47, 10.69 Hz, 1H)
C7-H	3.69 (d, *J* = 1.90 Hz, 1H)	20a	4.39 (d, *J* = 1.13 Hz)
$-OCH_3$	3.76 (s, 3H, $-OCH_3$)	-	-
2a	3.84 (dd, *J* = 4.50, 13.70 Hz)	14a	3.81(dd, *J* = 4.52, 13.19 Hz)

2.7.1.2 Relative stabilities and bulkiness of the *β*-lactam diastereomers 217 and 218.

Using VIs computer modelling, the energy differences of the *cis*- and *trans*-*β*-lactam diastereomers **217** and **218** were calculated:

$E_{cis\text{-isomer}}$ - $E_{trans\text{-isomer}}$ = -631.0110152–(–631.0129177) Hartree = 0.0019025*627.509391 kcal/mol = 1.1938 kcal/mol. Thus, the lower energy *trans*-diastereomer would be expected to be the favoured isomer at equilibrium in free solution.

Thus, from VIs computer modelling and Chem 3D model structures calculation showed that the *trans*-form, with the less stable energy transition state should be favoured as a major isomer in free solution reaction.

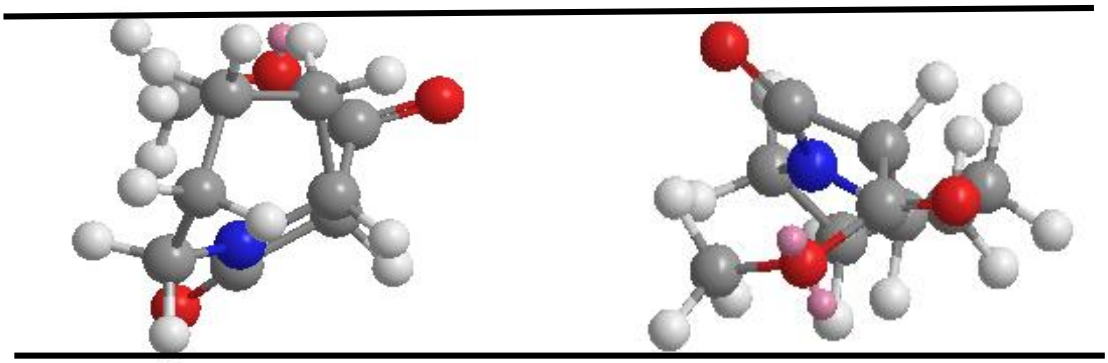

cis isomer *trans* isomer

Figure 47 Chem 3D model structures of *cis*- 217 and *trans*- 218 diastereomers.

There is a slight increase in bulkiness with the *cis*-isomer due to additional interactions between the carbonyl oxygen and the hydrogens of the piperidine ring. Due to these interactions the *cis*-isomer **217** is the slightly more bulky and stable isomer whereas for the flatter *trans*-isomer **218**, there is no such interaction and from Chem 3D models (Figure 47) the *cis*-isomer **217** looks more bulky than the *trans*-isomer **218**.

2.7.1.3 Results of carbene reactions of methyl *N*-piperidinodiazomalonate 187

Similar to other diazo carbonyl compounds, methyl *N*-piperidinodiazomalonate **187** reacted without catalyst at 75°C in acetonitrile solvent to give a mixture of *β*-lactam diastereomers **217** and **218** with *cis-/trans*-isomer ratio 2 : 98 (isolated yield *ca*. 66%). Reaction was faster when compared to uncatalysed, i.e. without catalyst under thermal conditions. In contrast, when a free solution catalysed reaction of methyl *N*-piperidinodiazomalonate **187**, heated under reflux with ($Cu(acac)_2$) as catalyst at 75°C in acetonitrile solvent overnight, the result was a complex mixture containing several by-products, with no *β*-lactam isomers being formed. When the same reaction was performed under photolytic conditions using dichloromethane as a solvent, the less bulky *trans*-isomer was formed as the major product with (*ca*. 60% isolated yield).

From the literature,[170] the photolysis of bicyclic diazo tetramic acid **221** gave *β*-lactams **217** and **218** with 65% yield as a 2 : 5 mixture (Scheme 73). *β*-Lactam **217** epimerised to **218** with great ease, even in the apparent absence of a proton carrier, thus leaving the relative amounts of **217** and **218** initially formed open to question.

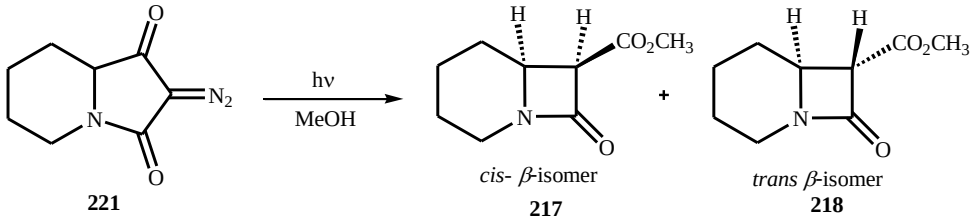

Scheme 73 Photolysis of tetramic acid to *β*-lactam isomers.

When the carbene insertion reactions (Scheme 71) were performed with the Cu(II)-exchanged mineral catalysts in acetonitrile or benzonitrile solvent, it was surprising that this reaction once again formed the *trans*-isomer **218** as the major product with a *cis*-/*trans*-isomer ratio of 2 : 98. This may be due to the restrictions in the interlayer space of clay minerals or zeolites. Benzonitrile solvent gave the highest yield with acetonitrile next and other solvents forming various solvent insertion products.

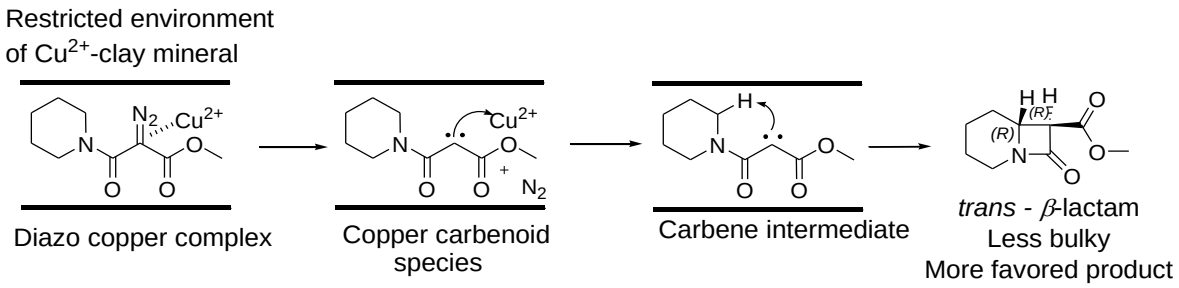

Figure 48 Mechanism of carbene formation in cation exchanged–clay mineral in order to form less bulky *β*-lactam.

For example, when this reaction was performed with a series of catalysts (as shown in Table 9, Section 2.4.1.5) and in various different solvents (Table 11) like toluene, tetrahydrofuran,

ethylbenzene and 1,4-dioxane the major products were the carbene dimers **219** and **220** (Scheme 72). This was similar to the dimer formation from ethyl diazoacetate **33** giving the dimers diethyl fumarate **232** and diethyl maleate **233**, which will be discussed in Chapter 3.

2.7.1.4 Effects of varying the solvent on the interlayer spacing of clay minerals

Table 11 shows the effect of changing solvent on the yields of the carbene insertion reaction of **187**.

Table 11 Measured (XRD) Δd values for Cu(II)-Wyoming bentonite in various solvents

Solvent	%Yield of *β*-lactams **217** & **218**	*trans*-diastereomer ratio	Interlayer distance of Wyoming bentonite, Δd (Å), assuming the clay layers ≈ 9.6 Å[164]
Acetonitrile	66	98 (*trans*)	3.52
Benzonitrile	72	98 (*trans*)	5.90
Toluene	28	98 (*trans*)	3.36
Acetone	-	-	3.40
Tetrahydrofuran	-	-	3.80
Others: Chloroform D_2O	 60 -	 98 (*trans*) -	3.56
Ethylbenzene	-	-	5.02
Dichloromethane	-	-	3.52
1,4-Dioxane	-	-	5.02

Thus good yields were obtained in benzonitrile, acetonitrile and chloroform whereas in other solvents like ethylbenzene, 1,4-dioxane, etc., there may be the difficulty of insertion at the active –CH position of the solvent and also the starting material was leading to carbene dimer products. Dichloromethane was a low boiling solvent and the reaction was only initiated at >75°C.

Due to the complexities with identification by ^{1}H-NMR spectroscopy, GC/MS was used to quantify the isomer ratios, Figure 49. The GC-MS spectra of *cis*- **217** and *trans*- **218**

diastereomers showed *m/z*: 183 (M^+), 155 (M^+ –CO), 124 (M^+ –CO_2Me) and 83 ($C\text{-}N{=}CH(CH_2)_4^+$).

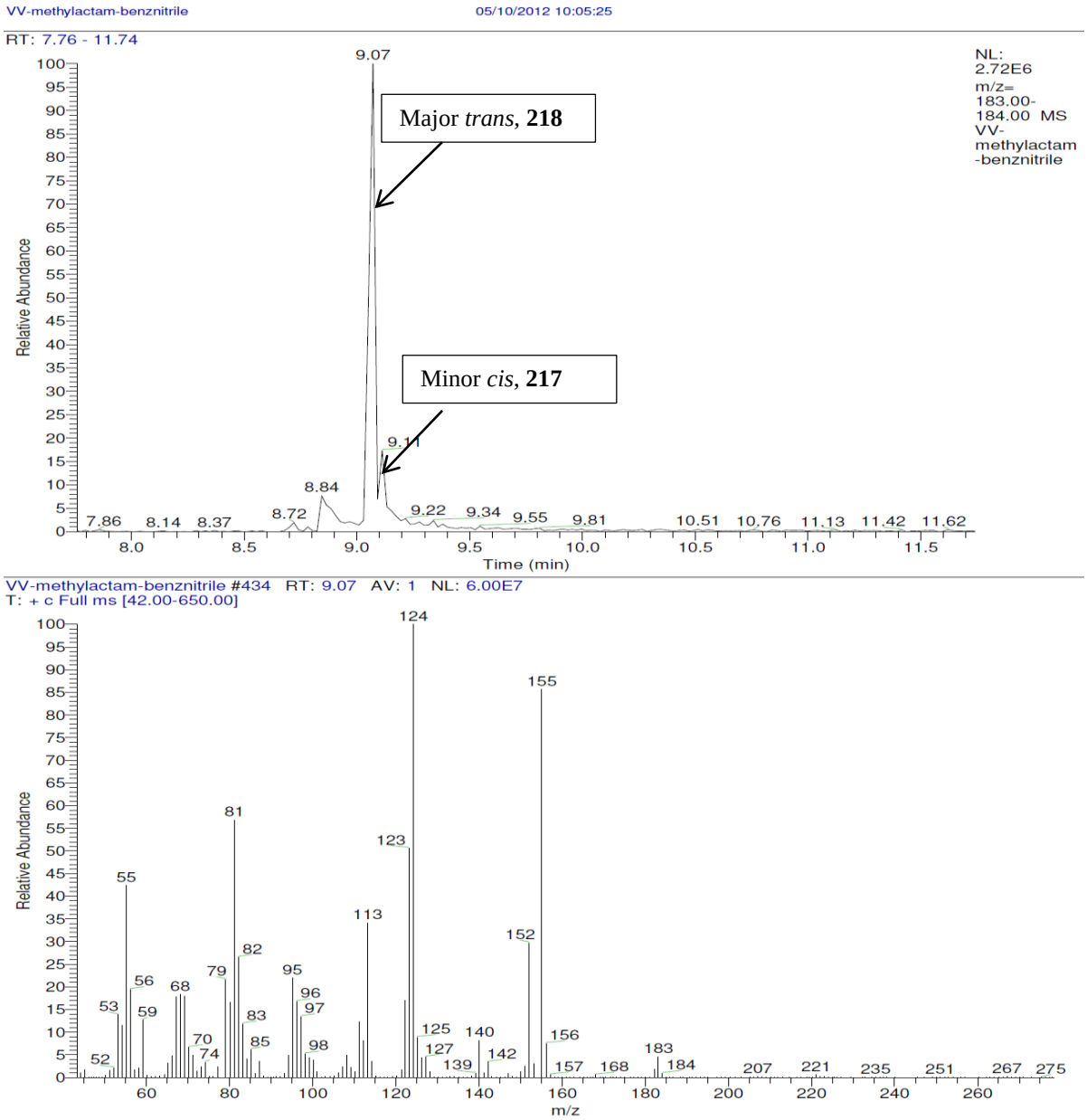

Figure 49 Reaction in benzonitrile solvent using clay mineral catalyst.

2.7.1.5 Conclusions for reactions of methyl *N*-piperidinodiazomalonate 187

Due to the arrangement of the bulky piperidine and ester methyl groups in the *cis*- and *trans*-*β*-lactam isomers **217** and **218** there is a noticeable difference in the smallest molecular dimension; there is a reasonable difference in the width of the two isomers, the *trans*-isomer being narrower, may lead to size selectivity. The bulkiness of the *cis*-isomer was further increased by interaction of the carbonyl oxygen and the hydrogen of the piperidine group, thus we found that size selectivity during the catalysed reaction within the restricted interlamellar region of the Cu^{2+}-exchanged clay mineral, favoured the more planar/less bulky *trans*-isomer. However, we found some interesting results: in most cases when using Cu(II)-exchanged clay mineral and zeolite catalysts in the carbene insertion reaction of **187**, the reactions were much faster than the uncatalysed reactions in all solvents and tended to give higher yields of the *β*-lactam products **217** (minor) and **218** (major) together with small amounts of carbene dimer by-products **219** and **220** and some ring-opened lactam acid.

Thus, it then led us to explore the effects of the more sterically demanding bulky benzyl ester group attached as in **188**, to see if this would show differences in size similar to that observed for the other two isomers.

2.8 Carbene reactions of benzyl piperidinodiazomalonate compound (benzyl 2-diazo-3-oxo-3-(piperidin-1-yl)propanoate) 188

Carbene intermediates were formed from benzyl piperidinodiazomalonate **188** by photolysis, thermolysis and catalysis with: copper(II) sulfate, Cu(II) clay minerals or Cu(II) zeolites, to yield a mixture of the *β*-lactam diastereomers **221** and **222** (Scheme 74), with small amounts of dimers **223** and **224** (Scheme 75) and the lactam acid formed by *β*-lactam ring cleavage.

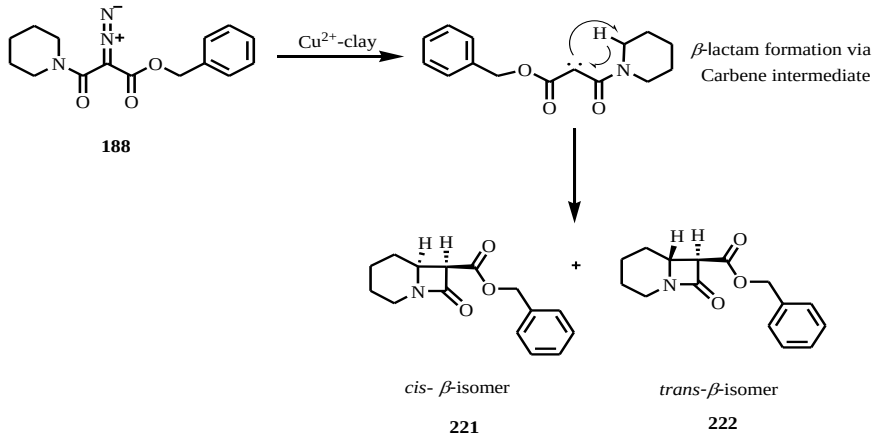

Scheme 74 Carbene insertion reaction of piperidine benzyl diazo compound 188 forming *β*-lactams 221 and 222.

Possibility:

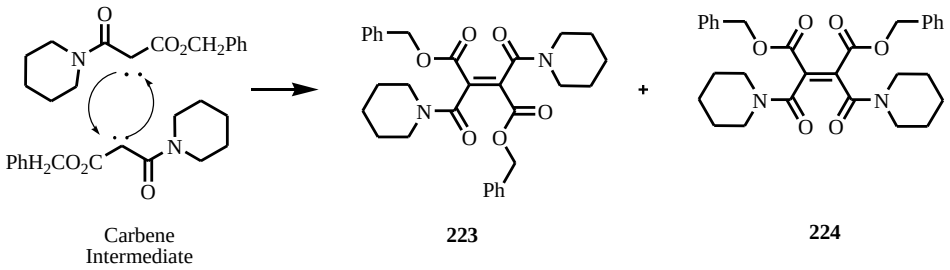

Scheme 75 Carbene addition reaction forming dimers 223 and 224.

2.8.1.1 Assignment of the structures of the *β*-lactam isomers 221 and 222

This was done in the usual manner from the nmr spectra (including Figure 51).

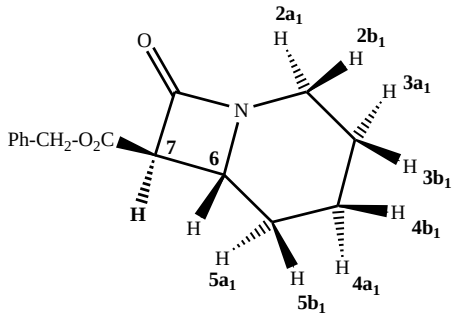

222

Figure 50 ***trans*-isomer of *β*-lactam 222**

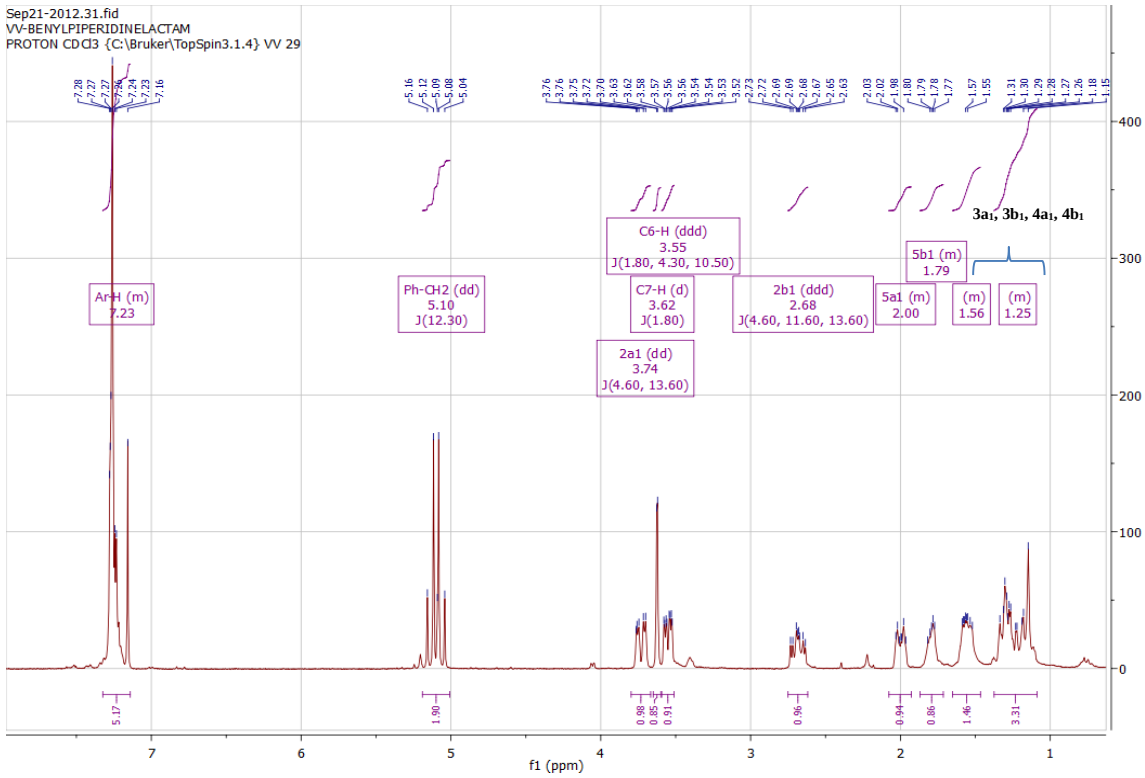

Figure 51 **^{1}H-NMR of *trans β*-lactam 222.**

Table 12 Assignments of the ^{1}H NMR Spectra of bicyclic *β*-lactams 222 and 218b

	δ values and (*J*) coupling Constants of **222**		δ values and (*J*) coupling Constants of **218b**
$3a_1$, $3b_1$, $4a_1$, $4b_1$	1.09 – 1.65 (m, 4H)	15a, 15b, 16a, 16b	1.18 – 1.70 (m, 4H)
$5b_1$	1.71 – 1. 87 (m, 1H)	18b	1.85 (m, 1H)
$5a_1$	1.93 – 2.08 (m, 1H)	18a	2.12 (m, 1H)
$2b_1$	2.68 (ddd, *J* = 4.60, 11.60, 13.60 Hz, 1H)	14b	2.74 (ddd, *J* = 4.33, 11.77, 13.47 Hz, 1H)
C6-H	3.55 (ddd, *J* = 1.80, 4.30, 10.50 Hz, 1H)	19a	3.51 (ddd, *J* = 1.04, 4.47, 10.69 Hz, 1H)
C7-H	3.62 (d, *J* = 1.80 Hz, 1H)	20a	4.39 (d, *J* = 1.13 Hz)
$2a_1$	3.74 (dd, *J* = 4.60, 13.60 Hz)	14a	3.81 (dd, *J* = 4.52, 13.19 Hz)
$-OCH_2$	5.10 (dd, *J* = 12.30 Hz, 2H, $-OCH_2Ph$)	-	-
Ar-H	7.14 – 7.32 (m, 5H, Ar-H)	-	-

From Table 12, the δ values of the benzyl *trans β*-lactam **222** were consistent with those reported for the *trans β*-lactam methoxy and bromo compounds **218** and **218b**. The singlet peak at δ 5.22 that corresponds to the benzylic CH_2 (PhC**H**$_2$) of the diazo compound **188** had disappeared and a new dd had formed at δ 5.10, which represents the diastreomeric CH_2 of the benzylic group and also the C7-H of the *β*-lactam ring, with a coupling constant *J* = 1.80 Hz, which was also consistent with the data for **218** and **218b**.

2.8.1.2 Relative stabilities and bulkiness of the *β*-lactam diastereomers 221 and 222

Using VIs computer modelling, the energy differences of the *cis*- and *trans*-*β*-lactam diastereomers **221** and **222** were calculated:

$E_{cis\text{-isomer}}$ - $E_{trans\text{-isomer}}$ = -862.0131511–(–862.0156775) Hartree = 0.0025264*627.509391 kcal/mol = 1.5853 kcal/mol. Thus, the lower energy *trans*-diastereomer **222** would be expected to be the favoured isomer at equilibrium in free solution.

Thus in comparison with the methyl ester and benzyl ester *cis*- **221** and the *trans*-isomer **222** and the more bulky *cis*- and less bulky *trans* will be assumed to be size difference by width of

both isomers. Thus, under thermodynamic conditions the less stable *trans*-isomer should form as a major isomer and the *cis*-isomer as the minor isomer.

2.8.1.3 Effects of varying the solvent on the interlayer spacing of clay minerals

Similar to those listed in Table 11, Table 13 shows that there is also an effect on the yields of the carbene insertion reactions of **188**. When compared, the yields from benzonitrile to acetonitrile and chloroform are good. This shows that by judicious choice of solvents such as acetonitrile and benzonitrile, the interlayer space of the clay mineral can be kept just wide enough to form the less bulky *trans*-isomer. In other solvents like ethylbenzene and 1,4-dioxane, there may be loss of yield due to the insertion at the active –CH position of the starting material, which leads to dimer products and other major impurities; whereas dichloromethane is a low boiling solvent and the reaction appears to be initiated at > 75°C.

Table 13 Measured (XRD) Δd values for Cu(II)-Wyoming bentonite in various solvents

Solvent	%Yield of *β*-lactams **221** & **222**	*trans-/cis*-diastereomer ratio	Interlayer distance of Wyoming bentonite, Δd (Å), assuming the clay layers ≈ 9.6 Å[164]
Acetonitrile	64	98% (*trans*)	3.52
Benzonitrile	68	98% (*trans*)	5.90
Toluene	20	98% (*trans*)	3.36
Acetone	-	-	3.40
Tetrahydrofuran	-	-	3.80
Others Chloroform	58	98% (*trans*)	3.56
D_2O	-	-	-
Ethylbenzene	-	-	5.02
Dichloromethane	-	-	3.52
1,4-Dioxane	-	-	5.02

2.8.1.4 Results of carbene reactions of benzyl piperidinodiazomalonate compound 188

By using chloroform as a solvent with Cu^{2+}-clay mineral we observed four different products. One pair is the *trans*- and *cis*-*β*-lactam isomers, of which the *trans*-isomer was the major

product and the second pair are the *cis*- and-*trans* alkenes due to carbene dimer formation from the carbene intermediates. This reaction is proof that, the syntheses of cyclopropane rings using ethyl diazoacetate with various alkenes will form diethyl fumarate and diethyl maleate (Scheme 80) as minor products along with cyclopropane rings as will be discussed in Chapter 3. This reaction was also carried out thermally without using catalyst and also by using catalysts such as Brett's Fullers earth, Los Trancos and Cu^{2+}-Al-O-EA in various solvents such as 1,4-dioxane, toluene, chloroform and benzonitrile.

2.8.1.5 Conclusions for reactions of benzyl piperidine diazomalonate 188

Similar to the reaction with **187**, the benzyl piperidino diazo compound **188** should undergo reaction within the restricted interlamellar region of the Cu^{2+}-exchanged clay mineral to favour the more planar/less bulky *trans*-isomer. By using Cu(II)-exchanged clay mineral and zeolite catalysts in the carbene insertion reaction of **188**, the reactions were much faster than the uncatalysed reactions in all solvents and tended to give higher yields of the *β*-lactam products **221** (minor) and **222** (major), as well as carbene dimer by-products **223** and **224**. When compared to the uncatalysed reaction in free solution, the mineral catalysed processes gave a mixture of the *cis*-isomer **221** (minor) and the more thermodynamically stable *trans*-isomer **222**, with good yields. The proportion of the less bulky *cis*-isomer could be improved by judicious choice of solvent, clay mineral layer charge or zeolite type, but even with the best of these the proportion of the slightly less bulky *cis*-isomer could not be improved over the catalyst free reaction. This suggests that the catalysed reaction, which usually favours the thermodynamic *trans*-product **222**, can be overcome to a small degree during the reaction of diazo compound **188** in the restricted inner regions of the mineral catalysts, but that the size difference of the *β*-lactam diastereomers **221** and **222** is not great enough to allow great size selection.

Thus we were led to choose to examine five membered ring heterocyclic ring systems which showed a greater difference in size of the two diastereomers from Chem 3D modelling and to find out whether the restricted environment will show greater stereoselectivity for diastereomer formation within the clay mineral interlayers or in fixed pores of zeolites.

2.9 Carbene reactions of methyl pyrrolidinodiazomalonate (methyl 2-diazo-3-oxo-3-(pyrrolidin-1-yl)propanoate) 189

The conversion of methyl pyrrolidinodiazomalonate **189** to the *β*-lactams **225** and **226** (Scheme 76) was attempted by the usual means, however only carbene dimers **227** and **228** (Scheme 77) were formed.

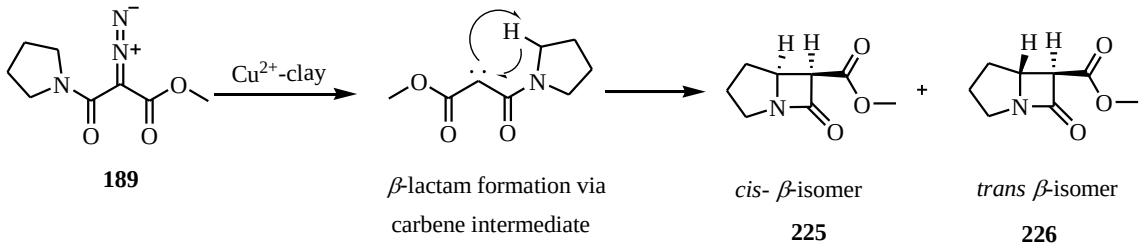

Scheme 76 Carbene insertion reaction of methyl pyrrolidinodiazomalonate 189 to form *β*-lactams 225 and 226.

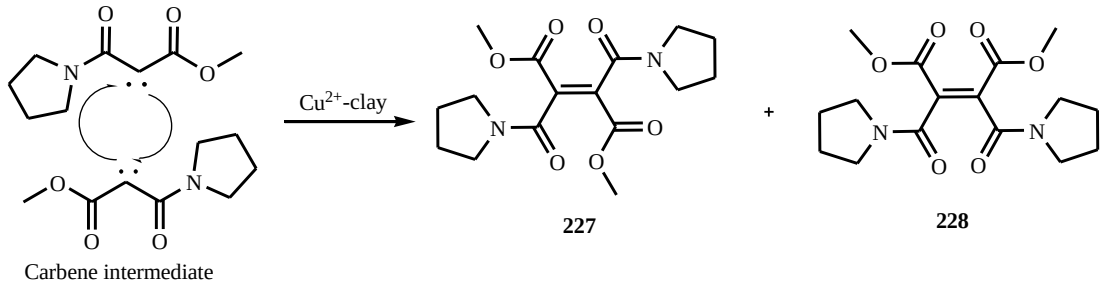

Scheme 77 Carbene addition reaction forming dimers 227 and 228.

2.9.1.1 Attempted assignment of the structures of the *β*-lactam isomers 225 and 226

The complex ^{1}H-NMR spectrum (Figure 52) shows the formation of carbene dimer products only, with broad resonances attributed to the pyrrolidine protons at δ 3.45 and δ 1.80 - 1.93,

the methoxy peaks in the δ 3.7 - 3.8 region with a complex mixture of *cis*- and *trans*-dimers and small amounts of the lactam acid were also seen.

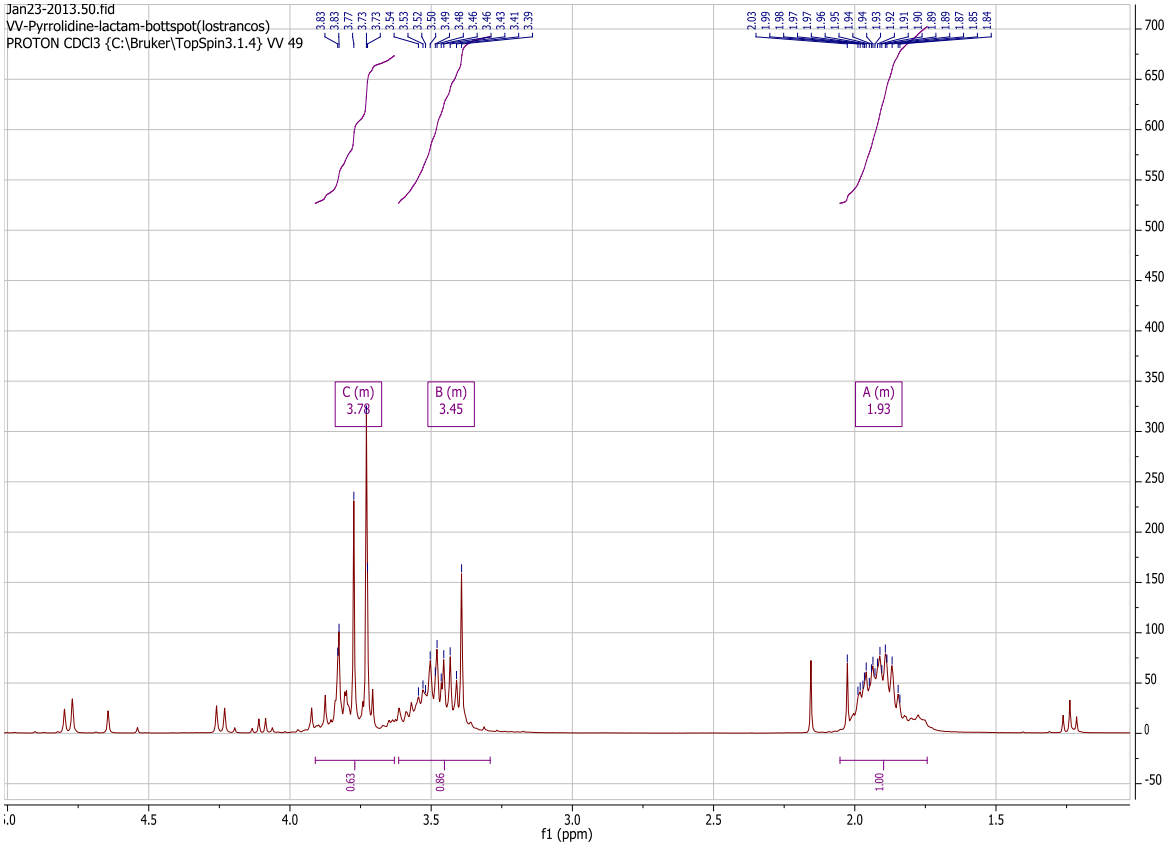

Figure 52 Dimer products from methyl pyrrolidinodiazomalonate 189.

2.9.1.2 Relative stabilities and bulkiness of the *β*-lactam diastereomers 225 and 226

Using VIs computer modelling, the energy differences of the *cis*- and *trans*-*β*-lactam diastereomers **225** and **226** were calculated:

$E_{cis\text{-isomer}}$ - $E_{trans\text{-isomer}}$ = -862.0131511–(–862.0156775) Hartree = 0.0025264*627.509391 kcal/mol = 1.5853 kcal/mol. Thus, the lower energy *trans*-diastereomer would be expected to be the favoured isomer at equilibrium in free solution.

Thus from VIs computer modelling and the Chem 3D model structures (Figure 53) shows the *cis*-isomer should be less stable, but could still form as the major isomer in free kinetic controlled solution reactions.

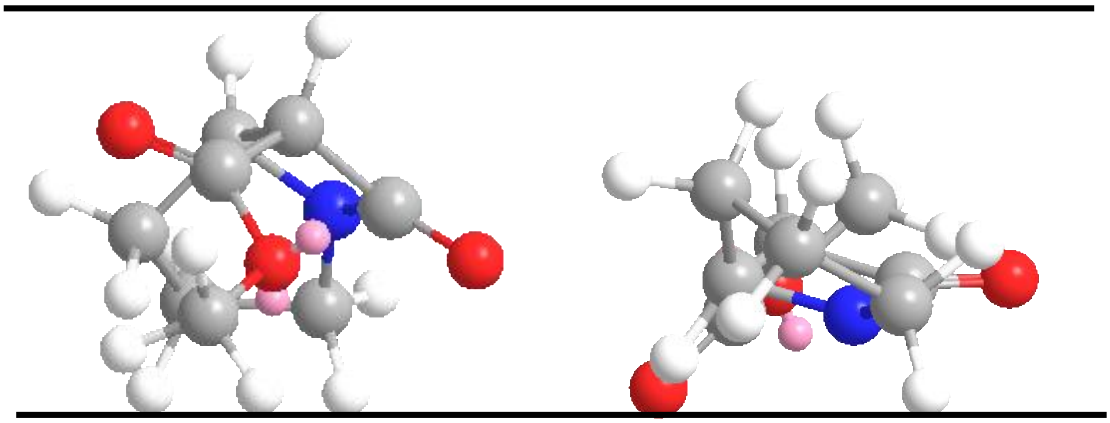

cis isomer *trans* isomer

Figure 53 Chem 3D structures of the diastereomers 225 and 226.

2.9.1.3 Conclusions for reactions of methyl pyrrolidinodiazomalonate 189

On using uncatalysed and clay mineral catalysed reactions we found that there were no *β*-lactam products from this precursor **189**, the five membered ring of pyrrolidine was unable to undergo carbene addition reactions, but instead formed carbene dimers. This suggests that either the pyrolidine C-H bonds are too far away to allow easy carbene insertion, or the very strained 4,5-bicyclic ring system would be expected to ring open rapidly under the hydrolytic conditions within the clay mineral. This is supported by the literature,[7] when diazo compound **189** was treated with dirhodium tetraacetate in dichloromethane solvent, the reaction did not proceed as expected from Scheme 77 and only starting material **189** was recovered.

2.10 Carbene insertion reaction of methyl 1-phenylethylamidodiazo-malonate (methyl 2-diazo-2-[(1-phenylethyl)carbamoyl]acetate) 191.

It was hoped that the diazo compound **191** would present the possibility of greater steric hindrance, so helping choice of the less bulky isomer and giving either *β*-lactams **229** or **230** or a *γ*-lactam product (Scheme 78).

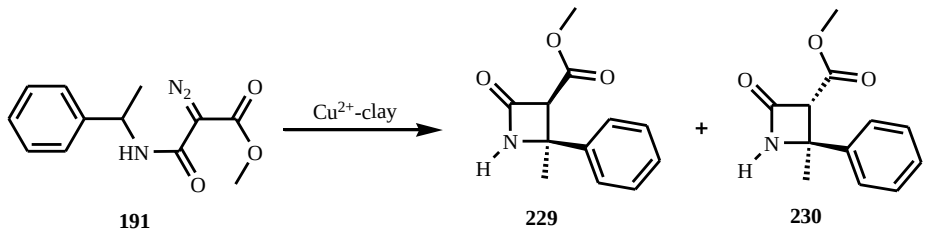

Scheme 78 Proposed reaction of methyl 1-phenylethylamidodiazomalonate 191 in the presence of Cu^{2+}-Wyoming bentonite catalyst.

When this reaction was performed in acetonitrile and benzonitrile solvents with clay and zeolite catalysts, none of the desired compounds formed, only complex crude mixtures were formed that did not appear to contain the desired *β*-lactams **229** and **230**.

2.10.1.1 Relative stabilities and bulkiness of the *β*-lactam diastereomers 229 and 230

Using VIs computer modelling, the energy differences of the *cis*- and *trans*-*β*-lactam diastereomers **229** and **230** were calculated:

$E_{cis\text{-isomer}}$ - $E_{trans\text{-isomer}}$ = -745.3047582–(–745.3059464) Hartree = 0.0011882*627.509391 kcal/mol = 0.74560 kcal/mol. Thus, the lower energy *trans*-diastereomer would be expected to be the favoured isomer at equilibrium in free solution.

As no useful products were found this line of investigation was discontinued.

2.11 Attempted carbene insertion reaction of methyl *N,N*-diphenyl-diazomalonamide (methyl 2-diazo-2-(*N,N*-diphenylcarbamoyl)-acetate) 192.

It was hoped that carbene insertion into one of the *ortho*- CH groups of the phenyls of the *N,N*-diphenyl malonamide **192** would produce the N-phenyl indolone **231** (Scheme 79).

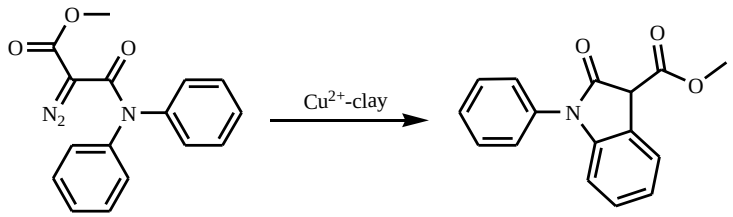

192 **231**

Scheme 79 Proposed carbene insertion reaction of methyl *N,N*-diphenyldiazomalonate 192 to form cyclised product 231.

However, once again this compound proved to be too bulky and difficult to fit into the interlayer space of clay catalysts or zeolite pores. As feared this molecule **192** did not form cyclised product **231** even in solvents such as acetonitrile, benzonitrile and toluene that had previously been shown to give good yields.

2.12 Conclusions

Small carbene precursors such as diazo esters **183 - 186** in Cu(II)-exchanged clay mineral or zeolite catalysts gave good yields of β-lactam compounds with small quantities of γ-lactam by-product, but little carbene dimers. The benzyl esters **184** and **186** gave small quantities of the benzyl C-H insertion β-lactam products also. As the bulkiness of the products increased, some selectivity for the less bulky isomer could be achieved within the mineral, the best results being within the restricted pores of the zeolites. Changes in solvent gave some useful

selectivity as long as the solvent did not have active C-H groups in the solvent, which competed with the intramolecular C-H insertion reactions. *N*-Phenyl substituted compounds showed strong competition for indolidine formation over *β*-lactams. Six membered ring piperidino compounds **187** and **188**, showed excellent selectivity for the *trans*-*β*-lactam isomers (> 98%), but the C-H groups of the corresponding five membered ring pyrrolidine compounds appeared to be too far away from the carbene centre for ring formation and carbene dimers were the only recognisable products. Very sterically demanding 1-phenylethylamido and *N*,*N*-diphenylamido compounds did not give any of the desired products as, presumably they had difficulty entering the clay or zeolite catalysts.

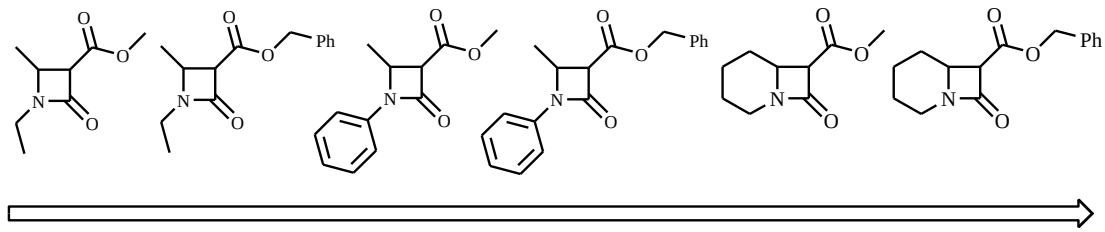

Figure 54 Increase in bulkiness as the *N*-substituent changes.

It appears that as the bulkiness increases from mono lactam ring with less bulky methoxy group to benzyl group and up to the *β*-lactam rings with phenyl groups (Figure 54) it becomes difficult to enter into the interlayer space of the clay mineral and as a result the reaction favours reaction outside the mineral, *i.e.* as that in free solution. However, the *β*-lactam ring can cleave in the presence of water and the clay mineral contains water in the interlayer space meaning that it can be difficult to maintain the lactam rings that have been formed, but in many cases good yields can be obtained. For these molecules we tried different catalysts (Zeolites ZSM-5, 4A and Cu^{2+}-Al-O-EA) and solvents such as dichloromethane, 1,4-dioxane, toluene, chloroform and benzonitrile to produce the more favoured less bulky/more planar isomer within the catalysts.

3 Chapter: Carbene Addition Reactions

3.1 Introduction of catalysed reactions of carbene addition

Cyclopropane is the highly strained smallest cycloalkane, which can be easily isolated and stored. The estimated total ring strain in cyclopropane is 28 kcal/mol (from heats of combustion measurements). For the cyclopropane ring C-C bond, when this value is compared with the strength of a typical C–C bond (*ca.* 88 kcal/mol), it has been shown that ring strain considerably weakens the C–C bonds of the ring. Hence, cyclopropane is much more reactive than acyclic alkanes and other cycloalkanes such as cyclohexane and cyclopentane.

In the current project we attempted diastereoselective cyclopropanation, by catalysed carbene addition onto alkenes within the interlamellar region of the cation exchanged Cu^{2+}-clay mineral catalyst to determine whether we could modify the stereo-chemical outcome of reactions within the clay layers compared to free solution reactions, i.e. reactions via less bulky intermediates should be more favoured in the restricted interlamellar region of the clay mineral.

For example:–

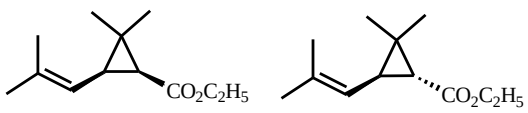

cis, **244** *trans*,**134**

Figure 55 Formation of the less bulky *cis*-isomer (pyrethrin pesticide) should be more favoured in the interlamellar region of the clay mineral.

By exchanging the usual sodium ions present in between the aluminosilicate layers of clay minerals, for a low valent transition metal, such as Cu^{2+}, a catalytic site highly restricted in size and shape will be produced. This leads to the possibility that the less bulky diastereomer

should be formed in this restricted environment. Due to steric constraints, chemical reactions carried out in the interlamellar region of clay minerals prefer to proceed via less bulky intermediates. Our primary aim was to study the chemoselectivity and diastereoselectivity of the cyclopropanation reactions. So, in the first instance, we wished to determine whether the less bulky diastereomer would be preferred in model catalysed reactions of a diazoalkane with simple alkenes within the interlamellar region of a cation exchanged Cu^{2+}-clay mineral, using dry dichloromethane as the solvent. Initially, we focused on three different types of alkenes (see Table 14) styrene **87**, linear alkenes (1–hexene **234**), cyclic alkenes (cyclohexene **131**, 1,5-cyclooctadiene **238**), dienes (isoprene **241**, 2,5–dimethyl–2,4–hexadiene **133** (DMHD)) and *trans*-cinnamic acid **245** with EDA **33** (ethyl diazoacetate) as the cyclopropanating agent. To evaluate the catalysed reactions, we performed reactions in different solvents with various catalysts such as Cu^{2+}-cation exchanged clay minerals (mainly Wyoming Bentonite) and zeolites (ZSM-5 and 4A molecular sieves).

3.2 Synthesis of cyclopropane rings from various alkenes

Cyclopropane ring formation reactions are amongst the most important reactions of carbenes. Alkenes such as styrene **87**, 1-hexene **234**, cyclohexene **131**, 1,5-cyclooctadiene **238**, isoprene **241** and 2,5–dimethyl–2,4–hexadiene **133** were reacted with a diazo compound (ethyl diazoacetate **33**), that forms a carbene intermediate in the presence of Cu^{2+}-cation exchanged clay mineral and zeolite catalysts, using dichloromethane as a solvent, to give cyclopropane rings showing *cis*-/*trans*-diastereomers and *endo*-/*exo*-isomers (Table 14).

Table 14 Cyclopropanes synthesised from alkenes and ethyl diazoacetate.

Starting material	Cyclopropanes, *cis*-/*trans*- or *endo*-/*exo*-	% Yield
Styrene **87**	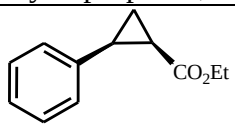 ***cis*, 127** 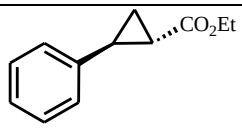 ***trans*, 128**	75
*1-Hexene **234**	 ***cis*,235**  ***trans*, 236**	-
Cyclohexene **131**	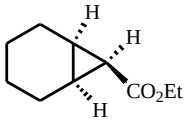 ***endo*, 132** 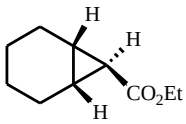 ***exo*, 237**	15
1,5-Cyclooctadiene **238**	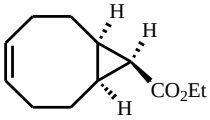 ***endo*, 239** 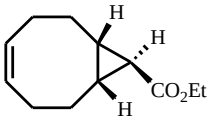 ***exo*, 240**	12
*Isoprene **241**	 ***cis*, 242** 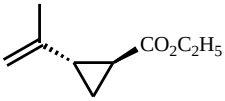 ***trans*, 243**	-
2,5–Dimethyl–2,4–hexadiene **133**	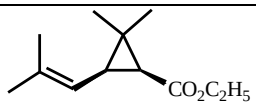 ***cis*, 244** 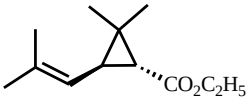 ***trans*,134**	48
trans-cinnamic acid **245**	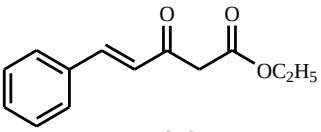 **246**	54

***** Reactions of EDA with 1-hexene and isoprene formed complex mixture.

3.3 Carbene addition reaction with EDA and styrene 87

From the literature,[8,173] carbene intermediates have been generated from ethyl diazoacetate **33** (EDA) in the presence of platinum and rhodium complexes and they have been reacted with styrene **87** to form *cis*- and *trans*-cyclopropanes **127** and **128**, as major products and diethyl fumarate **232** and diethyl maleate **233** carbene dimers as minor products of the carbene addition reaction. Similarly, we have used Cu^{2+}-Wyoming bentonite as catalyst to form the *cis*- and *trans*-cyclopropanes **127** and **128** from styrene **87** (Scheme 80).

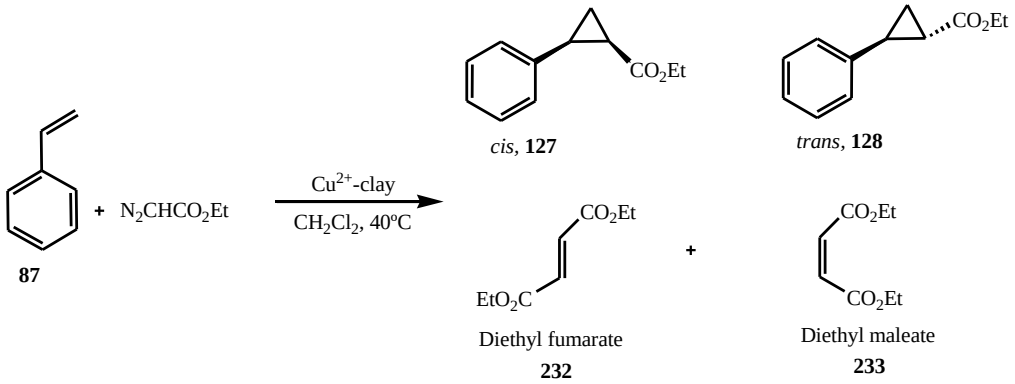

Scheme 80 Cyclopropanation of styrene with EDA in the presence of Cu^{2+}-Wyoming bentonite with minor by-products diethyl fumarate 232 and diethyl maleate 233.

3.3.1 Assignment of the structures of the *cis*- 127 and *trans*-isomers 128 of the cyclopropane from styrene 87

The *cis*- and *trans*-diastereomers **127** and **128** (45 : 55) were identified based on the assignment of their ^{1}H NMR (Figures 57 and 59), ^{13}C NMR, ^{1}H-^{1}H 2D COSY and ^{1}H-^{1}H 2D NOESY spectra.

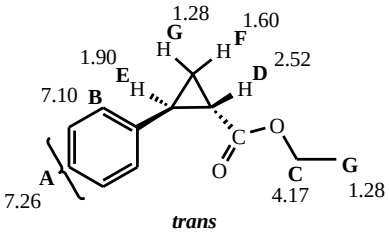

Figure 56 ***trans*-Isomer 128 from styrene cyclopropanation.**

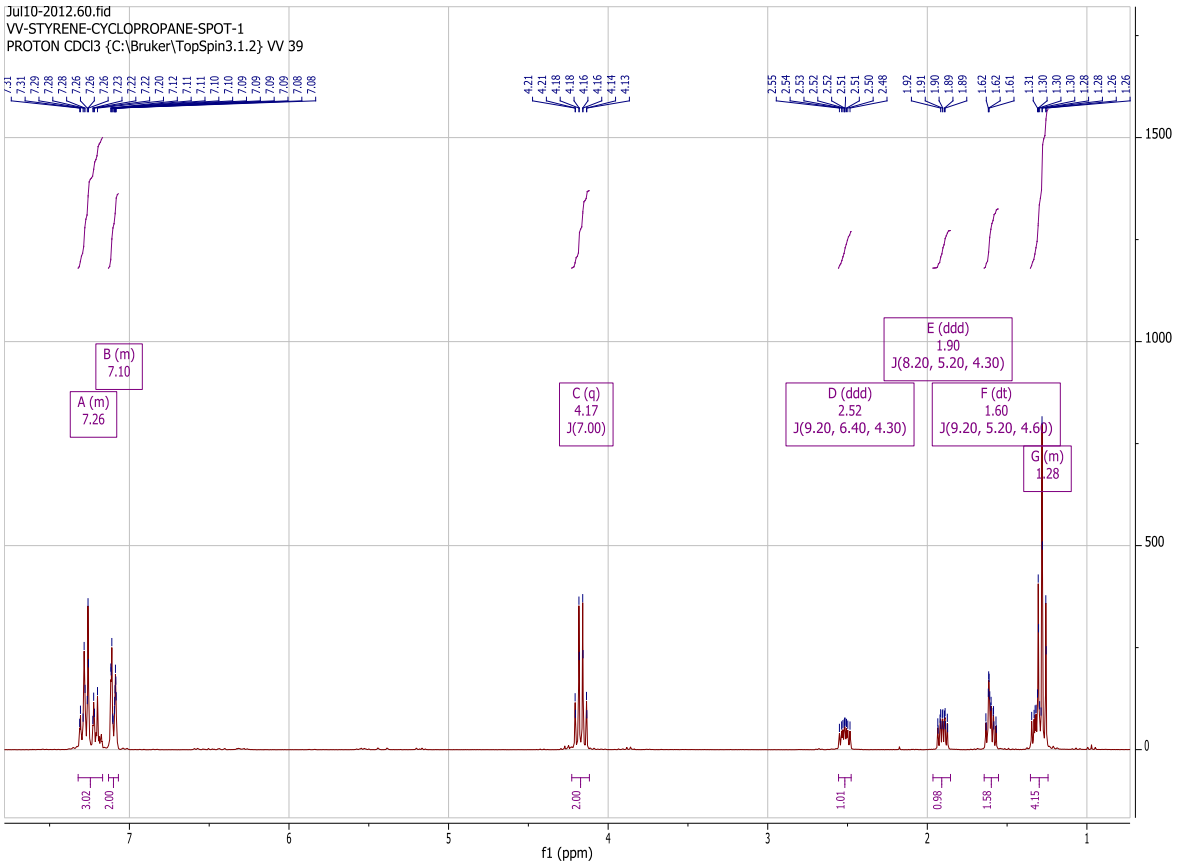

Figure 57 **^{1}H-NMR spectrum of the *trans*-cyclopropane isomer 128 from styrene 87.**

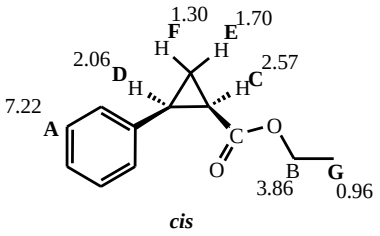

Figure 58 ***cis*-Isomer 127 from styrene cyclopropanation.**

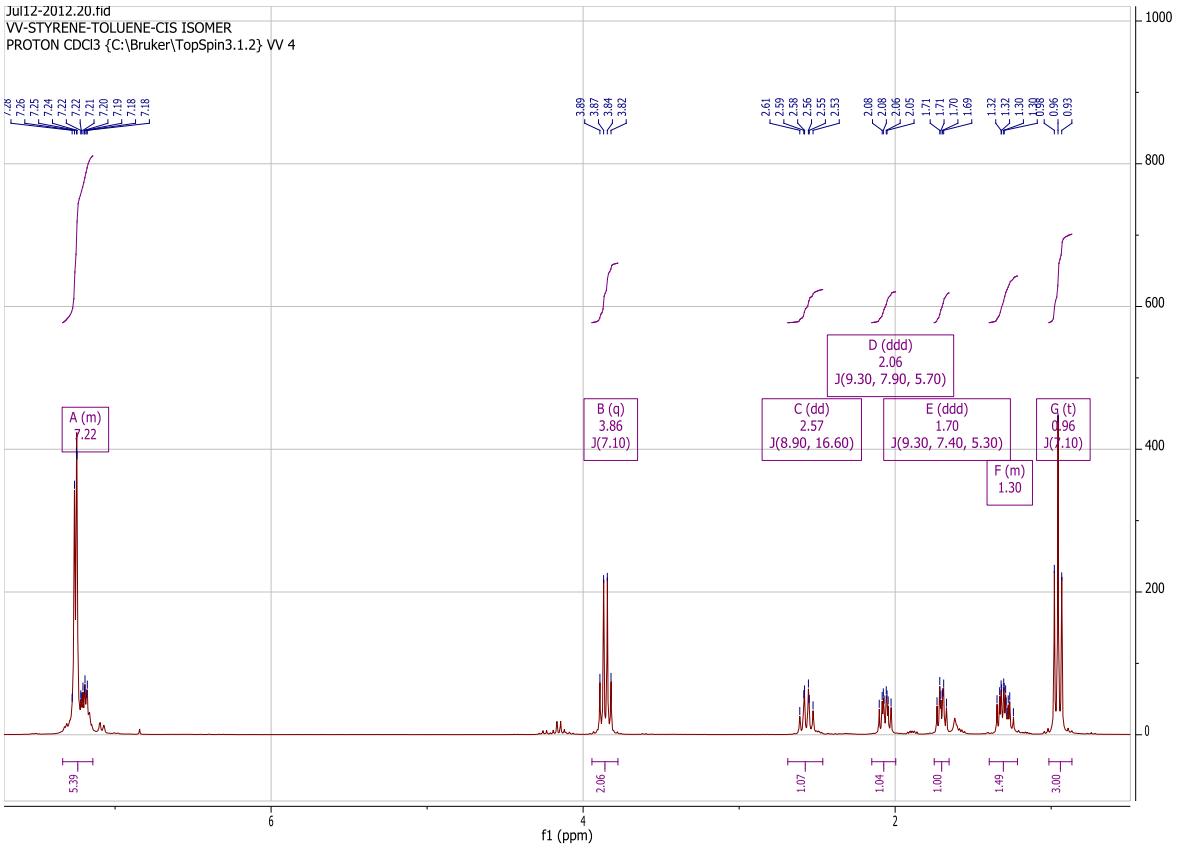

Figure 59 **^{1}H-NMR spectrum of the *cis*-isomer 127 from styrene cyclopropanation.**

Based on the literature values,[8,174] the protons at δ 1.90 (Figure 57) and 2.06 (Figure 59) were assigned to *trans*-isomer **128** and *cis*-isomer **127**. The other values were also consistent with the literature comparative data shown below in Table 15, and also from the crude spectra the minor products diethyl fumarate **132** and diethyl maleate **133** showed, the peaks at δ 6.88 (2H, s, -CH_{trans}) and 6.20 (2H, s, -CH_{cis}) consistent with the literature.[175]

Table 15 Comparative ^{1}H NMR data for *cis*- 127 and *trans*-isomers 128

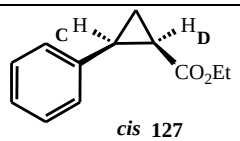 *cis* **127**		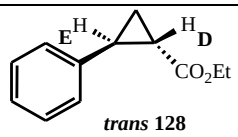 *trans* **128**	
Experimental	Literature	Experimental	Literature
2.06 (ddd, 1H, *J* = 9.30, 7.90, 5.70 Hz, $ArCH_C$)	2.06 (ddd, 1H, *J* = 9.30, 7.90, 5.70 Hz, $ArCH_C$)	1.90 (1H, ddd, *J* = 8.20, 5.20, 4.30 Hz $ArCH_E$)	1.90 (1H, ddd, *J* = 8.20, 5.20, 4.30 Hz $ArCH_E$)
2.57 (dd, 1H, *J* = 8.90, 16.60 Hz, CH_DCO_2Et	2.56 (dd, 1H, *J* = 8.90, 16.55 Hz, CH_DCO_2Et)	2.52 (1H, ddd, *J* = 9.20, 6.40, 4.30, CH_DCO_2Et)	2.52 (1H, ddd, *J* = 9.20, 6.40, 4.30, CH_DCO_2Et)

3.3.2 Relative bulkiness of the diastereomers 127 and 128 from Chem 3D models

Energy minimised Chem 3D structures give an estimate of the relative sizes of the diastereomers (Figure 60).

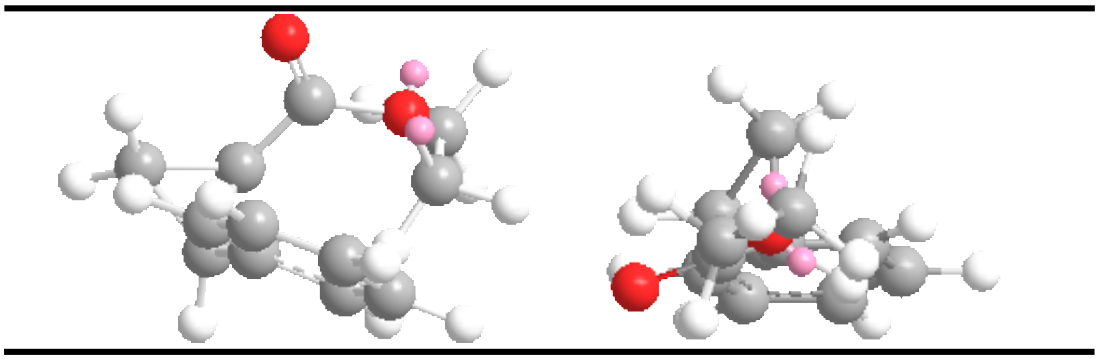

cis **127**, bulky *trans* **128**, less bulky

Figure 60 Chem 3D models of the structures of diastereomers 127 and 128.

The Chem 3D model structures (Figure 60) were generated by drawing the "all *trans*" conformation (longest open chain arrangement of the molecules) of both the *cis*- **127** and *trans*- styrene **128** cyclopropanes in Chem Draw and copying them to Chem 3D. The structures were energy minimised using the MM2 procedure and the structures checked to

ensure that the "all *trans*" configuration had been retained: if not then the structures were altered and re-minimised to produce the lowest energy "all *trans*" configurations. The *trans*-isomer showed the lower energy in MM2 process (by about 6 kcal mol^{-1}). The structures were copied to Microsoft Word and resized so that all atoms of each type were the same size in both structures. Two horizontal lines were used to help compare the sizes of the structures. Figure 60 shows that the *cis*-isomer **127** is more bulky than the *trans*-isomer **128** across its smallest dimension. Thus we expect that within the restricted environment of the clay minerals or the pores of the zeolite the less bulky *trans*-isomer **128** should be formed as the major product and the *cis*-isomer **127** as the minor product.

Using VIs computer modelling, the energy differences of the *cis*- and *trans*-cyclopropane isomers **127 - 128** were calculated:

$E_{cis\text{-isomer}} - E_{trans\text{-isomer}}$ = –576.8477579 – (–576.8525282) Hartree = 0.00477037*627.509391 kcal/mol = 2.993451974 kcal/mol.

This more accurate method, considering all conformations confirms that the *trans*-isomer **128** is more stable by about 3 kcal mol^{-1}.

As the *trans*-diastereomer **128** is more stable it would be expected to predominate slightly in free solution at high temperatures and to become more predominant in low energy catalysed processes. Furthermore, from the Chem 3D structures the relative "heights" of the diastereomers *cis*- and *trans*- show that the *trans*-diastereomer **128** should be less bulky with respect to a clay mineral interlayer and should be formed more readily if the environment is more restricted. Thus, the lower energy, less sterically constrained *trans*-isomer **128** should predominate both in solution and within the interlayer region of a clay mineral.

3.3.3 Results of the carbene addition reaction of EDA to styrene 127

Under thermal, uncatalysed conditions, reaction of ethyl diazoacetate **33** with styrene **127** gave carbene dimers (diethyl fumarate **232** and diethyl maleate **233**) as the major products with a complex mixture of impurities, while in the presence of Cu^{2+}-Wyoming bentonite

formed *cis*- **127** and *trans*-cyclopropanes **128** as major products with the carbene dimers **232** and **233** as minor products. When a similar reaction was catalysed by copper complexes of biaryldiimine, the ratio of *cis*- **127** and *trans*-cyclopropanes **128** obtained was 18 : 82 (ca. isolated yield 94%) whereas in Wyoming bentonite with dichloromethane as solvent, the ratio of *cis*- **127** and *trans*-cyclopropanes **128** was 45 : 55 (*ca*. isolated yield 75%), see Table 16. This ratio was about as expected from the small energy difference of the two isomers and suggests that there is little constraining effect by the clay mineral layers in this case. From the Chem 3D model, the *cis*-isomer **127** has an approximate "height" of 4.1 Å, which is larger than the estimated interlayer distance (Δδ) of 3.52 Å (Table 16) at ambient temperature for the Cu^{2+}-Wyoming bentonite expanded with dichloromethane. Thus, it is possible that the reactants themselves may be increasing the Δδ so that there is little constraining effect.

3.3.4 Effects of varying the solvent on the interlayer spacing of clay mineral and the ratio of diastereomers 127 and 128.

Different solvents (Table 16), such as chloroform, toluene and ethyl acetate, affect the Δδ of the Cu^{2+}-Wyoming bentonite, thus, if a significantly smaller Δδ can be achieved then the proportion of the more bulky *cis*-isomer **127** should be decreased. The estimated Δδ for the Cu^{2+}-Wyoming bentonite with toluene as solvent (3.36 Å) was lower than that with dichloromethane and the *cis*-/*trans*-isomer ratio decreased, as hoped, to 34 : 66, showing that the clay mineral layers were beginning to exert a constraining effect on the reaction. Unfortunately, the lower Δδ also made access of the reactants to the interlayer catalytic sites more difficult and the yield (49%) was reduced as a consequence. These effects were also seen with chloroform as solvent, where a lower proportion of the *cis*-isomer **127** (32 : 68) was accompanied by an lower yield (30%). The Δδ value with chloroform as solvent (3.56 Å) suggests that the degree of constraint should be similar to that with dichloromethane, however, the yield and isomer ratio suggests that the strongly hydrogen-bonding chloroform may hold the layers together much tighter and so preventing the reactants from increasing the Δd value. Ethyl acetate showed intermediate results, but unfortunately the XRD measurement of the Δd value was unreliable in this case.

Table 16 Measured (XRD) Δd values for Cu(II)-Wyoming bentonite in various solvents.

Solvents	% Yield of isomers **127** & **128**.	*cis-/trans-* diastereomer ratio.	Interlayer distance of Cu(II) Wyoming bentonite, Δd (Å), assuming the clay layers ≈ 9.6 Å[164]
$CHCl_3$	30	32 : 68	3.56
CH_2Cl_2	75	45 : 55	3.52
Ph-CH_3	49	34 : 66	3.36
EtOAc	45	43 : 57	-

Using carbene modified (Al-O-EA) Cu^{2+}-Wyoming bentonite (see Section 2.3.1.7) as catalyst (Table 17) increased the proportion of the more bulky *cis*-isomer **127** to about parity with the *trans*-isomer (*cis-/trans-* (52 : 48, *ca*. isolated yield 50%)) (Table 17), suggesting that there is little constrain in this case and carbene insertion into the AlO-H bonds of the Cu^{2+}-Wyoming bentonite is increasing the Δd value for all solvents. The zeolite, ZSM-5, should not show this problem of carbene insertion as there are no bridging AlO-H groups in its structure and we found that a lower proportion of the *cis*-isomer (30 : 70, yield 52%) was indeed obtained within the 5.4 - 5.6 Å zeolite pores (Table 17).

Table 17 Measured yield, isomer ratios and Δd values for clay minerals in various catalysts.

Cu^{2+}-exchanged mineral	Solvents	% Yield of isomers **127** & **128**	*cis-/trans-* diastereomer ratio	Interlayer distance of Cu(II)-clay mineral, Δd (Å), assuming the clay layers ≈ 9.6 Å[164] or smaller pore diameter of zeolites
Wyoming bentonite	CH_2Cl_2	75	45 : 55	3.52
Carbene Modified clay	CH_2Cl_2	50	52 : 48	3.09 (no solvent)
ZSM-5	CH_2Cl_2	52	30 : 70	5.4 - 5.6 Å

3.3.5 Conclusions

By considering the relative sizes of the smallest molecular dimensions of the *cis-* **127** and *trans*-**128** styrene cyclopropane isomers, formation of the more bulky and higher energy

cis-isomer should be less favoured both in free solution and within the interlayer region of a clay mineral. However, the "height" of the more bulky *cis*-isomer **127** (*ca*. 4.1 Å) is not too much larger than the Δδ of the clay mineral in most solvents (*ca*. 3.5 Å) (Table 16) and so there is little selection for the less bulky *trans*-isomer **128** until the Δδ is decreased to *ca*. 3.36 Å by using toluene as solvent (*cis*-/*trans*- 34 : 66). The yield of cyclopropane product decreases as the *cis*-/*trans*-isomer ratio decreases, suggesting that access to the interlayer region is becoming more difficult. The fixed pore size (*ca*. 5.5 Å) of the zeolite ZSM-5 gives a similar selectivity (*cis*-/*trans*- 30 : 70) (Table 17) to that with the Wyoming bentonite and toluene, suggesting that the reactants and/or products are also increasing the Δδ of the clay mineral.

To see what effect a less polar alkene would have on the selectivity, we then chose a linear alkene (1-hexene **234**) to determine whether there would be less effect on the Δδ of the clay mineral.

3.4 Carbene addition reaction to 1-hexene 234.

Ruthenium-catalysed asymmetric cyclopropanation of 1-hexene **234** has been reported to form both *cis*- **235** and *trans*- isomers **236** of the cyclopropane (*cis*-/*trans*- 52 : 48, yield 73%).[176] Thus, we attempted the same reaction with Cu^{2+}-Wyoming bentonite to see whether we could form both the *cis*- **235** and *trans*-cyclopropane **236** isomers (Scheme 81).

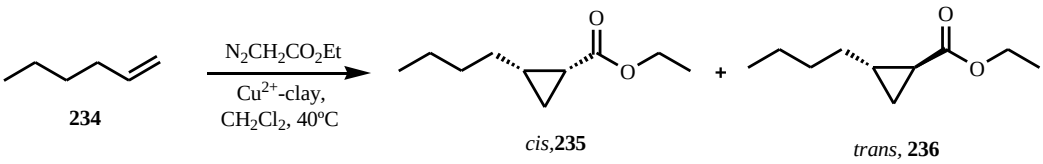

Scheme 81 Cyclopropanation of 1-hexene in the presence of Wyoming bentonite

3.4.1 Relative bulkiness of the diastereomers 235 and 236 from Chem 3D models.

Energy minimised Chem 3D structures give an estimate of the relative sizes of the diastereomers (Figure 61).

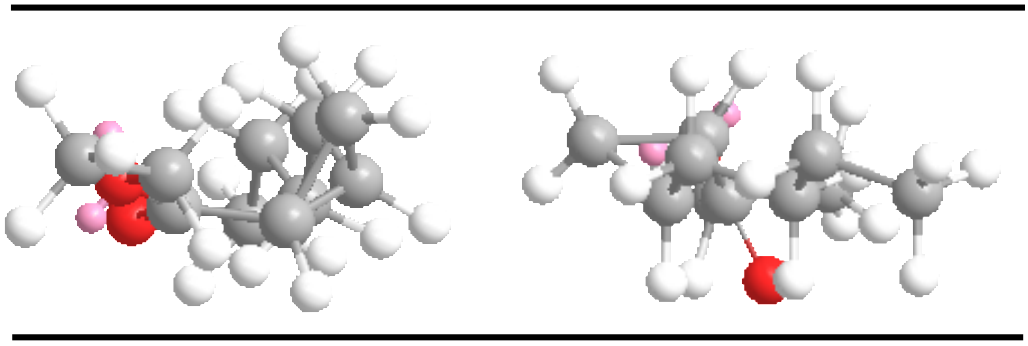

cis- bulky *trans*- less bulky

Figure 61 Chem 3D structures of *cis*- 235 and *trans*- 236 1-hexene cyclopropanes.

Using VIs computer modelling, the energy differences of the *cis*- and *trans*-cyclopropane isomers **235** and **236** were calculated:

$E_{cis\text{-isomer}} - E_{trans\text{-isomer}}$ = –385.1062298 –(–385.1087901) Hartree = 0.00256*627.509391 kcal/mol = 1.606574643 kcal/mol.

From the Chem 3D modelling (Figure 61) the higher energy *cis*-isomer **235** looks more bulky than the *trans*-isomer **236**, so the *trans*-isomer **236** should be more favoured within the interlamellar region of clay mineral or pores of zeolite.

3.4.2 Results of carbene addition reaction of 1-hexene 234

The Cu^{2+}-Wyoming bentonite catalysed reaction appeared to form both the *cis*- **235** and *trans*-cyclopropane **236** isomers. However, the reaction mixture was complex and it was very difficult to purify the crude material. Thus, we were unable to get useful results with this linear alkene and we decided that no more time could be spent on this reaction.

3.4.3 Conclusions

The failure of this reaction may be due to the low polarity alkane chain not "pushing" the layers of the clay mineral far enough apart to allow reaction to occur. Thus we were led to choose more hindered cyclic alkenes, such as cyclohexene **131** and 1,5-cyclooctadiene **238** to find whether reaction would take place and if diastereoselectivity of the cyclopropanation within the interlamellar region of clay mineral and pores of zeolite could be observed.

3.5 Carbene addition reaction to cyclohexene 131.

When an EDA carbene addition to cyclohexene reaction was attempted with rhenium(I) bipyridine or terpyridine tricarbonyl complexes, cyclopropane products were not observed.[2] Whereas in the presence of Cu^{2+}-Wyoming bentonite as catalyst, *endo*- **132** and *exo*- **237** cyclopropanes were formed as major products and diethyl fumarate **232** and diethyl maleate **233** carbene dimers as minor products (Scheme 82).

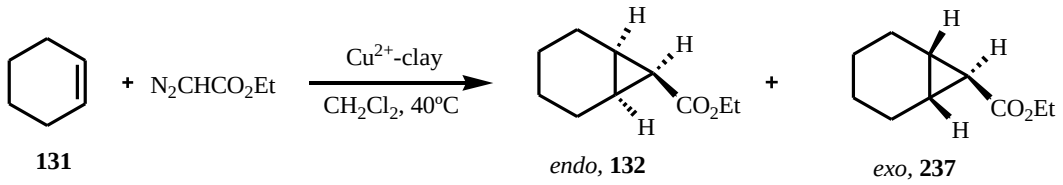

Scheme 82 Cyclopropanation of cyclohexene 131 in the presence of Cu^{2+}-Wyoming bentonite catalyst

3.5.1 Assignment of the structure of the 7-*exo*-ethoxycarbonylbicyclo[4.1.0]heptane 237

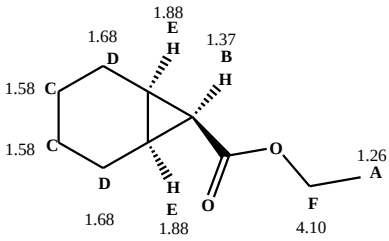

Figure 62 7-*exo*-ethoxycarbonylbicyclo[4.1.0]heptane

The ^{1}H NMR spectrum (Figure 63) of partially purified 7-*exo*-ethoxycarbonylbicyclo[4.1.0]heptane **237** was consistent with reported values,[13,177] however, the literature values for both *endo*- **132** and *exo*- **237** isomers were simply given as a range of protons (Table 18) and no coupling constant (*J*) values were mentioned to help differentiate the cyclopropane C-Hs from the *endo*- **132** or *exo*- **237** isomers. The literature[178] values for a similar example, for the cyclopropane from 1,5-cyclooctadiene **238** showed the protons as clearly differentiated for both the *endo*- **239** and *exo*- **240** isomers with distinct *J* values and triplets at δ 1.18 (*J* = 4.80 Hz) for the *exo*- isomer **240** and 1.70 (*J* = 8.80 Hz) for the *endo*-isomer. These compounds are discussed in more detail in Section 3.6 (Table 20). With the aid of the δ and *J* values for the *endo*- **239** and *exo*- **240** isomers from 1,5-cyclooctadiene, the major cyclopropane isomer from cyclohexene **131** was identified as the *exo*-isomer **237** from a triplet δ 1.37 with *J* = 4.35 Hz (Figure 63).

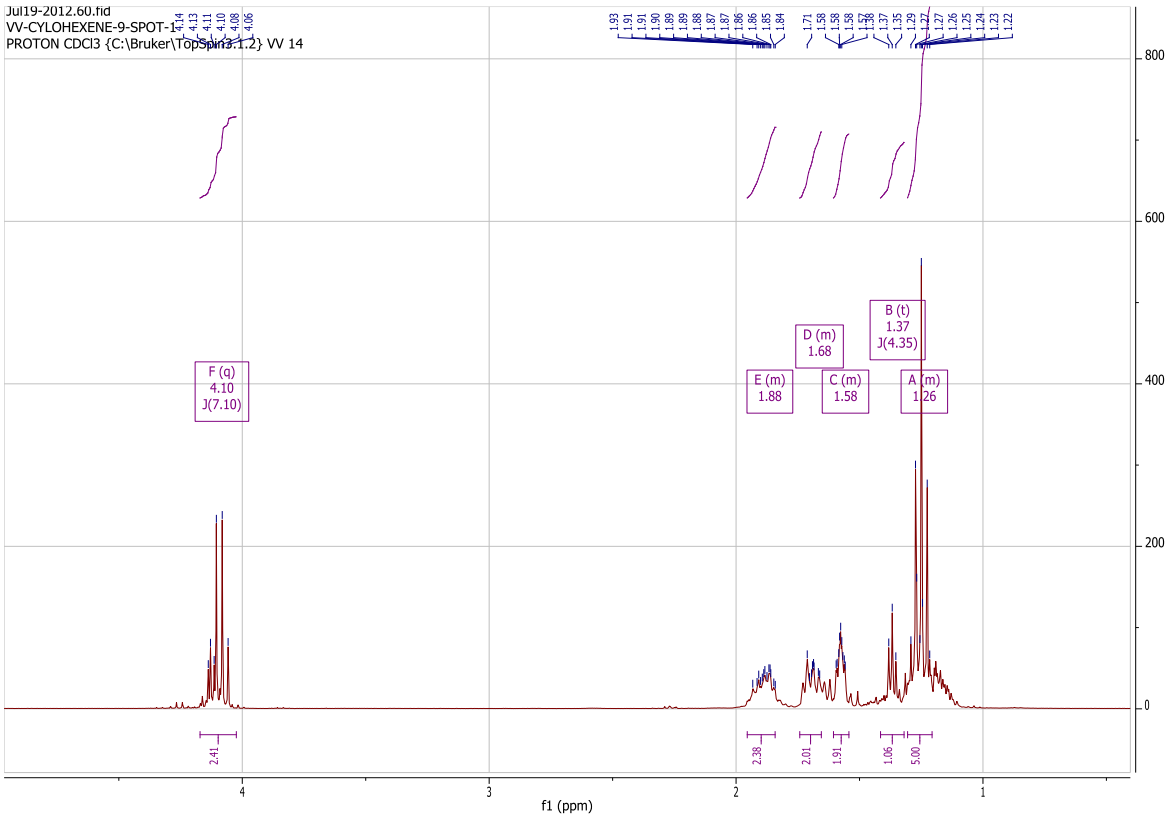

Figure 63 **^{1}H-NMR spectrum of the partially purified *exo*-isomer 237 of the EDA cyclopropanated cyclohexene.**

Table 18 **Literature ^{1}H NMR assignments and comparison of *endo*- 132 and *exo*- 237 isomers of EDA cyclopropanated cyclohexene 131.[13]**

7-*endo*-ethoxycarbonylbicyclo[4.1.0] heptane **132**	7-*exo*-ethoxycarbonylbicyclo[4.1.0] heptane **237**
δ 1.20 - 1.39 (m, 5H, CH_2 and OCH_2CH_3)	1.05 – 1.98 (11 H, m)
1.40 - 1.45 (m, 1H, CH)	1.25 (3H, t, $CO_2CH_2CH_3$, 3*J*H H = 7.10 Hz)
1.46 - 1.56 (dd, 1H, *J* = 9.80, 7.80 Hz, CH)	-
1.56 - 1.73 (m, 2H, CH_2)	-
1.75 - 1.93 (m, 2H, CH_2)	-
4.10 (q, 2H, *J*=7.10 Hz, OCH_2CH_3)	4.10 (2H, q, $CO_2CH_2CH_3$, 3*J*H H = 7.10 Hz)

3.5.2 Relative bulkiness of the diastereomers 132 and 237 from Chem 3D model

Energy minimised Chem 3D structures give an estimate of the relative sizes of the diastereomers (Figure 64).

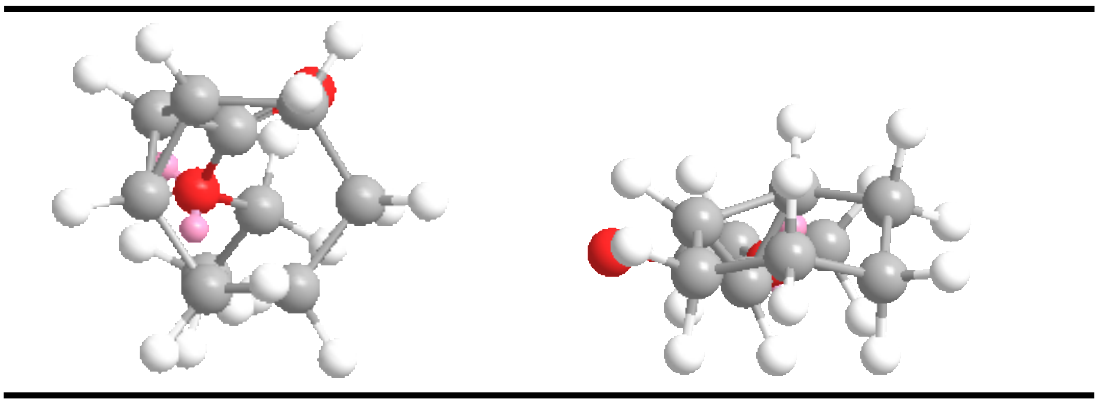

endo bulky *exo* less bulky

Figure 64 Chem 3D model structures of *endo*- 132 and *exo*- 237 cyclopropane isomers from cyclohexene 131

Using VIs computer modelling, the energy difference of the *endo*- **132** and *exo*-diastereomers **237** were calculated:

$E_{endo\text{-isomer}} - E_{exo\text{-isomer}} = -501.8338082 - (-501.8389947)$ Hartree = 0.005186*627.509391 kcal/mol = 3.254571 kcal/mol.

Thus, showing that the higher energy *endo*-isomer **132** should be disfavoured in the reaction. Chem 3D model structures of the *endo*- **132** and *exo*- **237** isomers (Figure 64) showed that the *endo*-isomer **132** is more bulky than the *exo*-isomer **237** isomer. Thus we expect that within the restricted environment of the clay minerals or the pores of the zeolite the less bulky *exo*-isomer **237** should be formed as the major product and the *endo*-isomer **132** as a minor product. The *exo*-diastereomer **237** is more stable and expected to predominate slightly in free solution at high temperatures and to become more predominant in low energy catalysed processes.

3.5.3 Results of carbene addition reaction of cyclohexene 131

Similar to styrene **87** and 1-hexene **234**, cyclohexene **131** was reacted first under uncatalysed conditions, unfortunately without using catalyst, thermally formed major products were the carbene dimers (diethyl fumarate **232** and diethyl maleate **233**) and with no cyclopropane ring formation. From the literature, when the similar reaction was performed in rhenium(I) bipyridine and terpyridine tricarbonyl complexes[2] reaction was not progressed at all. Whereas in Cu^{2+}-exchanged Wyoming bentonite in dichloromethane solvent favoured in the formation of *endo*-**132** and *exo*- **237** isomer (34 : 66 ca isolated yield 15%). The experimental results shown *ex*o- **237** isomer as a major product based on the ^{1}H NMR and GC-MS.

3.5.4 Effects of varying the solvent on the interlayer spacing of clay mineral and the ratio of diastereomers 132 and 237.

In order to see the effects of changing the solvent on the selectivity of the cyclopropanation of cyclohexene, the reaction was performed with various solvents such as toluene, ethyl acetate, 1,4-dichloromethane, 1,4-dioxane and 1,2-dichloroethane (Table 19). The best results were obtained with dichloromethane (Δd 3.52) (31 : 69 *ca*. isolated yield 15%) and we also expected toluene to have similar selectivity having (Δd 3.36) but the results from the crude mixture showed carbene dimers (diethyl fumarate **232** and diethyl maleate **233**) as major products, with less than 10% yield of cyclopropanes. Other solvents gave complex mixtures with no cyclopropane product evident.

Table 19 Measured (XRD) Δd values for Cu(II)-Wyoming bentonite in various solvents.

Solvents	% Yield of *endo*-/*exo*-**132** & **237**	*endo*-/*exo*-ratio	Interlayer distance of Cu(II) Wyoming bentonite, Δd (Å), assuming the clay layers ≈ 9.6 Å[164]
Dichloromethane	15	31 : 69	3.52
*Toluene	< 10	-	3.36
*Ethyl acetate	-	-	-
*1,4-Dioxane	-	-	5.02
*1,2-Dichloroethane	-	-	-

* Solvents showed complex mixtures and in toluene < 10 product with major impurities.

Both Cu(II) Wyoming bentonite and carbene modified (Al-O-EA) Cu^{2+}-Wyoming bentonite as catalyst (Table 20) gave the less bulky *exo*-isomer **237** as the major product, 31 : 69 *ca*. isolated yield 15% and 34 : 66 *ca*. isolated yield 12%, respectively showing that both Wyoming bentonite and modified clay were giving good selectivity for the less bulky *exo*-isomer **237**.

Table 20 Measured yield, isomer ratios and Δd values for clay minerals in various catalysts.

Cu^{2+}-exchanged mineral	Solvents	% Yield of *endo*-/*exo*-**132** & **237**	*endo*-/*exo*-diastereomer ratio	Interlayer distance of Cu(II)-clay mineral, Δd (Å), assuming the clay layers ≈ 9.6 Å[164] or smaller pore diameter of zeolites
Wyoming bentonite	CH_2Cl_2	15	31 : 69	3.52
Carbene Modified clay	CH_2Cl_2	12	34 : 66	3.09 (no solvent)

3.5.5 Conclusions

The Chem 3D model structures of the *endo*- **132** and *exo*- **237** isomers (Figure 64) showed the the *endo*-isomer **132** to be more bulky than the *exo*-isomer **237**. As expected under catalytic conditions the less bulky *exo*-isomer **237** formed as the major product and the *endo*-isomer **132** as the minor product (*endo*-/*exo*- ratio 31 : 69 *ca*. isolated yield 15%) with

Cu^{2+}-Wyoming bentonite (*endo*-/*exo*- ratio 34 : 66 *ca*. isolated yield 12%) with modified clay (Table 20). These results show that with dichloromethane as solvent we are getting more selectivity of the less bulky *exo*-isomer **237**. The failure of the other solvents: 1,4-dioxane, ethyl acetate and 1,2-dichloroethane, may be due to competing carbene insertion into solvent molecules in the highly restricted mineral interlayer.

We then decided to use 1,5-cyclooctadiene **238** as reactant to see if two possible alkene reaction sites per molecule might improve the yield of cyclopropane products with clay minerals or zeolite catalysts.

3.6 Carbene addition reaction of 1,5-cyclooctadiene 238

Dirhodium tetraacetate has been reported in the literature,[178,179] to catalyse the reaction of 1,5-cyclooctadiene **238** with EDA to form the *endo*- **239** and *exo*-isomers **240** (46 : 54). Similar to cyclohexene **131**, 1,5-cyclooctadiene reacted in the presence of cation exchanged clay catalyst formed *endo*- **239** and *exo*- **240** isomers (Scheme 83).

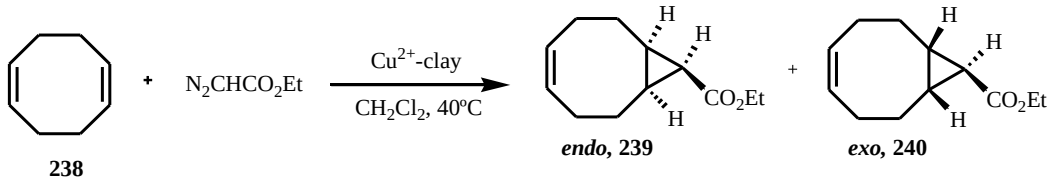

Scheme 83 Mixture of *endo*-/*exo*-isomers of cyclopropanated 1,5-cyclooctadiene 238.

3.6.1 Assignment of the structures of the *endo*-/*exo*-isomers 239 and 240.

The ^{1}H NMR spectrum (Figure 65) of the partially purified *exo*-isomer **240** showed triplets at δ 1.18 (J = 4.80 Hz) for the *exo*-isomer **240** and 1.70 (J = 8.80 Hz) for the *endo*-isomer **239**. These values were consistent with the literature values for the *exo*- **240** and *endo*- **239**

isomers,[178] triplet at 1.18 (J = 4.80 Hz) and 1.70 (J = 8.80 Hz). Table 21 compares the experimental and literature ^{1}H NMR data.

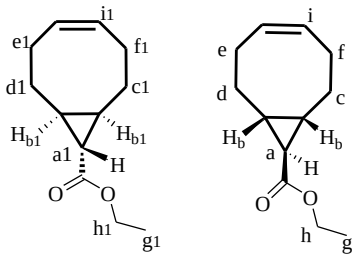

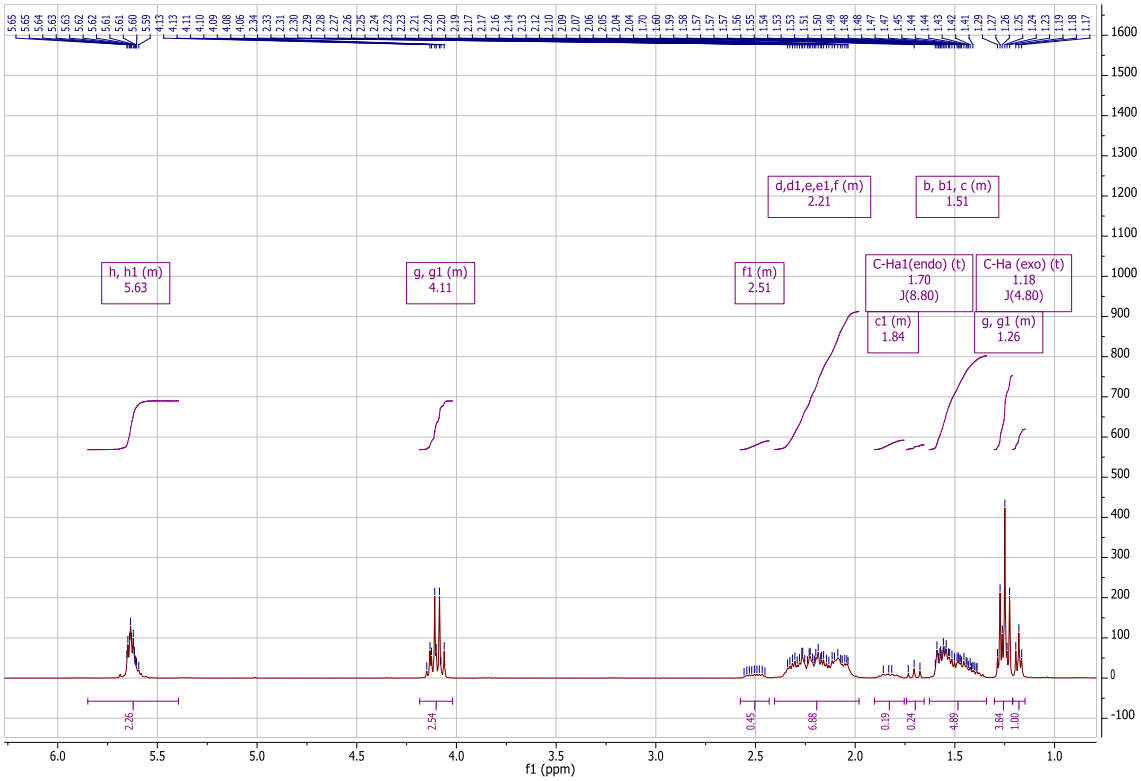

Figure 65 Partially purified *exo*- 240 (major) and *endo*- 239 (minor) isomers cyclopropanated 1,5-cyclooctadiene 238.

Table 21 *Exo*-ethyl bicyclo[6.1.0]non-4-ene-9-carboxylate 240

Experimental values	Literature values
1.18 (t, *J* = 4.80 Hz, 1H)	1.18 (t, *J* = 4.80 Hz, 1H)
1.25 (t, *J* = 7.20 Hz, 3H)	1.25 (t, *J* = 7.20 Hz, 3H)
1.49 – 1.59 (m, 4H)	1.43 – 1.53 (m, 2H) 1.53 – 1.59 (m, 2H)
2.04 – 2.31 (m, 6H)	2.04 – 2.13 (m, 2H) 2.16 – 2.24 (m, 2H) 2.27 – 2.35 (m, 2H)
4.11 (q, *J* = 7.20 Hz, 2H)	4.10 (q, *J* = 7.20 Hz, 2H)
5.39 – 5.65 (m, 2H)	5.60 – 5.68 (m, 2H)

3.6.2 Relative bulkiness of the diastereomers 239 and 240 from Chem 3D model

Energy minimised Chem 3D structures give an estimate of the relative sizes of the diastereomers (Figure 66).

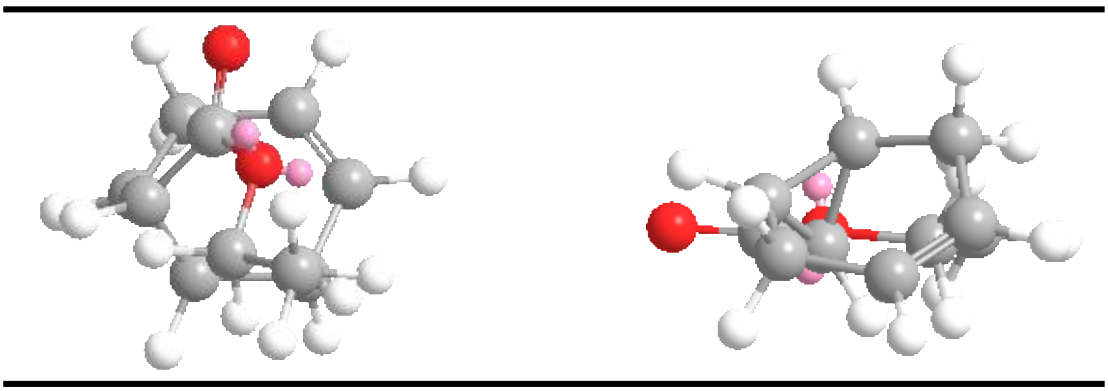

endo bulky *exo* less bulky

Figure 66 Chem 3D structures of *endo*- 239 and *exo*- 240 cyclopropane isomers from 1,5-cyclooctadiene

Using VIs computer modelling, the energy differences of the *endo*- and *exo*- diastereomers **239** and **240** were calculated:

$E_{endo\text{-isomer}} - E_{exo\text{-isomer}}$ = –579.2194379 –(–579.2317306) Hartree = 0.012293*627.509391 kcal/mol = 7.713772 kcal/mol.

Chem 3D model structures (Figure 66) for the cyclopropanated 1,5-cyclooctadiene isomers, showed that just as with the cyclopropanated cyclohexene isomers **132** and **237**, the *endo*-isomer **239** was more bulky than the *exo*-isomer **240**. Thus we expect that within the restricted environment of a clay mineral or the pores of a zeolite the less bulky *exo*-isomer **239** should be formed as the major product and the *endo*-isomer **240** as a minor product. The *exo*-isomer **240** is more stable and would be expected to be more predominant in low energy catalysed processes and to predominate slightly in free solution at high temperatures, whereas the bulky *endo*-isomer **239** should form as the minor product in both cases.

3.6.3 Results of carbene addition reaction of EDA to 1,5-cyclooctadiene 238

The dirhodium tetraacetate catalysed reaction of EDA with 1,5-cyclooctadiene **238** has been reported to form the *endo*-/*exo*-isomers **239** and **240** in the ratio: 46 : 54,[178,179] Under uncatalysed conditions only carbene dimers **232** and **233** were formed with no cyclopropane formation. In the presence of both Cu^{2+}-Wyoming bentonite or Cu^{2+}-ZSM-5 catalyst both *endo*- **239** and *exo*- **240** isomers were formed with an isomer ratio 20 : 80 with the clay (*ca*. isolated yield 12%) and ratio 10 : 90 with ZSM-5 (*ca*. isolated yield 10%), based on ^{1}H NMR spectroscopic and GC-MS data (Table 22).

3.6.4 Conclusions

When compared to the literature,[178] the proportion of the less bulky *exo*-isomer **240** has increased quite dramatically from 46 : 54 to 20 : 80 in the Wyoming bentonite and 10 : 90 in the more restricted ZSM-5. However, the yields were still low and having twice as many alkene bonds does not seem to affect the yield.

We then focused on the simple 1,3-diene **133**, isoprene **241** followed by the more complex chrysanthemic acid precursor 2,5–dimethyl–2,4–hexadiene **133** to determine whether diastereoselectivity can be achieved in the cyclopropanation reaction when using clay and zeolite catalysts.

3.7 Carbene addition reaction of EDA to isoprene 241

Isoprene **241** was reacted with EDA using Cu^{2+}-Wyoming bentonite to form both *cis*- **242** and *trans*-cyclopropanes **243** (Scheme 84).

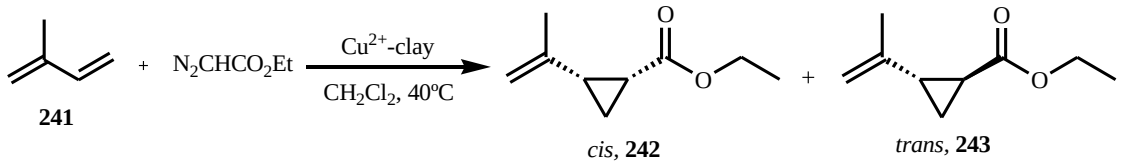

Scheme 84 Cyclopropanation of isoprene 241 with EDA in the presence of Cu^{2+}-Wyoming bentonite catalyst.

3.7.1 Assignment of the structures of the *cis*-/*trans*-isomers 242 and 243 from the EDA cyclopropanation of isoprene 241

The literature values for the ^{1}H NMR spectrum of ethyl 2-(2-isopropenyl)cyclopropane-l-carboxylate **242** and **243**,[180] were given as ranges of δ values for a mixture of *E*-, (*trans*) **243** and *Z*-, (*cis*) **242** isomers, δ 4.05 and 4.00 (q, 2H, CH_2CH_3, *E* and *Z*) and a triplet at δ 1.25 (CH_2CH_3, *E*) and a triplet at 1.20 (CH_2CH_3, Z).

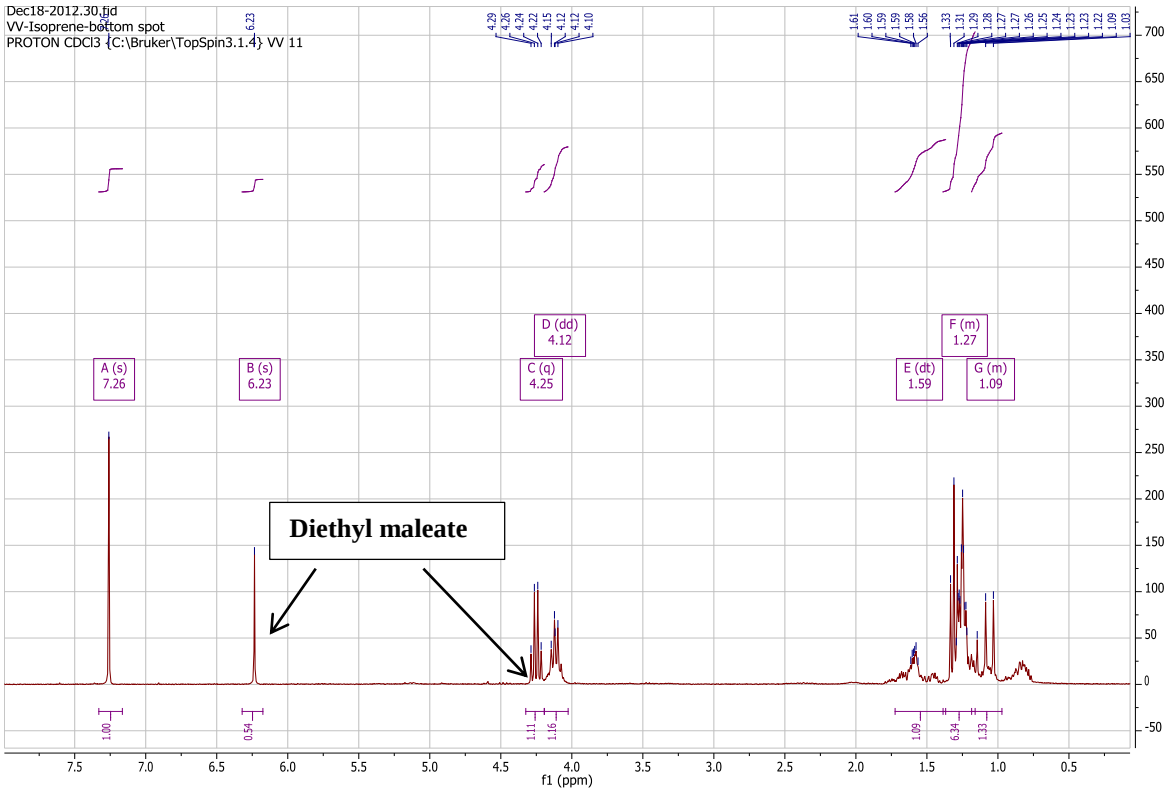

Figure 67 ^{1}H-NMR spectrum of the partially purified crude isoprene reaction mixture.

The Cu^{2+}-Wyoming bentonite catalysed cyclopropanation of isoprene **241** with EDA in dichloromethane gave less than 10% yield. The ^{1}H-NMR spectrum of the partially purified crude material showed a mixture of roughly equal amounts of *cis*- **242** and *trans*- **243** cyclopropane isomers and the carbene dimer (δ 6.23 (double bond C=CH) and C**H**$_2$CH$_3$ of diethyl maleate). Based on only ^{1}H-NMR data (Figure 67) it was difficult to differentiate between the *cis*- **24**2 and *trans*- **243** isomers. Due to the low yields obtained for this reaction and the apparently roughly equal amounts of the *cis*- **242** and *trans*-isomers **243**, it was decided not to continue with this reaction.

3.7.2 Relative bulkiness of the diastereomers 242 and 243 from Chem 3D model

Energy minimised Chem 3D structures give an estimate of the relative sizes of the diastereomers (Figure 68).

Using VIs computer modelling, the energy differences of the *cis*- and *trans*-β-lactam diastereomers **242** and **243** were calculated:

$E_{cis\text{-isomer}}$ - $E_{trans\text{-isomer}}$ = -462.5035312– (-462.5084723) Hartree = 0.004941*627.509391 kcal/mol = 3.100612 kcal/mol.

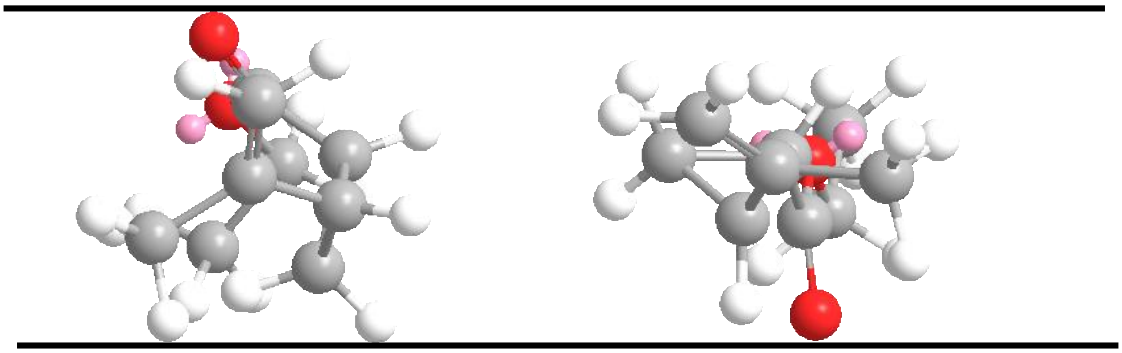

cis- bulky *trans*- less bulky

Figure 68 Chem 3D structures of *cis*- 242 and *trans*- 243 cyclopropanes from addition of EDA to isoprene 241.

3.7.3 Results of carbene addition reaction of EDA to isoprene 241

Under uncatalysed conditions there are no cyclopropane products formed and shows only a complex mixture. When reacted with EDA in the presence of Cu^{2+}-Wyoming bentonite in dichloromethane solvent the reaction did not proceeded smoothly and formed only a complex, crude and difficult to analyse product mixture, the investigation was discontinued.

3.7.4 Conclusions

Even though the same reaction is reported in the literature[180] proceeded smoothly, similarly to the attempted 1-hexene cyclopropanation reaction, this reaction failed to give recognisable *cis*- **242** and *trans*-cyclopropane **243** products and we found that this reaction is of no use under mineral catalysed conditions due to the complex mixture formed. Failure of this

reaction may be due to competition of the two double bonds in isoprene or to a Diels-Alder dimerisation reaction of the diene, which can be catalysed by Cu^{2+}-exchanged clay minerals.[12]

We then choose to investigate the cyclopropanation of the hindered symmetrical diene, 2,5–dimethyl–2,4–hexadiene **133**, to determine whether stereoselectivity can be achieved under mineral catalysed conditions.

3.8 Carbene addition reaction of 2,5–dimethyl–2,4–hexadiene 133 with EDA.

Carbenes generated from EDA have been reported[2,151] to undergo addition reactions to the diene **133** to form both the *cis*- **244** and *trans*- **134** cyclopropanes as the major products and diethyl fumarate **232** and diethyl maleate **233** carbene dimers as the minor products. Cu^{2+}-exchanged Wyoming bentonite with dichloromethane as solvent gave the *cis-/trans*-isomers **244** and **134** (45 : 55) (Scheme 85) in reasonable yield (*ca.* isolated 48%) (Table 21).

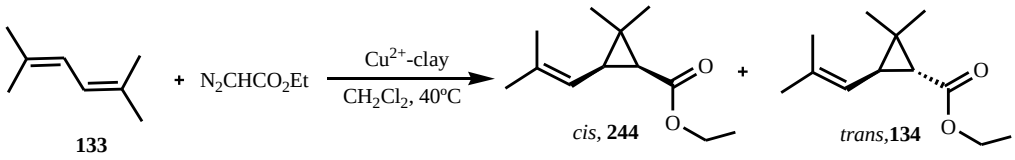

Scheme 85 Cyclopropane formation of 2,5–dimethyl–2,4–hexadiene 133.

3.8.1 Assignment of the structures of the *cis*- 244 and *trans*- 134 isomers

The *cis*- **244** and *trans*- **134** diastereomers were identified based on the assignment of their ^{1}H-NMR (Figures 70), ^{13}C NMR, ^{1}H-^{1}H 2D COSY and ^{1}H-^{1}H 2D NOESY spectra.

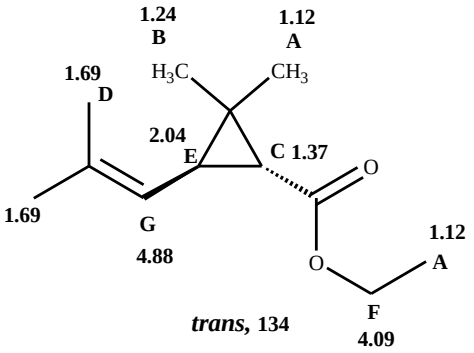

Figure 69 ***trans*-Isomer 134 of the cyclopropane from 2,5–dimethyl–2,4–hexadiene 133 and EDA.**

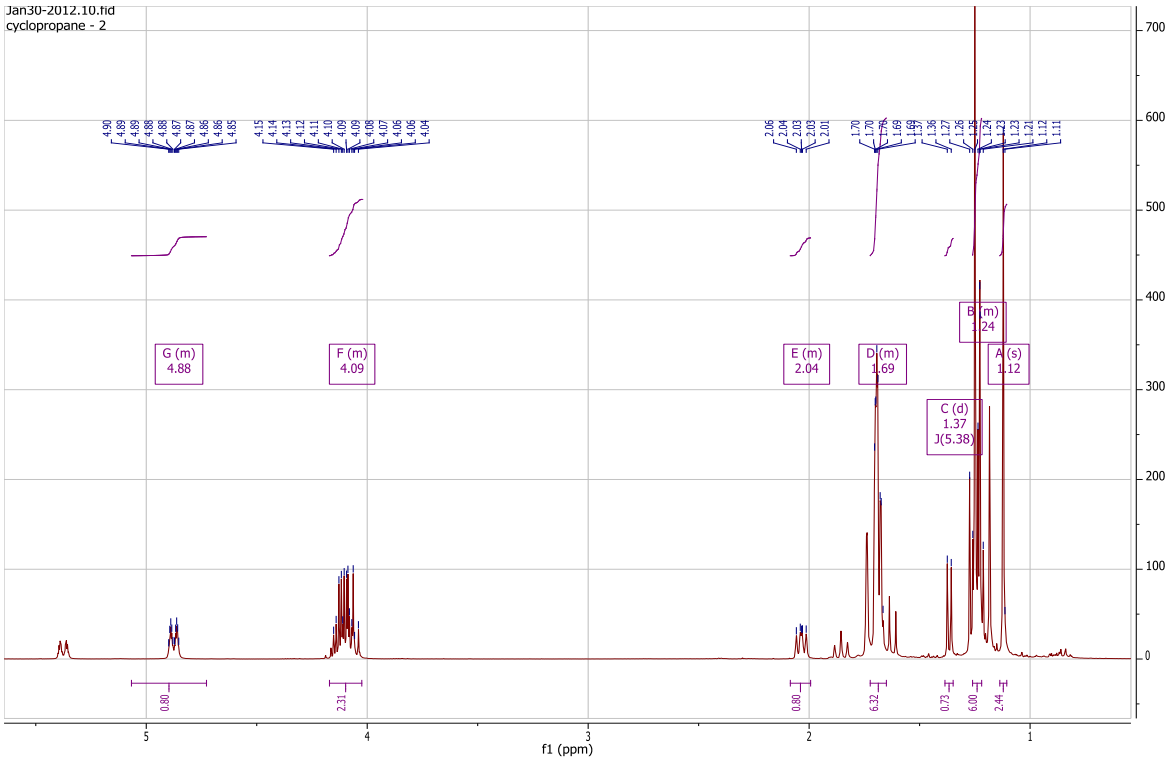

Figure 70 **^{1}H-NMR spectrum of the (major) *trans*-isomer 134 from the partially purified mixture of *cis-/trans*-cyclopropanes from 2,5–dimethyl–2,4–hexadiene 133 and EDA 33.**

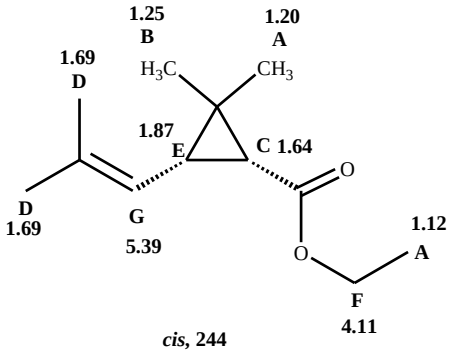

Figure 71 The *cis*-cyclopropane 244 from 2,5–dimethyl–2,4–hexadiene 131 and EDA

Based on the literature values,[8,181] the ^{1}H–NMR spectrum of *trans*-isomer **134** from diene **131** should show a characteristic resonance at δ 4.89 (d, 1H, C=C**H**) and the *cis*-isomer **244** at δ 5.39 (d, 1H, -C=C**H**). The *cis*-/*trans*- isomer ratios were calculated from the ^{1}H-NMR spectra, based on the integration values of the characteristic doublets at δ 4.88 (1H, -C=C**H**) and δ 5.39 (1H, -C=C**H**) (Figure 70).

3.8.2 Relative bulkiness of the diastereomers 244 and 134 from Chem 3D model

Energy minimised Chem 3D structures give an estimate of the relative sizes of the diastereomers (Figure 72).

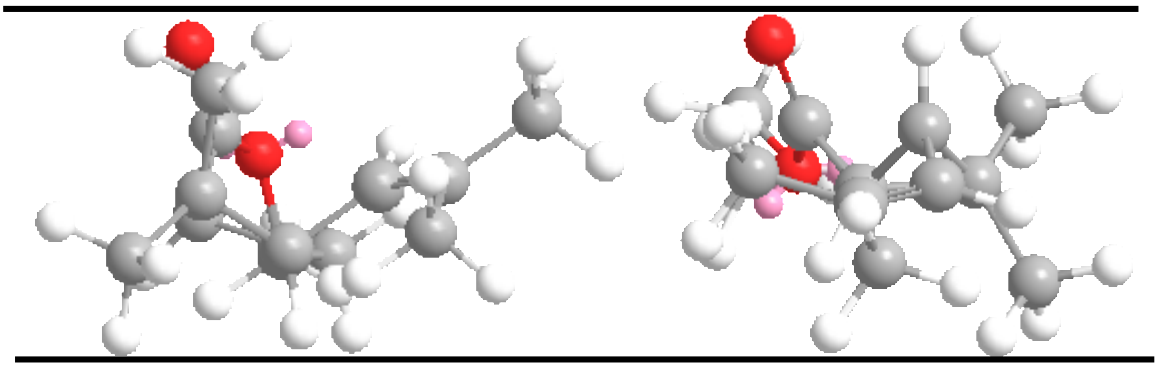

cis slightly less bulky *trans* bulky, lower energy

Figure 72 Chem 3D structures of *cis*- 244 and *trans*- 134 isomers of the cyclopropane from 2,5-dimethyl–2,4–hexadiene 133 and EDA.

Using VIs computer modelling, the energy difference of the *cis*- and *trans*-*β*-lactam diastereomers **244** and **134** were calculated:

$E_{cis\text{-isomer}}$ - $E_{trans\text{-isomer}}$ = -580.4559561– (-580.4586209) Hartree = 0.002665*627.509391 kcal/mol = 1.672206 kcal/mol

The Chem 3D model structures (Figure 72) of the *cis*- **244** and *trans*- **134** cyclopropanes from 2,5-dimethyl–2,4–hexadiene **133** showed that the *cis*-isomer **244** was very slightly less bulky than the *trans*-isomer **134**, but is of higher energy in its extended conformation. Thus we expect the less bulky *cis*-isomer **244** as the major product and the *trans*-isomer **134** as a minor product when the reaction occurs within the restricted environment of the clay minerals or the pores of the zeolites, but from their relative energies the *trans*-isomer **134** may be preferred in a non-constrained environment.

3.8.3 Effects of varying the solvent or the interlayer spacing of clay minerals on the ratio of diastereomers 244 and 134

Reaction in 1,4-dioxane as solvent gave an isolated yield of *ca.* 35% with *cis-/trans*-isomer ratio of 30 : 70, while in 1,2-dichloroethane the *ca.* isolated yield was 40% with *cis-/trans*-isomer ratio of 36 : 64. In chloroform or ethyl acetate as solvent the ratio of the *cis-/trans*-isomers was lower compared to other solvents (Table 22). Dichloromethane and toluene were found to be the best solvents for selection of the less bulky *cis*-isomer due to their keeping the interlayer distance fairly close (3.52 Å and 3.36 Å) respectively (Table 22).

Table 22 Measured (XRD) Δd values for Cu(II)-Wyoming bentonite in various solvents.

Solvents	% Yield of *cis*-/*trans*-diastereomers **244** & **134**	*cis*-/*trans*-diastereomer ratio	Interlayer distance of Cu(II) exchanged Wyoming bentonite, Δd (Å), assuming the clay layers ≈ 9.6 Å[164]
Dichloromethane	48	45 : 55	3.52
Chloroform	46	33 : 67	-
Ethyl acetate	45	37 : 63	-
Toluene	32	42 : 58	3.36
1,4-Dioxane	35	30 : 70	-
1,2-Dichloroethane	40	36 : 64	-

3.8.4 Effect of varying the layer charge of a clay mineral on the ratios of diastereomers 244 and 134

The Cu^{2+}-carbene modified clay (Al-O-EA) catalyst gave similar results to those of Cu^{2+}-Wyoming bentonite (Table 23). While Cu^{2+}-ZSM-5 gave a slightly increased proportion of the more energetically favoured *trans*-isomer **134**.

Table 23 Measured yield, isomer ratios and Δd values for clay minerals in various solvents.

Cu^{2+}-exchanged clay mineral	Solvent	% Yield of cyclopropanes **244** & **134**	*cis*-/*trans*-diastereomer ratio	Interlayer distance of Cu(II)-clay mineral, Δd (Å), assuming the clay layers ≈ 9.6 Å[164]
Wyoming bentonite	CH_2Cl_2	48	45 : 55	3.52
Modified clay	CH_2Cl_2	44	45 : 55	> 3.09
ZSM-5	CH_2Cl_2	47	38 : 62	5.4 - 5.6

3.8.5 Conclusions

Chem 3D model structures (Figure 72) of both the *cis*- **244** and *trans*- isomers **134** showed that the *cis*-isomer **244** is slightly less bulky than the *trans*-isomer **134**. However,

thermodynamically more stable *trans*-isomer **244** should be favoured in free solution reactions, whereas under constrained catalytic conditions the less bulky *cis*-isomer **134** should be favoured. When this reaction is compared with the literature[2] (30 : 70 ca. isolated yield 68%) the proportion of the *cis*-isomer has increased within the Cu^{2+}-Wyoming bentonite (45 : 55 ca. isolated yield 48%) suggesting that there is some size selectivity occurring.

The final reactant choosen was *trans*-cinnamic acid **245** to see if the carbene would select the alkene or carboxylic acid OH on reaction with EDA in the presence of the mineral catalysts.

3.9 Carbene addition reaction of EDA to *trans*-cinnamic acid 245

When *trans*-cinnamaldehyde was reacted with EDA in the presence of a rhodium catalyst,[182] only CH the insertion product was formed. Similarly, the insertion product was also produced when the *trans*-cinnamic acid **245** was reacted in the presence of Cu^{2+}-clay catalysts (Scheme 86). These demonstrate that carbene insertion into activated CH's is preferred to addition across a conjugated C=C.

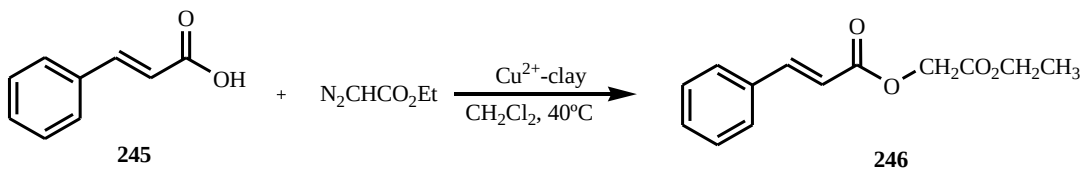

Scheme 86 Carbene insertion into *trans*-cinnamic acid 245.

3.9.1 Assignment of the structure of the insertion product of *trans*-cinnamic acid 245

The ^{1}H-NMR spectrum (Figure 74) of the purified product from Cu^{2+}-Wyoming bentonite catalysed carbene insertion of EDA into the OH of *trans*-cinnamic acid (Figure 73) in dichloromethane showed doublet peaks at δ 6.41 (1H, *J* = 16.00 Hz, Ar-CH=C**H**) and δ 7.64 (1H, *J* = 16.00 Hz, Ar-C**H**=CH), which confirms that the *trans*-double bond is still in the

molecule, while the singlet at δ 4.60 for the CH_2 (methylene group) confirms the formation of the ester.

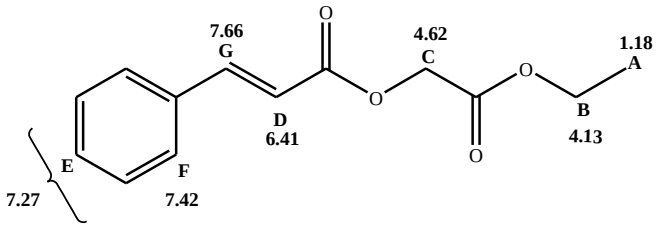

Figure 73 Insertion product of *trans*-cinnamic acid 245 to form the *β*-keto ester 246.

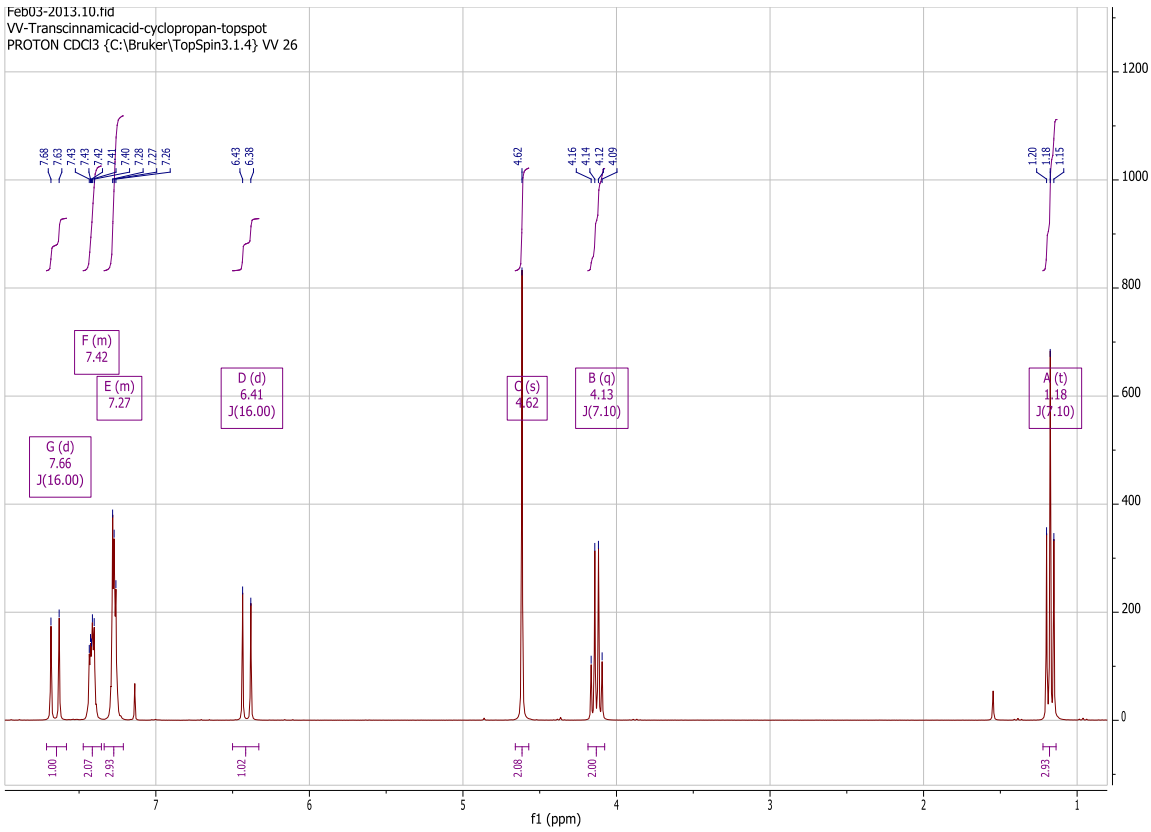

Figure 74 Insertion product of *trans*-cinnamic acid 245 forming *β*-keto esters.

3.9.2 Conclusions

Similar to the carbene insertion reactions in Chapter 2, carbene addition reactions across double bonds are expected to favour the formation of less bulky products within the interlamellar region of caly catalysts or pores of zeolite. Except for very non-polar alkenes, some cyclopropanes were formed, even for poor substrates like cyclohexene **131** and 1,5-cyclooctadiene **238**. Generally, if reaction occurred at all, reaction within the restricted region of Cu^{2+}-exchanged clay minerals showed only modest selectivity for the less bulky isomer, probably due to the reactants themselves altering the Δd of the clay mineral. Somewhat better selectivity was seen with Cu^{2+}-ZSM-5, but only in cases where the size of the molecule approached the pore diameter. In many cases the generated carbenes from EDA favoured the formation of the carbene dimers, diethyl fumarate **232** and diethyl maleate **233**. The yields were very low in most of the carbene additions compared to literature values, probably due to the competing reaction of carbene insertion into the Al-O-H of the octahedral layer of the clay mineral. Carbene insertion reaction into the functional groups of compounds such as *trans*-cinnamic acid **245** to give the ester **246**, also occurred readily.

In order to get around the apparent problems of carbene insertion into the AlO-H bond of the clay mineral we decided to see whether a more bulky diazo compound would have more difficulty in carrying out this insertion reaction and, so improve the yield of the cyclopropanation reaction. Thus, we used a series of more sterically demanding azo dicarbonyl compounds for Cu^{2+}-mineral catalysed cyclopropanation reactions.

3.10 Cyclopropane formation with more sterically demanding diazodicarbonyl compounds

The cyclopropane ring is an important component of many natural products and synthetic drugs.[183] Cyclopropane rings having two geminal electron-withdrawing groups are required precursors of biologically important cyclopropyl α- and β-amino acids.[184] Generation of cyclopropane *gem*-diesters by transisition metal catalysed intermolecular cyclopropanation from readily available alkenes and the corresponding diazo reagent appears to be an efficient and easy process.[185]

Our aim was to synthesise cyclopropane rings bearing geminal dicarboxy groups (Table 24) to, hopefully, give increased yields over EDA reactions and to improve stereoselectivity of the reactions within the restricted environment of mineral catalysts. In order to prepare a racemic cyclopropane, we chose the diazodicarbonyl compound 1,3–dimethyl 2-diazopropanedioate **247**, as it can be synthesised easily from dimethyl malonate and *p*-TSAz.[186] Methyl *N*-piperidinodiazomalonate **187** and methyl pyrrolidinodiazomalonate **189** were available from our previous work on *β*-lactam formation (Chapter 2). The methyl piperidinodiazomalonate **187** did not give any *β*-lactam in dichloromethane as solvent and the more strained pyrolidino-*β*-lactam possible from the diazodicarbonyl **189** was not formed under the usual reaction conditions. Each of these diazodicarbonyl compounds were reacted with styrene as this tended to give reasonable yields with EDA (Table 24).

Table 24 Cyclopropane ring formation with various diazo reagents with styrene in the presence of Cu(II) exchanged Wyoming bentonite.

Diazo reagents	Cyclopropanes	% Yield
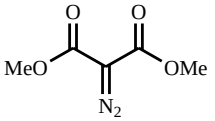 **247**	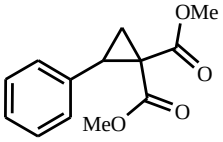 **248**	10
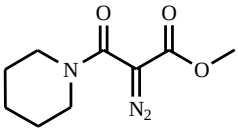 **187**	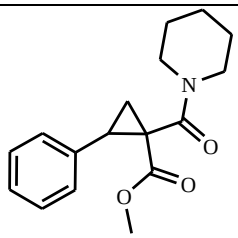 **249**	12
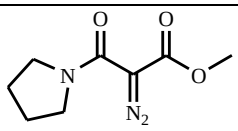 **189**	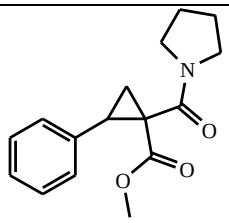 **250**	12

3.11 Catalysed cyclopropane ring formation between styrene 87 and 1,3–dimethyl 2–diazopropanedioate 247

1,3–Dimethyl 2-diazopropanedioate **247** has been reported to react with styrene **87** in the presence of the rhodium catalyst ($Rh_2(esp)_2$) to form the cyclopropane product **248**.[185] The same reaction performed in the presence of Cu^{2+}-Wyoming bentonite also formed the cyclopropane product **248** (Scheme 87).

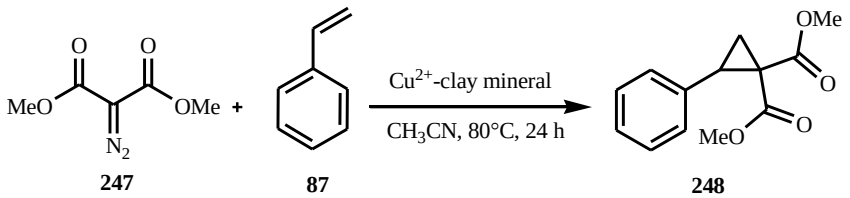

Scheme 87 Synthesis of methyl 2-phenyl-cyclopropane-1,1-dicarboxylic acid methyl ester 248 in the presence of Cu(II) Wyoming bentonite.

3.11.1 Assignment of the structure of the 2-phenyl-cyclopropane-1,1-dicarboxylic acid methyl ester 248

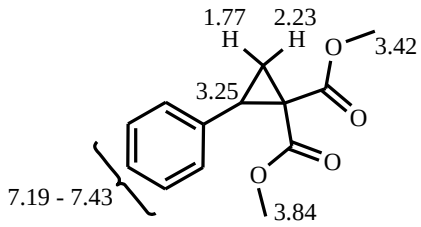

248

The data from the ^{1}H NMR spectrum, showed two double doublets at δ 1.77 (*J* = 9.20, 5.20 Hz cyclopropyl CH), δ 2.23 (*J* = 8.0, 5.20 Hz, cyclopropyl CH) and a triplet at δ 3.25 (*J* = 8.70 Hz, Ph-CH) which matched reasonably well with the literature values dds at 1.73 (dd, *J* = 9.20, 5.20 Hz, 1H) and 2.19 (dd, *J* = 8.0, 5.20 Hz, 1H) and a triplet at 3.23 (t, *J* = 8.60 Hz,

1H); other values were also consistent with the literature[185,187] comparative data shown in Table 25.

Table 25 Comparative ^{1}H NMR data for 2-phenyl-cyclopropane-1,1-dicarboxylic acid methyl ester 248.

Literature[187]	Experimental
1.73 (dd, *J* = 9.20, 5.20 Hz, 1H)	1.77 (dd, 1H, *J* = 9.20, 5.20 Hz, CH (cyclopropyl))
2.19 (dd, *J* = 5.20, 8.00 Hz, 1H)	2.23 (dd, 1H, *J* = 5.20, 8.00 Hz, CH (cyclopropyl))
3.23 (t, *J* = 8.60 Hz, 1H)	3.25 (t, 1H, *J* = 8.70 Hz, Ar-CH)
3.36 (s, 3H)	3.42 (s, 3H, -OCH_3)
3.79 (s, 3H)	3.84 (s, 3H, -OCH_3)
7.18 - 7.29 (m, 5H)	7.19 – 7.43 (m, 5H, Ar-H)

3.11.2 Results for 2-phenyl-cyclopropane-1,1-dicarboxylic acid methyl ester 248.

Initially, styrene **87** was reacted with 1,3–dimethyl 2–diazopropanedioate **247** without catalyst under thermal conditions and the reaction gave no cyclopropane product. In the literature reaction catalysed by the rhodium catalyst, ($Rh_2(esp)_2$), 2-phenyl-cyclopropane-1,1-dicarboxylic acid methyl ester **248** was formed with an isolated yield of *ca*. 93%).[186] When the same reaction was performed using Cu^{2+}-Wyoming bentonite as a catalyst in dichloromethane, no reaction was seen. However, in acetonitrile the cyclopropane **248** was formed in low yield (*ca*. isolated yield 10%). Unfortunately, in this case, the hoped for increase in yield were not obtained.

3.12 Catalysed cyclopropane ring formation between styrene 87 and *N*-piperidinodiazomalonate 187

Methyl *N*-piperidinodiazomalonate **187** was reported to react with styrene **87** in the presence of the rhodium catalyst ($Rh_2(oct)_4$) to form cyclopropane **249** in 29% yield.[188] Similarly, when the same reaction was performed in the presence of Cu^{2+}-Wyoming bentonite in dichloromethane, there was no reaction, but in acetonitrile, the intramolecular insertion

reaction products *cis*- **217** and *trans*-*β*-lactams **218** were obtained as the major product, with the cyclopropane **249** as minor product (Scheme 88).

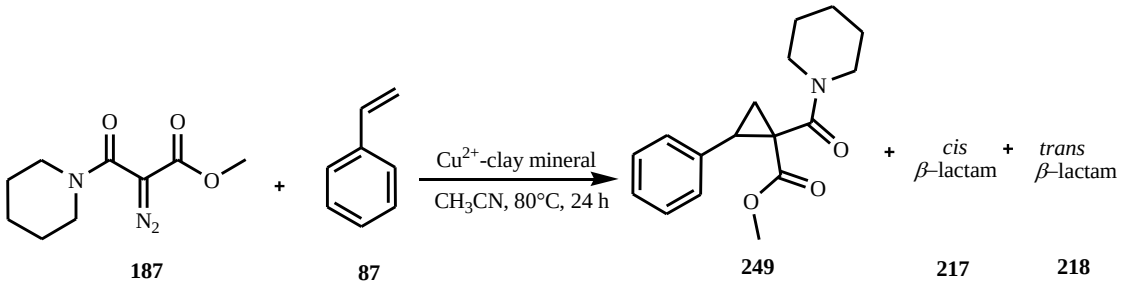

Scheme 88 Synthesis of methyl 2-phenyl-1-(piperidine-1-carbonyl) cyclopropane carboxylate 249 in the presence of Cu(II) Wyoming bentonite.

3.12.1 Assignment of the structure of the methyl 2-phenyl-1-(piperidine-1-carbonyl) cyclopropane carboxylate 249.

The data from the ^{1}H NMR spectra (Table 26) showed the dd at δ 2.13 (*J* = 5.10, 8.02 Hz, -CH, cyclopropane ring) and a triplet at δ 3.18 (*J* = 8.40 Hz, PhCH) were consistent with the literature dd at 2.16 (*J* = 5.0, 8.20 Hz, 1H) and a triplet at 3.18 (*J* = 8.40 Hz, 1H); other values matched with the literature[151,188] comparative data shown in Table 26.

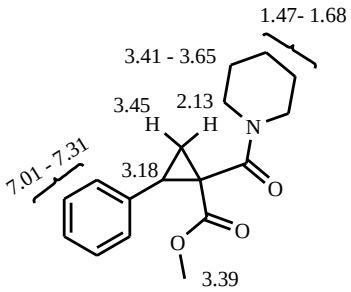

249

Table 26 Comparative ^{1}H NMR data for methyl 2-phenyl-1-(piperidine-1-carbonyl) cyclopropane carboxylate

Literature[188]	Experimental
1.52 - 1.63 (m, 7H)	1.47 – 1.68 (m, 7H, C-H piperidine ring)
2.16 (dd, *J* = 5.0, 8.20 Hz, 1H)	2.13 (dd, *J* = 5.10, 8.02 Hz, 1H, C-H (cyclopropyl))
3.18 (t, *J* = 8.40 Hz, 1H)	3.18 (t, *J* = 8.40 Hz, 1H, Ar-CH)
3.39 (s, 3H)	3.39 (s, 3H, -OCH3)
3.40 - 3.58 (m, 4H)	3.41 – 3.65 (m, 4H, CH piperidine ring, C-H (cyclopropyl))
7.18 - 7.26 (m, 5H)	7.01 – 7.31 (m, 5H, Ar-H)

3.12.2 Results for methyl 2-phenyl-1-(piperidine-1-carbonyl) cyclopropane carboxylate 249.

Methyl *N*-piperidinodiazomalonate **187** did not react with styrene without catalyst. The same reaction catalysed by Cu^{2+}-Wyoming bentonite in dichloromethane, once again, failed. However, in acetonitrile cyclopropane **249** was formed in low yield (*ca*. isolated yield 12%), the major products being the carbene insertion reaction *β*-lactam products **217** and **218** as expected from Section 2.7. The yield might have been improve if the reaction had occurred in dichloromethane, which we had found did not give *β*-lactam products with Cu^{2+}-Wyoming bentonite, but these did show that intramolecular carbene insertion occurs more readily than carbene addition to a double bond. A higher yield of cyclopropane product **249** might have been achieved if a large excess of styrene were used in the reaction, but this was not done as styrene can polymerise within cation exchanged clay minerals.

3.13 Catalysed cyclopropane ring formation between styrene 87 and *N*-pyrrolidinediazomalonate 189

Methyl *N*-pyrrolidine diazomalonate **189** has been reported to react with styrene **87** in the presence of rhodium tetraoctanoate catalyst to form the cyclopropane **250**.[188] Once again, the same reaction performed in the presence of Cu^{2+}-Wyoming bentonite in dichloromethane

failed to occur. Again, in acetonitrile the cyclopropane product **250** were formed as minor products with carbene dimers **227** and **228** as major products (Scheme 89).

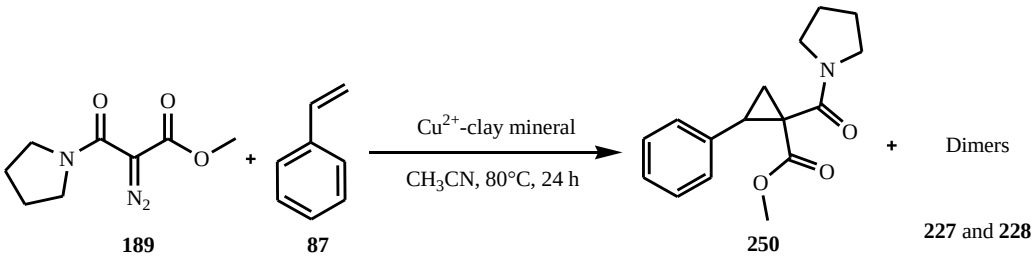

Scheme 89 Synthesis of methyl 2-phenyl-1-(pyrrolidine-1-carbonyl) cyclopropane carboxylate 250 in the presence of Cu(II) Wyoming bentonite.

3.13.1 Assignment of the structure methyl-2-phenyl-1-(pyrrolidine-1-carbonyl) cyclopropane carboxylate 250

The data from the ^{1}H NMR spectrum showed dds at δ 1.52 (*J* = 4.90, 9.10 Hz, CH cyclopropane) and at 2.19 (*J* = 4.90, 8.00 Hz, CH cyclopropane) which were consistent with the literature[188] comparative data as shown in Table 27.

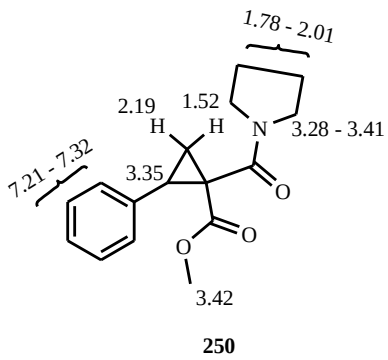

Table 27 Comparative ^{1}H-NMR data for methyl 2-phenyl-1-(pyrrolidine-1-carbonyl) cyclopropane carboxylate 250

Literature[188]	Experimental
1.53 (dd, *J* = 4.70, 9.10 Hz, 1H)	1.52 (dd, *J* = 4.90, 9.10 Hz, 1H, C-H cyclopropyl ring)
1.87 – 2.01 (m, 4H)	1.78 - 2.01 (m, 4H, *pyrrolidine ring*)
2.21 (dd, *J* = 4.70, 7.90 Hz, 1H)	2.19 (dd, *J* = 4.90, 8.00 Hz, 1H, Cyclopropyl-CH)
3.27 – 3.41 (m, 2H)	3.28 – 3.41 (m, 2H, *N*-CH, Ar-CH cyclopropyl)
3.42 (s, 3H)	3.42 (s, 3H, -OCH_3)
3.50 – 3.78 (m, 3H)	3.72 – 3.96 (m, 3H, C-H *pyrrolidine ring*)
7.22 - 7.30 (m, 5H)	7.21 – 7.32 (m, 5H, Ar-H)

3.13.2 Results for methyl 2-phenyl-1-(pyrrolidine-1-carbonyl)cyclopropane carboxylate 250

In a similar manner to **247** and **187**, methyl *N*-pyrrolidinediazomalonate **189** did not react with styrene without catalyst or with Cu^{2+}-Wyoming bentonite in dichloromethane. Once again, under catalytic conditions in acetonitrile in the presence of Cu^{2+}-Wyoming bentonite, cyclopropanes **250** were formed in low yield (*ca*. isolated yield 12%) with the major products being the carbene dimers **227** and **228** (> 50% yield from the crude). Compared to the reported yield with the rhodium catalyst ($Rh_2(oct)_4$) (79%),[187] methyl 2-phenyl-1-(pyrrolidine-1-carbonyl)cyclopropane carboxylate **250** was formed in low yield (ca isolated yield 10%) with Cu^{2+}-Wyoming bentonite.

3.14 Conclusions

Similar to carbene addition reaction with alkene and EDA, we were also attempted the same reaction with different diazo reagent which are readily available **247**, **187** and **189** to form respective cyclopropane rings. The first diazo molecule **247** having less bulky geminal ester groups when it reaches the interlayer space unable to push the layers expand and resulting in less selectivity cyclopropane ring formation (ca isolated yield 10%) compared to literature (ca isolated yield 93%). Similarly, the methyl *N*-piperidinodiazomalonate **187**, having carbonyl

groups from methyl ester and piperidine amide were more bulkier than in the **247**, but this molecule **187** is more preferred to carbene insertion reaction products **217** and **218** β-lactams (> 50% yield from the crude) and with minor cyclopropane ring **249** (ca isolated yield 12%) reasonable to literature (ca isolated yield 29%). The *N*-pyrrolidinediazomalonate **189**, similar to **187** favoured to carbene insertion reaction dimer formation **227** and **228** as a major product and minor cyclopropane ring **250** product (ca isolated yield 12%) obtained with low yield compared to literature (ca isolated yiled 79%).

4 Chapter: Nitrenes

4.1 Introduction of nitrenes addition reactions

Nitrenes are uncharged, electron deficient molecular species that contain a monovalent nitrogen atom surrounded by a sextet of electrons.[139] Aziridines are useful synthetic intermediates, which can be used in the preparation of nitrogen–containing functional compounds via ring opening and ring expansion reactions.[189] They are also found in some natural products as well as biologically active compounds such as mitomycins and azinomycins.[82]

Metal catalysed nitrene transfer reactions such as aziridination of alkenes have an important applications in synthetic chemistry. In the recently reported literature,[190] there has been a wide range of interest in the use of organic azides as nitrogen-transfer reagents because nitrogen gas is formed as a by-product, which is non-hazardous to the environment. In the literature,[191] copper-catalysed aziridination of styrene with copper-exchanged zeolite Y (CuHY) and copper (ii) triflate (trifluoromethanesulfonate) ($Cu(OTf)_2$) have been reported as catalysts. Thus, reactions in the pores of zeolites have been demonstrated as effective immobilised catalysts and we wanted to explore the possibility of using other mesoporous materials for generating nitrene intermediates to form aziridine rings. Similar to the catalysed carbene addition and insertion reactions described in Chapter 2 and 3, we attempted to generate nitrenes within the restricted environment of the Cu^{2+}-exchanged clay mineral or zeolites.

Table 28 Aziridination of styrene with various aryl azides in the presence of Cu^{2+}-Wyoming bentonite catalyst

Aryl azides	Product (% yield)
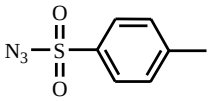 **182**	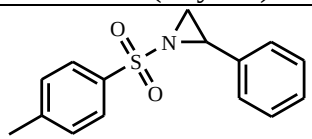 **251** 12%
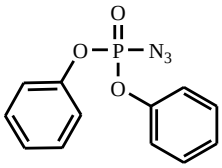 **252**	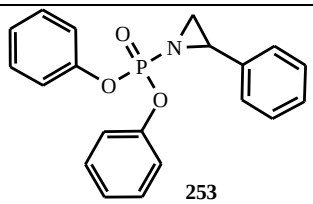 **253** Complex crude
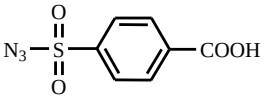 **254**	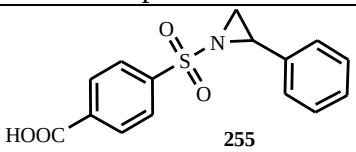 **255** Complex crude

4.2 Catalysed nitrene addition reaction

The literature reports that when styrene **87** was reacted with *p*-toluenesulfonyl azide in the presence of 4A MS an aziridine **251** was formed.[192] When the same reaction was performed thermally under uncatalysed condition there was no product formed. Whereas, on using Cu^{2+}-Wyoming bentonite as a catalyst we were able to form aziridine **251** from styrene **87** and *p*-toluenesulfonyl azide **182** (Scheme 90).

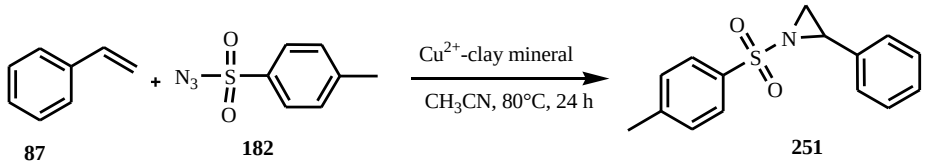

Scheme 90 Nitrene addition reaction in the presence of Cu^{2+}-Wyoming bentonite.

4.2.1 Assignment of the structure *N*-(*p*-tolylsulfonyl)-2-phenylaziridine 251

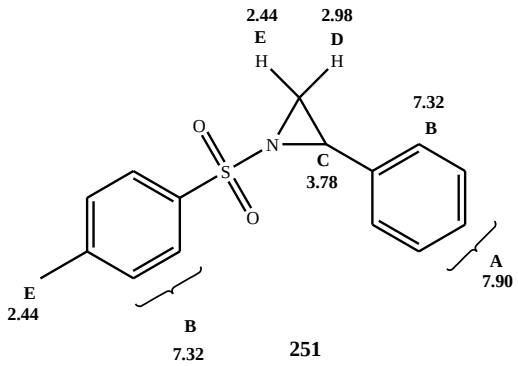

Figure 75 ***N*-(*p*-Tolylsulfonyl)-2-phenylaziridine 251**

From the ^{1}H NMR spectrum of the partially purified of *N*-(*p*-tolylsulfonyl)-2-phenylaziridine **251** (Figure 76) the δ values at 2.98 (d, *J* = 7.20 Hz, 1H) corresponds to the aziridine ring hydrogen, which is consistent with the literature[139] value at 2.99 (d, *J* = 7.20 Hz, 1H). The other values also consistent with the literature comparative data shown in Table 29.

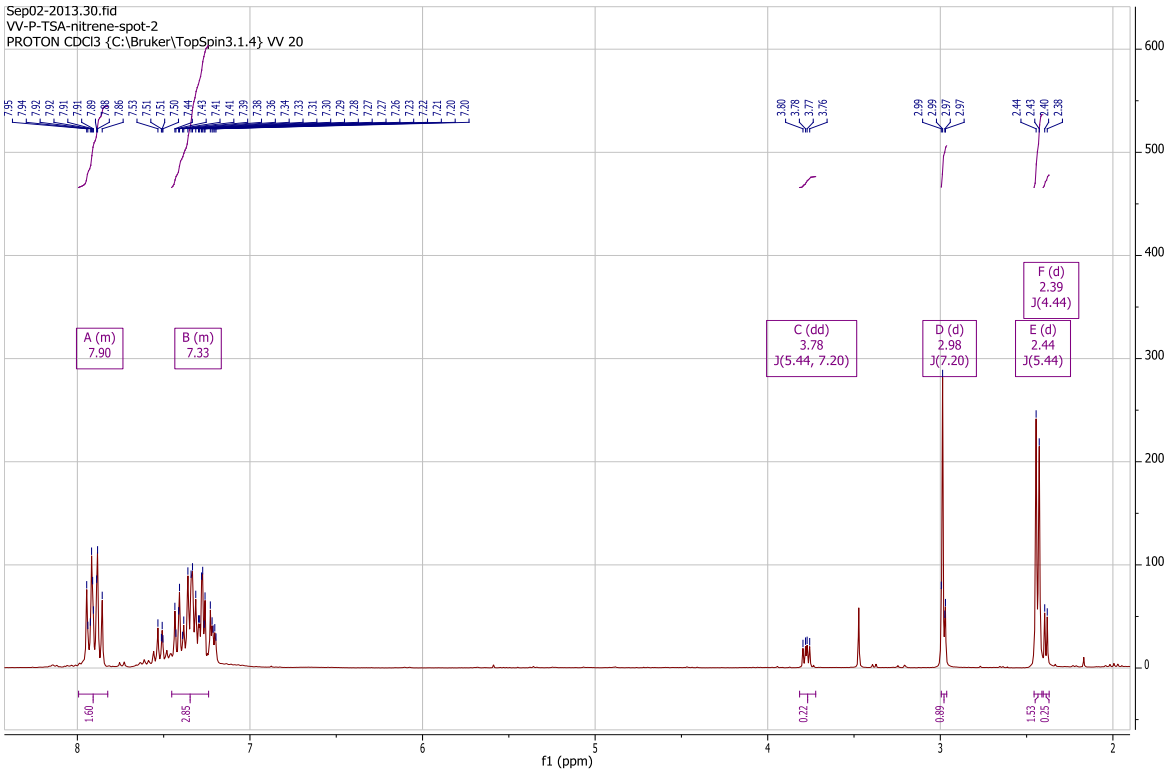

Figure 76 **^{1}H-NMR of the partially purified *N*-(*p*-tolylsulfonyl)-2-phenylaziridine**

Table 29 Comparative ^{1}H NMR data of *N*-(*p*-tolylsulfonyl)-2-phenylaziridine 251

Literature	Experimental
2.38 (d, *J* = 4.40 Hz, 1H) 2.43 (s, 3H)	2.41 – 2.47 (m, 4H, Ph-CH_3, CH_E aziridine)
2.98 (d, *J* = 7.20 Hz, 1H)	2.98 (d, *J* = 7.20 Hz, 1H, CH_D aziridine)
3.78 (dd, *J* = 4.40, 7.20 Hz, 1H)	3.78 (dd, *J* = 5.44, 7.20 Hz, 1H, Ar-CH)
7.20 (m, 2H) 7.27 – 7.31 (m, 3H) 7.33 (d, *J* = 8.40 Hz, 2H) 7.87 (d, *J* = 8.40 Hz, 2H)	7.17 – 7.47 (m, 6H, Ar-H) 7.82 – 7.99 (m, 3H, Ar-H)

4.2.2 Results for *p*-toluenesulfonyl azide 182 addition onto styrene 87

Our initial aim was to show whether the restricted environment of a Cu^{2+}-clay mineral will allow a nitrene intermediate to be produced and then lead to aziridine ring formation in a similar manner to that reported in the literature for a zeolite:[192] where styrene was reacted with *p*-toluenesulfonyl azide in dichloromethane in the presence of 4A MS to yield 94% aziridine **251**. We attempted the same nitrene addition reaction with Cu^{2+}-Wyoming bentonite, initially using dichloromethane as a solvent, but found no reaction even under reflux conditions. Then by using acetonitrile as the solvent, with Cu^{2+}-Wyoming bentonite as catalyst, we succeded in forming the aziridine **251** in low yield (*ca*. isolated yield 12%).

Although the yield was low and we did not have time to try optimisation of solvents, etc., this result still made us optimistic that there was for future development of syntheses for various pharmaceutical products by using different alkenes to react with *p*-toluenesulfonyl azide within the interlamellar region of clay catalysts.

We then attempted the nitrene addition reaction with two different aryl azide diazo reagents **252** and **254** available in our laboratory to see if reaction within the clay minerals would favour aziridine ring formation.

4.2.3 Results for nitrene addition reaction onto the styrene 87 with diphenylphosphoryl azide 252

In accord with a literature synthesis,[193] we attempted to form an aziridine ring using diphenylphosphoryl azide **252** as a nitrene source for reaction with styrene in the presence of Cu^{2+}-Wyoming bentonite (Scheme 91). The ^{1}H-NMR spectrum of the crude reaction product showed a complex mixture. The failure of this reaction may be due to the bulkiness of the arylphosphorylazide reagent **252**, which has two benzoxy groups that could be hindering access to the interlayer space of the clay mineral.

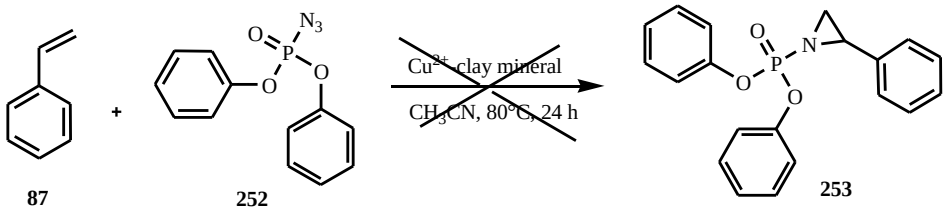

Scheme 91 Attempted synthesis of an aziridine ring with diphenylphosphoryl azide 252 and styrene 87 using Cu^{2+}-Wyoming bentonite as catalyst.

Aziridine ring formation was attempted using 4-(azidosulfonyl)benzoic acid **254** in the presence of Cu^{2+}-Wyoming bentonite catalyst (Scheme 92), but once again the reaction showed a complex mixture from the crude ^{1}H NMR spectrum. The reaction failure may be due to the acid group present in the aryl azide reagent ring-opening the aziridine to give amines, which may go on to form a complex mixture.

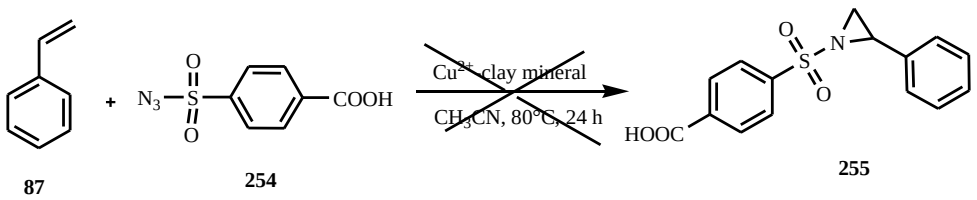

Scheme 92 Attempted synthesis of an aziridine ring with 4-(azidosulfonyl)benzoic acid 254 and styrene 87 using Cu^{2+}-Wyoming bentonite as catalyst.

4.3 Conclusions for nitrene addition reactions of styrene 87

We attempted the nitrene addition reaction with three different aryl azide diazo reagents **182**, **252** and **254** (Table 28)3 to see if reaction within the clay minerals would favour aziridine ring formation. Only the *p*-toluenesulfonyl azide gave a recognisable aziridine **251** in low yield; while both the other azides gave complex mixtures. This suggests that care must be taken in the choise of azides if the aziridination reaction is to succeed.

5 Chapter: Experimental

5.1 Instruments and Materials

Nuclear magnetic resonance spectra (^{1}H, ^{13}C, DEPT 135, COSY, HMQC, NOESY) were recorded either on a Bruker DPX 250 MHz or on Bruker Avance 300 MHz or 400 MHz spectrometers with tetramethylsilane (TMS) as internal standard for ^{1}H NMR and deuteriochloroform ($CDCl_3$, δ_C 77.23 ppm) for ^{13}C–NMR unless otherwise stated. Chemical shifts for ^{1}H NMR spectra are recorded in parts per million (ppm) from TMS with the solvent resonance as the internal standard (chloroform, δ 7.27 ppm) if TMS was not present. Data are reported as follows: chemical shift (δ), the abbreviations used for the multiplicity of the ^{1}H NMR signals are (s = singlet, d = doublet, t = triplet, q = quartet, m = multiplet, dd = doublet of doublets, dt = double triplet, dq = double quartet and br = broad), coupling constant (*J*) in Hertz (Hz), then integration. Chemical shifts for ^{13}C NMR spectra are recorded in parts per million from tetramethylsilane using the central peak of deuterochloroform (77.23 ppm) as the internal standard. When ambiguous, proton and carbon assignments were established using COSY, HSQC and DEPT experiments. Mass spectra were recorded on a Thermo Scientific Trace GC Ultra DSQ II using Electron Ionisation (GCMS–EI) Infrared spectra were recorded on a NICOLET IR 2000 FT-IR spectrometer and are reported in reciprocal centimeters (cm^{-1}), Thin Layer Chromatography (TLC) was carried out on Machery–Nagel polygram Sil/G/UV_{254} pre–coated plates. X–Ray diffraction (XRD) was recorded on an EQUINOX-2000 X-ray diffractometer for measuring the interlayer distance of clay minerals and XRF elemental analyses were carried out on a BRUKER D2 PHASER.

5.2 Purification and cation exchange of the minerals

Clay samples were first purified by a sedimentation process. This process was based on Stokes Law[25]. Stokes law relates the force on a particle (**F**), the particle radius (**r**), the viscosity (η) of the liquid that the particle is in and the terminal velocity (**v**) of the particle. The mathematical statement of Stokes law is:

$$F = 6\pi r\eta v$$

If we consider the density of the particle (ρ), minus the density of water to be **ρ*** and for convenience assume that all the particles are spherical,[194] then:

$$F = mg$$

$$\text{But } m = \rho^*$$

$$F = \rho^* gV$$

$$= 1.33\pi r^3 \rho^* g$$

$$\text{Thus } 6r\pi\eta v = 1.33\pi r^3 \rho^* g$$

$$v = 1.33\pi r^2 \rho^* g / (6\eta)$$

As time (t) = distance (d) /velocity (v)

$$t = 6\eta d / (1.33\pi r^2 \rho^* g)$$

Using this equation, we can calculate the time required for the clay particles below a certain size to drop below a certain level from a well–dispersed clay/water suspension.

If we take the viscosity of water,η, as 10^{-3} $Kgm^{-1}s^{-1}$ at 20ºC, the particle density, ρ, as $2.65x10^{-3}$ Kgm^{-3} then ρ^* is $1.65x10^{-3}$ Kgm^{-3}. The acceleration due to gravity, g, is 9.81 ms^{-2}. As we require clay particles of less than 2μm the radius of the particle, r, is 10^{-6}m. This gives a settling time of at least 7.7 h.

Typically, Wyoming bentonite (25 g) was taken in a 5 L beaker marked with a line about 2 cm from the top and another line10 cm below. 1M NaCl solution was added up to the top line and the mixture was stirred well before sonicating for 15–20 min in a sonicator bath. The

suspension was allowed to settle for about 7 h 15 min and the top 10 cm were siphoned off or decanted, if the solution were clear, from the 5 L beaker. The remaining suspension was topped up to the upper 10 cm line with deionised water and the stirring, sonication, settling, siphoning and topping up sequence repeated until little or no clay suspension was received. The siphoned suspensions were collected in 2.5 litre bottles and allowed to settle until clear. The majority of the clear liquid was decanted off and the clay mineral re-suspended and transferred to a centrifuge bottle and centrifuged for 15-30 minutes until a tight deposit was obtained. The aqueous layer was decanted and tested with $AgNO_3$ solution to check the presence of chloride ions by precipitation of AgCl (silver chloride). The clay deposit was washed until chloride free by repeated re-suspendion in deionised water and centrifugation. When the clay layer was chloride free it was transferred to a filter paper under suction on a Buchner funnel until no more water was removed. The filter cake was transferred to a watch glass and kept at 75ºC for 16 h until dry, then ground to a fine powder using a mortar and pestle.

5.3 XRD Characterisation

X–ray diffraction of clay minerals wetted with different solvents can help determine the alterations in the interlayer spacing by assuming that the montmorillonite layers themselves are 9.66 Å. Thus, the interlayer distance (Δd Å) of clay minerals wetted with solvents of interest were measured by using XRD.

Sample preparation: About 0.05 g of clay mineral samples were placed on the sample holder and the sample was wetted by careful spraying of the respective solvents onto the flat clay surface which was then covered and sealed with Mylar film to avoid solvent evaporation. The sample holder was placed in the powder X-ray diffractometer and the diffraction trace (Intensity vs. 2θ) recorded. The 2θ value is converted to a distance, d, by means of the Bragg relationship[195]: $n\lambda = 2d \sin(\theta)$, which for n = 1 and small angles, θ, approximates closely to: $d = \lambda / 2\theta$ $\lambda = 1.54184$ Å α x-ray wavelength used. The initial broad peak (d_{001}) of the diffraction trace represents the interlayer spacing ($d_{spacing}$) from which the interlayer distance (Δd) is calculated on the basis of the formula: $\Delta d = d_{spacing} - 9.66$ Å. Where the value 9.66 Å represents the repeat distance of a fully collapsed clay mineral layer.

The value of Δd depends upon the degree of hydration of the clay mineral, the size of the interlayer cation and the stacking/interaction of solvent molecules within the interlayer. Thus, e.g. the dried Cu^{2+}-exchanged Wyoming bentonite has a 0.85 Å larger Δd than the non-exchanged Wyoming bentonite, due to the relative sizes of the Cu^{2+} and Na^{+} cations. The effects of changing solvents on the Δd are recorded in Table 30.

Table 30 The interlayer distance, Δd (Å) of clay minerals are measured by using XRD.

S. No	Clay minerals and in different solvents	$\Delta d = s_{pacing} - 9.66$ Å
1	Purified clay	1.89
2	Cu^{2+}–clay	2.74
3	Acetonitrile	3.52
4	Dichloromethane	3.52
5	Toluene	3.36
6	1,4–Dioxane	5.02
7	Ethyl benzene	5.02
8	Benzonitrile	5.90
9	Cu^{2+}–Al–O–EA	3.09

5.4 Synthesis and characterisation of *β*-lactams

5.4.1 Synthesis of monomethyl malonic acid (3-methoxy-3-oxopropanoic acid) 167 from dimethyl malonate 165

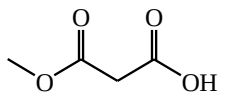

167

This was synthesised according to a reported procedure.[145]

Potassium hydroxide (25.0 g, 445.0 mmol) in methanol (58.0 mL) was added dropwise (15 min) to a stirring solution of dimethyl malonate **165** (50.0 g, 378.0 mmol) in methanol (100.0 mL) with occasional cooling to room temperature. After further stirring for 15 min, the reaction mixture was acidified with concentrated HCl (hydrochloric acid) and filtered. The filter cake (KCl potassium chloride) was washed with methanol (200.0 mL) and the combined filtrate and washings were concentrated on a rotary evaporator. The residual liquid was dissolved in dichloromethane (500.0 mL) and the small amount of salts filtered off. The filtrate was again evaporated on a rotary evaporator to give methyl malonate **167** (30.0 g, 67%) as a colourless oil. ^{1}H NMR (300 MHz, $CDCl_3$): δ 3.47 (s, 2H, CH_2), 3.79 (s, 3H, -OCH_3), 10.0 (s, COOH); ^{13}C NMR (75 MHz, $CDCl_3$): δ 40.80, 52.81, 167.29, 171.42; IR (ATR): 593, 659, 776, 891, 1014, 1154, 1206, 1327, 1408, 1438, 1712, 2958; GC–MS: *m/z:* 118, 119, 101, 74, 59, 44.

5.4.2 Synthesis of benzyl malonate (3-(benzyloxy)-3-oxopropanoic acid) 170 from malonic acid 168

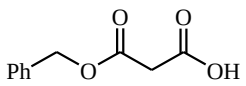

170

This was synthesised according to a reported procedure.[196]

Triethylamine (19.40 g, 191.0 mmol) was added to a solution of malonic acid **168** (20.0 g, 192.0 mmol) in acetonitrile (50.0 mL). To the cooled reaction mixture benzyl bromide (32.80 g, 191.0 mmol) was added dropwise over 30 min. The reaction mixture was heated under reflux for 1 h and the solvent evaporated under vacuum to give the crude product. The crude oil was dissolved in dichloromethane (50.0 mL) and washed with brine solution (40.0 mL) and water (40.0 mL). The solvent was evaporated under vacuum to get the crude product (26.0 g) the crude compound was purified by silica gel column chromatography and the compound **170** was eluted (solvents: (30 : 70) EtOAc : pet ether) as a white solid (15.0 g, 40%). ^{1}H NMR (300 MHz, $CDCl_3$,) δ 3.49 (s, 2H, CH_2), 5.22 (s, 2H, Ph–CH_2), 7.37 (m, 5H, Ar–H), 11.00 (br s, 1H, COOH); ^{13}C NMR (75 MHz, $CDCl_3$): δ 40.71, 67.71, 128.44, 128.65, 128.69, 134.86, 166.71, 171.30; IR (ATR): 596, 698, 665, 698, 753, 841, 900, 979, 1164, 1306, 1331, 1432, 1706, 2947; GC–MS: *m/z* 194, 107, 91, 79, 60, 51.

5.4.3 Synthesis of methyl-2-(diethylcarbamoyl)acetate 171

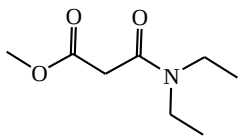

171

This was synthesised according to a reported procedure.[148]

N,N'-Dicyclohexylcarbodiimide (1.65 g, 8.00 mmol) in dichloromethane (8.00 mL) was added to a stirred solution of methyl malonate **167** (1.00 g, 8.00 mmol) in dichloromethane (10.0 mL) and diethylamine (1.60 g, 8.80 mmol) was added to the reaction mixture in a drop wise manner for 30 min. The reaction mixture was stirred for 4 h at 40°C and then cooled to room temperature, filtered off and the solid was washed with dichloromethane (10.0 mL), filtrate was washed with water (10.0 mL) and brine solution (20.0 mL). Then the dichloromethane was evaporated under vacuum to get the crude oily compound 1.40 g. The crude compound was purified by silica gel column chromatography, solvents: (40 : 60) EtOAc : pet ether as eluent to get the pure yellow oil. **171** (0.82 g, 63%). ^{1}H NMR (300 MHz, $CDCl_3$): δ 1.13 (t, *J* = 7.20 Hz, 3H, N-CH_2C**H**$_3$), 1.19 (t, *J* = 7.20 Hz, 3H, N-CH_2C**H**$_3$), 3.29 (q, *J* = 7.20 Hz, 2H, N–CH_2), 3.38 (q, *J* = 7.20 Hz, 2H, N–CH_2), 3.43 (s, 2H, CH_2), 3.74 (s,

3H, –OCH_3); ^{13}C NMR (75 MHz, $CDCl_3$): δ 12.94, 14.25, 40.40, 41.16, 42.74, 52.53, 165.13, 168.46; IR (ATR): 573, 626, 788, 899, 950, 1025, 1097, 1137, 1163, 1216, 1247, 1322, 1364, 1433, 1638, 1740, 2162, 2934; GC–MS: RT (8.21): 173, 156, 143, 124, 112, 96, 84, 68.

5.4.4 Synthesis of benzyl 2–(diethylcarbamoyl) acetate 172

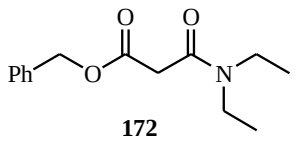

172

This was synthesised according to a reported procedure.[78,148]

172 was synthesised as for **171** using benzyl malonic acid **170** (1.00 g, 5.15 mmol), DCC (1.07 g, 5.15 mmol) and diethyl amine (0.37 g, 5.10 mmol) to give the product **172** as a yellow oil (0.80 g, 62%). ^1H NMR (300 MHz, $CDCl_3$): δ 1.07 (dt, *J* = 7.07, 7.07 Hz, 6H, N-CH_2C**H**$_3$), 3.19 (q, *J* = 7.07 Hz, 2H, N-CH_2), 3.32 (q, *J* = 7.07 Hz, 2H, N-CH_2), 3.41 (s, 2H, CH_2), 5.12 (s, 2H, Ph–CH_2), 7.19 - 7.31 (m, 5H, Ar–H); ^{13}C NMR (75 MHz, $CDCl_3$): δ 12.73, 14.01, 40.13, 41.06, 42.61, 66.72, 128.23, 128.27, 128.49, 135.47, 167.64, 164.95; IR (ATR): 491, 592, 742, 787, 906, 998, 1098, 1137, 1241, 1279, 1319, 1377, 1452, 1640, 1738, 2030, 2160, 2934, 2973; GC–MS: 250, 181, 158, 140, 115, 100, 91, 72.

5.4.5 Synthesis of methyl 2–[ethyl (phenyl) carbamoyl] acetate 173

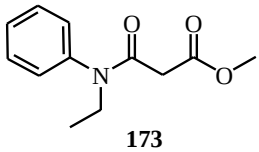

173

173 was synthesised as for **171** using methyl malonate (1.00 g, 8.46 mmol), DCC (1.74 g, 8.46 mmol) and *N*–ethyl aniline (1.02 g, 8.46 mmol) to give the product **173** as a colourless oil (0.80 g, 43%). ^1H NMR (300 MHz, $CDCl_3$): δ 1.04 (t, *J* = 7.10 Hz, 3H, N-CH_2C**H**$_3$), 3.07 (s, 2H, CH_2), 3.56 (s, 3H, -OCH_3), 3.67 (q, *J* = 7.10, 2H, N–CH_2), 7.11 (d, *J* = 7.10 Hz, 2H,

Ar–H *ortho*), 7.28 - 7.43 (m, 3H, Ar–H *para* and *meta*); ^{13}C NMR (75 MHz, $CDCl_3$): δ 12.83, 41.66, 44.15, 52.13, 52.33, 128.28, 128.40, 129.84, 141.51, 165.33, 168.18; IR (ATR): 559, 663, 701, 952, 1090, 1130, 1157, 1240, 1323, 1404, 1494, 1593, 1655, 1741, 1973, 2032, 2156, 2935; GC–MS: 222, 190, 148, 121, 120, 106, 93, 77, 59.

5.4.6 Synthesis of benzyl 2–[ethyl (phenyl) carbamoyl] acetate 174

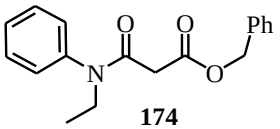

174

174 was synthesised as for **171** using benzyl malonic acid (1.00 g, 5.15 mmol), DCC (1.07 g, 5.15 mmol) and *N*–ethyl aniline (0.62 g, 5.19 mmol) to give the product **174** as a yellow oil (0.75 g, 48%). ^{1}H NMR (300 MHz, $CDCl_3$): δ 1.12 (t, *J* = 7.20 Hz, 3H, N-CH_2C**H**$_3$), 3.20 (s, 2H, N-CH_2), 3.77 (q, *J* = 7.20 Hz, 2H, CH_2), 5.10 (s, 2H, Ph–CH_2), 7.06 – 7.19 (m, 2H, Ar–H), 7.29 - 7.45 (m, 8H, Ar–H); ^{13}C NMR (75 MHz, $CDCl_3$): δ 12.91, 31.13, 41.96, 44.31, 66.96, 76.86, 128.35, 128.38, 128.54, 129.84, 135.45, 141.70, 165.27, 167.64; IR (ATR): 494, 562, 664, 699, 746, 769, 908, 997, 1089, 1130, 1153, 1232, 1321, 1405, 1451, 1493, 1593, 1655, 1738, 2934; GC-MS : *m/z* 297.

5.4.7 Synthesis of methyl 3–Oxo–3–(piperidin–1–yl)propanoate 175

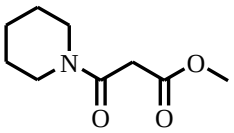

175

This was synthesised according to a reported procedure.[87]

175 was synthesised as for **171** using methyl malonate **167** (1.00 g, 8.46 mmol), DCC (1.74 g, 8.46 mmol) and piperidine (0.72 g, 8.45 mmol) to give the product **175** as a yellow oil (1.00

g, 63%). ^{1}H NMR (300 MHz, $CDCl_3$): δ 1.44 - 1.64 (m, 6H, -N-$(CH_2)_3$), 3.30 (t, *J* = 5.60 Hz, 2H, N-CH_2), 3.39 (s, 2H, CH_2), 3.49 (t, *J* = 5.60 Hz, 2H, N–CH_2), 3.71 (s, 3H, -OCH_3); ^{13}C NMR (75 MHz, $CDCl_3$): δ 24.29, 25.33, 26.18, 40.98, 42.90, 47.70, 52.30, 164.02, 168.22; IR (ATR): 604, 668, 754, 856, 914, 945, 989, 1021, 1153, 1189, 1227, 1254, 1312, 1433, 1632, 1736, 2023, 2876, 2954, 3470; GC–MS: *m/z* 185, 154, 126, 97, 84, 69, 59.

5.4.8 Synthesis of benzyl 3–oxo–3–(pyrrolidin–1–yl) propanoate 176

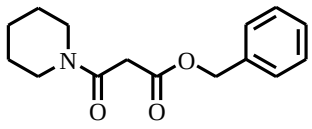

176

176 was synthesised as for **171** using benzyl malonic acid (1.00 g, 5.15 mmol), DCC (1.07 g, 5.15 mmol) and piperidine (0.44 g, 5.16 mmol) to give the product **176** as a colourless oil (0.90 g, 66%). ^{1}H NMR (300 MHz, $CDCl_3$): δ 1.35 - 1.60 (m, 6H, -$(CH_2)_3$), 3.23 (t, *J* = 5.70 Hz, 2H, N-CH_2), 3.47 (t, *J* = 5.70 Hz, 2H, N-CH_2), 3.41 (s, 2H, CH_2), 5.22 (s, 2H, Ph-CH_2), 7.18 - 7.36 (m, 5H, Ar-H); ^{13}C NMR (75 MHz, $CDCl_3$): δ 24.30, 26.10, 25.33, 41.55, 42.95, 47.51, 66.97, 128.40, 128.56, 163.93, 167.63; IR (ATR): 460, 535, 587, 640, 697, 741, 852, 894, 998, 1084, 1153, 1219, 1311, 1373, 1443, 1639, 1739, 1979, 2853, 2930, 3318; GC–MS: 262, 170, 91, 84.

5.4.9 Synthesis of methyl 3–oxo–3–(pyrrolidine–1–yl) propanoate 177

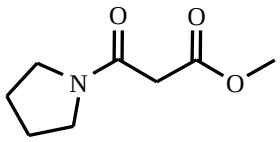

177

177 was synthesised as for **171** using methyl malonate (1.00 g, 8.46 mmol), DCC (1.74 g, 8.46 mmol) and pyrrolidine (0.60 g, 8.46 mmol) to give the product **177** as a colourless oil

(0.99 g, 68%). ^{1}H NMR (300 MHz, $CDCl_3$): δ 1.80 - 1.20 (m, 4H, N-(C**H**$_2$)$_2$), 3.33 – 3.53 (m, 6H, N-CH_2C**H**$_2$ & CH_2), 3.70 (s, 3H, -OCH_3); ^{13}C NMR (75 MHz, $CDCl_3$): δ 24.37, 25.98, 42.17, 42.28, 45.89, 52.40, 164.23, 168.03; IR (ATR): 3470, 2954, 2876, 2023, 1736, 1632, 1433, 1312, 1254, 1227, 1189, 1153, 1021, 989, 945, 914, 856, 754, 668, 604; GC–MS: *m/z* 171, 101, 84, 70, 59.

5.4.10 Synthesis of benzyl 3–oxo–3–(pyrrolidine–1–yl) propanoate 178

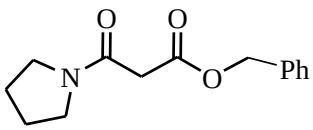

178

178 was synthesised as for **171** using benzyl malonic acid (1.00 g, 5.15 mmol), DCC (1.07 g, 5.15 mmol) and pyrrolidine (0.38 g, 5.20 mmol) to give the product **178** as a colourless oil (0.80 g, 64%). ^{1}H-NMR (300 MHz, $CDCl_3$): δ 1.75 - 2.05 (m, 4H, N-CH_2), 3.40 (t, *J* = 6.60 Hz, 2H, N-CH_2), 3.45 (s, 2H, CH_2), 3.50 (t, *J* = 6.60 Hz, 2H, N-CH_2), 5.17 (s, 2H, Ph–CH_2), 7.29 - 7.43 (m, 5H, Ar–H); ^{13}C NMR (75 MHz, $CDCl_3$): δ 26.18, 47.10, 43.03, 46.37, 67.29, 128.56, 128.40, 135.40, 163.95, 167.60; IR (ATR): 492, 606, 697, 742, 844, 996, 1029, 1143, 1267, 1328, 1373, 1454, 1498, 1729, 1968, 2163, 2982; GC-MS : *m/z* 247.

5.4.11 Synthesis of methyl 2–[(1–phenylethyl) carbamoyl] acetate 179

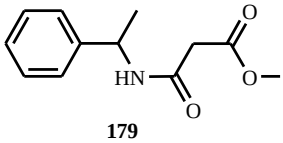

179

179 was synthesised as for **171** using methyl malonate (1.00 g, 8.46 mmol), DCC (1.74 g, 8.46 mmol) and 1–phenylethan–1–amine (1.02 g, 8.46 mmol) to give the product **179** as a colourless oil (0.80 g, 43%). ^{1}H NMR (300 MHz, $CDCl_3$): δ 1.54 (d, *J* = 7.20 Hz, 3H, CH_3), 3.40 (s, 2H, CH_2), 3.70 (s, 3H, -OCH_3), 5.20 (q, *J* = 7.20 Hz, 1H, Ar-CH), 7.24 - 7.50 (m, 5H,

Ar–H), 7.99 (brs, 1H, N–H); ^{13}C NMR (75 MHz, $CDCl_3$): δ 21.00, 49.00, 52.00, 125.00, 127.00, 128.23, 145.00, 165.00, 168.00; IR (ATR): 555, 596, 680, 745, 945, 1025, 1278, 1346, 1428, 1509, 1637, 1679, 3324; GC-MS: *m/z* 221.

5.4.12 Synthesis of 4–methylbenzene–1–sulfonyl azide

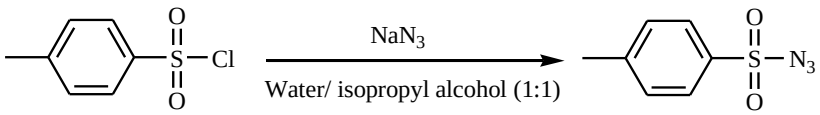

181 **182**

This was synthesised according to a reported procedure.[197]

p–Toluenesulfonyl chloride **181** (1.0 g, 5.24 mmol) and sodium azide (0.34 g, 5.24 mmol) dissolved in 1 : 1 ratio of water (15.0 mL) and isopropyl alcohol (15.0 mL) and stirred overnight. From this reaction mixture, solvent was evaporated on the rotavapor to get the crude compound and then the crude compound was purified by silica gel column chromatography (solvents (10 : 90) EtOAc : hexane) to get pure colourless oil **182** (0.75 g, 67%). ^{1}H NMR (300 MHz, $CDCl_3$): δ 2.35 (s, 3H, Ph-CH_3), 7.27 (d, *J* = 8.20 Hz, 2H, Ar-H), 7.70 (d, *J* = 8.20 Hz, 2H, Ar-H); ^{13}C NMR (75 MHz, $CDCl_3$): δ 21.40, 127.00, 130.10, 135.10, 146.12; IR (ATR): 500, 535, 586, 657, 701, 741, 812, 1084, 1161, 1297, 1366, 1452, 1594, 2122, 2358; GC–MS: 197, 185, 155, 121, 91, 65, 45.

5.4.13 Synthesis of methyl N,N-diethylamidodiazomalonate (methyl 2-diazo-2-(diethylcarbamoyl)acetate) 183

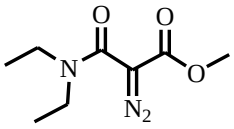

183

This was synthesised according to a reported procedure.[7]

p–Toluenesulfonyl azide **182** (0.68 g, 3.46 mmol) was suspended in a stirred solution of methyl 2–(diethylcarbamoyl)acetate **171** (0.50 g, 2.89 mmol) in dry acetonitrile (4.00 mL). The mixture was stirred at room temperature for 30 min and dry triethylamine (0.35 g, 3.46 mmol) was added all at once, and then stirred for 36 h. The reaction mixture was filtered and washed with excess dichloromethane (20.0 mL) the filtrate was washed with water (10.0 mL) and brine solution (20.0 mL) dried, and evaporated to give crude compound (1.00 g). The crude compound was purified by column chromatography on silica gel using (solvent (60 : 40) EtOAc/pet ether) to get the pure compound **183** (0.40 g, 70%) as a yellow oil. ^{1}H NMR (300 MHz, $CDCl_3$): δ 1.19 (t, *J* = 7.10 Hz, 6H, N-($CH_2C\mathbf{H}_3)_2$), 3.39 (q, *J* = 7.10 Hz, 4H, N-$(CH_2)_2$), 3.79 (s, 3H, -OCH_3); ^{13}C NMR (75 MHz, $CDCl_3$): δ 13.23, 41.84, 52.16, 66.06, 160.48, 163.10; IR (ATR): 606, 646, 716, 754, 799, 861, 931, 954, 1009, 1088, 1143, 1187, 1215, 1271, 1292, 1347, 1361, 1379, 1421, 1618, 1710, 2120, 2876, 2972, 3498; GC–MS: 199, 184, 155, 140, 122, 99.

5.4.14 Synthesis of benzyl N,N-diethylamidodiazomalonate (benzyl 2-diazo-2-(diethylcarbamoyl)acetate) 184

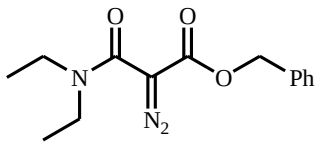

184

184 was synthesised as for **183** using benzyl 2–(diethyl carbamoyl) acetate (1.0 g, 4.04 mmol), *p*–toluenesulfonyl azide (0.94 g, 4.80 mmol) and dry triethylamine (0.48 g, 4.80 mmol) to give the product **184** (0.80 g, 72%) as a yellow oil. ^{1}H–NMR (300 MHz, $CDCl_3$): δ 1.20 (t, *J* = 7.10 Hz, 6H, N-($CH_2C\mathbf{H}_3)_2$), 3.41 (q, *J* = 7.10 Hz, 4H, N-($C\mathbf{H}_2)_2$), 5.24 (s, 2H, Ph-CH_2), 7.32 – 7.44 (m, 5H, Ar-H); ^{13}C NMR (75 MHz, $CDCl_3$): δ 13.31, 41.96, 66.28, 128.27, 128.56, 128.64, 128.72, 135.49, 160.51, 162.51; IR (ATR): 496, 525, 559, 595, 647, 697, 750, 779, 859, 909, 949, 1069, 1142, 1213, 1270, 1377, 1423, 1620, 1706, 2123, 2972; GC–MS: 276, 248, 219, 176, 158, 131, 128, 91.

5.4.15 Synthesis of methyl *N*-ethyl-*N*-phenylamidodiazomalonate (methyl 2-diazo-2-[ethyl(phenyl)carbamoyl]acetate) 185

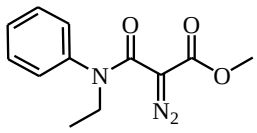

185

185 was synthesised as for **183** using methyl 2–[ethyl (phenyl) carbamoyl] acetate (1.0 g, 4.52 mmol), *p*–toluenesulfonyl azide (1.06 g, 5.40 mmol) and dry triethylamine (0.54 g, 5.33 mmol) to give the product **185** (0.58 g, 54%) as a yellow oil. ^{1}H–NMR (300 MHz, $CDCl_3$): δ 1.62 (t, *J* = 7.05 Hz, 3H, N-CH_2C**H**$_3$), 3.56 (s, 3H, -OCH_3), 3.84 (q, *J* = 7.05 Hz, 2H, N-C**H**$_2$), 7.17 (d, 2H, *J* = 7.10 Hz, Ar-H *ortho*), 7.23 - 7.31 (m, 1H, Ar-H *para*), 7.37 (t, *J* = 7.10 Hz, 2H, Ar–H *meta*); ^{13}C-NMR (75 MHz, $CDCl_3$): δ 12.81, 45.81, 52.11, 66.37, 126.71, 127.16, 129.47, 141.81, 160.18, 162.72; IR (ATR): 487, 532, 578, 697, 748, 766, 861, 963, 1034, 1104, 1141, 1190, 1301, 1387, 1435, 1493, 1591, 1628, 1689, 1723, 2115, 2952; MS: *m/z* 247.

5.4.16 Synthesis of methyl *N*-piperidinodiazomalonate (methyl 2-diazo-3-oxo-3-(piperidin-1-yl)propanoate) 187

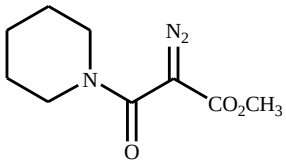

187

187 was synthesised as for **183** using methyl 3–oxo–3–(piperidin–1–yl)propanoate (1.00 g, 5.40 mmol), *p*–toluenesulfonyl azide (1.27 g, 6.40 mmol) and dry triethylamine (0.65 g, 6.42 mmol) to give the product **187** (0.70 g, 62%) as a yellow oil. ^{1}H–NMR (300 MHz, $CDCl_3$): δ 1.59 (br s, 6H, N–$(CH_2)_3$), 3.42 (br s, 4H, N–$(CH_2)_2$), 3.78 (s, 3H, -OCH_3); ^{13}C NMR (75

MHz, $CDCl_3$): δ 24.38, 25.82, 46.88, 52.18, 66.36, 160.16, 162.8; IR (ATR): 877, 952, 1007, 1097, 1141, 1186, 1264, 1293, 1351, 1427, 1620, 1711, 2121, 2937; GC-MS: *m/z* 211, 184, 155, 113.

5.4.17 Synthesis of benzyl piperidinodiazomalonate (benzyl 2-diazo-3-oxo-3-(piperidin-1-yl)propanoate) 188

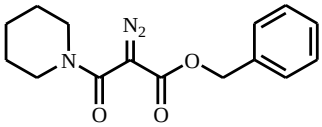

188

188 was synthesised as for **183** using benzyl 3–oxo–3–(piperidin–1–yl)propanoate (1.0 g, 3.83 mmol), *p*–toluenesulfonyl azide (0.90 g, 4.59 mmol) and dry triethylamine (0.46 g, 4.59 mmol) to give the product **188** (0.71 g, 71%) as a yellow oil. ^{1}H NMR (300 MHz, $CDCl_3$): δ 1.50 - 1.68 (m, 6H, *N*–$(CH_2)_3$), 3.25 - 3.45 (m, 4H, *N*–$(CH_2)_2$), 5.22 (s, 2H, Ph–CH_2), 7.25 - 7.45 (m, 5H, Ar–H); ^{13}C-NMR (75 MHz, $CDCl_3$): δ 24.29, 25.33, 26.10, 41.55, 42.99, 47.55, 66.74, 128.40, 128.56, 128.60, 135.42, 163.95, 167.62; IR (ATR): 594, 649, 697, 750, 852, 907, 951, 1004, 1086, 1142, 1179, 1285, 1376, 1429, 1497, 1621, 1706, 1762, 2124, 2855, 2936; GC-MS: *m/z* 287.

5.4.18 Synthesis of methyl *N*-pyrrolidinodiazomalonate (methyl 2-diazo-3-oxo-3-(pyrrolidin-1-yl)propanoate) 189

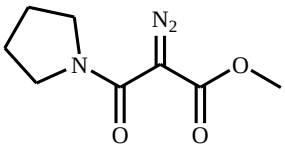

189

189 was synthesised as for **183** using methyl 3–oxo–3–(pyrrolidine–1–yl) propanoate (1.0 g, 5.84 mmol), *p*–toluenesulfonyl azide (1.37 g, 6.96 mmol) and dry triethylamine (0.70 g, 6.96 mmol) to give the product **189** (0.69 g, 60%) as a yellow oil ^{1}H NMR (300 MHz, $CDCl_3$): δ 1.81 – 1.98 (m, 4H, *N*-$(CH_2)_2$), 3.20 - 3.90 (m, 4H, *N*-$CH_2(C\mathbf{H}_2)_2$), 3.80 (s, 3H, -OCH_3); ^{13}C NMR (75 MHz, $CDCl_3$): δ 25.12, 47.89, 52.10, 66.68, 159.39, 162.48; IR (ATR): 455, 535, 566, 647, 710, 752, 795, 845, 887, 917, 955, 1033, 1101, 1188, 1230, 1288, 1343, 1405, 1612, 1711, 2122, 2882, 2956; GC–MS: 198, 139, 110, 98, 82, 70, 55.

5.4.19 Synthesis of benzyl *N*-pyrrolidinodiazomalonate (benzyl 2-diazo-3-oxo-3-(pyrrolidin-1-yl)propanoat) 190

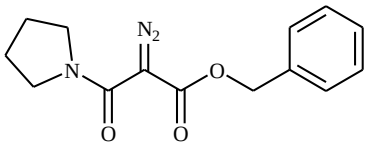

190

190 was synthesised as for **183** using benzyl 3–oxo–3–(pyrrolidine–1–yl) propanoate (1.0 g, 4.04 mmol), *p*–toluenesulfonyl azide (0.94 g, 4.80 mmol) and dry triethylamine (0.48 g, 4.80 mmol) to give the product **190** (0.70 g, 64%) as a yellow oil. ^{1}H NMR (300 MHz, $CDCl_3$): δ 1.70 - 1.86 (m, 4H, N-$(CH_2)_2$), 3.31 - 3.49 (m, 4H, N-$CH_2(C\mathbf{H}_2)_2$), 5.23 (s, 2H, Ph–CH_2), 7.19 - 7.38 (m, 5H, Ar–H); ^{13}C NMR (75 MHz, $CDCl_3$): δ 24.01, 47.96, 66.70, 128.17, 128.47, 128.65, 135.43, 159.44, 161.88; IR (ATR): 492, 606, 697, 742, 844, 996, 1029, 1143, 1267, 1328, 1373, 1454, 1498, 1729, 1968, 2163, 2982. MS: *m/z* 273.

5.4.20 Synthesis of methyl 1-phenylethylamidodiazo-malonate (methyl 2-diazo-2-[(1-phenylethyl)carbamoyl]acetate) 191

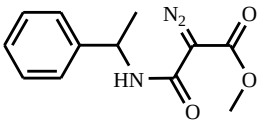

191

191 was synthesised as for **183** using methyl 2–[(1–phenylethyl) carbamoyl] acetate(1.0 g, 4.52 mmol), *p*–toluenesulfonyl azide (1.06 g, 5.40 mmol) and dry triethylamine (0.54 g, 5.33 mmol) to give the product **191** (0.60 g, 54%) as a yellow oil. ^{1}H NMR (300 MHz, $CDCl_3$): δ 1.56 (d, *J* = 7.20 Hz, 3H, CH_3), 3.70 (s, 3H, -OCH_3), 5.20 (q, *J* = 7.20 Hz, 1H, Ar-CH), 7.21 - 7.44 (m, 5H, Ar–H), 8.0 (brs, 1H, N–H); ^{13}C NMR (75 MHz, $CDCl_3$): δ 22.52, 36.72, 49.00, 52.00, 127.32, 127.49, 128.67, 143.28, 159.66, 164.99; IR (ATR): 533, 555, 596, 698, 755, 950, 1017, 1268, 1326, 1438, 1519, 1647, 1689, 2135, 3344; GC-MS: *m/z* 247.

5.4.21 Syntheses of methyl (±)-*cis* –1–ethyl–2–methyl–4–oxoazetidine–3–carboxylate 193 and methyl (±)-*trans* –1–ethyl–2–methyl–4–oxoazetidine–3–carboxylate 194 (*β*-lactams) and methyl 1–ethyl–2–oxopyrrolidine–3–carboxylate 195 (*γ*-lactam)

This was synthesised according to a reported procedure.[7]

Cu^{2+}-clay mineral (0.05 g) in dry acetonitrile (1.00 mL) was stirred for 1 h at room temperature under a nitrogen atmosphere and to this stirred solution methyl *N*,*N*-diethylamidodiazomalonate **183** (0.10 g, 0.50 mmol) was added and the reaction mixture was heated at 80ºC overnight. The reaction mixture was cooled to room temperature and the catalyst was removed by simple vacuum filtration and washed with excess of dichloromethane (4.00 mL). The filtrate was concentrated *in vaccuo* using a rotavapor to get the crude compound, which was purified by silica gel column chromatography using (solvents: (20 : 80) EtOAc : hexane) to obtain the top spot *γ*-lactam **195** (10 mg, 11%), (solvents: (30 : 70) EtOAc : hexane) to obtain upper spot *trans*-isomer **194** (34 mg, 40%) and (solvents: (40 : 60) EtOAc : hexane) bottom spot *cis*-isomer **193** (26 mg, 30%).

5.4.21.1 Methyl (±)-*cis* –1–ethyl–2–methyl–4–oxoazetidine–3–carboxylate 193

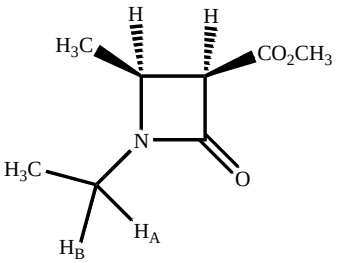

***cis*, 193**

^{1}H NMR (300 MHz, $CDCl_3$): δ 1.17 (t, *J* = 7.20 Hz, 3H, N-CH_2C**H**$_3$), 1.32 (d, *J* = 6.30 Hz, 3H, CH_3), 3.12 (dt, *J* = 7.20, 14.30 Hz, 1H, N-C**H$_A$**CH_3), 3.41 (dt, *J* = 7.20, 14.30 Hz, 1H, N-C**H$_B$**CH_3), 3.76 (s, 3H, -OCH_3), 3.95 (dq, *J* = 5.67, 6.30 Hz, 1H, -C**H**-N-CH_2CH_3), 4.05 (d, *J* = 5.67 Hz, 1H, C**H**-CO_2CH_3); ^{13}C NMR (75 MHz, $CDCl_3$): δ 12.81, 14.43, 17.65, 34.82, 49.29, 56.65, 161.59, 167.17; IR (ATR): 552, 717, 790, 950, 1023, 1061, 1172, 1229, 1381, 1411, 1641, 1438, 1730, 2975; GC–MS: 172, 156, 143, 128, 100, 85, 69, 56.

5.4.21.2 Methyl (±)-*trans*–1–ethyl–2–methyl–4–oxoazetidine–3–carboxylate 194

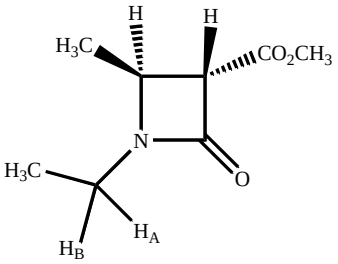

***trans*, 194**

^{1}H NMR (300 MHz, $CDCl_3$): δ 1.19 (t, *J* = 7.20 Hz, 3H, N-CH_2**CH**$_3$), 1.38 (d, *J* = 6.30 Hz, 3H, CH_3), 3.10 (dt, *J* = 7.20, 14.30 Hz, 1H, N-C**H**), 3.39 (dt, *J* = 7.20, 14.30 Hz, 1H, *N*-C**H**), 3.56 (d, *J* = 2.25 Hz, 1H, C**H**-CO_2CH_3), 3.76 (s, 3H, -OCH_3), 3.97 (dq, *J* = 2.25, 6.30 Hz, 1H, -C**H**-N-CH_2CH_3); ^{13}C NMR (75 MHz, $CDCl_3$): δ 13.29, 18.05, 35.45, 50.53, 52.70, 60.68, 161.35, 167.96; IR (ATR): 552, 717, 790, 950, 1023, 1061, 1172, 1229, 1381, 1411, 1641, 1438, 1730, 2975; GC–MS: 172, 156, 143, 128, 100, 85, 69, 56.

5.4.21.3 Methyl 1–ethyl–2–oxopyrrolidine–3–carboxylate 195

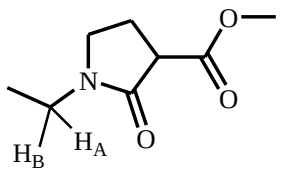

195

^{1}H NMR (300 MHz, $CDCl_3$): δ 1.12 (m, 3H, N-CH_2C**H**$_3$), 1.20 - 1.25 (m, 2H, N-CH_2), 2.30 - 2.39 (m, 1H, N-C**H**$_A$H$_B$), 2.20 - 2.27 (m, 1H, N-CH$_A$**H**$_B$), 3.36 (m, 3H, N-C**H**$_2$ *pyrrolidine ring*, CH), 3.76 (s, 3H, -OCH_3); ^{13}C NMR (75 MHz, $CDCl_3$): δ 12.51, 23.40, 39.99, 43.18, 48.90, 52.00, 169.31, 170.39; IR (ATR): 490, 596, 697, 739, 914, 973, 1024, 1079, 1160, 1225, 1275, 1332, 1379, 1454, 1494, 1684, 1734, 1979, 2038, 2163, 2337, 2360, 2935; MS *m/z*: 171.

5.4.22 Synthesis of benzyl(±)-*cis*–1–ethyl–2–methyl–4–oxoazetidine–3–carboxylate 202, benzyl(±)-*trans*–1–ethyl–2–methyl–4–oxoazetidine–3–carboxylate 203 (*β*-lactams) and benzyl-1–ethyl–2–oxopyrrolidine–3–carboxylate 204 (*γ*-lactam).

202, **203** and **204** were synthesised as for **193**, **194** and **195** using benzyl *N*,*N*-diethylamidodiazomalonate **184** (0.10 g, 0.36 mmol), Cu^{2+}-clay mineral (0.05 g) to give the benzyl (±)-*cis*–1–ethyl–2–methyl–4–oxoazetidine–3–carboxylate **202** (23.0 mg, 25%), benzyl (±)-*trans*–1–ethyl–2–methyl–4–oxoazetidine–3–carboxylate **203** (30.0 mg, 34%) and (*γ*-lactam) benzyl-1–ethyl–2–oxopyrrolidine–3–carboxylate **204** (10.0 mg, 11%) as a yellow oil.

5.4.22.1 Benzyl (±)-*cis* –1–ethyl–2–methyl–4–oxoazetidine–3–carboxylate 202

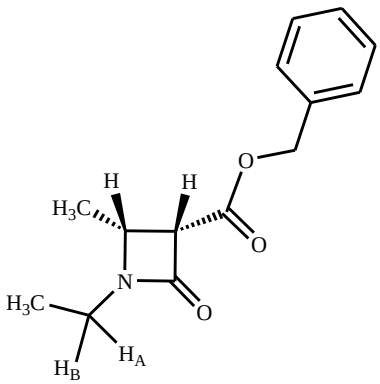

***cis*, 202**

^{1}H NMR (300 MHz, $CDCl_3$): δ 1.18 (t, *J* = 7.20 Hz, 3H, N-CH_2C**H**$_3$), 1.37 (d, *J* = 6.20 Hz, 3H, CH_3), 3.11 (dt, *J* = 7.20, 14.30 Hz, 1H, N-CH_A), 3.41 (dt, *J* = 7.20, 14.30 Hz, 1H, N-CH_B), 3.97 (dq, *J* = 5.65, 6.20 Hz, 1H, -C**H**-N-CH_2CH_3), 4.08 (d, *J* = 5.65, 1H, C**H**-CO_2CH_2Ph), 5.21 (dd, *J* = 8.20 Hz, 2H, Ph-CH_2), 7.36 - 7.40 (m, 5H, Ar-H); ^{13}C NMR (75 MHz, $CDCl_3$): δ 12.66, 17.93, 35.17, 49.86, 60.19, 67.05, 128.21, 128.47, 128.55, 135.47, 167.54, 164.85; IR (ATR): 480, 590, 697, 720, 949, 1008, 1071, 1168, 1220, 1287, 1380, 1411, 1453, 1485, 1647, 1720, 1750, 2979; GC–MS: 247, 219, 156, 128, 107, 91, 69.

5.4.22.2 Benzyl (±)-*trans*–1–ethyl–2–methyl–4–oxoazetidine–3–carboxylate 203

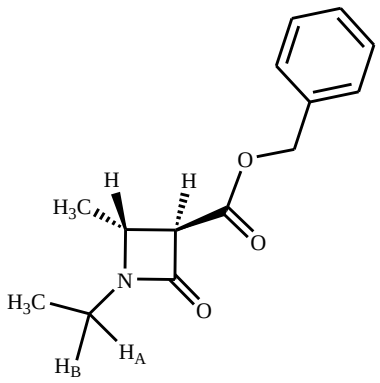

***trans*, 203**

^{1}H NMR (300 MHz, $CDCl_3$) δ 1.19 (t, *J* = 7.20 Hz, 3H, N-CH_2C**H**$_3$), 1.37 (d, *J* = 6.20 Hz, 3H, CH_3), 3.11 (dt, *J* = 7.20, 14.30 Hz, 1H, N-CH_A), 3.40 (dt, *J* = 7.20, 14.30 Hz, 1H, N-

CH_B), 3.98 (dq, *J* = 2.20, 6.20 Hz, 1H, C**H**-N-CH_2CH_3), 3.60 (d, *J* = 2.20 Hz, 1H, C**H**-CO_2CH_2Ph), 5.20 (dd, *J* = 8.20 Hz, 2H, Ph-C$\mathbf{H}_2$), 7.31 – 7.40 (m, 5H, Ar-H); ^{13}C NMR (75 MHz, $CDCl_3$): δ 13.17, 17.92, 35.55, 49.80, 60.19, 67.18, 128.22, 128.36, 128.60. 135.47, 167.54, 164.85; IR (ATR): 491, 596, 697, 742, 949, 1008, 1081, 1168, 1226, 1297, 1380, 1411, 1453, 1495, 1647, 1728, 1754, 2975; GC–MS: 247, 219, 156, 128, 107, 91.

5.4.22.3 Benzyl 1–ethyl–2–oxopyrrolidine–3–carboxylate 204

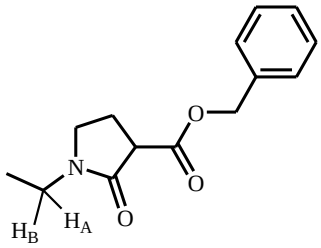

204

^{1}H NMR (300 MHz, $CDCl_3$): δ 1.12 (t, *J* = 7.20 Hz, 3H, N-$CH_2C\mathbf{H}_3$), 1.22 - 1.31 (m, 2H, *N*-CH_2, *pyrrolidine ring*), 2.20 - 2.34 (m, 1H, *N*-C$\mathbf{H}_A$$H_B$, *pyrrolidine ring*), 2.35 - 2.48 (m, 1H, *N*-$CH_A\mathbf{H}_B$, *pyrrolidine ring*), 3.30 – 3.60 (m, 3H, *N*-C$\mathbf{H}_2CH_3$, CH), 5.21 (s, 2H, Ph-CH_2), 7.30 - 7.40 (m, 5H, Ar-H); ^{13}C NMR (75 MHz, $CDCl_3$): δ 12.51, 22.46, 37.81, 45.18, 48.84, 67.29, 128.20, 128.30, 128.68, 135.70, 169.31, 170.39; IR (ATR): 1160, 1225, 1275, 1332, 1379, 1454, 1494, 1684, 1734, 2038, 2163, 2337, 2360, 2958; GC-Ms: *m/z*: 247, 156, 138, 113, 91.

5.4.23 Syntheses of 1–ethyl–2,3–dihydro–1H–indol–2–one 207 and benzyl (±)–2-*cis*–methyl–4–oxo–3–phenylcyclobutane–1–carboxylate 205 and benzyl (±)–2-*trans*–methyl–4–oxo–3–phenylcyclobutane–1–carboxylate 206 (*β*-lactams, minor products).

205, **206** and **207** were synthesised as for **193** and **194** using ethyl 2–diazo–2–[ethyl (phenyl) carbamoyl] acetate (0.10 g, 0.40 mmol), Cu^{2+}-clay mineral (0.05 g) to give the products 1–ethyl–2,3–dihydro–1H–indol–2–one **207** (0.015 g, 0.06 mmol) (major product), benzyl (±)–

2-*cis*–methyl–4–oxo–3–phenylcyclobutane–1–carboxylate **205** and benzyl (±)–2-*trans*–methyl–4–oxo–3–phenylcyclobutane–1–carboxylate **206** (*β*-lactams, minor products).

5.4.23.1 benzyl (±)–2-*cis*–methyl–4–oxo–3–phenylcyclobutane–1–carboxylate 205 and benzyl (±)–2-*trans*–methyl–4–oxo–3–phenylcyclobutane–1–carboxylate 206

These minor compounds **205** and **206** were only identified by GC-MS (*m/z*: 219) as there was insufficient product to even give a crude ^{1}H NMR spectrum.

5.4.23.2 1–Ethyl–2,3–dihydro–1H–indol–2–one 207

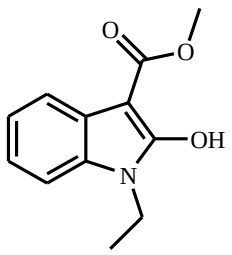

207

^{1}H NMR (300 MHz, $CDCl_3$): δ 1.29 (t, *J* = 7.30 Hz, 3H, N-CH_2C**H**$_3$), 3.72 – 3.82 (m, 5H, N-C**H**$_2$$CH_3$ & -OCH_3), 4.23 (s, 1H, OH), 6.89 (d, *J* = 7.90 Hz, 1H), 7.09 (t, *J* = 7.80 Hz, 1H), 7.29 (d, *J* = 7.90 Hz, 1H), 7.38 (t, *J* = 7.80 Hz, 1H); ^{13}C NMR (75 MHz, $CDCl_3$): δ 17.13, 59.0, 80.0, 121.92, 123.22, 123.79, 124.07, 126.64, 127.32, 130.78, 166.0, 173.0; IR (ATR): 550, 674, 799, 960, 1000, 1120, 1139, 1170, 1228, 1257, 1340, 1465, 1609, 1756, 1957, 1999, 2021, 2083, 2168, 2361, 2922, 3329; MS: *m/z* 219.

5.4.24 Syntheses of benzyl (±)-*cis*–2–methyl–4–oxo–3–phenylcyclobutane–1–carboxylate 214 and benzyl (±)-*trans*–2–methyl–4–oxo–3–phenylcyclobutane–1–carboxylate 215 and 1-ethyl-2-methyl-1H-indole-3-carboxylate 216.

214, **215** and **216** were synthesised as for **193**, **194** & **195** using benzyl *N*,*N*-diethylamidodiazomalonate **184** (0.10 g, 0.31 mmol), Cu^{2+}-clay mineral (0.05 g) to give the

products benzyl (±)-*cis*–2–methyl–4–oxo–3–phenylcyclobutane–1–carboxylate **214**, benzyl (±)-*trans*–2–methyl–4–oxo–3–phenylcyclobutane–1–carboxylate **215** (*β*-lactams **214** and **215** (0.010 g, 11%)) and 1-ethyl-3a-methoxy-3H-cyclohepta[b]pyrrol-2-one **216** as a yellow oil (0.015 g, 23%) (cyclised product).

5.4.24.1 benzyl (±)-*cis*–2–methyl–4–oxo–3–phenylcyclobutane–1–carboxylate 214

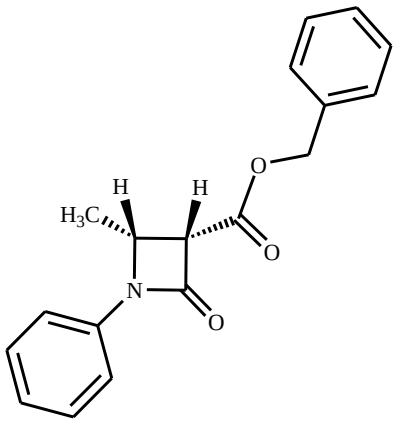

***cis*, 214**

^{1}H NMR (300 MHz, $CDCl_3$): δ 1.34 (d, *J* = 6.27 Hz, 3H, CH_3), 4.20 (d, *J* = 6.20 Hz, 1H, C**H**-CO_2CH_2Ph), 4.40 (dq, *J* = 6.39, 6.20 Hz, 1H, N-CH), 5.20 (m, 2H, Ph-C**H**$_2$), 7.05 - 7.10 (m, 2H, Ar-H), 7.19 - 7.28 (m, 8H, Ar-H); ^{13}C NMR (75 MHz, $CDCl_3$): δ 17.76, 45.34, 50.86, 60.91, 67.48, 124.00, 128.25, 128.47, 128.68, 135.15, 136.0, 158.0, 166.0; IR (ATR): 481, 596, 697, 742, 940, 1008, 1079, 1148, 1226, 1297, 1378, 1400, 1423, 1485, 1647, 1718, 1744, 2985; GC-MS: *m/z*: 295.

5.4.24.2 benzyl (±)-*trans*–2–methyl–4–oxo–3–phenylcyclobutane–1–carboxylate 215

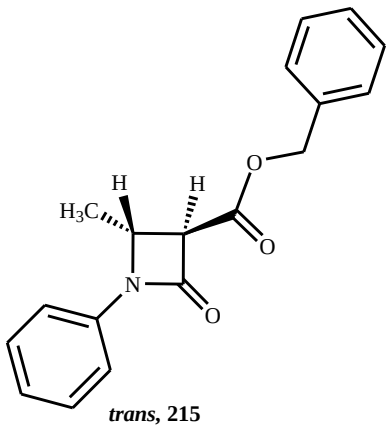

***trans*, 215**

^{1}H NMR (300 MHz, $CDCl_3$): δ 1.46 (d, *J* = 6.27 Hz, 3H, CH_3), 3.70 (d, *J* = 2.49 Hz, 1H, C**H**-CO_2CH_2Ph), 4.40 (dq, *J* = 6.11, 2.49 Hz, 1H, N-CH), 5.21 (m, 2H, Ph-C**H**$_2$), 7.05 - 7.19 (m, 2H, Ar-H), 7.23 - 7.28 (m, 8H, Ar-H); ^{13}C NMR (75 MHz, $CDCl_3$): δ 14.45, 45.90, 50.86, 60.84, 67.48, 124.00, 128.25, 128.47, 128.68, 135.15, 136.0, 158.0, 166.0; IR (ATR); 489, 586, 687, 732, 940, 1059, 1140, 1226, 1287, 1368, 1405, 1420, 1490, 1637, 1720, 1734, 2975; GC-MS: *m/z*: 295.

5.4.24.3 1-Ethyl-2-methyl-1H-indole-3-carboxylate 216a

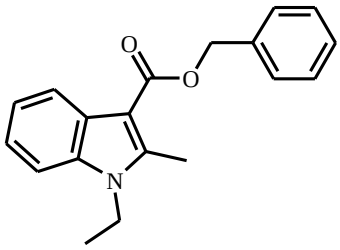

216a

^{1}H NMR (300 MHz, $CDCl_3$): δ 1.21 (t, *J* = 7.10 Hz, 3H), 2.41 (s, 3H), 3.83 (q, *J* = 7.10 Hz, 2H), 5.15 (s, 2H), 6.77 – 7.05 (m, 3H), 7.21 – 7.30 (m, 7H); ^{13}C NMR (75 MHz, $CDCl_3$): δ 13.21, 14.45, 46.0, 65.51, 117.65, 117.95, 118.05, 121.81, 128.38, 128.93, 129.54, 136.41, 144.00, 155.00, 156.00, 160.75; IR (ATR): 1122, 1149, 1190, 1228, 1259, 1350, 1377, 1465, 1489, 1609, 1700, 1756, 1957, 1999, 2021, 2083, 2168, 2361, 2922, 3329; MS: 294.

5.4.25 Syntheses of methyl (±)-*cis*–8–oxo–1–azabicyclo [4.2.0] octane–7–carboxylate 217 and methyl (±)-*trans*–8–oxo–1–azabicyclo [4.2.0]octane–7–carboxylate 218

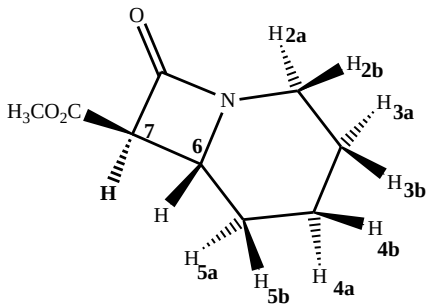

218

217 and **21**8 were synthesised as for **193**, **194** using methyl *N*-piperidinodiazomalonate **187** (0.12 g, 0.57 mmol), Cu^{2+}-clay mineral (0.05 g) to give the products methyl (±)*trans*–8–oxo–1–azabicyclo [4.2.0] octane–7–carboxylate **218** (0.066 g, 66%) (*major*) and methyl (±)*cis*–8–oxo–1–azabicyclo [4.2.0] octane–7–carboxylate **217** (*minor*) as a yellow oil.

5.4.25.1 methyl (±)-*cis*–8–oxo–1–azabicyclo [4.2.0] octane–7–carboxylate 217

There was insufficient of the product **217** for characterisation by spectroscopic means, only identified by GC–MS: (RT 9.11 *minor*): 183, 155, 124, 96, 81, 55.

5.4.25.2 Methyl (±)-*trans*–8–oxo–1–azabicyclo [4.2.0]octane–7–carboxylate 218

^{1}H NMR (300 MHz, $CDCl_3$): δ 1.16 – 1.73 (m, 4H, 3a, 3b, 4a, 4b), 1.83 - 1.95 (m, 1H, 5b), 2.05 – 2.18 (m, 1H, 5a), 2.79 (ddd, *J* = 4.50, 11.60, 13.70 Hz, 1H, 2b), 3.65 (ddd, *J* = 1.90, 4.50, 10.50 Hz, 1H, C6-H), 3.69 (d, *J* = 1.90 Hz, 1H, C7-H), 3.76 (s, 3H, -OCH_3), 3.84 (dd, *J* = 4.50, 13.70 Hz, 2a); ^{13}C NMR (75 MHz, $CDCl_3$): δ 22.01, 24.16, 29.77, 39.36, 51.00, 52.65, 61.84, 161.52, 167.02; IR (ATR): 511, 568, 702, 771, 803, 867, 916, 1039, 1082, 1136, 1203, 1340, 1444, 1584, 1635, 1697, 1739, 1972, 2027, 2160, 2199, 2882, 2955, 3342; GC–MS: (RT 9.07*major*): 183, 155, 124, 113, 81, 55;

5.4.26 Syntheses of benzyl (±)-*trans*–8–oxo–1–azabicyclo [4.2.0] octane–7–carboxylate 222 and benzyl (±)-*cis*–8–oxo–1–azabicyclo [4.2.0] octane–7–carboxylate 221 (*β*-lactams)

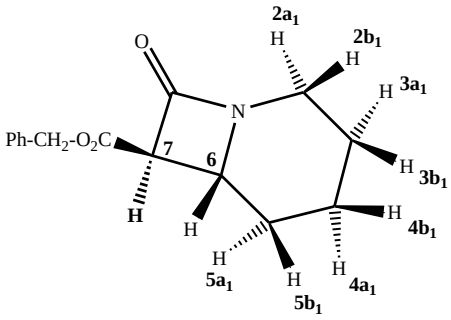

222

221 and **222** were synthesised as for **193** and **194** using benzyl *N*-piperidinodiazomalonate **188** (0.10 g, 0.35 mmol), Cu^{2+}-clay mineral (0.05 g) to give the products benzyl (±)*trans*–8–oxo–1–azabicyclo [4.2.0] octane–7–carboxylate **222** (*major*) (0.068 g, 68%) and benzyl (±)*cis*–8–oxo–1–azabicyclo [4.2.0] octane–7–carboxylate **221** (*minor*) as a yellow oil

5.4.26.1 Benzyl (±)-*cis*–8–oxo–1–azabicyclo [4.2.0] octane–7–carboxylate 221

There was insufficient of the product **221** for characterisation by spectroscopic means, only identified by GC–MS (RT= 9.12): *m/*z: 243.

5.4.26.2 Benzyl (±)-*trans*–8–oxo–1–azabicyclo [4.2.0] octane–7–carboxylate 222

^{1}H NMR (300 MHz, $CDCl_3$): δ 1.09 – 1.65 (m, 4H, $3a_1$, $3b_1$, $4a_1$, $4b_1$), 1.71 – 1.87 (m, 1H, $5b_1$), 1.93 - 2.08 (m, 1H, $5a_1$), 2.68 (ddd, *J* = 4.60, 11.60, 13.60 Hz, 1H, $2b_1$), 3.55 (ddd, *J* = 1.80, 4.30, 10.50 Hz, 1H, C6-H), 3.62 (d, *J* = 1.80 Hz, 1H, C7-H), 3.74 (dd, *J* = 4.60, 13.60 Hz, $2a_1$), 5.10 (dd, *J* = 12.30 Hz, 2H, $-OCH_2Ph$), 7.14 – 7.32 (m, 5H, Ar-H); ^{13}C NMR (75 MHz, $CDCl_3$): δ 21.81, 24.09, 29.56, 39.15, 50.77, 61.85, 67.08, 128.49, 128.26, 128.18, 135.23, 160.16, 167.26; IR (ATR): 411, 463, 582, 697, 743, 834, 941, 976, 1027, 1081, 1151,

1177, 1216, 1304, 1274, 1330, 1380, 1404, 1447, 1497, 1650, 1726, 1755, 2858, 2941; GC-MS (RT): *m/z:* 243.

5.5 Synthesis and characterisation of cyclopropanation reactions

5.5.1 General method for the preparation of cyclopropanes; synthesis of ethyl *cis*–2–phenylcyclopropane–1–carboxylate 127 and ethyl *trans*–2–phenylcyclopropane–1–carboxylate 128 from styrene 87 and EDA 33.

This was synthesised according to a reported procedure.[8]

Cu^{2+}-clay mineral (0.05 g) in dry dichloromethane was stirred for 1 h at room temperature under nitrogen atmosphere and to this stirred solution, styrene **87** (0.39 g, 4.63 mmol) was added and further stirred for 30 min at room temperature. Then ethyl diazoacetate (0.10 g, 0.87 mmol) was added slowly in a dropwise manner over 10 h at room temperature. The resulting mixture was heated to 40ºC overnight. The course of the reaction was monitored by TLC and IR until the complete disappearance of diazo peak 2220 cm^{-1} from ethyl diazoacetate. The reaction mixture was then cooled to room temperature and the catalyst removed by simple filtration and washed with excess dichloromethane (4.0 mL). The filtrate was concentrated *in vaccu*o and purified by silica gel column chromatography using (solvents (0.5 : 9.5) EtOAc : hexane) to obtain pure compounds **127** (0.050 g, 30%) and **128** (0.075 g, 45%).

5.5.1.1 Ethyl *cis*–2–phenylcyclopropane–1–carboxylate 127

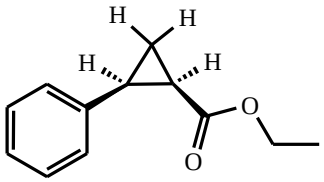

***cis*, 127**

^{1}H NMR (300 MHz, $CDCl_3$): δ 0.96 (d, *J* = 7.10 Hz, 3H, C**H**$_3$CH$_2$O), 1.27 – 1.38 (m, 1H, CH$_2$, cyclopropyl C-H), 1.70 (ddd, *J* = 9.30, 7.40, 5.30 Hz, 1H, CH$_2$, cyclopropyl C-H), 2.06

(ddd, *J* = 9.30, 7.90, 5.70 Hz, 1H, Ar-C**H**), 2.57 (dd, *J* = 8.90, 16.60 Hz, 1H, C**H**CO_2Et), 3.86 (d, *J* = 7.10 Hz, 2H, OC**H**$_2$$CH_3$), 7.16 – 7.33 (m, 5H, Ar-H); ^{13}C NMR (75 MHz, $CDCl_3$): δ 10.98, 13.80, 21.17, 25.57, 60.26, 126.48, 127.92, 129.31, 136.4, 170.69; IR (ATR): 613, 696, 722, 754, 781, 793, 851, 907, 952, 1019, 1039, 1078, 1176, 1219, 1268, 1324, 1336, 1382, 1404, 1457, 1497, 1604, 1720, 2774, 2030, 2343, 2904, 2980, 3027, 3090; GC–MS: (RT = 8.56 *cis* minor): *m/z*: 190 (M^+), 162 (PhCH (CH_2) $CHCO_2^+$), 145 (PhCH (CH_2) $CHCO^+$), 117 (PhCH (CH_2) CH^+).

5.5.1.2 Ethyl *trans*–2–phenylcyclopropane–1–carboxylate[174] 128

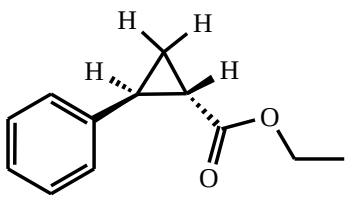

***trans*, 128**

^{1}H NMR (300 MHz, $CDCl_3$): δ 1.24 – 1.35 (m, 4H, CH_2 (cyclopropyl C-H), C**H**$_3$$CH_2$O), 1.60 (ddd, *J* = 9.20, 5.20, 4.60 Hz, 1H, CH_2 (cyclopropyl C-H)), 1.90 (ddd, *J* = 8.20, 5.20, 4.30 Hz, 1H, Ar-CH), 2.52 (ddd, *J* = 9.20, 6.40, 4.30 Hz, 1H, C**H**CO_2Et), 4.17 (q, *J* = 7.0 Hz, 2H, OC**H**$_2$$CH_3$), 7.07 – 7.13 (m, 2H, Ar-H), 7.17 – 7.32 (m, 3H, Ar-H); ^{13}C NMR (75 MHz, $CDCl_3$): δ 14.51, 17.40, 24.75, 26.40, 61.00, 126.66, 126.99, 128.99, 140.64, 173.96; IR (ATR): 696, 722, 754, 786, 790, 851, 907, 952, 1010, 1039, 1070, 1176, 1219, 1268, 1324, 1336, 1382, 1404, 1457, 1497, 1604, 1720, 2774, 2030, 2343, 2904, 2980, 3027; GC–MS (RT = 8.28 *trans* major): 190 (M^+), 162 (PhCH (CH_2) $CHCO_2^+$), 145 (PhCH (CH_2) $CHCO^+$), 117 (PhCH (CH_2) CH^+).

5.5.2 Syntheses of 7–*endo*–ethoxycarbonyl bicyclo[4.1.0]heptane 132 and 7-*exo*-ethoxycarbonylbicyclo[4.1.0]heptane 237.

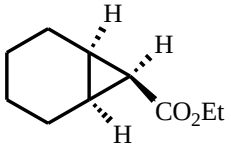

endo, **132**

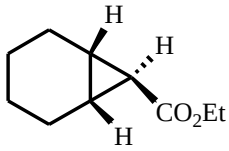

exo, **237**

132 and **237** was synthesised as for **127** and **128** using Cu^{2+}-clay mineral (0.05 g) in dry dichloromethane (4.0 mL), cyclohexene **131** (0.35 g, 4.26 mmol) with ethyl diazoacetate (0.10 g, 0.87 mmol) to give a mixture of **132** (*endo*, minor) and **237** (*exo*, major) (0.022 g, 15%) as an oil.

5.5.2.1 7-*endo*-Ethoxycarbonylbicyclo[4.1.0]heptane 132

Because of insufficient of the product **132** for characterisation by spectroscopic means, only identified by GC–MS: (RT 7.10 *endo* minor): 168, 140, 122, 94, 79, 67.

5.5.2.2 7-*exo*-Ethoxycarbonylbicyclo[4.1.0]heptane 237

^{1}H NMR (300 MHz, $CDCl_3$): δ 1.10 – 1.34 (m, 5H, $OCH_2C\mathbf{H}_3$, CH_2 cyclohexane ring), 1.38 (t, *J* = 4.30 Hz, C**H**CO_2Et), 1.56 – 1.63 (m, 2H, CH_2), 1.64 - 1.76 (m, 2H, CH_2), 1.82 – 1.92 (m, 2H, CH_2), 4.12 (q, *J* = 7.10 Hz, 2H, $OC\mathbf{H}_2CH_3$); ^{13}C NMR (75 MHz, $CDCl_3$): δ 14.02, 17.08, 20.95, 22.05, 130.29, 134.51, 174.7, 171.8; IR (ATR): 701, 734, 844, 1031, 1112, 1174, 1266, 1456, 1380, 1715, 1943, 2034, 2167, 2337, 2360, 2980, 3443, 3729; GC–MS (RT = 7.31 *exo* major): 168, 140, 122, 94, 79, 67.

5.5.3 Syntheses of *endo*-ethyl bicyclo[6.1.0]non-4-ene-9-carboxylate 239 and *exo*-ethyl bicyclo[6.1.0]non-4-ene-carboxylate 240.

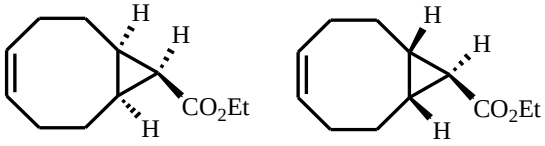

***endo*, 239** ***exo*, 240**

239 and **240** were synthesised as for **127** and **128** using Cu^{2+}-Wyoming bentonite (0.05 g) in dry dichloromethane (4.0 mL), 1,5-cyclooctadiene **238** (0.47 g, 4.33 mmol) with ethyl diazoacetate (0.10 g, 0.87 mmol) to give **242** (*endo*, minor) and **243** (*exo*, major) (0.020 g, 12%) as an oil.

5.5.3.1 *endo*-Ethyl bicyclo[6.1.0]non-4-ene-9-carboxylate 239

Because of insufficient of the product **239** for characterisation by spectroscopic means, only identified by GC–MS: (RT 8.64 *endo* minor): 195, 166, 138, 105, 91.

5.5.3.2 *exo*-Ethyl bicyclo[6.1.0]non-4-ene-9-carboxylate 240.

^{1}H NMR (300 MHz, $CDCl_3$): δ 1.18 (t, *J* = 4.80 Hz, 1H, C-H *exo*), 1.25 (t, *J* = 7.20 Hz, 3H, $CH_2C\mathbf{H}_3$), 1.49 - 1.59 (m, 4H), 2.04 – 2.31 (m, 6H), 4.11 (q, *J* = 7.20 Hz, 2H, $C\mathbf{H}_2CH_3$), 5.39 – 5.65 (m, 2H, -HC = CH); ^{13}C NMR (75 MHz, $CDCl_3$): δ 14.33, 26.67, 27.70, 27.78, 28.20, 60.82, 129.61, 174.66. IR (ATR): 1027, 1096, 1157, 1261, 1375, 1454, 1719, 2155, 2360, 2952, 3479; GC-MS: (RT 8.82): 195, 166, 138, 105, 91.

5.5.4 Syntheses of *cis*-ethyl 2,2–dimethyl–3–(2–methylpropenyl)cyclopropane–1–carboxylate 244 and *trans*-ethyl 2,2–dimethyl–3–(2–methylpropenyl)cyclo-propane–1–carboxylate 134.

244 and **134** was synthesised as for **127** and **128** using Cu^{2+}-clay mineral (0.05 g) in dry dichloromethane (4.0 mL), 2,5-dimethyl-2,4-hexadiene **133** (0.48 g, 4.30 mmol) with ethyl diazoacetate (0.10 g, 0.87 mmol) to give **244** and **134** (0.070 g, 48%) as an oil.

5.5.4.1 *cis*-Ethyl 2,2–dimethyl–3–(2–methylpropenyl)cyclopropane–1–carboxylate 244

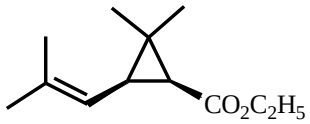

cis, **244**

^{1}H NMR (300 MHz, $CDCl_3$): δ 1.20 (s, 3H, C(C**H**$_3$)), 1.21 – 1.28 (m, 6H, C(C**H**$_3$)$_2$/CH$_2$C**H**$_3$), 1.64 (d, *J* = 8.80 Hz, 1H, H-C1), 1.69 (s, 6H, (C**H**$_3$)$_2$C=CH$_{cis}$), 1.87 (t, *J* = 8.70 Hz, 1H, H-C2), 4.00 – 4.20 (m, 2H, C**H**$_2$CH$_3$), 5.34 – 5.44 (m, 1H, C=C**H**); ^{13}C NMR (75 MHz, $CDCl_3$): δ 14.40, 22.18, 24.14, 26.00, 28.00, 60.21, 125.74, 128.27, 131.19, 173.29; IR (ATR): 856, 1028, 1160, 1100, 1374, 1437, 1722, 2064, 2183, 2220, 2970, 3456; GC–MS: (RT = 6.94 *cis minor*): *m/z* 196, 181, 153, 123, 107, 95, 91, 81.

5.5.4.2 *trans*-Ethyl 2,2–dimethyl–3–(2–methylpropenyl)cyclopropane–1–carboxylate 134

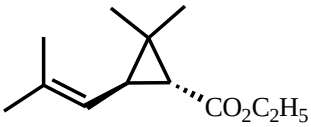

trans,**134**

^{1}H NMR (300 MHz, $CDCl_3$): δ 1.12 (s, 3H, C(C**H**$_3$)), 1.22 – 1.26 (m, 6H, C(C**H**$_3$)$_2$/CH$_2$C**H**$_3$), 1.37 (d, *J* = 5.40 Hz, 1H, H-C1), 1.71 (s, 6H, (C**H**$_3$)$_2$C=CH$_{trans}$), 1.99 – 2.09 (m, 1H, H-C2), 4.02 (m, 2H, C**H**$_2$CH$_3$), 4.73 - 5.07 (m, 1H, C=C**H**); ^{13}C NMR (75 MHz, $CDCl_3$): δ 18.50,

22.18, 25.50, 26.00, 28.00, 60.21, 121.19, 128.25, 135.40, 172.54; IR (ATR): 444, 856, 1028, 1175, 1115, 1374, 1447, 1722, 2002, 2064, 2173, 2226, 2978, 3456; GC–MS: (RT = 6.99 *trans major*): *m/z* 196, 181, 153, 123, 107, 95, 91, 81.

5.5.5 Synthesis of 3–hydroxy–5–phenyl–pent–4–enolic acid ethyl ester

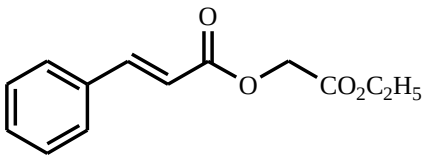

246

246 was synthesised as for **127** and **128** using Cu^{2+}-clay mineral (0.05 g) in dry dichloromethane, *trans*-cinnamic acid **245** (0.30 g, 2.02 mmol) with ethyl diazoacetate (0.10 g, 0.87 mmol) to give **246** (0.10 g, 54%) as a oil. ^{1}H NMR (300 MHz, $CDCl_3$): δ 1.18 (t, *J* = 7.10 Hz, 3H, $CH_2C\mathbf{H}_3$), 4.13 (q, *J* = 7.10 Hz, 2H, $C\mathbf{H}_2CH_3$), 4.62 (s, 2H, CH_2), 6.41 (d, *J* = 16.0 Hz, 1H, Ar-CH=C**H**), 7.20 - 7.27 (m, 3H, Ar-H), 7.32 – 7.42 (m, 2H, Ar-H), 7.66 (d, *J* = 16.0 Hz, 1H, Ar-C**H**=CH); ^{13}C NMR (75 MHz, $CDCl_3$): δ 14.16, 60.89, 61.50, 116.75, 128.26, 128.94, 130.61, 134.14, 146.27, 166.20, 167.98; MS: *m/z* 234.

5.6 Synthesis and characterisation of cyclopropanes from other diazo compounds

5.6.1 General method for the preparation of cyclopropanes: 2–phenyl–cyclopropane–1,1–dicarboxylic acid methyl ester 248

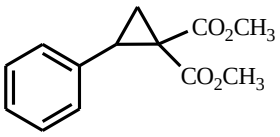

248

Cu^{2+}–clay mineral (0.10 g) was dissolved in acetonitrile (2.0 mL) and stirred for 1 h at room temperature. Styrene **87** (0.32 g, 3.07 mmol) was added to this reaction mixture and 1,3–dimethyl 2–diazopropanedioate **247** (0.10 g, 0.63 mmol) was added slowly in a dropwise manner over 2 h. The reaction mixture was then heated under reflux overnight, cooled to room temperature, filtered under vacuum and washed with excess of dichloromethane. The combined filtrate was evaporated on a rotavapor to give the crude product, which was purified by column chromatography; the pure compound **248** was eluted with (20 : 80) EtOAc/hexane, which on rotary evaporation gave a colourless oil (0.015 g, 10%).

^{1}H NMR (300 MHz, $CDCl_3$): δ 1.77 (dd, 1H, *J* = 9.20, 5.20 Hz, CH (cyclopropyl)), 2.23 (dd, 1H, *J* = 8.0, 5.20 Hz, CH (cyclopropyl)), 3.25 (t, 1H, *J* = 8.70 Hz, Ar-CH), 3.42 (s, 3H, -OCH_3), 3.84 (s, 3H, -OCH_3), 7.19 – 7.43 (m, 5H, Ar-H); ^{13}C NMR (75 MHz, $CDCl_3$): δ 19.0, 32.40, 37.10; 52.0, 52.60, 127.30, 128.0, 128.30, 134.50, 166.90, 170.10; IR (ATR): 1082, 1130, 1207, 1277, 1332, 1416, 1726, 2980; GC-MS: 234.

5.6.2 Synthesis of c*is*–methyl 2–phenyl–1–(piperidine–1–carbonyl) cyclopropane carboxylates 249

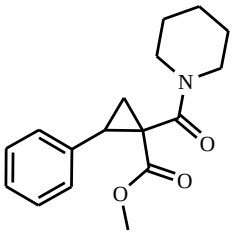

249

The compound **249** was synthesised by using Cu^{2+}–clay mineral (0.10 g) in acetonitrile (2.0 mL), styrene **87** (0.24 g, 2.3.0 mmol), methyl *N*-piperidinodiazomalonate **187** (0.10 g, 0.47 mmol) which gave the pure compound as a colourless oil **249** (0.015 g, 12%). ^{1}H-NMR (300 MHz, $CDCl_3$): δ 1.47 – 1.68 (m, 7H, C-H *piperidine ring*), 2.13 (dd, *J* = 8.02, 5.10 Hz, 1H, C-H (cyclopropyl)), 3.18 (t, *J* = 8.40 Hz, 1H, Ar-CH), 3.39 (s, 3H, -OCH_3), 3.41 – 3.65 (m, 4H, CH *piperidine ring*, C-H (cyclopropyl)), 7.01 – 7.31 (m, 5H, Ar-H); ^{13}C-NMR (75 MHz, $CDCl_3$): δ 18.0, 24.7, 25.5, 26.0, 32.1, 37.7, 43.6, 46.8, 52.3, 129.2, 128.1, 127.2, 135.3, 166.6, 168.8; IR (ATR) 1135, 1334, 1434, 1511, 1638, 1715, 2884, 2946, 3008, 3039; GC-MS: 287, 255, 227, 202, 170, 144, 115, 84.

5.6.3 Methyl–2–phenyl–1–(pyrrolidine–1–carbonyl) cyclopropane carboxylate 250

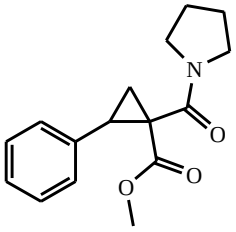

250

The compounds **250** were synthesised by using Cu^{2+}–clay mineral (0.10 g) in acetonitrile (2.0 mL) and styrene **87** (0.26 g, 2.5 mmol), methyl pyrrolidinodiazomalonate **189** (0.10 g, 0.50 mmol) was reacted to form the compound **250** as a colourless oil (0.016 g, 12%). ^{1}H NMR (300 MHz, $CDCl_3$): δ 1.52 (dd, *J* = 4.90, 9.10 Hz, 1H, C-H cyclopropyl ring), 1.78 - 2.01 (m, 4H, *pyrrolidine ring*), 2.19 (dd, *J* = 4.90, 8.00 Hz, 1H, Ar-CH), 3.28 – 3.41 (m, 2H, N-CH, C-H cyclopropyl), 3.42 (s, 3H, $-OCH_3$), 3.72 – 3.96 (m, 3H, C-H *pyrrolidine ring*), 7.21 –7.32 (m, 5H, Ar-H); ^{13}C NMR (75 MHz, $CDCl_3$): δ 14.10, 17.60, 24.40, 26.30, 31.40, 38.80, 46.60, 46.70, 61.30, 129.20, 128.10, 127.20, 135.50, 166.60, 168.30; IR (ATR): 1142, 1310, 1426, 1637, 1724, 2875, 2973, 3008, 3038; GC-MS: 274.

5.7 Synthesis and characterisation of nitrene addition reaction products

5.7.1 General method for the preparation of aziridines: *N*-(*p*-tolylsulfonyl)-2-phenylaziridine 249

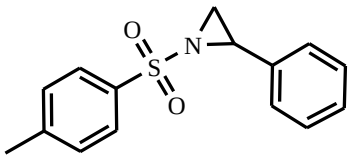

251

Cu^{2+}-clay mineral (0.10 g) was dissolved in acetonitrile (2.0 mL) and stirred for 1 h at room temperature to this reaction mixture styrene **87** (0.26 g, 2.50 mmol) was added and the *p*–toluenesulfonyl azide **182** (0.10 g, 0.50 mmol) was added slowly dropwise for 2 h. Then the reaction mixture was refluxed for overnight and then cooled to room temperature, filtered under vacuum, washed with excess of dichloromethane. Then the filtrate was collected and evaporated under rotavapor to get crude product, the crude product was purified by column chromatography to elute the pure compound **249** at (solvent (40 : 60) EtOAc/hexane) as a colourless oil (0.016 g, 12%). ^{1}H NMR (300 MHz, $CDCl_3$): δ 2.41 – 2.47 (m, 4H, Ph-CH_3, CH_2), 2.98 (d, *J* = 7.20 Hz, 1H, CH_2), 3.78 (dd, *J* = 7.20, 5.44 Hz, 1H, Ar-CH), 7.17 – 7.47 (m, 6H, Ar-H), 7.82 – 7.99 (m, 3H, Ar-H); ^{13}C NMR (75 MHz, $CDCl_3$): δ 21.71, 36.00, 41.09, 126.62, 127.99, 128.36, 128.62, 129.83, 135.02, 135.09, 144.72; IR (ATR): 3267, 3062, 2360, 2336, 2924, 2131, 2003, 1682, 1597, 1493, 1450, 333, 1161, 1088, 813, 750, 698, 667, 592, 543, 414; MS: *m/z*: 274.

5.7.2 Attempted synthesis of diphenyl (2-phenylaziridin-1-yl)phosphonate

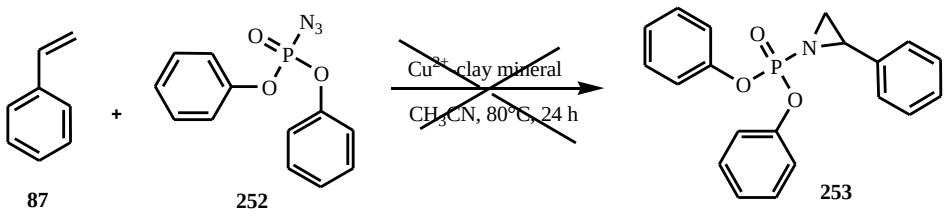

The synthesis of compound **253** was attempted as for **251** by using Cu^{2+}-Wyoming bentonite (0.10 g) in acetonitrile (2.0 mL) with styrene **87** (0.20 g, 1.90 mmol) and diphenylphosphoryl azide **252** (0.10 g, 0.36 mmol). The reaction showed a complex mixture and when the crude product was purified by column chromatography the desired product **253** was not found by ^{1}H NMR spectroscopy.

5.7.3 Attempted synthesis of 4-[(2-phenylaziridin-1-yl)sulfonyl]benzoic acid 255

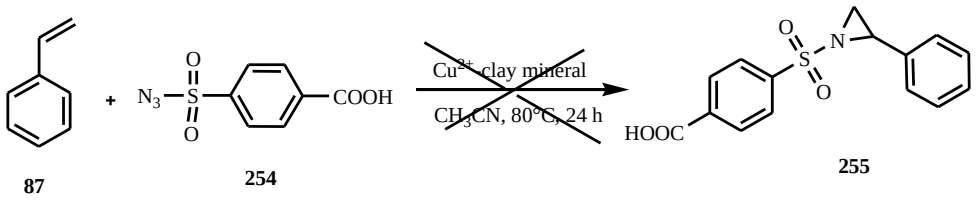

The synthesis of compound **255** was attempted as for **251** using Cu^{2+}-Wyoming bentonite (0.10 g) in acetonitrile (2.0 mL) with styrene **87** (0.20 g, 1.90 mmol) and 4-(azidosulfonyl)benzoic acid **254** (0.10 g, 0.44 mmol). The reaction gave a complex crude mixture which on attempted purification by column chromatography showed none of the required product **255** by ^{1}H NMR spectroscopy.

6 Future work

6.1 Asymmetric synthesis with carbocations

The following work should be examined to further understand these catalytic systems:

6.2 Asymmetric synthesis with carbocations

As many pharmaceuticals, flavours, fragrances, food and feed additives and agrochemicals contain elements of chirality and most are required to be enantiomerically pure before they can be used. Introduction of a chiral unit into the currently achiral groups to determine whether a chiral centre can induce preference for one of the possible stereoisomers, which will give an advantage as we can use biologically active chiral compounds.[198]

6.3 Chiral carbanion reactions

Clay minerals have been used for supporting Grignard reagents without decomposition. Asymmetric syntheses via chiral carbanions derived from these organometallic reagents are well known.[199] We would aim to determine whether we can improve the stereo–selectivity of reactions of chiral Grignard reagents with prochiral carbonyl compounds or achiral Grignard reagents with chiral carbonyl compounds, on intercalating the Grignard reagent into a clay interlayer.

6.4 Enantioselective reactions within clay interlayers

Up to now we will have examined the potential for regio– and stereo–control of reactions by clay minerals. However, it may be possible to exert improved enantio–selectivity on reactions if the clay interlayer is made into a chiral environment. There are two simple methods for creating a chiral environment within the clay interlayer; the first is simply to make the clay interlayer chiral. This can be done either by displacing the water from the interlayer with an

optically active solvent, e.g. an ether for Grignard reactions, an alcohol for aldol reactions, a haloalkane for carbene reactions, etc., or by having an un–reactive optically active compound either in solution or intercalated into the interlayer, e.g. a chiral tetra–alkyl ammonium ion (forming a chiral organoclay).

The second method would be to convert the clay layer to an optically active organoclay layer. Carbenes generated in the clay interlayer have been observed to insert into the H–O–Al bond of the clay layers. This work will be extended by generation and insertion of a chiral carbene into the clay interlayer surface, thus creating a chiral interlayer environment. This chiral clay material will then be used to induce stereo–selectivity into catalysed reactions, for example other carbene insertions, carbocation rearrangements and carbanion reactions carried out in the clay interlayer.

7 References:

1. Wulfman, D. S.; Peace, B. W.; McDaniel Jr, R. S., Metal salt catalysed carbenoids - XIV: The mechanisms of carbene dimer formation from diazoacetic ester and dimethyl diazomalonate in the presence of some soluble copper catalysts. *Tetrahedron* **1976,** *32* (11), 1251-1255.

2. Yeung, C.-T.; Teng, P.-F.; Yeung, H.-L.; Wong, W.-T.; Kwong, H.-L., Catalytic and asymmetric cyclopropanation of alkenes catalysed by rhenium(I) bipyridine and terpyridine tricarbonyl complexes. *Organic and Biomolecular Chemistry* **2007,** *5* (23), 3859-3864.

3. Maier, T. C.; Fu, G. C., Catalytic Enantioselective O−H Insertion Reactions. *Journal of the American Chemical Society* **2006,** *128* (14), 4594-4595.

4. Morilla, M. E.; Molina, M. J.; Díaz-Requejo, M. M.; Belderraín, T. R.; Nicasio, M. C.; Trofimenko, S.; Pérez, P. J., Copper-catalysed carbene insertion into OH bonds: High selective conversion of alcohols into ethers. *Organometallics* **2003,** *22* (14), 2914-2918.

5. Corey, E. J.; Felix, A. M., A New Synthetic Approach to the Penicillins. *Journal of the American Chemical Society* **1965,** *87* (11), 2518-2519.

6. Ye, T.; McKervey, M. A., Organic synthesis with α-diazo carbonyl compounds. *Chemical Reviews* **1994,** *94* (4), 1091-1160.

7. Box, V. G. S.; Marinovic N.; Yiannikouros G. P., The synthesis of β-lactones and β-lactams from malonates and malonamides. *Heterocycles* **1991,** *22* (32), 245-251.

8. Sanders, C. J.; Gillespie, K. M.; Scott, P., Catalyst structure and the enantioselective cyclopropanation of alkenes by copper complexes of biaryldiimines: the importance of ligand acceleration. *Tetrahedron: Asymmetry* **2001,** *12* (7), 1055-1061.

9. Godula, K.; Sames, D., C-H bond Functionalization in Complex Organic Synthesis. *Science* **2006,** *312* (5770), 67-72.

10. McCabe, R. W., *"Clay Chemistry"*. 2nd ed.; John Wiley and Sons: (1996); Vol. in: "Inorganic Materials", p 313-376.

11. Chiche, B.; Finiels, A.; Gauthier, C.; Geneste, P.; Graille, J.; Pioch, D., Friedel-Crafts acylation of toluene and *p*-xylene with carboxylic acids catalysed by zeolites. *The Journal of Organic Chemistry* **1986,** *51* (11), 2128-2130.

12. Adams, J. M.; Dyer, S.; Martin, K.; Matear, W. A.; McCabe, R. W., Diels-Alder reactions catalysed by cation-exchanged clay minerals. *Journal of the Chemical Society, Perkin Transactions 1* **1994,** (6), 761-765.

13. Rosenberg, M. L.; Krivokapic, A.; Tilset, M., Highly *cis*-selective cyclopropanations with ethyl diazoacetate using a novel Rh(I) catalyst with a chelating *N*-heterocyclic iminocarbene ligand. *Organic Letters* **2008,** *11* (3), 547-550.

14. Hu, W.; Timmons, D. J.; Doyle, M. P., In search of high stereocontrol for the construction of *cis*-disubstituted cyclopropane compounds. Total synthesis of a cyclopropane-configured urea-PETT analogue that is a HIV-1 reverse transcriptase inhibitor. *Organic Letters* **2002,** *4* (6), 901-904.

15. Adams, J. M.; McCabe, R. W., *Clay minerals as catalysts*. in: Handbook of Clay Science, Vol. 1; Elsevier, Eds. F. Bergaya, B.K.G. Theng, G. Lagaly; **2006**; p 541-581.

16. Graham, R. C., X-ray diffraction and the identification and analysis of clay minerals. *Soil Science* **1999,** *164* (1), 72-73.

17. Brindley, G. W.; Brown G., Crystal structures of clay minerals and their x-ray identification. *Mineralogical Society*: (**1980**).

18. Fraile, J. M.; García, J. I.; Mayoral, J. A.; Tarnai, T., Clay-supported bis(oxazoline)-copper complexes as heterogeneous catalysts of enantioselective cyclopropanation reactions. *Tetrahedron: Asymmetry* **1998,** *9* (22), 3997-4008.

19. Gorski, C. A.; Klüpfel, L. E.; Voegelin, A.; Sander, M.; Hofstetter, T. B., Redox Properties of Structural Fe in Clay Minerals: 3. Relationships between Smectite Redox and Structural Properties. *Environmental Science and Technology* **2013,** *47* (23), 13477-13485.

20. Padwa, A.; Hornbuckle, S. F., Ylide formation from the reaction of carbenes and carbenoids with heteroatom lone pairs. *Chemical Reviews* **1991,** *91* (3), 263-309.

21. Warkentin, J., 2,5-Dihydro-1,3,4-oxadiazoles and bis(heteroatomsubstituted)carbenes. *Accounts of Chemical Research* **2008,** *42* (1), 205-212.

22. Velde, B., Composition and mineralogy of clay minerals. In *Origin and Mineralogy of Clays*, Velde, B., Ed. Springer Berlin Heidelberg: **1995**; pp 8-42.

23. Bergaya, F.; Lagaly, G., *Handbook of Clay Science*. Elsevier Science: **2013**.

24. Weiss, A.; Russow, J., Über die Lage der austauschbaren kationen bei Kaolinit. *Proceedings of the International Clay Conference, Stockholm* **1963** *1*,203–13.

25. Caine, M.; Dyer, G.; Holder, J.; Osborne, B.; Matear, W.; McCabe, R.; Mobbs, D.; Richardson, S.; Wang, L., The use of clays as sorbents and catalysts. In *Natural Microporous Materials in Environmental Technology*, Springer: **1999**; pp 49-69.

26. Brunauer, S.; Emmett, P. H.; Teller, E., Adsorption of gases in multimolecular layers. *Journal of the American Chemical Society* **1938,** *60* (2), 309-319.

27. Franz W.; Gunther, P.; Hofstadt, C. E., Catalysts on the basis of acid-activated montmorillonites. *Proc. 5th World Petrol. Congr.* **1960,** *3* 123-132.

28. Fahn, R.; Fenderl K., Reaction products of organic dye molecules with acid-treated montmorillonite. *Clay Minerals* **1983,** *18* (4), 447-458.

29. Chen, Y.; Banin, A., Scanning electron microscope (SEM) observations of soil structure changes induced by sodium-calcium exchange in relation to hydraulic conductivity. *Soil Science* **1975,** *120* (6), 428-436.

30. Mills, G. A.; Holmes, J.; Cornelius, E. B., The acid activation of some bentonite clays. *The Journal of Physical and Colloid Chemistry* **1950,** *54* (8), 1170-1185.

31. Thomas, C. L.; Hickey, J.; Stecker, G., Chemistry of clay cracking catalysts. *Industrial and Engineering Chemistry* **1950,** *42* (5), 866-871.

32. Breen, C., Thermogravimetric study of the desorption of cyclohexylamine and pyridine from an acid-treated Wyoming bentonite. *Clay Minerals* **1991,** *26* (4), 473-486.

33. Gonzalez-Pradas, E.; Villafranca-Sanchez, M.; Valverde-Garcia, A.; Villafranca-Sanchez, E., Adsorption of *β*-Carotene from acetone solution on natural and chemically modified bentonite. *Materials Chemistry and Physics* **1991,** *27* (3), 307-319.

34. Stockmeyer. M; K. Kruse, Adsorption of Zn and Ni ions and phenol and diethylketones by bentonites of different organophilicities. *Clay Minerals* **1991,** *26* 431-434.

35. González-Pradas, E.; Villafranca-Sánchez, M.; Socias-Viciana, M.; Castillo-Sánchez, J.; Fernández-Pérez, M., Removal of 3—(3, 4—dichlorophenyl)—1, 1 dimethylurea from aqueous solution by natural and activated bentonite. *Journal of Chemical Technology and Biotechnology* **1993,** *56* (1), 67-71.

36. Ueda, H.; Hamayoshi, M., Sepiolite as a deodorant material: an ESR study of its properties. *Journal of Materials Science* **1992,** *27* (18), 4997-5002.

37. Aznar, A.; Casal, B.; Ruiz-Hitzky, E.; Lopez-Arbeloa, I.; Lopez-Arbeloa, F.; Santaren, J.; Alvarez, A., Adsorption of methylene blue on sepiolite gels: spectroscopic and rheological studies. *Clay Minerals* **1992,** *27* (1), 101-108.

38. Bernal, M.; Lopez-Real, J., Natural zeolites and sepiolite as ammonium and ammonia adsorbent materials. *Bioresource Technology* **1993,** *43* (1), 27-33.

39. Breen, C., Thermogravimetric, infrared and mass spectroscopic analysis of the desorption of tetrahydropyran, tetrahydrofuran and 1, 4-dioxan from montmorillonite. *clay minerals* **1994,** *29* (1), 115-122.

40. Breck, D. W.; Eversole, W. G.; Milton, R. M.; Reed, T. B.; Thomas, T. L., Crystalline Zeolites. I. The Properties of a New Synthetic Zeolite, Type A. *Journal of the American Chemical Society* **1956,** *78* (23), 5963-5972.

41. http://www.molecularsieve.org/Zeolite_Molecular_Sieve.htm accessed 28 June 2014.

42. Broussard, L.; Shoemaker, D. P., The structures of synthetic molecular sieves. *Journal of the American Chemical Society* **1960,** *82* (5), 1041-1051.

43. Shannon, R. t., Revised effective ionic radii and systematic studies of interatomic distances in halides and chalcogenides. *Acta Crystallographica Section A: Crystal Physics, Diffraction, Theoretical and General Crystallography* **1976,** *32* (5), 751-767.

44. Database of periodic table. http://abulafia.mt.ic.ac.uk/shannon/ptable.php accessed 28 June 2014.

45. Zeolite. http://www.cchem.berkeley.edu/molsim/teaching/fall2009/mto/cat.html

accessed 28 June 2014.

46. International Zeolite Association. http://iza-online.org accessed 28 June 2014.

47. Adams J. M.; Clement D. E.; Graham S. H., Reactions of Alcohols with Alkenes over an Aluminum-Exchanged Montmorillonite. *Clays and Clay Minerals* **1983,** *31* 129-136.

48. Mortland, M. M.; Raman, K. V., Surface Acidity of Smectites in Relation to Hydration, Exchangeable Cation, and Structure. *Clays and Clay Minerals* **1968,** *16* 393-398.

49. Kubota, M.; Sakamoto, A.; Komatsu, M.; Maeno, K.; Masuyama, A., Selective Preparation of Monobenzyl Glyceryl Ethers by the Condensation Reaction of Glycerol with Benzyl Alcohols in the Presence of Zeolite Catalysts. *Journal of Oleo Science* **2014,** *63* (10), 1057-1062.

50. Eggers S. H.; Kane, V. V.; Lowe, G., Studies related to cephalosporin C. Part III. A synthetical route to 6H-1,3-thiazines and the synthesis of a new fragmentation product of a cephalosporanic acid derivative. *Journal of the Chemical Society (Resumed)* **1965,** (0), 1262-1270.

51. Jeganathan, M.; Pitchumani, K., Synthesis of substituted isoquinolines via iminoalkyne cyclization using Ag(I) exchanged K10-montmorillonite clay as a reusable catalyst. *RSC Advances* **2014,** *4* (73), 38491-38497.

52. Roesch, K. R.; Zhang, H.; Larock, R. C., Synthesis of Isoquinolines and Pyridines by the Palladium-Catalysed Iminoannulation of Internal Alkynes. *The Journal of Organic Chemistry* **2001,** *66* (24), 8042-8051.

53. Varma R. S.; Kumar D.; Liesen P.J., Solid state synthesis of 2-aroylbenzo[*b*]furans, 1,3-thiazoles and 3-aryl-5,6-dihydroimidazo[2,1-*b*][1,3]thiazoles from *α*-tosyloxyketones using microwave irradiation. *Journal of the Chemical Society, Perkin Transactions 1* **1998,** (24), 4093-4096.

54. Fefer, M.; King, L. C., Reaction of Ethylenethiourea with Phenacyl and *para*-Substituted Phenacyl Halides. *The Journal of Organic Chemistry* **1961,** *26* (3), 828-835.

55. Prakash, O.; Saini, N.; Sharma, P. K., Hypervalent iodine reagents in the synthesis of heterocyclic compounds. *Synlett* **1994,** (04), 221-227.

56. Azzallou, R.; Mamouni, R.; Stieglitz, K.; Saffaj, N.; El Haddad, M.; Lazar, S., Al-Pillared Ghassoulite Clay as a New Green Catalyst for the Synthesis of Benzothiazoles and Benzimidazoles: Effect of Amine/CEC Ratio. *International Journal of Organic Chemistry* **2013,** *3*, 151.

57. Elmchaouri, A.; Mahboub, R., Effects of preadsorption of organic amine on Al-PILCs structures. *Colloids and Surfaces A: Physicochemical and Engineering Aspects* **2005,** *259* (1-3), 135-141.

58. Varma, R. S., Clay and clay-supported reagents in organic synthesis. *Tetrahedron* **2002,** *58* (7), 1235-1255.

59. Saoudi, A.; Hamelin, J.; Benhaoua, H., Rapid Synthesis of Aziridine Derivatives over Bentonite in "Dry Media". *Journal of Chemical Research* **1996,** (11), 492-493.

60. Larhed, M.; Moberg, C.; Hallberg, A., Microwave-accelerated homogeneous catalysis in organic chemistry. *Accounts of Chemical Research* **2002,** *35* (9), 717-727.

61. Nagendrappa, G., Organic synthesis using clay and clay-supported catalysts. *Applied Clay Science* **2011,** *53* (2), 106-138.

62. Borkin, D.; Carlson, A.; Török, B., K-10-Catalysed Highly Diastereoselective Synthesis of Aziridines. *Synthesis Letters* **2010,** (05), 745-748.

63. Gutierrez, E.; Ruiz-hitzky, E., Intracrystalline Pinacol Rearrangement in Layer Silicates. *Molecular Crystals and Liquid Crystals Incorporating Nonlinear Optics* **1988,** *161* (1), 453-458.

64. Nagendrappa, G., Organic synthesis using clay catalysts. *Resonance* **2002,** *7* (1), 64-77.

65. Traynelis, V. J.; Hergenrother, W. L.; Hanson, H. T.; Valicenti, J. A., Dehydration of alcohols, diols, and related compounds in dimethyl sulfoxide. *The Journal of Organic Chemistry* **1964,** *29* (1), 123-129.

66. Ramesh S.; Bhat Y. S.; Jai Prakash B. S., Microwave-activated *p*-TSA dealuminated montmorillonite - a new material with improved catalytic activity. *Clay Minerals* **2012,** *47* (2), 231-242.

67. Martil, E. N.; Aragon de la Cruz, F., Formation of monosaccharides form glycolaldehyde in a water suspension of Na^+-montmorillonite. *Anales de Quimica Serie B - Quimica Inorganica y Quimica Analytica* **1986,** *82*, 256-259.

68. Kim, S. H.; Yoon, S.; Kim, Y.; Verkade, J. G., Mukaiyama Aldol Reactions Catalysed by a Trimeric Organo Aluminum(III) Alkoxide. *Phosphorus, Sulfur, and Silicon and the Related Elements* **2014,** *189* (7-8), 1193-1206.

69. Ainsworth, C.; Chen, F.; Kuo, Y.-N., Ketene alkyltrialkylsilyl acetals: synthesis, pyrolysis and NMR studies. *Journal of Organometallic Chemistry* **1972,** *46* (1), 59-71.

70. Kawai, M.; Qnaka, M.; Izumi, Y., Solid acid-catalysed allylation of acetals and carbonyl compounds with allylic silanes. *Chemistry Letters* **1986,** *15* (3), 381-384.

71. Newton, L., Dimer Acids and their Derivatives-Potential Applications. *Specialty Chemicals* **1984,** *17*, 22-24.

72. Downing, R. S., Van Austel, J., and Joustra, A. H. Dimerization Process Catalyst : *U.S. Patent* 4,125,483. (1978).

73. Ruiz-López, M. F.; Assfeld, X.; García, J. I.; Mayoral, J. A.; Salvatella, L., Solvent effects on the mechanism and selectivities of asymmetric Diels-Alder reactions. *Journal of the American Chemical Society* **1993,** *115* (19), 8780-8787.

74. Sheehan, M. E.; Sharratt, P. N., Molecular dynamics methodology for the study of the solvent effects on a concentrated Diels-Alder reaction and the separation of the post-reaction mixture. *Computers and Chemical Engineering* **1998,** *22, Supplement 1* (0), S27-S33.

75. Mitsudome, T.; Nose, K.; Mizugaki, T.; Jitsukawa, K.; Kaneda, K., Reusable montmorillonite-entrapped organocatalyst for asymmetric Diels–Alder reaction. *Tetrahedron Letters* **2008,** *49* (38), 5464-5466.

76. Ahrendt, K. A.; Borths, C. J.; MacMillan, D. W. C., New strategies for organic catalysis: The first highly enantioselective organocatalytic Diels - Alder reaction. *Journal of the American Chemical Society* **2000,** *122* (17), 4243-4244.

77. Pauling, L., The structure of singlet carbene molecules. *Journal of the Chemical Society, Chemical Communications* **1980,** (15), 688-689.

78. Kirmse, W., *Carbene Chemistry 2e*. Elsevier: 2013; Vol. 1.

79. Forrester, A. R.; Sadd, J. S., Detection of carbenes by electron spin resonance spectroscopy: 'triplet trapping'. *Journal of the Chemical Society, Chemical Communications* **1976,** (16), 631-632.

80. Davidson, E. R., Singlet-triplet energy separation in carbenes and related diradicals. *Diradicals, edited by WT Borden (Wiley, Weinheim, Germany)* **1982**, 73.

81. Curtius, T., Clays and Clay Minerals. *Berichte der Deutschen Chemischne Gesellschaft* **1883,** *16*, 2230-2231.

82. Regitz, M., New Methods of Preparative Organic Chemistry. Transfer of Diazo Groups. *Angewandte Chemie International Edition in English* **1967,** *6* (9), 733-749.

83. Stork, G.; Kazuhiko, N., Regiocontrol by electron withdrawing groups in the Rh-catalysed CH insertion of *α*-diazoketones. *Tetrahedron Letters* **1988,** *29* (19), 2283-2286.

84. Rando, R., Conformational and solvent effects on carbene reactions. *Journal of the American Chemical Society* **1970,** *92* (22), 6706-6707.

85. Corey, E. J.; Myers, A. G., Efficient synthesis and intramolecular cyclopropanation of unsaturated diazoacetic esters. *Tetrahedron Letters* **1984,** *25* (33), 3559-3562.

86. Aratani, T.; Yoneyoshi, Y.; Nagase, T., Asymmetric synthesis of chrysanthemic acid. An application of copper carbenoid reaction. *Tetrahedron Letters* **1975,** *16* (21), 1707-1710.

87. Brookhart, M.; Studabaker, W. B., Cyclopropanes from reactions of transition metal carbene complexes with olefins. *Chemical Reviews* **1987,** *87* (2), 411-432.

88. Demonceau, A.; Noels, A. F.; Hubert, A. J.; Teyssie, P., Transition-metal-catalysed reactions of diazoesters. Insertion into C-H bonds of paraffins by carbenoids. *Journal of the Chemical Society, Chemical Communications* **1981,** (14), 688-689.

89. Demonceau, A.; Noels, A. F.; Anciaux, A. J.; Hubert, A. J.; Teyssié, P., Transition-Metal-Catalysed Reactions of Diazoesters: Synthesis of Chrysanthemic and Permethric Acid Esters by Cyclopropanation of Conjugated Dienes. *Bulletin des Sociétés Chimiques Belges* **1984,** *93* (11), 949-952.

90. Maas, G., New syntheses of diazo compounds. *Angewandte Chemie International Edition in English* **2009,** *48* (44), 8186-8195.

91. Holton, T. L.; Schechter, H., Advantageous Syntheses of Diazo Compounds by Oxidation of Hydrazones with Lead Tetraacetate in Basic Environments. *The Journal of Organic Chemistry* **1995,** *60* (15), 4725-4729.

92. Bamford, W. R.; Stevens, T. S., The decomposition of toluene-*p*-sulfonylhydrazones by alkali. *Journal of the Chemical Society (Resumed)* **1952,** (0), 4735-4740.

93. Aggarwal, V. K.; Alonso, E.; Bae, I.; Hynd, G.; Lydon, K. M.; Palmer, M. J.; Patel, M.; Porcelloni, M.; Richardson, J.; Stenson, R. A.; Studley, J. R.; Vasse, J.-L.; Winn, C. L., A New Protocol for the In Situ Generation of Aromatic, Heteroaromatic, and Unsaturated Diazo Compounds and Its Application in Catalytic and Asymmetric Epoxidation of Carbonyl Compounds. Extensive Studies To Map Out Scope and Limitations, and Rationalization of Diastereo- and Enantioselectivities. *Journal of the American Chemical Society* **2003,** *125* (36), 10926-10940.

94. Farnum, D. G., Preparation of Aryldiazoalkanes by the Bamford-Stevens Reaction. *The Journal of Organic Chemistry* **1963,** *28* (3), 870-872.

95. Staudinger, H., Ketene, eine neue Körperklasse. *Berichte der Deutschen Chemischen Gesellschaft* **1905,** *38* (2), 1735-1739.

96. Nozaki, H.; Kondô, K.; Takaku, M., A stable sulfonium ylide. *Tetrahedron Letters* **1965,** *6* (4), 251-254.

97. McGarrigle, E. M.; Aggarwal, V. K., Ylide-Based Reactions. In *Enantioselective Organocatalysis*, Wiley-VCH Verlag GmbH & Co. KGaA: 2007; pp 357-389.

98. Sulikowski, G. A.; Cha, K. L.; Sulikowski, M. M., Stereoselective intramolecular carbon–hydrogen insertion reactions of metal carbenes. *Tetrahedron: Asymmetry* **1998,** *9* (18), 3145-3169.

99. Siddall, J. B.; Marshall, J. P.; Bowers, A.; Cross, A. D.; Edwards, J. A.; Fried, J. H., Synthetic Studies on Insect Hormones. I. Synthesis of the Tetracyclic Nucleus of Ecdysone1. *Journal of the American Chemical Society* **1966,** *88* (2), 379-380.

100. Herrmann, W. A.; Elison, M.; Fischer, J.; Köcher, C.; Artus, G. R., N-Heterocyclic Carbenes: Generation under Mild Conditions and Formation of Group 8–10 Transition Metal Complexes Relevant to Catalysis. *Chemistry-A European Journal* **1996,** *2* (7), 772-780.

101. Braslavsky, S.; Heicklen, J., The gas-phase thermal and photochemical decomposition of heterocyclic compounds containing nitrogen, oxygen, or sulfur. *Chemical Reviews* **1977,** *77* (4), 473-511.

102. Hine, J.; Pollitzer, E. L.; Wagner, H., The Dehydration of Alcohols in the Presence of Haloforms and Alkali. *Journal of the American Chemical Society* **1953,** *75* (22), 5607-5609.

103. Nakamura, E.; Yoshikai, N.; Yamanaka, M., Mechanism of C−H Bond Activation/C−C Bond Formation Reaction between Diazo Compound and Alkane Catalysed by Dirhodium Tetracarboxylate. *Journal of the American Chemical Society* **2002,** *124* (24), 7181-7192.

104. Doyle, M. P.; Westrum, L. J.; Wolthuis, W. N. E.; See, M. M.; Boone, W. P.; Bagheri, V.; Pearson, M. M., Electronic and steric control in carbon-hydrogen insertion reactions of diazoacetoacetates catalysed by dirhodium(II) carboxylates and carboxamides. *Journal of the American Chemical Society* **1993,** *115* (3), 958-964.

105. Taber, D. F.; Petty, E. H., General route to highly functionalized cyclopentane derivatives by intramolecular C-H insertion. *The Journal of Organic Chemistry* **1982,** *47* (24), 4808-4809.

106. Taber, D. F.; Ruckle, R. E., Cyclopentane construction by dirhodium tetraacetate-mediated intramolecular CH insertion: steric and electronic effects. *Journal of the American Chemical Society* **1986,** *108* (24), 7686-7693.

107. Doyle, M. P.; Dorow, R. L.; Tamblyn, W. H.; Buhro, W. E., Regioselectivity in catalytic cyclopropanation reactions. *Tetrahedron Letters* **1982,** *23* (22), 2261-2264.

108. Doyle, M. P.; Shanklin, M. S.; Oon, S. M.; Pho, H. Q.; Van der Heide, F. R.; Veal, W. R., Construction of *β*-lactams by highly selective intramolecular carbon-hydrogen insertion from rhodium(II) carboxylate catalysed reactions of diazoacetamides. *The Journal of Organic Chemistry* **1988,** *53* (14), 3384-3386.

109. Padwa, A.; Austin, D. J.; Price, A. T.; Semones, M. A.; Doyle, M. P.; Protopopova, M. N.; Winchester, W. R.; Tran, A., Ligand effects on dirhodium(II) carbene reactivities. Highly effective switching between competitive carbenoid transformations. *Journal of the American Chemical Society* **1993,** *115* (19), 8669-8680.

110. Davies, H. M. L.; Beckwith, R. E. J., Catalytic Enantioselective C−H Activation by Means of Metal−Carbenoid-Induced C−H Insertion. *Chemical Reviews* **2003,** *103* (8), 2861-2904.

111. Yoon, C. H.; Zaworotko, M. J.; Moulton, B.; Jung, K. W., Regio- and Stereocontrol Elements in Rh(II)-Catalysed Intramolecular C−H Insertion of *α*-Diazo-*α*-(phenylsulfonyl)acetamides. *Organic Letters* **2001,** *3* (22), 3539-3542.

112. Gois, Pedro M. P.; Afonso, Carlos A. M., Regio- and stereoselective dirhodium(II)-catalysed intramolecular C−H insertion reactions of *α*-diazo-*α*-(dialkoxyphosphoryl)acetamides and acetates. *European Journal of Organic Chemistry* **2003,** (19), 3798-3810.

113. Jones, M.; Moss, R. A., Singlet Carbenes. *Reactive Intermediate Chemistry* **2004**, 273-328.

114. Cang, H.; Moss, R. A.; Krogh-Jespersen, K., Nucleophilic Intermolecular Chemistry and Reactivity of Dimethylcarbene. *Journal of the American Chemical Society* **2015**.

115. Bourissou, D.; Guerret, O.; Gabbai, F. P.; Bertrand, G., Stable carbenes. *Chemical Reviews* **2000,** *100* (1), 39-92.

116. Nozaki, H.; Moriuti, S.; Takaya, H.; Noyori, R., Asymmetric induction in carbenoid reaction by means of a dissymmetric copper chelate. *Tetrahedron Letters* **1966,** *7* (43), 5239-5244.

117. Corma, A.; Iglesias, M.; Llabrés i Xamena, F. X.; Sánchez, F., Cu and Au Metal-Organic Frameworks Bridge the Gap between Homogeneous and Heterogeneous Catalysts for Alkene Cyclopropanation Reactions. *Chemistry – A European Journal* **2010,** *16* (32), 9789-9795.

118. Tiemann, F., Zur Kenntniss der Amidoxime und Azoxime. *Berichte der Deutschen Chemischen Gesellschaft* **1891,** *24* (2), 3420-3426.

119. Linke, S.; Tisue, G. T.; Lwowski, W., Curtius and Lossen rearrangements. II. Pivaloyl azide. *Journal of the American Chemical Society* **1967,** *89* (24), 6308-6310.

120. Bentiss, F.; Lagrenée, M.; Barbry, D., Rapid synthesis of 2,5-disubstituted 1,3,4-oxadiazoles under microwave irradiation. *Synthetic Communications* **2001,** *31* (6), 935-938.

121. Loreto, M. A.; Pellacani, L.; Tardella, P. A., The regiochemistry of the (ethoxycarbonyl)nitrene addition reaction to siloxydienes. *Tetrahedron Letters* **1989,** *30* (37), 5025-5028.

122. Bodnar, B. S.; Miller, M. J., Reactions of Nitroso Hetero-Diels−Alder Cycloadducts with Azides: Stereoselective Formation of Triazolines and Aziridines. *The Journal of Organic Chemistry* **2007,** *72* (10), 3929-3932.

123. Doyle, M. P.; McKervey, A.; Ye, T., *Modern catalytic methods for organic synthesis with diazo compounds: from cyclopropanes to ylides*. Wiley: 1998.

124. Suematsu, H.; Kanchiku, S.; Uchida, T.; Katsuki, T., Construction of Aryliridium−Salen Complexes: Enantio- and *Cis*-Selective Cyclopropanation of Conjugated and Nonconjugated Olefins. *Journal of the American Chemical Society* **2008,** *130* (31), 10327-10337.

125. Wang, P.; Adams, J., Model Studies of the Stereoelectronic Effect in Rh(II) Mediated Carbenoid C-H Insertion Reactions. *Journal of the American Chemical Society* **1994,** *116* (8), 3296-3305.

126. Werner, H.; Vicha, R.; Gissibl, A.; Reiser, O., Improved Synthesis of Aza-bis(oxazoline) Ligands. *The Journal of Organic Chemistry* **2003,** *68* (26), 10166-10168.

127. Díaz-Requejo, M. M.; Belderraín, T. R.; Trofimenko, S.; Pérez, P. J., Unprecedented Highly *cis*-Diastereoselective Olefin Cyclopropanation Using Copper Homoscorpionate Catalysts. *Journal of the American Chemical Society* **2001,** *123* (13), 3167-3168.

128. Ramazani, A.; Kazemizadeh, A. R.; Ahmadi, E.; Noshiranzadeh, N.; Souldozi, A., Synthesis and reactions of stabilized phosphorus ylides. *Current Organic Chemistry* **2008,** *12* (1), 59-82.

129. Gilchrist, T. L.; Moody, C. J.; Rees, C. W., Photolysis and thermolysis of N-(N-arylimidoyl) sulfimides. *Journal of the Chemical Society, Perkin Transactions 1* **1975,** (19), 1964-1969.

130. Taylor, E. C.; Turchi, I. J., 1, 5-Dipolar cyclizations. *Chemical Reviews* **1979,** *79* (2), 181-231.

131. Williams, D. R.; Rojas, C. M.; Bogen, S. L., Studies of Acyl Nitrene Insertions. A Stereocontrolled Route toward Lankacidin Antibiotics. *The Journal of Organic Chemistry* **1999,** *64* (3), 736-746.

132. Morita, H.; Tatami, A.; Maeda, T.; Ju Kim, B.; Kawashima, W.; Yoshimura, T.; Abe, H.; Akasaka, T., Generation of Nitrene by the Photolysis of N-Substituted Iminodibenzothiophene. *The Journal of Organic Chemistry* **2008,** *73* (18), 7159-7163.

133. Johnson, M. C.; Hoffman, R. V., N,O-Bis(trimethylsilyl)hydroxylamine. In *Encyclopedia of Reagents for Organic Synthesis*, John Wiley & Sons, Ltd: 2001.

134. Fazio, A.; Loreto, M. A.; Tardella, P. A., Aziridination of *α,β*-unsaturated phosphonic esters. *Tetrahedron Letters* **2001,** *42* (11), 2185-2187.

135. Lwowski, W., Nitrenes and the Decomposition of Carbonylazides. *Angewandte Chemie International Edition in English* **1967,** *6* (11), 897-906.

136. Shainyan, B. A.; Kuzmin, A. V.; Moskalik, M. Y., Carbenes and nitrenes. An overview. *Computational and Theoretical Chemistry* **2013,** *1006* (0), 52-61.

137. Kemnitz, C. R.; Karney, W. L.; Borden, W. T., Why Are Nitrenes More Stable than Carbenes? An Ab Initio Study. *Journal of the American Chemical Society* **1998,** *120* (14), 3499-3503.

138. Knight, J., Carbenes and Nitrenes. *Organic Reaction Mechanisms*·**2003**, 253.

139. Taylor, S.; Gullick, J.; McMorn, P.; Bethell, D.; Page, P. C. B.; Hancock, F. E.; King, F.; Hutchings, G. J., Catalytic asymmetric heterogeneous aziridination of styrene using CuHY: effect of nitrene donor on enantioselectivity. *Journal of the Chemical Society, Perkin Transactions 2* **2001,** (9), 1714-1723.

140. Han, H.; Park, S. B.; Kim, S. K.; Chang, S., Copper−Nitrenoid Formation and Transfer in Catalytic Olefin Aziridination Utilizing Chelating 2-Pyridylsulfonyl Moieties. *The Journal of Organic Chemistry* **2008,** *73* (7), 2862-2870.

141. Doyle, M. P., Catalytic methods for metal carbene transformations. *Chemical Reviews* **1986,** *86* (5), 919-939.

142. Doyle, M. P.; Duffy, R.; Ratnikov, M.; Zhou, L., Catalytic Carbene Insertion into C-H Bonds. *Chemical Reviews* **2009,** *110* (2), 704-724.

143. Cowell, G. W.; Ledwith, A., Developments in the chemistry of diazo-alkanes. *Quarterly Reviews, Chemical Society* **1970,** *24* (1), 119-167.

144. Grakauskas, V.; Guest, A. M., Dinitromethane. *The Journal of Organic Chemistry* **1978,** *43* (18), 3485-3488.

145. Noszticzius, Z.; McCormick, W. D.; Swinney, H. L., Effect of trace impurities on a bifurcation structure in the Belousov-Zhabotinskii reaction: preparation of high-purity malonic acid. *The Journal of Physical Chemistry* **1987,** *91* (19), 5129-5134.

146. Niwayama, S.; Cho, H.; Lin, C., Highly efficient selective monohydrolysis of dialkyl malonates and their derivatives. *Tetrahedron Letters* **2008,** *49* (28), 4434-4436.

147. Sophie, A.-L.; Nadal, B.; Le Gall, T., Synthesis of Bis (tetronic acid) s via Double Dieckmann Condensation. *Synthesis* **2010,** *2010* (10), 1697-1701.

148. Manikowski, A.; Kolarska, Z., Facile and Versatile Room-Temperature Synthesis of N,N-Disubstituted Cyanoacetamides from Malonic Ester Chloride. *Synthetic Communications* **2009,** *39* (20), 3621-3638.

149. Liepa, A. J.; Nguyen, O.; Saubern, S., Synthesis of Some 4-Oxothiochromenes and Related Compounds. *Australian Journal of Chemistry* **2005,** *58* (12), 864-869.

150. Texier, F.; Marchand, E.; Carrié, R., Nouvelle methode de decarbomethoxylation. *Tetrahedron* **1974,** *30* (17), 3185-3192.

151. Marcoux, D.; Charette, A. B., trans-Directing Ability of Amide Groups in Cyclopropanation: Application to the Asymmetric Cyclopropanation of Alkenes with Diazo Reagents Bearing Two Carboxy Groups. *Angewandte Chemie International Edition* **2008,** *47* (52), 10155-10158.

152. Palasz, P. D.; Utley, J. H. P.; Hardstone, J. D., Electro-organic reactions. Part 23. Regioselectivity and the stereochemistry of anodic methoxylation of N-acylpiperidines and N-acylmorpholines. *Journal of the Chemical Society, Perkin Transactions 2* **1984,** (4), 807-813.

153. Zradni, F.-Z.; Hamelin, J.; Derdour, A., Synthesis of amides from esters and amines under microwave irradiation. *Synthetic Communications* **2002,** *32* (22), 3525-3531.

154. Wiitala, K. W.; Cramer, C. J.; Hoye, T. R., Comparison of various density functional methods for distinguishing stereoisomers based on computed ^{1}H or ^{13}C NMR chemical shifts using diastereomeric penam β-lactams as a test set. *Magnetic Resonance in Chemistry* **2007,** *45* (10), 819-829.

155. Seeman, J. I., The Curtin-Hammett principle and the Winstein-Holness equation: new definition and recent extensions to classical concepts. *Journal of Chemical Education* **1986,** *63* (1), 42.

156. Roth, M.; Damm, W.; Giese, B., The Curtin-Hammett principle: Stereoselective radical additions to alkenes. *Tetrahedron Letters* **1996,** *37* (3), 351-354.

157. Seeman, J. I., Effect of conformational change on reactivity in organic chemistry. Evaluations, applications, and extensions of Curtin-Hammett Winstein-Holness kinetics. *Chemical Reviews* **1983,** *83* (2), 83-134.

158. Otzenberger, R. D.; Lipkowitz, K. B.; Mundy, B. P., Quaternizations in the 8-azabicyclo[4.3.0]non-3-ene series. *The Journal of Organic Chemistry* **1974,** *39* (3), 319-321.

159. Leach, A. R., A Survey of Methods for Searching the Conformational Space of Small and Medium-Sized Molecules. *Reviews in Computational Chemistry, Volume 2* **2007**, 1-55.

160. Tomioka, H.; Kitagawa, H.; Izawa, Y., Photolysis of N,N-diethyldiazoacetamide. Participation of a noncarbenic process in intramolecular carbon-hydrogen insertion. *The Journal of Organic Chemistry* **1979,** *44* (17), 3072-3075.

161. Kabwadza-Corner, P.; Munthali, M. W.; Johan, E.; Matsue, N., Comparative Study of Copper Adsorptivity and Selectivity toward Zeolites. *American Journal of Analytical Chemistry* **2014,** *5* (07), 395.

162. Palomino, G. T.; Bordiga, S.; Zecchina, A.; Marra, G. L.; Lamberti, C., XRD, XAS, and IR Characterisation of Copper-Exchanged Y Zeolite. *The Journal of Physical Chemistry B* **2000,** *104* (36), 8641-8651.

163. Mortland, M.; Raman, K., Surface acidity of smectites in relation to hydration, exchangeable cation, and structure. *Clays and Clay Minerals* **1968,** *16* (5), 393-398.

164. Van Olphen, H. Interlayer forces in bentonite (**1954**).

165. Fraile, J. M.; López-Ram-de-Viu, P.; Mayoral, J. A.; Roldán, M.; Santafé-Valero, J., Enantioselective C–H carbene insertions with homogeneous and immobilized copper complexes. *Organic and Biomolecular Chemistry* **2011,** *9* (17), 6075-6081.

166. Díaz-Requejo, M. M.; Belderraín, T. R.; Nicasio, M. C.; Trofimenko, S.; Pérez, P. J., Intermolecular Copper-Catalysed Carbon−Hydrogen Bond Activation via Carbene Insertion. *Journal of the American Chemical Society* **2002,** *124* (6), 896-897.

167. Carballeira, L.; Pérez–Juste, I., Influence of calculation level and effect of methylation on axial/equatorial equilibria in piperidines. *Journal of Computational Chemistry* **1998,** *19* (8), 961-976.

168. Wee, A. G.; Liu, B.; Zhang, L., Dirhodium tetraacetate catalysed carbon-hydrogen insertion reaction in N-substituted.α-carbomethoxy-α-diazoacetanilides and structural analogs. Substituent and conformational effects. *The Journal of Organic Chemistry* **1992,** *57* (16), 4404-4414.

169. Miah, S.; Slawin, A. M. Z.; Moody, C. J.; Sheehan, S. M.; Marino Jr, J. P.; Semones, M. A.; Padwa, A.; Richards, I. C., Ligand effects in the rhodium(II) catalysed reactions of diazoamides and diazoimides. *Tetrahedron* **1996,** *52* (7), 2489-2514.

170. Stork, G.; Szajewski, R. P., Carboxy β-lactams by photochemical ring contraction. *Journal of the American Chemical Society* **1974,** *96* (18), 5787-5791.

171. Kaupang, Å.; Bonge-Hansen, T., α-Bromodiazoacetamides–a new class of diazo compounds for catalyst-free, ambient temperature intramolecular C–H insertion reactions. *Beilstein Journal of Organic Chemistry* **2013,** *9* (1), 1407-1413.

172. Bender, D. R.; Bjeldanes, L. F.; Knapp, D. R.; McKean, D. R.; Rapoport, H., Rearrangement of pyruvates to malonates. B-Lactams by ring contraction. *The Journal of Organic Chemistry* **1973,** *38* (19), 3439-3440.

173. Rosenberg, M. L.; Langseth, E.; Krivokapic, A.; Gupta, N. S.; Tilset, M., Investigation of ligand steric effects on a highly *cis*-selective Rh(I) cyclopropanation catalyst. *New Journal of Chemistry* **2011,** *35* (10), 2306-2313.

174. Solladié-Cavallo, A.; Diep-Vohuule, A.; Isarno, T., Two-Step Synthesis of *trans*-2-Arylcyclopropane Carboxylates with 98–100 % *ee* by the Use of a Phosphazene Base. *Angewandte Chemie International Edition* **1998,** *37* (12), 1689-1691.

175. Yoshino, T.; Imori, S.; Togo, H., Efficient esterification of carboxylic acids and phosphonic acids with trialkyl orthoacetate in ionic liquid. *Tetrahedron* **2006,** *62* (6), 1309-1317.

176. Hoang, V. D. M.; Reddy, P. A. N.; Kim, T.-J., Highly enantioselective and *cis*-diastereoselective cyclopropanation of olefins catalysed by ruthenium complexes of (iminophosphoranyl)ferrocenes. *Tetrahedron Letters* **2007,** *48* (45), 8014-8017.

177. Kamel, C. B.; Benno, R.; Francoise, T. B.; Jack, H.; Hadj, B., Reactivity of Ethyldiazoacetate Towards Alkenes under Microwave Irradiation. *Journal of Chemical Research* **2002,** *33* (37).

178. Taylor, M. T.; Blackman, M. L.; Dmitrenko, O.; Fox, J. M., Design and synthesis of highly reactive dienophiles for the tetrazine–*trans*-cyclooctene ligation. *Journal of the American Chemical Society* **2011,** *133* (25), 9646-9649.

179. Dommerholt, J.; Schmidt, S.; Temming, R.; Hendriks, L. J.; Rutjes, F. P.; van Hest, J.; Lefeber, D. J.; Friedl, P.; van Delft, F. L., Readily Accessible Bicyclononynes for Bioorthogonal Labeling and Three-Dimensional Imaging of Living Cells. *Angewandte Chemie International Edition in English* **2010,** *49* (49), 9422-9425.

180. Anciaux, A. J.; Hubert, A. J.; Noels, A. F.; Petiniot, N.; Teyssie, P., Transition-metal-catalysed reactions of diazo compounds. 1. Cyclopropanation of double bonds. *The Journal of Organic Chemistry* **1980,** *45* (4), 695-702.

181. Boldini, I.; Guillemot, G.; Caselli, A.; Proust, A.; Gallo, E., Polyoxometalates: Powerful Catalysts for Atom-Efficient Cyclopropanations. *Advanced in Synthesis and Catalysis* **2010,** *352* (14-15), 2365-2370.

182. Kanemasa, S.; Kanai, T.; Araki, T.; Wada, E., Lewis acid-catalysed reactions of ethyl diazoacetate with aldehydes. Synthesis of α-formyl esters by a sequence of aldol reaction and 1,2-nucleophilic rearrangement. *Tetrahedron Letters* **1999,** *40* (27), 5055-5058.

183. Wessjohann, L. A.; Brandt, W.; Thiemann, T., Biosynthesis and Metabolism of Cyclopropane Rings in Natural Compounds. *Chemical Reviews* **2003,** *103* (4), 1625-1648.

184. Brackmann, F.; de Meijere, A., Natural Occurrence, Syntheses, and Applications of Cyclopropyl-Group-Containing α-Amino Acids. 1. 1-Aminocyclopropanecarboxylic

Acid and Other 2,3-Methanoamino Acids. *Chemical Reviews* **2007,** *107* (11), 4493-4537.

185. González-Bobes, F.; Fenster, M. D. B.; Kiau, S.; Kolla, L.; Kolotuchin, S.; Soumeillant, M., Rhodium-Catalysed Cyclopropanation of Alkenes with Dimethyl Diazomalonate. *Advanced Synthesis and Catalysis* **2008,** *350* (6), 813-816.

186. de Nanteuil, F.; Serrano, E.; Perrotta, D.; Waser, J., Dynamic Kinetic Asymmetric [3 + 2] Annulation Reactions of Aminocyclopropanes. *Journal of the American Chemical Society* **2014,** *136* (17), 6239-6242.

187. Talukdar, R.; Tiwari, D. P.; Saha, A.; Ghorai, M. K., Diastereoselective Synthesis of Functionalized Tetrahydrocarbazoles via a Domino-Ring Opening–Cyclization of Donor-Acceptor Cyclopropanes with Substituted 2-Vinylindoles. *Organic Letters* **2014,** *16* (15), 3954-3957.

188. Marcoux, D.; Goudreau, S. R.; Charette, A. B., *trans*-Directing Ability of the Amide Group: Enabling the Enantiocontrol in the Synthesis of 1,1-Dicarboxy Cyclopropanes. Reaction Development, Scope, and Synthetic Applications. *The Journal of Organic Chemistry* **2009,** *74* (23), 8939-8955.

189. Padwa, A.; Woolhouse, A. D., Aziridines, Azirines and Fused-ring Derivatives. In *Comprehensive Heterocyclic Chemistry*, Katritzky, A. R.; Rees, C. W., Eds. Pergamon: Oxford, **1984**; pp 47-93.

190. Bagchi, V.; Paraskevopoulou, P.; Das, P.; Chi, L.; Wang, Q.; Choudhury, A.; Mathieson, J. S.; Cronin, L.; Pardue, D. B.; Cundari, T. R.; Mitrikas, G.; Sanakis, Y.; Stavropoulos, P., A Versatile Tripodal Cu(I) Reagent for C–N Bond Construction via Nitrene-Transfer Chemistry: Catalytic Perspectives and Mechanistic Insights on C–H Aminations/Amidinations and Olefin Aziridinations. *Journal of the American Chemical Society* **2014,** *136* (32), 11362-11381.

191. Jeffs, L.; Arquier, D.; Kariuki, B.; Bethell, D.; Page, P. C. B.; Hutchings, G. J., On the enantioselectivity of aziridination of styrene catalysed by copper triflate and copper-exchanged zeolite Y: consequences of the phase behaviour of enantiomeric mixtures of N-arene-sulfonyl-2-phenylaziridines. *Organic and Biomolecular Chemistry* **2011,** *9* (4), 1079-1084.

192. Omura, K.; Uchida, T.; Irie, R.; Katsuki, T., Design of a robust Ru(salen) complex: aziridination with improved turnover number using N-arylsulfonyl azides as precursors. *Chemical Communications* **2004,** (18), 2060-2061.

193. Gao, G.-Y.; Jones, J. E.; Vyas, R.; Harden, J. D.; Zhang, X. P., Cobalt-Catalysed Aziridination with Diphenylphosphoryl Azide (DPPA): Direct Synthesis of N-Phosphorus-Substituted Aziridines from Alkenes. *The Journal of Organic Chemistry* **2006,** *71* (17), 6655-6658.

194. Cunningham, E., On the velocity of steady fall of spherical particles through fluid medium. *Proceedings of the Royal Society of London. Series A, Containing Papers of a Mathematical and Physical Character* **1910,** *83* (563), 357-365.

195. Warren, B., X-Ray Diffraction Methods. *Journal of Applied Physics* **1941,** *12* (5), 375-384.

196. Sophie, A.-L.; Nadal, B.; Le Gall, T., Synthesis of Bis (tetronic acid) s via Double Dieckmann Condensation. *Synthesis* **2010,** (10), 1697-1701.

197. Bélanger, D.; Tong, X.; Soumaré, S.; Dory, Y. L.; Zhao, Y., Cyclic Peptide–Polymer Complexes and Their Self-Assembly. *Chemistry – A European Journal* **2009,** *15* (17), 4428-4436.

198. Carreno, M. C., Applications of Sulfoxides to Asymmetric Synthesis of Biologically Active Compounds. *Chemical Reviews* **1995,** *95* (6), 1717-1760.

199. Bennani, Y. L.; Hanessian, S., *trans*-1,2-Diaminocyclohexane Derivatives as Chiral Reagents, Scaffolds, and Ligands for Catalysis: Applications in Asymmetric Synthesis and Molecular Recognition. *Chemical Reviews* **1997,** *97* (8), 3161-3196.

Oral and Poster Presentations Related to this Work

2011 Centre for Material Science (UCLan)

Oral Presentation

2012 North West Organic Chemistry, University of Liverpool

Poster Presentation

2012 Peak dale Molecular Symposium, Sheffield

Poster Presentation

2012 UCLan Graduate School Research Conference

Poster Presentation

2013 UCLan Graduate School Research Conference

Oral Presentation

2013 Young Chem 2013, Poznan, Poland

Poster presentation (Abstract published in **congress book**)

2013 Clay Mineral Group Conference, Durham University
Oral Presentation

Cu^{2+} Clay Mineral Catalysed Reactions of Diazoalkanes: Effects of the Restrictions of the Interlayer Space on the Stereochemistry of the Carbene Reactions.

Richard W McCabe [1] and Vinod Kumar Vishwapathi [1]

[1] Centre for Material Sciences, School of Forensic and Investigative Sciences, University of Central Lancashire, Preston, PR1 2HE, UK

Abstract

Carbene intermediates can be generated by thermal, photochemical and transition metal catalysed processes from diazoalkanes.[i] The carbene intermediates are very reactive and can add across double bonds to give 3-membered rings (cyclopropanes),[ii] insert into OH bonds to give esters and insert into neighbouring C-H bonds to give 4 or 5-membered rings, such as β- and γ-lactams or β-lactones. Copper salts and complexes were amongst the first catalysts to be used for carbene generation from diazoalkanes.[iii] However, current tendencies are to use very expensive, especially, platinum group salts and complexes to generate the carbene intermediates, as yields and specificity tend to be higher. We have found. On the other hand, that Cu (II) exchanged clay minerals, e.g. Wyoming bentonite, have proven to be very competitive in yield with these transition metal catalysts and they have the added tendency that the restricted reaction space within the clay interlayer favours the more planar/less bulky product when the layer spacing is kept low by judicious choice of solvent.

Herein we report a wide range of carbene addition (cyclopropane formation) and C-H insertion reactions (β-lactam, γ-lactam and β-lactone formation) catalysed by the Cu(II) exchanged clay minerals and the stereochemical consequences of carrying out the reactions within the clay interlayer.

References

[i] Wulfman, D.S., McDaniel, Jr., R.S. and Peace, B.W. (1976) *Tetrahedron*, **32**, 1241-51.

[ii] e.g. Yeung, C, T., Teng, P, F., Yeung, H.L., Wong, W.T and Kwong, H.L (2007) "Catalytic and asymmetric cyclopropanation of alkenes catalysed by rhenium (I) bipyridine and terpyridine tricarbonyl complexes", *Organic and Biomolecular Chemistry,* (**5**) p-3859-3864.

[iii] e.g. Sanders, C.J., Gillespie, K.M., and Scott, P (2001) "Catalyst structure of the enantioselective cyclopropanation of alkenes by copper complexes of biaryldiimines: the importance of ligand acceleration", Tetrahedron: *Asymmetry* 12 p-1055-1061.